Syntheses and Functionalization of *N*-Heterocycles via Rhodium Catalysed C-H Activation

by

PRAGATI BISWAL

CHEM11201604007

National Institute of Science Education and Research,

Bhubaneswar, Odisha

A thesis submitted to the

Board of Studies in Chemical Sciences

In partial fulfillment of requirements

for the Degree of

DOCTOR OF PHILOSOPHY

of

HOMI BHABHA NATIONAL INSTITUTE

Jan, 2022

Homi Bhabha National Institute[1]

Recommendations of the Viva Voce Committee

As members of the Viva Voce Committee, we certify that we have read the dissertation prepared by **Pragati Biswal** entitled **"Syntheses and Functionalization of *N*-Heterocycles *via* Rhodium Catalyzed C-H Activation"** and recommend that it may be accepted as fulfilling the thesis requirement for the award of Degree of Doctor of Philosophy.

Chairman - Prof. A. Srinivasan   Date: 17.03.22

Guide / Convener - Dr. Ponneri C. Ravikumar   Date: 17/03/2022

Examiner - Prof. Dattatraya Dethe   Date: 17/03/2022

Member 1- Dr. S. Nembenna   Date: 17/3/22

Member 2- Dr. C. S. Purohit   Date: 17/03/22

Member 3- Dr. V. Badireenath Konkimalla   Date: 17/MAR/2022

Final approval and acceptance of this thesis is contingent upon the candidate's submission of the final copies of the thesis to HBNI.

I/We hereby certify that I/we have read this thesis prepared under my/our direction and recommend that it may be accepted as fulfilling the thesis requirement.

Date: 17/03/2022

Place: NISER, Bhubaneswar

Signature   17/03/2022

Guide

---

[1] This page is to be included only for final submission after successful completion of viva voce.

STATEMENT BY AUTHOR

This dissertation has been submitted in partial fulfillment of requirements for an advanced degree at Homi Bhabha National Institute (HBNI) and is deposited in the library to be made available to borrowers under rules of the HBNI.

Brief quotations from this dissertation are allowable without special permission, provided that accurate acknowledgement of source is made. Requests for permission for extended quotation from or reproduction of this manuscript in whole or in part may be granted by the Competent Authority of HBNI when in his or her judgment the proposed use of the material is in the interests of scholarship. In all other instances, however, permission must be obtained from the author.

Pragati Biswal

Pragati Biswal

DECLARATION

I, hereby declare that the investigation presented in the thesis has been carried out by me.

The work is original and has not been submitted earlier as a whole or in part for a degree

/ diploma at this or any other Institution / University.

Pragati Biswal

Pragati Biswal

List of Publications

a. Published

*1) **P. Biswal**; B. V. Pati; R. Chebolu; A. Ghosh; P. C. Ravikumar.* Hydroxylamine-*O*-Sulfonic Acid (HOSA) as a Redox-Neutral Directing Group: Rhodium Catalysed, Additive Free, One-Pot Synthesis of Isoquinolines from Arylketones. *Eur. J. Org. Chem*. **2020**, *2020*, 1006–1014.

Editor choice: **Very Important paper** (VIP), **Highlighted in Synfacts**: *Synfacts* **2020**; 16(07): 0776.

*2) **P. Biswal**; S. K. Banjare; B. V. Pati; S. R. Mohanty; P. C. Ravikumar.* Rhodium-Catalysed One-Pot Access to *N*-Polycyclic Aromatic Hydrocarbons from Aryl Ketones through Triple C–H Bond Activations. *J. Org. Chem*. **2021,** *86*, 1108–1117.

3) S. K. Banjare; **P. Biswal;** P. C. Ravikumar.* Cobalt-Catalysed One-Step Access to Pyroquilon and C-7 Alkenylation of Indoline with Activated Alkenes Using Weakly Coordinating Functional Groups. *J. Org. Chem*. **2020**, *85*, 5330–5341.

4) T. Nanda; **P. Biswal**; B. V. Pati; S. K. Banjare; P. C. Ravikumar.* Palladium-Catalysed C–C Bond Activation of Cyclopropenone: Modular Access to Trisubstituted *α, β*-Unsaturated Esters and Amides. *J. Org. Chem*. **2021**, *86*, 2682–2695.

5) S. K. Banjare; T. Nanda; B. V. Pati; **P. Biswal**; P. C. Ravikumar.* *O*-Directed C–H functionalization via cobaltacycles: a sustainable approach for C–C and C–heteroatom bond formations. *Chem. Commun*. **2021**, *57*, 3630–3647.

(* pertaining to thesis)

6) S. R. Mohanty; N. Prusty; L. Gupta; **P. Biswal**; P. C. Ravikumar.[*] Cobalt(III)-Catalysed C-6 Alkenylation of 2-Pyridones by Using Terminal Alkyne with High Regioselectivity. *J. Org. Chem*. **2021,** *86*, 9444−9454.

7) G. Das Adhikari; B. V. Pati; T. Nanda; **P. Biswal**; S. K. Banjare; P. C. Ravikumar.[*] Co (II)-Catalysed C-H/N-H Annulation of Cyclic Alkenes with Indole-2-Carboxamides at room temperature: A one step access to *β*-carboline-1-one derivatives. *J. Org. Chem*. **2022,** 87, 4438−4448.

b. Manuscripts Communicated

*1) **P. Biswal**,[†] T. Nanda,[†] S. K. Banjare, S. Prasad, S. R. Mohanty, D. J. Tantillo,[*] and P. C. Ravikumar[*] *N*-allylbenzimidazole as a Strategic Surrogate in the Rh-catalysed Stereoselective Mono-Alkenylation of Aryl C(sp^2)-H Bonds (**Under revision, [†]contributed equally**)

*2) **P. Biswal**; T. Nanda; N. Prusty; S. R. Mohanty; P. C. Ravikumar. Rhodium-Catalysed Synthesis of 2-Methylindole via C-N bond Cleavage of *N*-allylbenzimidazole (**Communicated**)

3) T. Nanda; S. K. Banjare; S. Prasad; **P. Biswal**; L. Gupta; B. V. Pati; S. R. Mohanty; D. J Tantillo; P. C. Ravikumar, Breaking the Monotony: Cobalt and Maleimide as a New Entrant to the Catellani Reaction. (**ChemRxiv, doi: 10.26434/chemrxiv-2022-l355m**)

c. Book Chapter

1) **P. Biswal**; N. Prusty; P. C. Ravikumar, 'Synthesis of Hetero-Polycyclic Aromatic Hydrocarbons through Directed C-H Functionalization' in "Handbook of C-H Functionalization" (**Wiley Publishers**, **in press**)

(* pertaining to thesis)

Conferences

1. 'Hydroxylamine-*O*-Sulfonic Acid (HOSA) as a Redox–Neutral Directing Group: Rhodium Catalysed, Additive Free, One-Pot Synthesis of Isoquinolines from Arylketones'; **P. Biswal**, B. V. Pati, R. Chebolu, A. Ghosh, and Ponneri. C. Ravikumar*; in National Conference on Organic Synthesis (**N-COS-2020**), Organized by PG Department of Chemistry, Berhampur University, Odisha. during 02-03 March, 2020. (**Poster presentation** and **Short oral presentation**).

2. 'Rhodium-catalysed, One-pot Strategy Towards the Synthesis of Isoquinolines and aza-Ploycyclic Aromatic Hydrocarbons (*N*-PAHs)'; **P. Biswal**, B. V. Pati, R. Chebolu, A. Ghosh, Ponneri C. Ravikumar*; in First Virtual JNOST Conference (**JNOST-16**) For Research Scholars, organized by the Indian Institute of Science, Bangalore, India during October 31–Nov. 1, 2020. (**Virtual oral presentation**).

3. 'C-H Activation: A Modern Synthetic Platform for the Synthesis of Heterocycles (isoquinoline & indoles)'; **P. Biswal** and Ponneri C. Ravikumar; in National Conference on Recent Advances in Heterocyclic Chemistry (**RAHC-2022**)' held at the Department of Chemistry, Ravenshaw University during January 15-16, 2022. (**Oral presentation**).

Pragati Biswal
Pragati Biswal

Dedicated to

My Family,

Dr. Padmanava Pradhan (Uncle)

&

all My Teachers

ACKNOWLEDGEMENTS

Pragati Biswal

Pragati   Biswal

CONTENTS

SYNOPSIS

This thesis has been organized into five chapters.

Chapter 1 represents a brief introduction to directed C-H functionalizations (**Scheme 1**).

Scheme 1: **Transition-metal catalysed directed C-H functionalization**
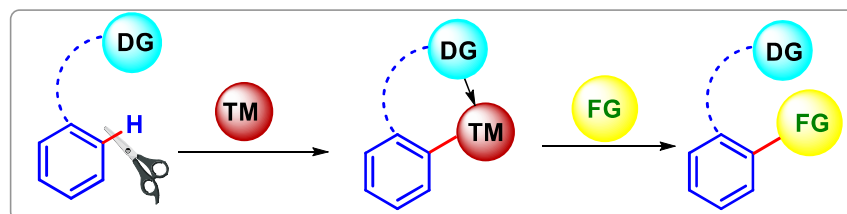
In **Chapter 2**, one-pot synthesis of isoquinolines has been reported from readily available aryl ketones **1** and internal alkynes **3** (**Scheme 2**). In this methodology, a well-known aminating reagent hydroxylamine-*O*-sulfonic acid (HOSA) **2** has been used as a redox-neutral directing group. This protocol works well with a series of aryl ketones including benzophenones, giving respective annulated compounds in good to excellent yields. This C-H/N-O annulation methodology gives excellent yields even without any silver additive, acid/base or metal oxidant. This is the first report wherein a directing group is simultaneously generated *in situ*, which acts as an acid additive, and also as an internal oxidant.

Scheme 2: Cp*Rh-catalysed, one-pot syntheses of isoquinolines and the catalytic cycle

R^1 = H, **4aa,** 89%
= OMe, **4ba,** 97%

4ca, 71%

4da, 70%

4ea, 71%

R^2 = Me, **4ab,** 75%
R^2 = H, **4ac,** 77%

4ab

R = H, **4fa**, 64%
= OMe, **4ga**, 72%

4ha, 70%
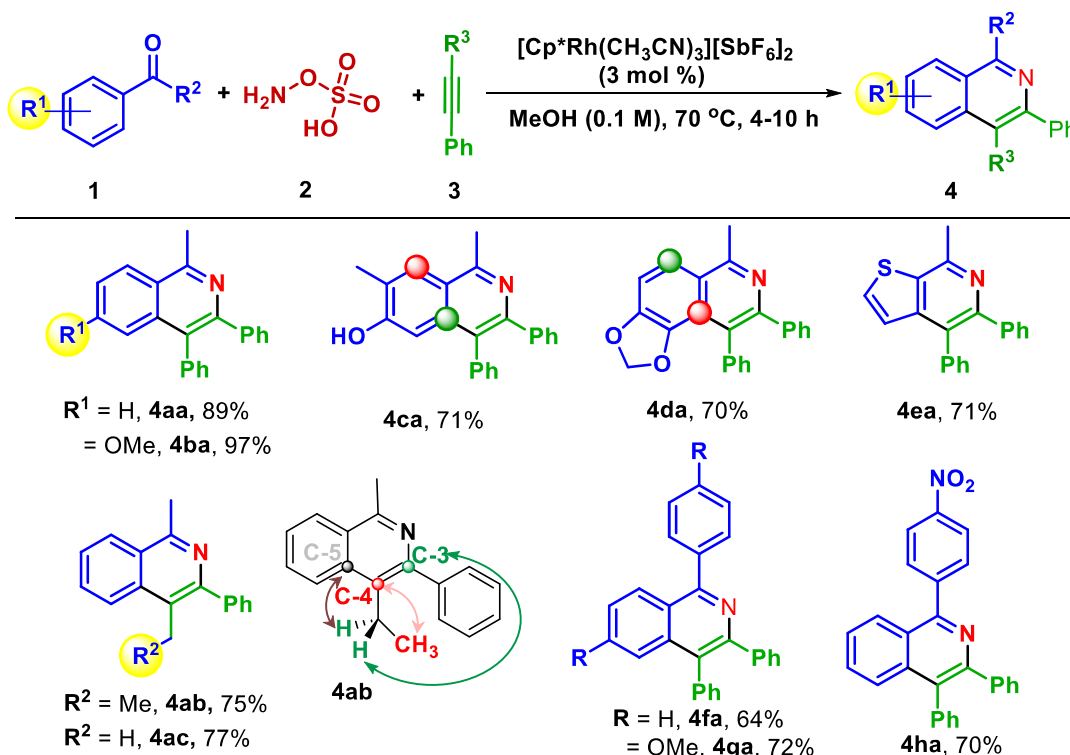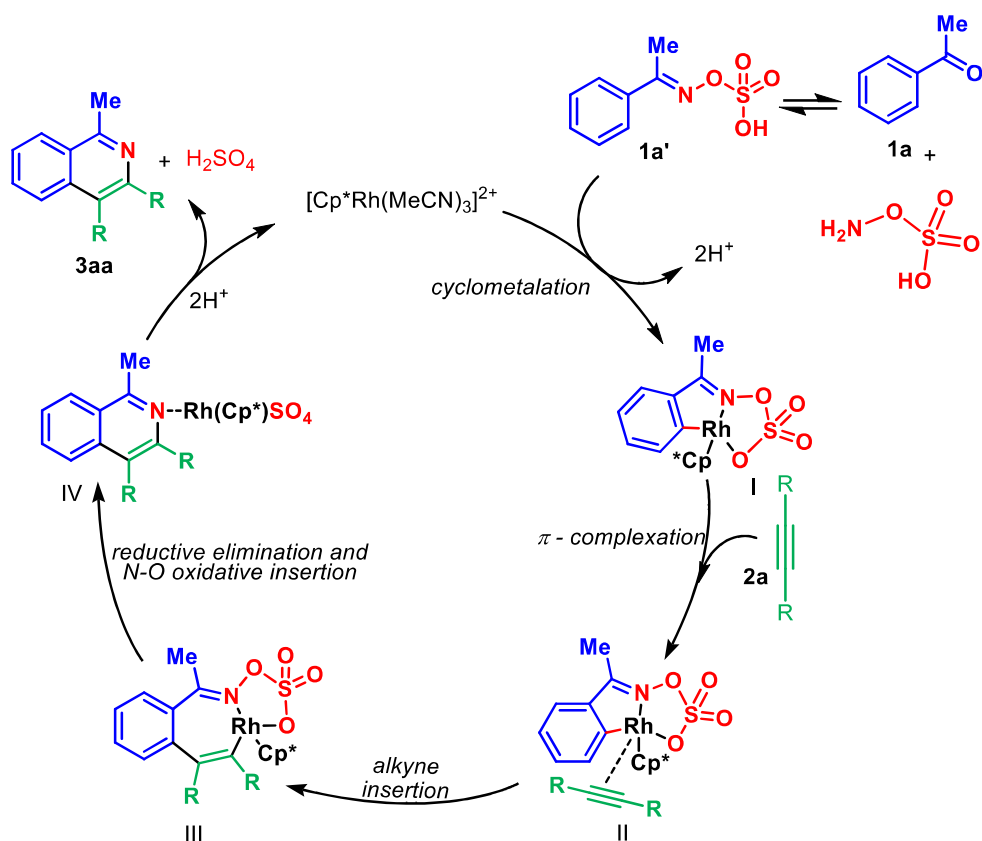
In **Chapter 3**, one-pot synthesis of *N*-polycyclic aromatic hydrocarbons (*N*-PAHs) has been presented from aryl ketone **1**, HOSA **2**, and internal alkyne **3** (**Scheme 3**). The reaction proceeds through a cascade of C-H activations followed by annulation with internal alkyne **3**. This methodology tolerates a wide range of functional groups including aryl halides, electron donating/withdrawing substituents and more importantly free hydroxy (-OH) group. It shows that, this protocol could be applicable with a substrate having unprotected hydroxy group. The well-known aminating reagent HOSA has been used here as *N*-transfer reagent, thus exploring the synthetic applications of the aminating reagent. Moreover, the easily synthesizable highly arylated *N*-PAH products could be applicable in optoelectronics. Mechanistic experiments were performed to understand the mechanism and the isoquinoline **4** was found as an active intermediate for the formation of **5**.

Scheme 3: Cp*Rh-catalysed synthesis of *N*-polycyclic aromatic hydrocarbons and the proposed catalytic cycle
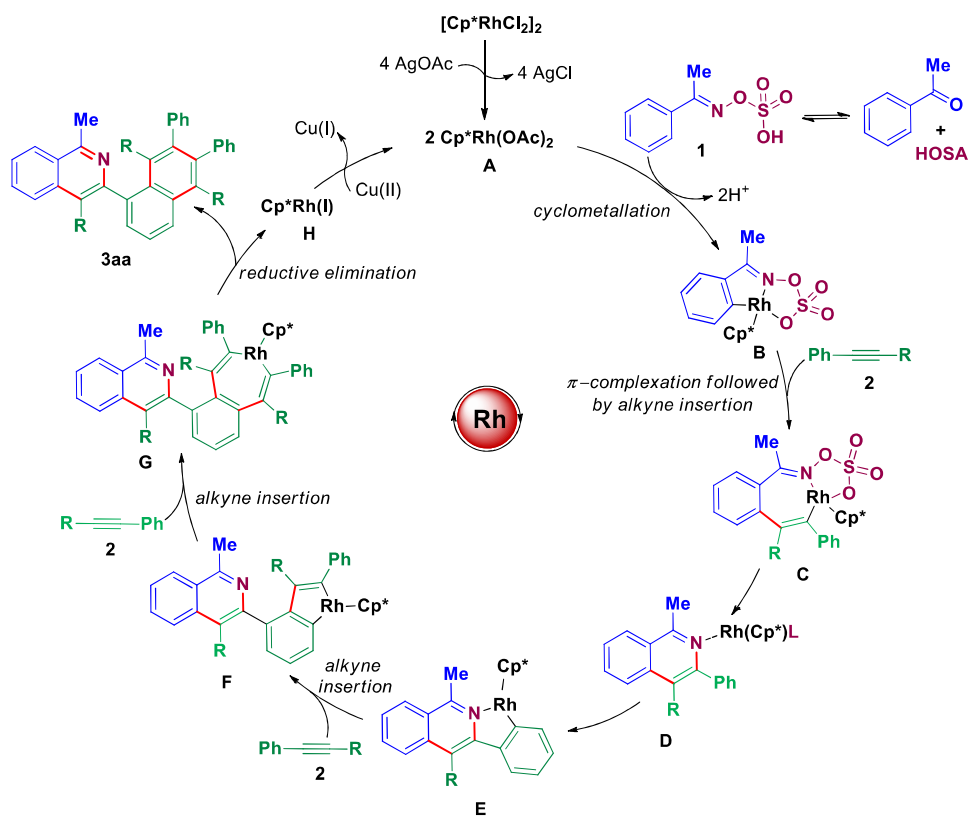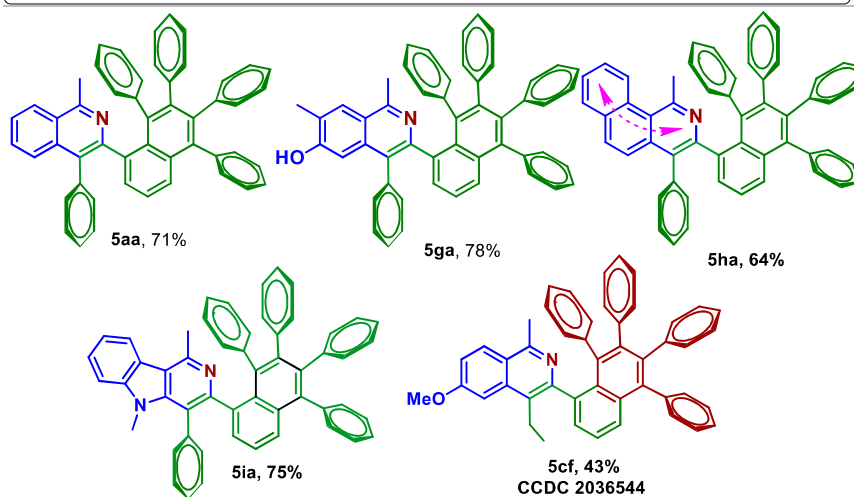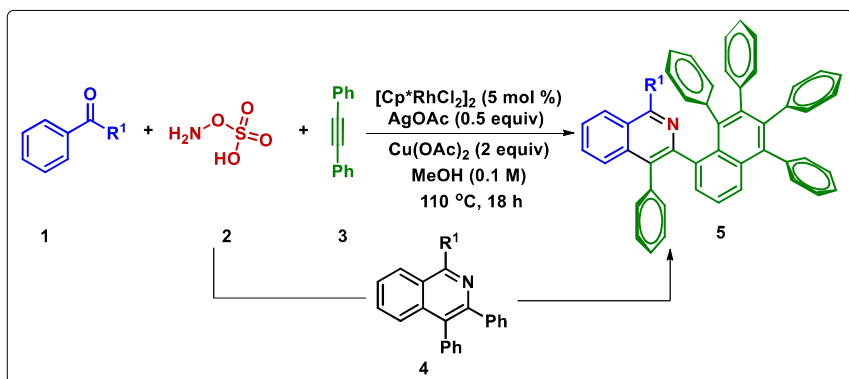
In **Chapter 4**, a Rh-catalysed $C(sp^2)$-H alkenylation **8** has been reported taking *N*-allylbenzimidazole **7** as an allylamine congener (**Scheme 4**). This distinctive transformation has been observed for the first time, where a tandem process of C-H allylation followed by alkene isomerization delivers a highly stereoselective *trans*-alkenylated product. The presence of Lewis acid enhances the reactivity by assisting the cleavage of $C(sp^3)$-N bond by coordinating to the N3 of *N*-allylbenzimidazole. Thus, herein we have demonstrated an unprecedented protocol of domino C-N bond cleavage followed by aryl $C(sp^2)$-H alkenylation. Further, detailed mechanistic studies, control experiments and computational studies have been conducted to understand the mechanism. The rhodacycle-intermediates involved in the reaction have been isolated and characterized through NMR, HRMS, and single crystal X-ray. This methodology has been found to be applicable with a wide range of functional groups and directing groups (pyridine, pyrimidine, pyrazole, purine). More importantly, the nucleobase

Scheme 4: Cp*Rh-catalysed $C(sp^2)$-H alkenylation directed by heteroarenes and the proposed catalytic cycle
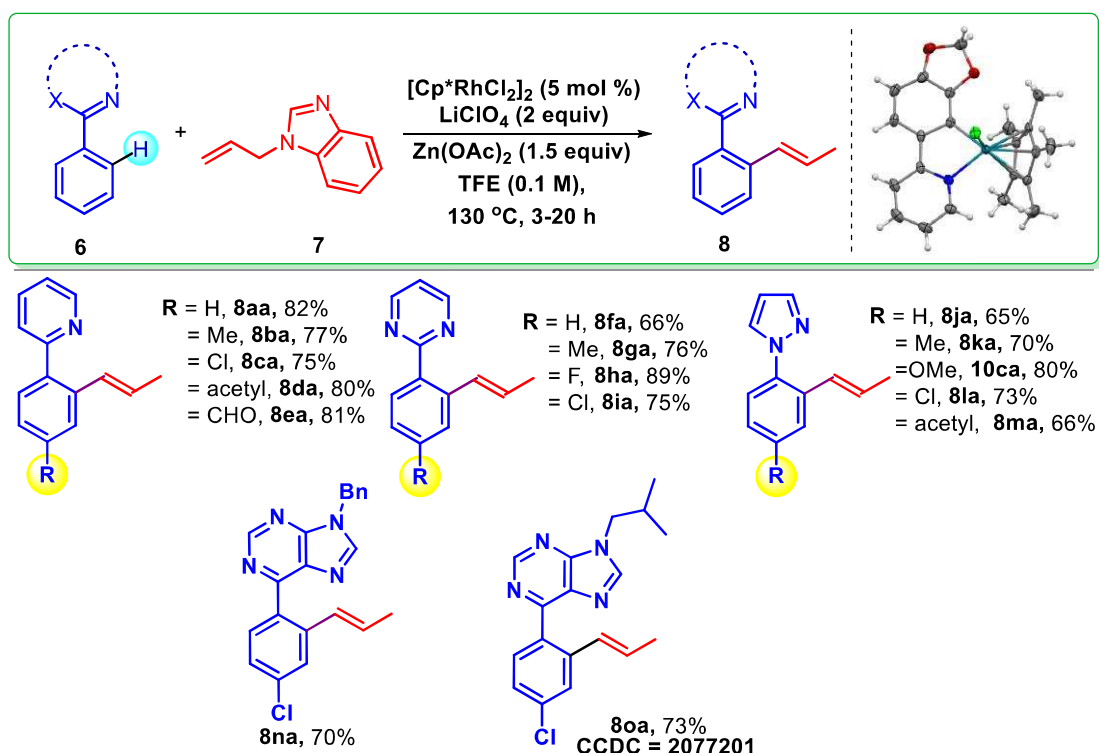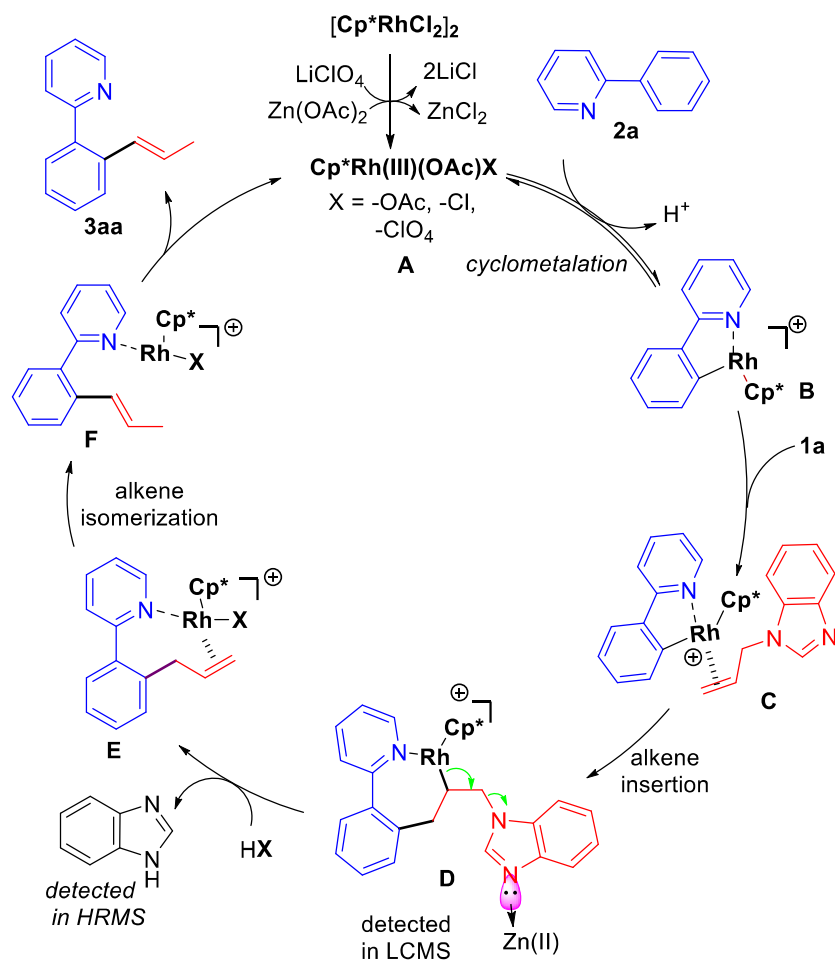
purine could be stereoselectivity monoalkenylated under the developed protocol. Mechanistic studies, organo-rhodium intermediate isolation and single crystal structure confirms the reaction pathway. The stereoselective formation of the *trans*-alkene among other possibilities such as allylation/cis-alkenylation is a key feature of this methodology.

Chapter 5 represents a rhodium catalysed oxidative C-H/N-H dehydrogenative [3+2] annulation strategy between anilines **9** and *N*-allylbenzimidazole **7** for the synthesis of 2-methylindole scaffolds **10** (**Scheme 5**). An un-activated alkene *N*-allylbenzimidazole has been used and more importantly, this transformation involves the cleavage of thermodynamically stable C-N bond of allylamine. Detailed mechanistic studies have

Scheme 5: Cp*Rh-catalysed synthesis of 2-methylindole and the proposed catalytic cycle
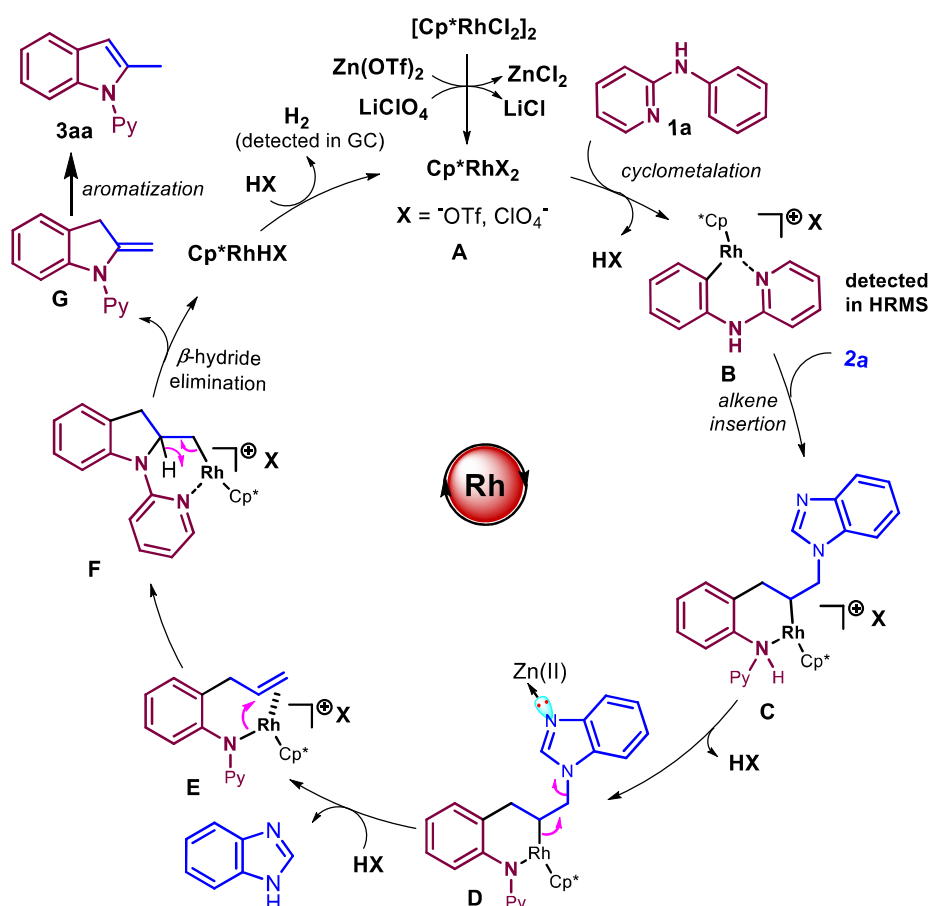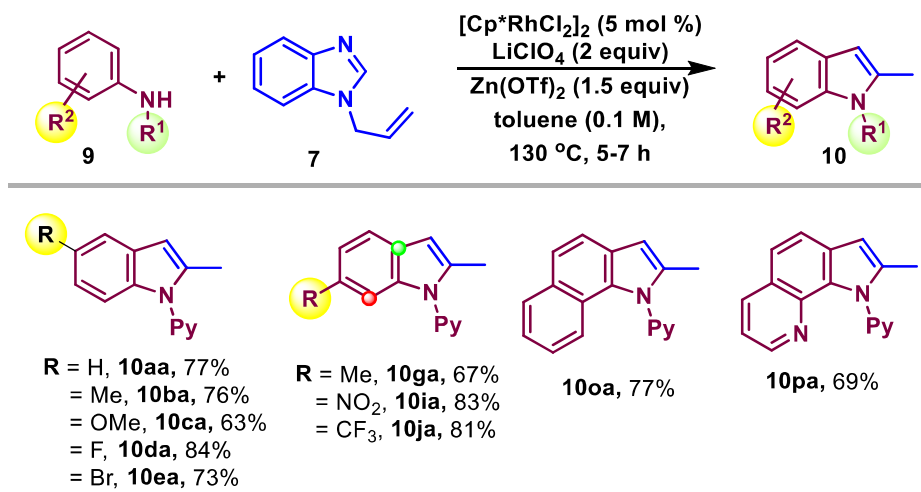
been performed and key intermediate was detected in HRMS. The product **10** has been used for the synthesis of the drug molecule MIPP (methuosis inducer).

List of figures

List of tables

List of schemes

List of Abbreviations

AcOH	Acetic acid
CH_3CN	Acetonitrile
S_EAr	Aromatic electrophilic substitution
BIES	Base-assisted intramolecular electrophilic substitution
NBS	*N*-Bromosuccinimide
BHT	Butylated hydroxytoluene
^{n}BuLi	*n*-Butyllithium
^{13}C NMR	Carbon nuclear magnetic resonance
$Cu(OAc)_2$	Copper (II) acetate
$CHCl_3$	Chloroform
$CDCl_3$	Chloroform-d
CMD	Concerted metalation deprotonation
DCE	1,2-dichloroethane
DCM/CH_2Cl_2	Dichloromethane
DMSO	Dimethyl sulfoxide
DMF	Dimethylformamide
DEPT-135	Distortionless enhancement by polarization transfer
DG	Directing group
EtOAc	Ethyl acetate
FG	Functional group
GC	Gas chromatography
HMBC	^{1}H-^{13}C Heteronuclear Multiple Bond Correlation Spectroscopy
HFIP	1,1,1,3,3,3-Hexafluoro isopropanol
HRMS	High resolution mass spectrometry
HOSA	Hydroxylamine-*O*-Sulfonic Acid
IR	Infrared
KIE	Kinetic Isotope Effect
$LiClO_4$	Lithium perchlorate
MeOH	Methanol

CD$_3$OD	d$_4$-Methanol	
OLED	Organic light emitting diode	
PAHs	Polycyclic aromatic hydrocarbons	
K$_2$CO$_3$	Potassium carbonate	
DG^{OX}	Redox neutral directing group	
AgOAc	Silver acetate	
AgTFA	Silver trifluoroacetate	
NaH	Sodium hydride	
Na$_2$SO$_4$	Sodium sulphate	
THF	Tetrahydrofuran	
TEMPO	(2,2,6,6-Tetramethylpiperidin-1-yl) oxyl	
TFA	Trifluoroacetic acid	
TFE	Trifluoroethanol	
TM	Transition metal	
^{2}D	Two dimensional	
Zn(OAc)$_2$	Zinc acetate	

Chapter 1

Introduction to directed C-H functionalization

1.1 Introduction

1.2 Non-directed C-H functionalization (Scope and limitations)

1.3 Basics of directed C-H functionalization

1.4 Directing groups and their classification

1.5 Conclusion

1.6 References

Chapter 1

Introduction to directed C-H functionalization
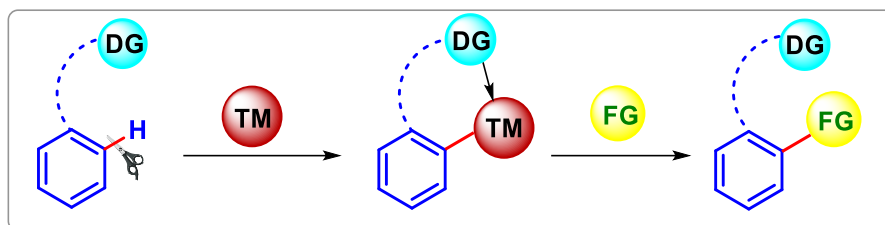
1.1 INTRODUCTION

Organic synthesis relies on the transformation of pre-existing functional groups. The reorganisation and cleavage of various covalent bonds is key to all organic transformations. Organic functional group transformations are helpful for the synthesis of structurally/ biologically important molecular architectures. The carbon-hydrogen (C-H), carbon-carbon (C-C), carbon-halogen (C-X), carbon-nitrogen (C-N), carbon-oxygen (C-O), and carbon-sulphur (C-S) bonds are prevalant in organic molecules. Among them, the C-H and C-C bonds are ubiquitous and are non-polar in nature as compared to C-X/C-N/C-O/C-S bonds. This polar/non-polar nature of the covalent bond is because of their electronegitivity difference between the bonded atoms. Consequently, the ease of substitution/functionalization of a polar covalent bond is quite easier than non-polar bond.

Since early 19th century, numerous methodologies have been discovered for the functionalization of covalent bond using traditional synthesis, which include (i) aromatic electrophilic/nucleophilic substitution, (ii) enolate chemistry with a substrate containing active methyl/methylene group, (iii) free radical chemistry, (iv) carbene chemistry, (v) Diels-Alder/Sigmatropic rearrangements. Additionally, the discovery of the Grignard reagent[1] (an organometallic reagent) evolved as a seminal methodology for many transformations. Similarly, palladium-catalysed cross coupling reactions increased the

scope for the functionalization of a covalent bond and have found high applicability in

organic synthesis (Figure 1.1).[2]

$$R\text{—}X + R^1\text{—}M \xrightarrow{\textbf{Pd}} R\text{—}R^1$$

R, R^1=aryl, alkenyl, alkyl   M = Mg   Kumada coupling
X=Cl, Br, I, OTf..   Zn   Negishi coupling
                                 B   Suzuki coupling
                                 Sn   Stille coupling
                                 Si   Hiyama coupling
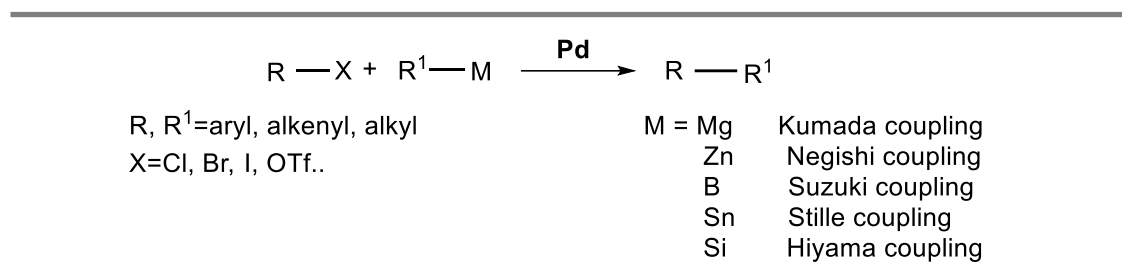
Figure 1.1: Palladium-catalysed cross coupling reactions

Limitations in Pd-catalysed cross-coupling reaction: In these cross coupling reactions, a prefunctionalized/activated bond (e.g., C-X, X = Br, I, boronic acid/boronate ester, -OTf etc.) is required for the generation of the organometallic intermediate and extra steps are required to prepare such functionalized substrate from inert C-H bond. So, this is both cost and step uneconomical. Additionally, generation of waste byproducts is another limitation associated with these coupling reactions. Thus, direct functionalization of inert C-H bond has streamlined organic synthesis by providing step and cost economical approach. It restricts waste generation by minimizing step and thus contributes to green chemistry.

1.2 NON-DIRECTED C-H FUNCTIONALIZATION

Significant effort has been devoted to design protocols which could form C-C/ C-hetero bond from direct functionalization of inert C-H bonds. In this context, the Fujiwara-Moritani olefination stands as a representative example of coupling reaction where an aryl C-H bond couples with olefins, forming a C-C bond (Figure 1.2).[3] This coupling reaction considered as a substitute of the well-known Heck reaction, as it obviates the need of preactivated substrates such as aryl halides or triflates for coupling with an olefinic carbon.[4] The Fujiwara-Moritani coupling reaction involves the C-H metalation of arene C-H bond followed by olefin insertion and reductive elimination to

deliver the arylated olefins. The scope of this protocol has been extended for the incorporation of olefinic unit into an arene unit containing different functional groups.
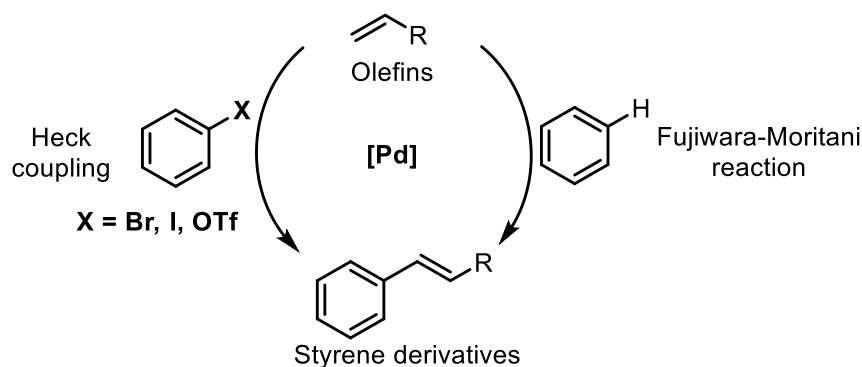
Figure 1.2: Heck reaction *vs* Fujiwara-Moritani olefination

For an example, the Obara group reported a highly selective *para*-olefination of *N,N*-dialkylanilines with palladium/molybdovanadophosphoric acid catalyst (Figure 1.3a).[5] *N,N*-dialkyl aniline is an *ortho/para*-directing group, still they obtained highly selective *para*-functionalization over *ortho*-functionalization. This high selectivity is a
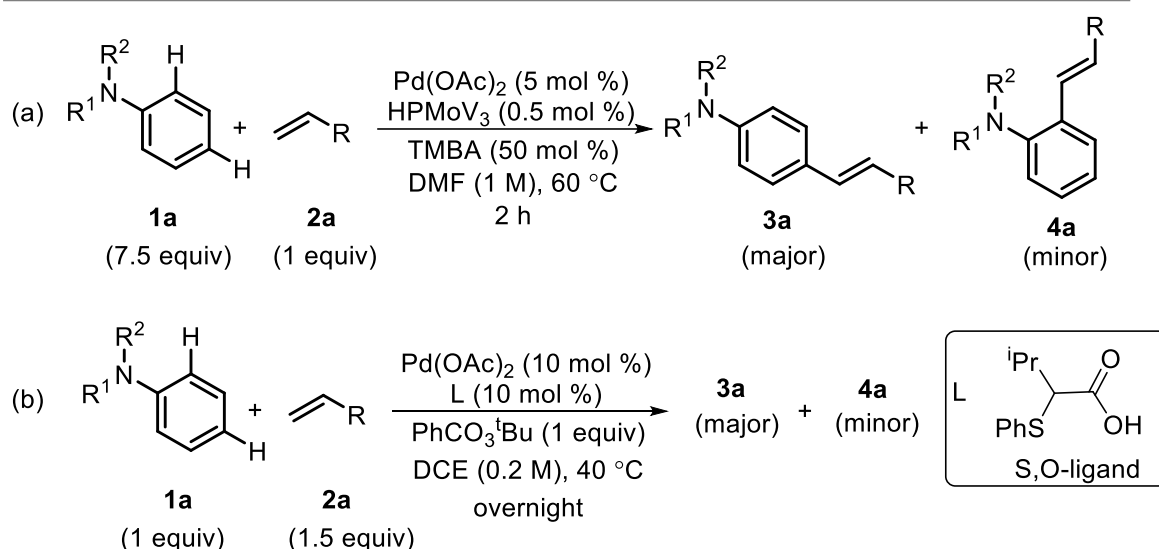
Figure 1.3: Palladium catalysed non-directed C-H functionalization

consequence of using sterically bulky TMB (trimethyl benzoate) ligand with the *ortho* *N,N*-dialkyl unit. Even though they got highly *para*-selective olefination, excess (>7 equiv) of arene must be used to enhance the C-H metalation step,[5] which renders the synthetic applicability of this methodology and hence, unsuitable for large scale

applications.

In the last few decades, significant progress has been made towards the development of a sustainable approach in non-directed C-H activation by tuning the reactivity of the catalyst with the help of diverse ligands. The Naksomboon group observed an enhanced reactivity of a Pd/*S,O*-ligand based catalytic system for a highly *para-* selective olefination (Figure 1.3b).[6] This methodology was found viable with tertiary, secondary, and primary aniline as well. Aniline moiety with electron withdrawing groups also successfully delivered the respective products. More importantly, a better yield, selectivity as well as reactivity was achieved with lower equivalence of aniline **1a**, as compared to Obara's report.
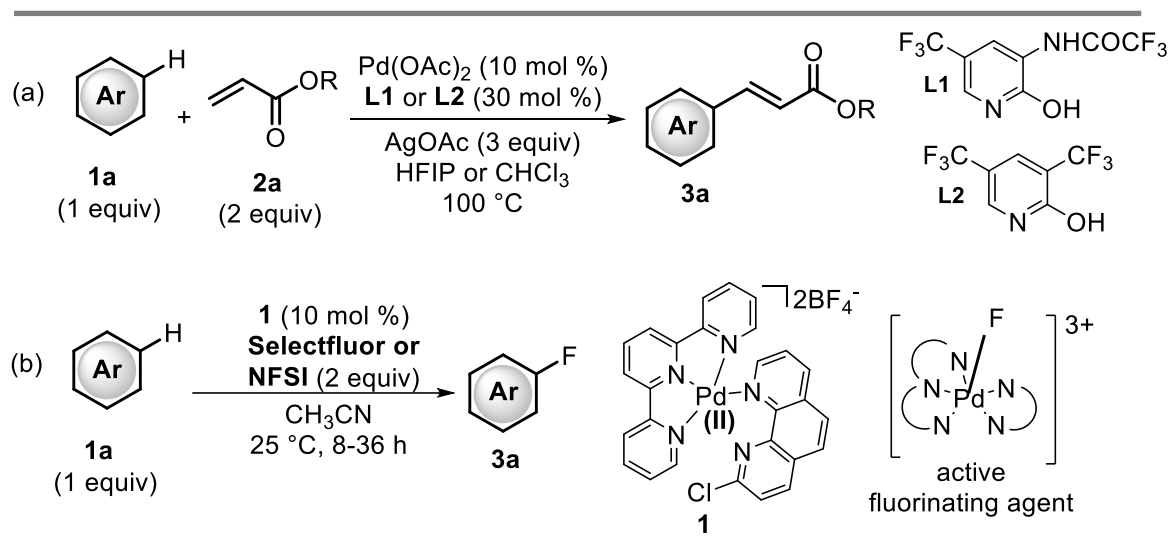
Figure 1.4: Ligand enabled Palladium-catalysed non-directed C-H functionalization

The Yu group discovered an enhanced reactivity of palladium catalyst by using a 2-pyridone ligand. This catalytic system was viable not only with electronically rich arenes, but also with electronically poor arenes (Figure 1.4a). Additionally, arenes with sensitive functional groups such as halogens, ester, and other carbonyl moieties have also been functionalized successfully.[7]

Fluorination of arene ring is one of the valuable transformations among many important functionalizations. It is because the fluorine containing molecules show enhanced activities in agrochemicals and pharmaceuticals.[8] By increasing the electrophilicity of fluorinating agent with the help of a reactive, high valent Pd-intermediate, the Ritter group has successfully performed fluorination on an arene ring via an electrophilic substitution reaction (Figure 1.4b).[9] In a similar way, by taking the advantages of acidic proton, there are several reports on non-directed C-H functionalizations for constructions of C-C/C-X bonds.[10]

Limitations of non-directed C-H functionalizations: Even though there are many reports on non-directed functionalization of inert C-H bonds, the reports are associated with common limitations such as:

(i) Functionalizations are highly biased with electronically rich arenes or reactive atom (i.e, electronically poor arenes are less reactive)

(ii) Regioselectivity of C-H functionalization is entirely controlled by the nature of substituent/functional group present in the (arene) molecule

(iii) Very poor regioselectivity between *ortho*/*para-* functionalization (particularly, when electron donating group is present in the arene ring)

As a solution to the above mentioned issues, directed C-H bond activation has evolved as an emerging methodology, providing highly regioselective functionalizations of inert C-H bond.[11]

1.3 BASICS OF DIRECTED C-H FUNCTIONALIZATION

Substrates bearing coordinating functional groups such as imine, amine, amide, and carbonyl groups, have the ability to coordinate with the transition metals. The coordinating atom (N, O, S, P) chelates the transition metal by donating its free lone pair of electrons to the empty *d*-orbitals of the metal (Figure 1.5). Hence, the substrate now

directs the metal towards the proximal C-H bond and it makes an agostic interaction (a 3c-2e transition state) with the proximal C-H bonds. This agostic interaction arises from the σ-donation by the C-H bond to the empty metal *d*-orbital and backbonding by the metal orbital synergestically. This interaction weakens the inert C-H bond and leads to the formation of an organometallic intermediate with reactive carbon-metal bond. This process is called as directed C-H bond activation. This organometallic species is even more nucleophilic and it can be coupled with a suitable coupling partner for the formation of C-C/C-N/C-O/C-S/C-X bonds.
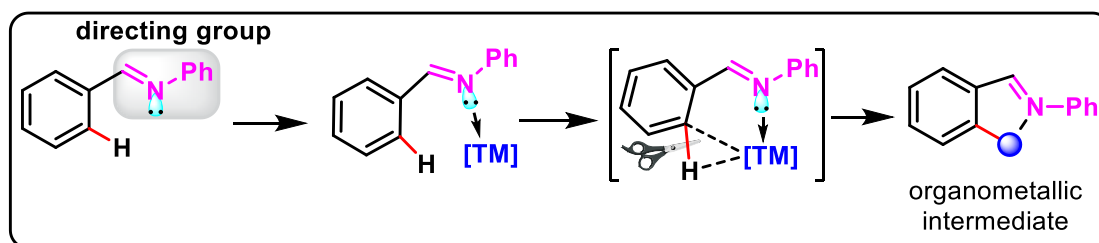
Figure 1.5: Basics of directed C-H activations

The overall process of directed C-H functionalization can be understood from a general catalytic cycle which proceeds through four-stages (Figure 1.6).

Stage-1: As mentioned in the previous section, the active transition metal catalyst chelates with the σ-donor atom of the directing group, which then makes an agostic interaction with the proximal C-H bond (C-H activation process) giving a reactive organometallic intermediate **I** {**C**-[**M**]}.

Stage-2: The intermediate I is functionalized with a secondary substrate (coupling partner) forming intermediate **II**, where both substrate and the coupling partner are bonded with the metal catalyst {**C**-[**M**+**R**]}.

Stage-3: Both the substrate and the coupling partner couple, delivering the final product (**C-R**) and the reduced metal catalyst [**M′**].

Stage-4: Involves catalyst regeneration from the reduced catalyst by copper salts/silver salts/molecular oxygen/organic oxidants.
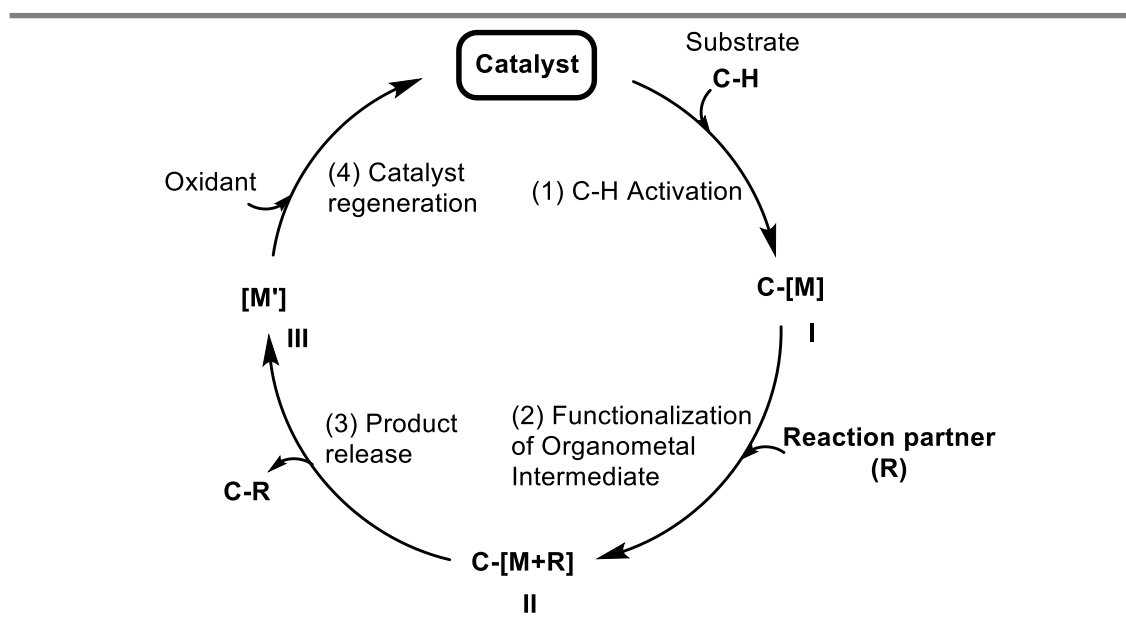
Figure 1.6: General catalytic cycle for directed C-H functionalization

Different mode of C-H activation

Six different modes of C-H bond activations have been documented in the literature.[12]

These are:

(1)   *Oxidative addition* (OA):[13a]
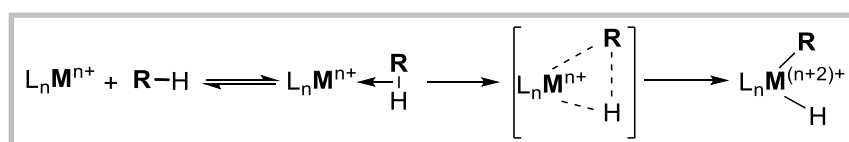
Such type of reactivities are commonly observed with metal catalysts having low a oxidation state M(0) or M(I), which undergoes oxidative insertion into the inert C-H bond. In this process, the oxidation state as well as coordination number of the metal increases by two units.

(2)   *Aromatic electrophilic substitution* (S_EAr):[13b]
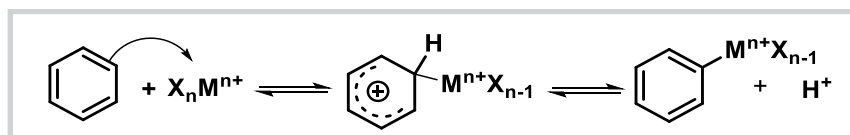
Transition metal catalysts are electron deficient due to the presence of empty *d*-orbitals. Therefore, the catalyst behaves as an electrophile. This metal electrophile can undergo

electrophilic substitution type reaction with electronically rich arene units generating reactive organometallic species.

(3) *σ-Bond metathesis (σBM):*

$$R{-}H + X_nM^{n+}{-}R^1 \longrightarrow \left[\begin{array}{c} X_nM^{n+}\cdots R^1 \\ \vdots \quad\quad \vdots \\ R\cdots H \end{array} \right] \longrightarrow X_nM^{n+}{-}R + R^1{-}H$$
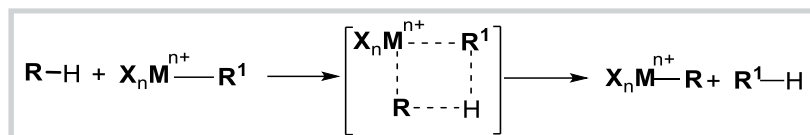
This is a four-membered concerted transition state, where a metal-ligand σ-bond undergoes exchange (metathesis) with the inert C-H bond. After exchange of the ligand, a reactive organometallic species is generated.

(4) *Single electron transfer (SET):*[13c-f]

$$R{-}H + L_nM^{n+} \xrightarrow{SET} L_nM^{(n+1)+}{-}H + R^{\bullet} \xrightarrow{SET} L_nM^{(n+2)+}\begin{array}{c} R \\ H \end{array}$$
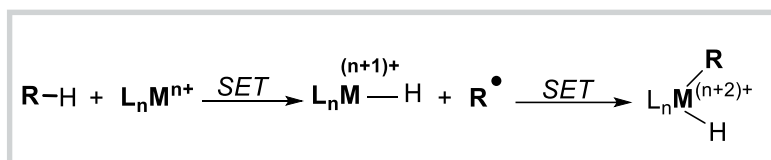
Such reactions are quite general with the catalysts such as Cu, Ni, Mn, and Fe. As transfer of single electron is involved in the mechanism for the generation of organometallic species, formation of the radical intermediate could be confirmed by using radical scavenger.

(5) **Concerted metalation deprotonation (CMD):**[13g]

$$L_nM^{n+}{-}B + R{-}H \longrightarrow \left[\begin{array}{c} L_nM^{n+}\cdots B \\ \vdots \quad\quad \downarrow \\ R\cdots H \end{array} \right] \longrightarrow L_nM^{n+}{-}R + BH$$
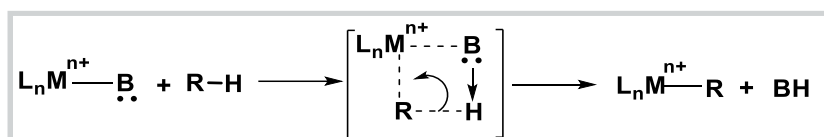
This mechanism is quite similar with *σ*-bond metathesis. Mostly, it is observed with electron-deficient arene substrates in presence of a base. The substrate undergoes metalation and deprotonation in a concerted manner by the help of base and forms carbon-metal bond.

(6) **Base-assisted intramolecular electrophilic substitution (BIES):**[13h]
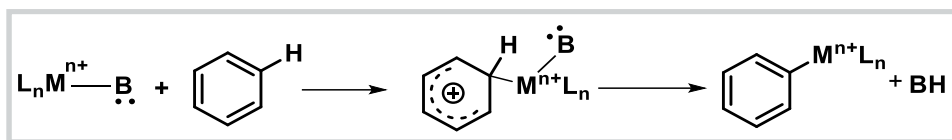
Since this mechanism is of the type of electrophilic substitution on an aromatic ring, it is observed mostly on the electronically rich aromatic ring. Thus, the presence of electron-donating groups favor this mechanism. Additionally, enhanced reactivity is observed by the addition of an additive (base or acid) into the reaction.

1.4 DIRECTING GROUPS AND THEIR CLASSIFICATION (mono/bidentate/ transient/ redox-neutral/ traceless DG)

In chelation assisted C-H functionalization methodology, different functional groups have been used as directing groups (**DG**). Based on the number of chelation sites and reactivities, the directing groups could be classified in to five-catagories.[14] These are:

(i) **Monodentate directing groups** (only one atom chelates the transition-metal):
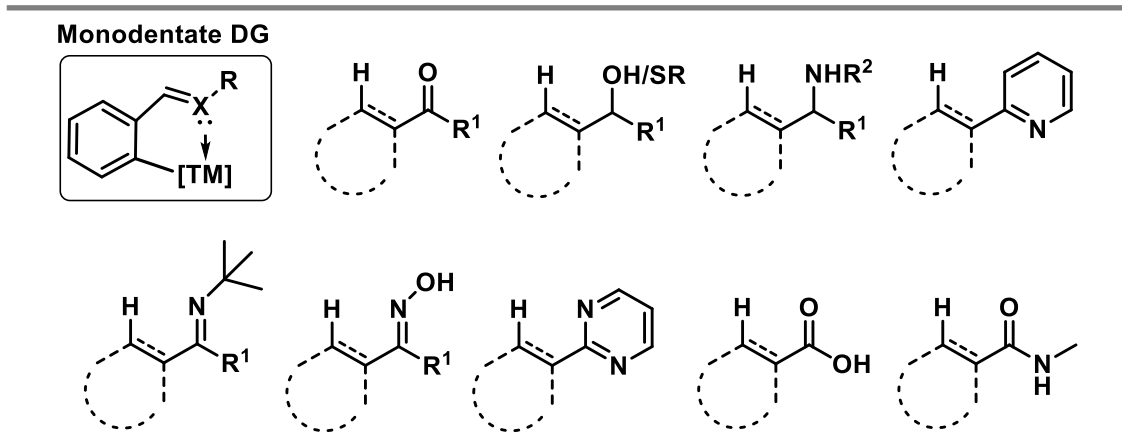
Figure 1.7: Monodentate directing groups

Functional groups such as aldehydes, ketones, alcohols, thiols, amines, and carboxylic acids are used as monodentate directing groups (Figure 1.7). The heteroatom present in this DG chelates with the transition-metal catalyst forming four-six membered metallacycle intermediates.

(ii) **Bidentate directing groups** (two donor atoms chelating the metal atom):

Such directing groups have two chelating sites, therefore the metal catalyst forms a CNN/CNO/CNS-based pincer-type organometallic intermediate after C-H activation (Figure 1.8). These bidentate DGs not only stabilize the intermediate (by the extra chelation) but also, improve the reactivity even in milder reaction conditions for valuable transformations.[14b]

Limitations: In the proximity-driven C-H activation strategy, installation/removal of the directing group to/from the substrate needs extra steps before/after the desired functionalization, which is a drawback of this methodology. In order to avoid the extra steps, transient directed C-H
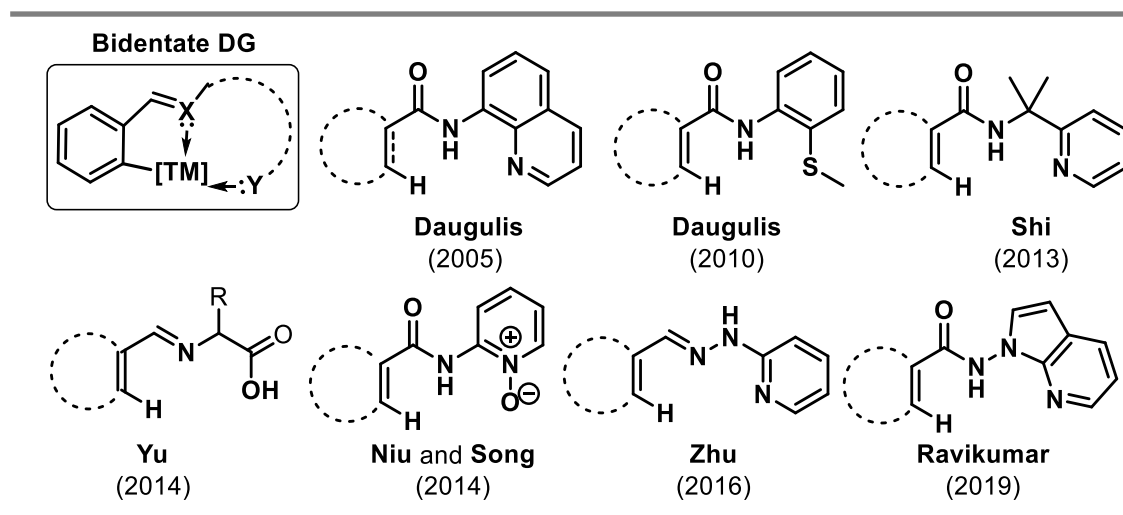
Figure 1.8: Bidentate directing groups

functionalization has emerged as a step economical approach.

(iii)   Transient directing groups (TDGs):

In this advanced concept, the directing group is installed into the substrate reversibly and also is detached after the desired functionalization without any additional steps. This concept has been used extensively with substrates having weak σ-donor DGs (such as phenol or carbonyl groups). Thereby, the transiently installed DG provides a better σ-donor chelation site for binding with the transition metal catalyst. With this strategy, the TDG can be installed with substrates containing alcohol, amine, formyl or

ketone functionalities.[15] In 1985, for the first time, *ortho-* di-deuteration of phenol was reported using a pre-synthesized ruthenium catalyst with a phosphite directing group (Figure 1.9a). Here, the phosphite group acts as a transient directing group via
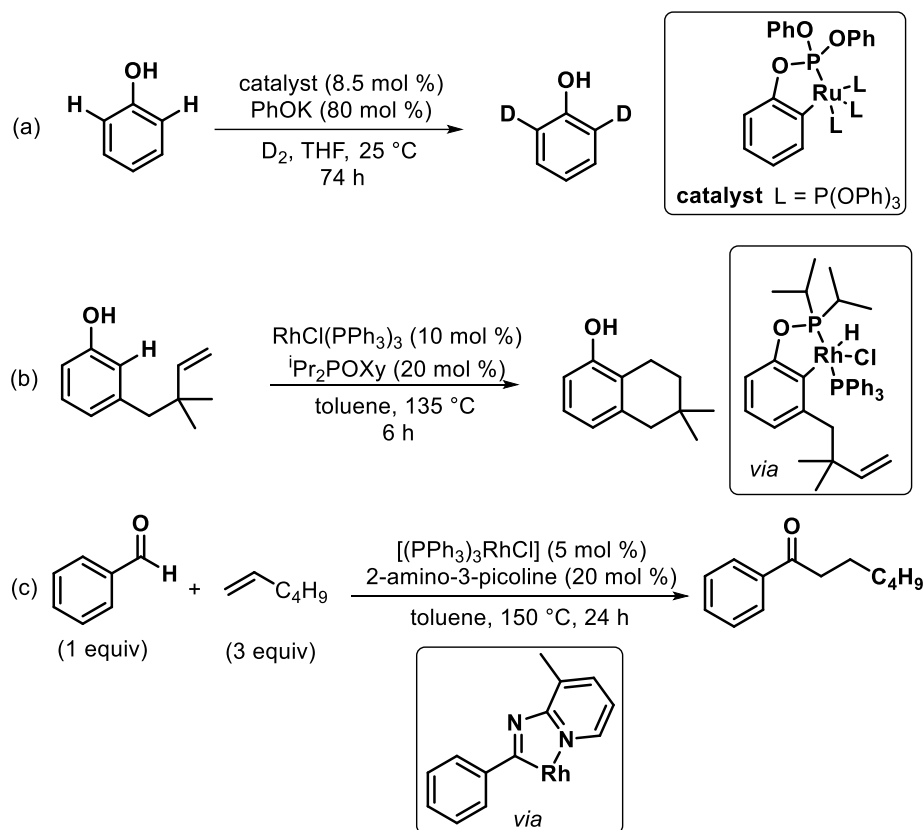
Figure 1.9: C-H functionalizations with transient directing group

transesterification. The use of a catalytic amount of KOPh was found to show better reactivity.[15e] Later in 1985, Lewis and Ellmann revealed the intramolecular *ortho-*alkylation of phenol under rhodium catalysis where *i*-Pr$_2$POXy act as TDG and installed *in situ* forming the active rhodium phosphinite complex followed by intramolecular alkylation with the alkene (Figure 1.9b).[15f] In 1997, Hong *et al.* reported hydroacylation of alkenes with benzaldehyde using 2-amino-3-picoline as TDG and 5 mol % of Wilkinson's catalyst (Figure 1.9c).[15g] 2-Amino-3-picoline undergoes imination with the aldehydic carbonyl group, which binds the active catalyst, activates the C(sp^2)-H bond, and then reacts with alkene to obtain functionalized ketones.

Generally, the carbonyl oxygen atom is considered as a poor σ-donor chelating atom. However, it can be transferred to an imine which can act as a strong directing group. Amino acids are zwitterionic, having both amine (-NH$_2$) and carboxylic (-COOH) groups. Amino acids have been used extensively as TDGs for the functionalization of aliphatic as well as aromatic carbonyl compounds. The pioneering work by the Yu research group for C(sp^3)-H arylation under palladium catalysis has shown the potential of amino acids as TDGs (Figure 1.10).[15h] After this seminal work, chiral amino acids have been also used for asymmetric synthesis under transient catalysis.
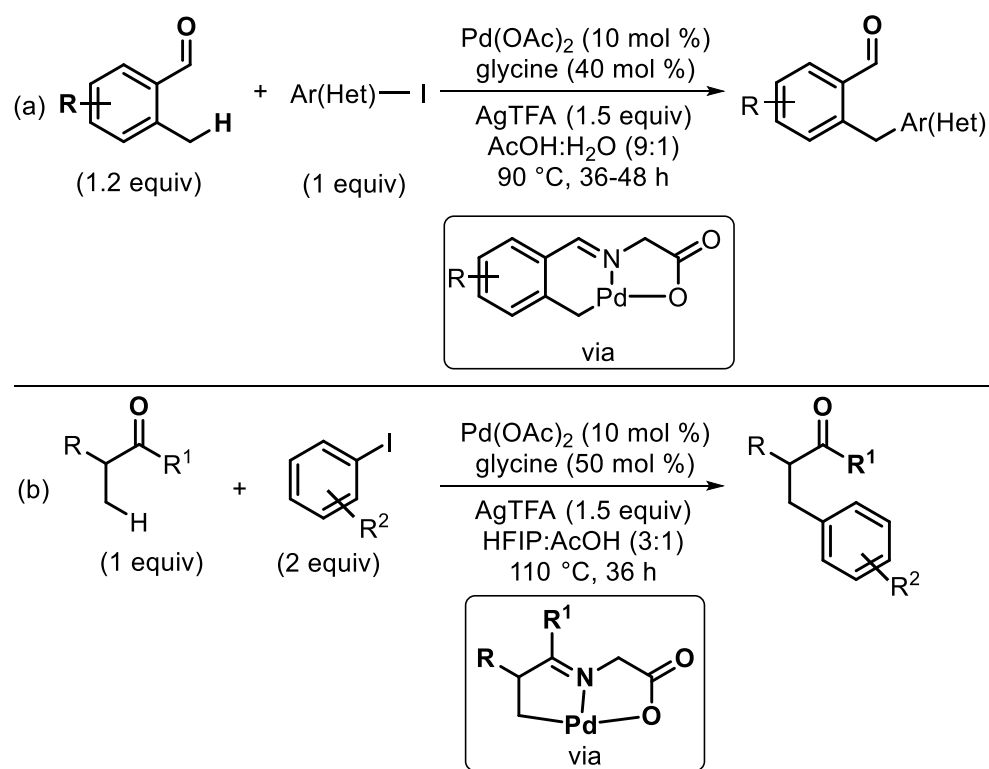
Figure 1.10: Pd-catalysed arylation of C(sp^3)-H bond of carbonyl compounds

Amines are important structural motifs and its compounds are found with agricultural, agrochemical, and pharmaceutical importance. In 2016, the Yu group reported palladium catalysed γ-C(sp^3)-H arylation of aliphatic amine by using 2-hydroxynicotinal-dehyde as TDG (Figure 1.11a).[15i] This TDG was found quite efficient and provided sufficient reactivity and stability to the organo-palladation intermediate

which is reflected from the lower loading of TDG as compared to their previous report (Figure 1.10).
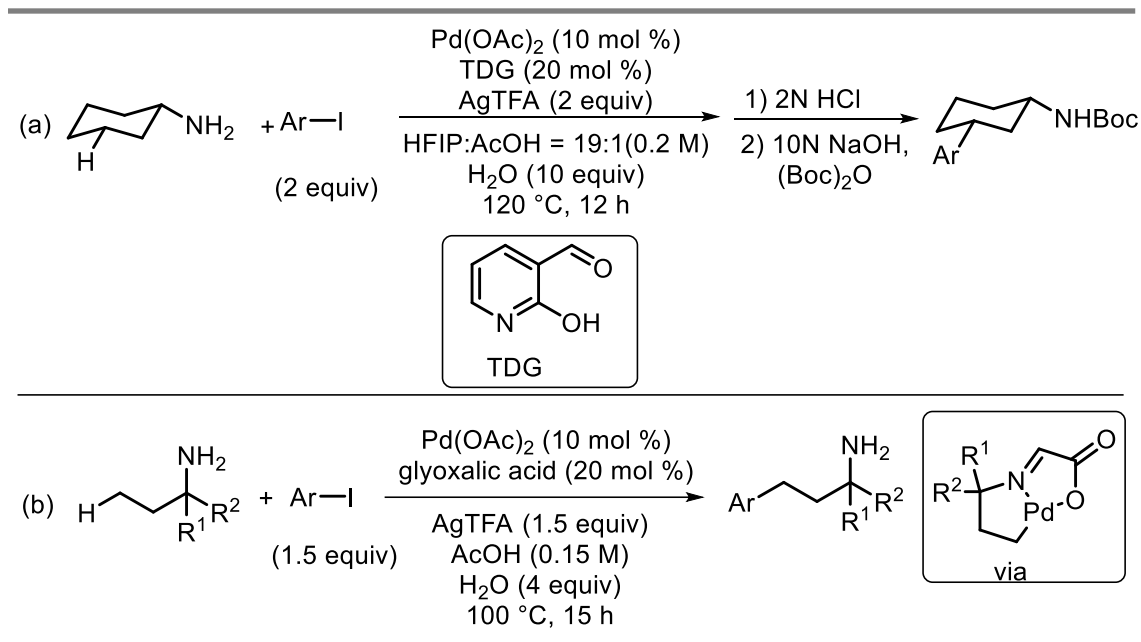
Figure 1.11: Pd-catalysed arylation of C(sp³)-H bond of amines

In the same vein, Liu and co-workers reported γ-C(sp^3)-H arylation of aliphatic acyclic amines using glyoxalic acid as the TDG (Figure 1.11b).[15j] This protocol eliminates extra steps of protection of amine group, and hence provides a straightforward methodology for targeted molecule synthesis.

(iv)   Redox-neutral directing groups:

In   transition   metal-catalysed   coupling   reactions/functionalization,   a stoichiometric amount of external oxidants is required to reoxidize the reduced metal catalyst. Very commonly, copper/silver/organic compounds are used as external oxidants and they produce stoichiometric amounts of their reduced by-products. As a substitute for these external oxidants, researchers have revealed the chemistry of internal oxidants, where organic compounds containing weak bonds such as N-O/N-N/N-Cl/N-S/S-Cl/Si-H have been used as internal oxidants.[16a,b] Therefore, chemists are using directing groups with weak bonds, and such directing groups are known as redox-neutral directing groups (DG^{ox}). In the last two decades, many types of redox-neutral directing group have been

used for valuable transformations.[16c] The commonly used redox-neutral directing groups

are as follows:
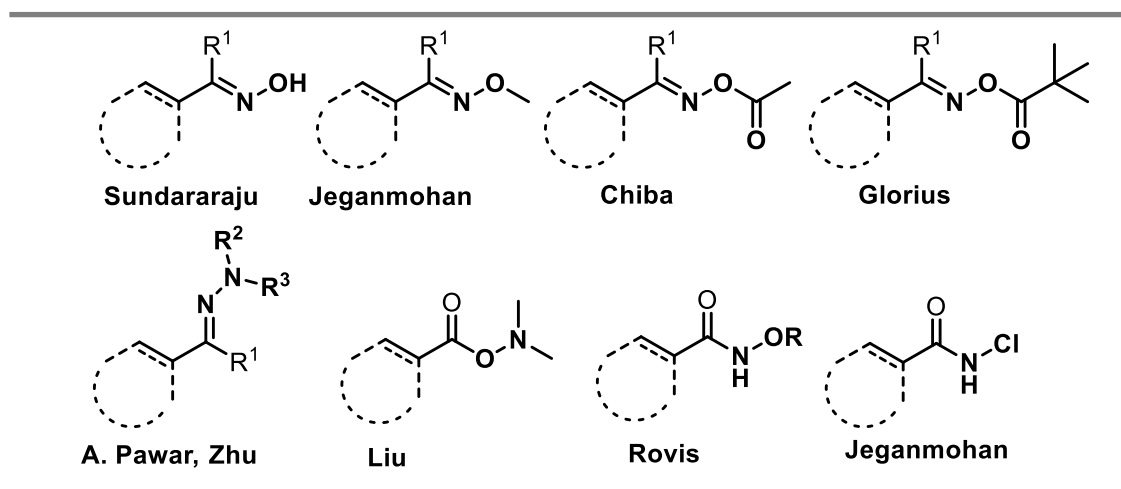
Figure 1.12: Commonly used DG^{ox}

For an example, Fagnou and coworkers have reported an imine directed, Cp*Rh-catalysed

isoquinoline synthesis by the [4+2] annulation of alkyne and aldimine where 2.1
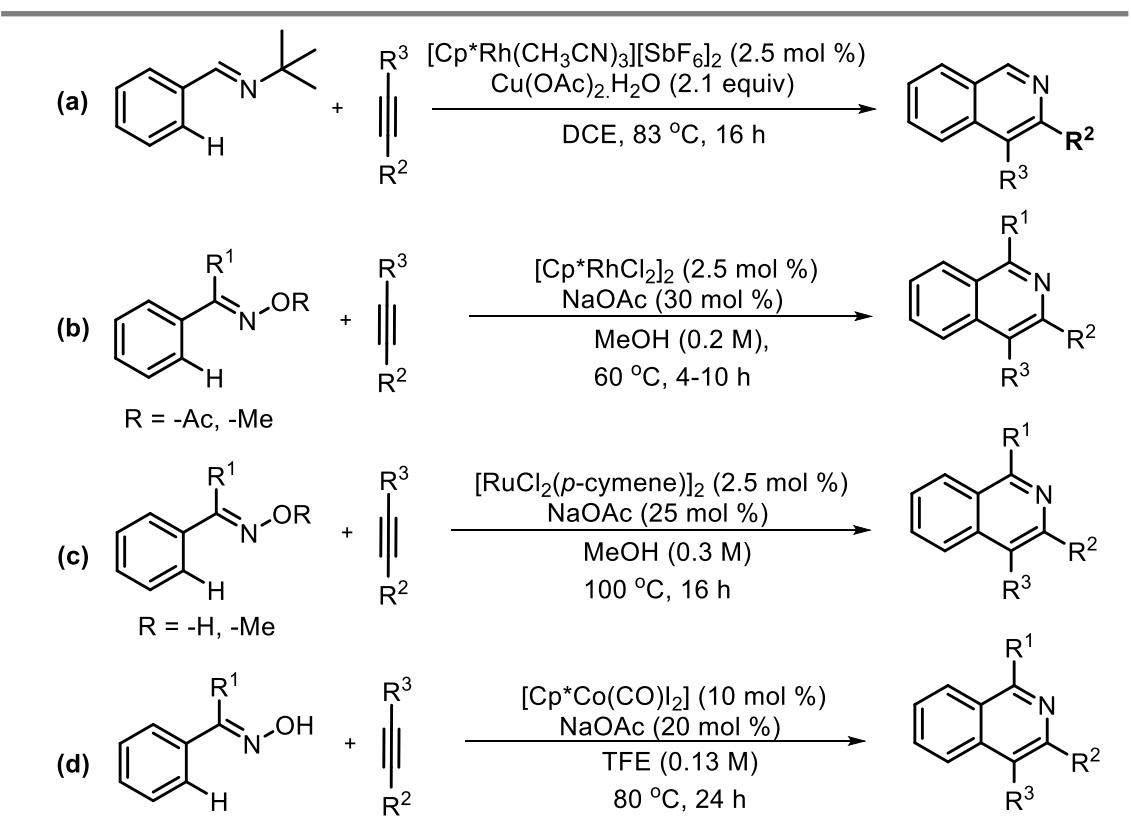
Figure 1.13: Isoquinoline synthesis using DG^{ox}

equivalents of Cu(OAc)$_2$.H$_2$O have been used as oxidant (Figure 1.13a).[16d] Researchers

have achieved isoquinoline synthesis using various types of redox-neutral directing

groups, obviating the use of external metal oxidants. In this context, Chiba,[16e] Jeganmohan,[16f] and Sundararaju[16g] research groups have reported isoquinoline synthesis with N-O bond-containing redox-neutral directing groups under Rh, Ru, and Co catalytic conditions respectively (Figure 1.13, b-d).

(v) **Traceless directing groups**:

In directed C-H functionalization strategies, after getting the desired functionalization, the DG either stays in the product as a non-removable DG or additional steps are required for its removal from the product. Either of these limits the scope of structural diversities of product. In last decade, many functionalizations are achieved by traceless directing group strategies wherein, C-H functionalization and DG removal are achieved in a one-pot fashion. This methodology became the most ideal in directed C-H
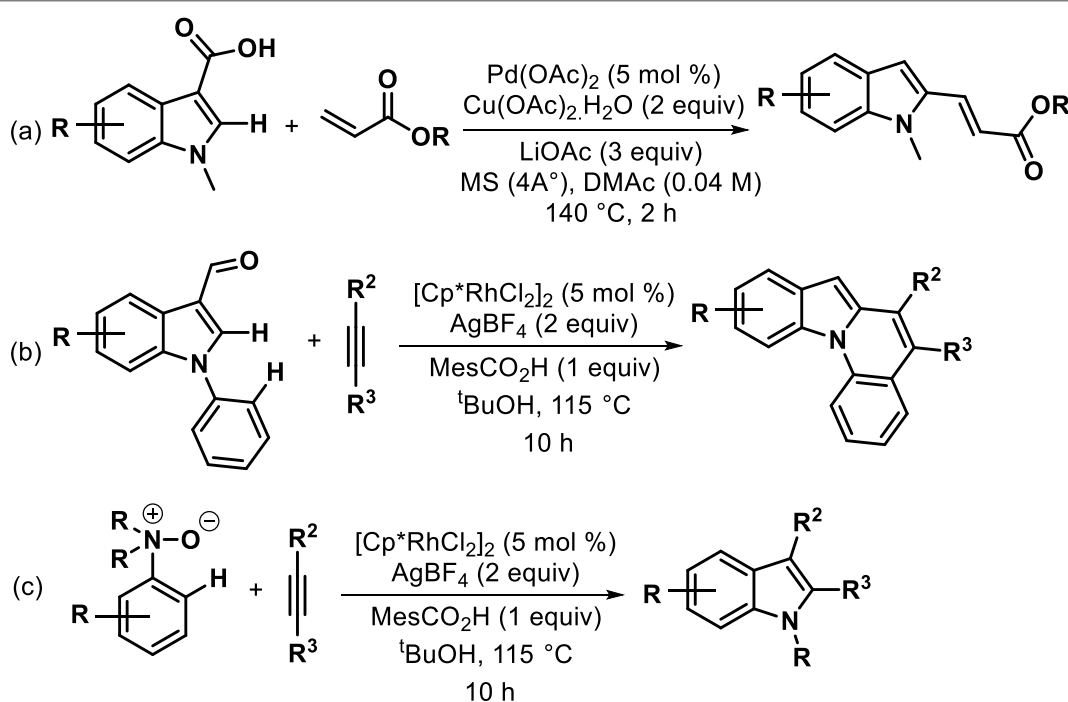
Figure-1.14: Use of traceless DG for various transformations

functionalization strategy. Functional groups such as carboxylic acid, formyl group, sulfoxonium ylides, *N*-oxides *etc*. have been used as traceless DG for different transformations.[17] In last decades, Miura,[17b] Yu,[17c] and Wang[17d] research groups have

reported various transformations independently by using carboxylic acid, formyl group and *N*-oxide as traceless DG (Figure-1.14).

1.5. CONCLUSION

In this chapter, we have discussed the functionalizations of a covalent bond by traditional organic approaches and then Pd-catalysed cross coupling reactions. The need of preactivated starting materials were the major limitations of Pd-catalysed cross-coupling reactions, which led to the discovery of non-directed C-H functionalizations and this worked well in many transformations. Even though non-directed C-H functionalization is more eco-friendly, it is also associated with major issues such as (i) reactivity is highly biased with electronically rich arenes, and (ii) very poor regioselectivity. These limitations gave birth to directed C-H activation, which is an active research area. Important aspects of directed C-H functionalizations are (i) highly regioselective transformation, (ii) no need of pre-activated bond for coupling, and (iii) it works efficiently, overcoming the inherent electronics of the substrate.

1.6 REFERENCES

1.   Seyferth, D. The Grignard Reagents. *Organometallics* **2009**, *28*, 1598–1605.

2.   (a) Devendar, P.; Qu, R.-Y.; Kang, W.-M.; He, B.; Yang, G.-F. Palladium-Catalysed Cross-Coupling Reactions: A Powerful Tool for the Synthesis of Agrochemicals. *J. Agric. Food Chem.* **2018**, *66*, 8914–8934. (b) Dorel, R.; Grugel, C. P.; Haydl, A. M. The Buchwald–Hartwig Amination After 25 Years. *Angew. Chem., Int. Ed.* **2019**, *58*, 17118–17129. (c) Magano, J.; Dunetz, J. R. Large-Scale Applications of Transition Metal-Catalysed Couplings for the Synthesis of Pharmaceuticals. *Chem. Rev.* **2011**, *111*, 2177–2250.

3.   (a) Fujiwara, Y.; Moritani, I. Aromatic substitution of styrene-palladium chloride complex, *Tetrahedron Lett.* **1967**, *8*, 1119-1122. (b) Fujiwara, Y.; Moritani, I.;

Matsuda, M.; Teranishi, S. Aromatic substitution of styrene-palladium chloride complex. II effect of metal acetate, *Tetrahedron Lett*. **1968**, *9*, 633–636. (c) Fujiwara, Y.; Moritani, I.; Danno, S.; Asano, R.; Teranishi, S. Aromatic substitution of olefins. VI. Arylation of olefins with palladium (II) acetate, *J. Am. Chem. Soc*. **1969**, *91*, 7166–7169.

4. (a) Heck, R. F.; Nolley, J. P. Palladium-catalysed vinylic hydrogen substitution reactions with aryl, benzyl, and styryl halides. *J. Org. Chem.* **1972**, *37*, 2320–2322. (b) Dieck, H. A.; Heck, R. F. Organophosphine palladium complexes as catalysts for vinylic hydrogen substitution reactions. *J. Am. Chem. Soc.* **1972***, 96,* 1133-1136*.

5. Mizuta, Y.; Obora, Y.; Shimizu, Y.; Ishii, Y. *para*-Selective Aerobic Oxidative C-H Olefination of Aminobenzenes Catalysed by Palladium/Molybdovanadophosphoric acid/2,4,6-Trimethylbenzoic Acid System. *ChemCatChem* **2012**, *4*, 187-191.

6. Naksomboon, K.; Poater, J.; Bickelhaupt, F. M.; Fernández-Ibáñez, M. Á. *para*-Selective C–H Olefination of Aniline Derivatives via Pd/*S,O*-Ligand Catalysis. *J. Am. Chem. Soc.* **2019**, *141*, 6719–6725.

7. Wang, P.; Verma, P.; Xia, G.; Shi, J.; Qiao, J. X.; Tao, S.; Cheng, P. T.; Poss, M. A.; Farmer, M. E.; Yeung, K.-S. Ligand-accelerated non-directed C−H functionalization of arenes. *Nature* **2017**, *551*, 489-493.

8. (a) Müller, K.; Faeh, C.; Diederich, F. Fluorine in pharmaceuticals: looking beyond intuition Science **2007**, *317*, 1881-1886. (b) Gillis, E. P.; Eastman, K. J.; Hill, M. D.; Donnelly, D. J.; Meanwell, N. A. Applications of Fluorine in Medicinal Chemistry *J. Med. Chem*. **2015**, *58*, 8315–8359.

9.   Yamamoto, K.; Li, J.; Garber, J. A. O.; Rolfes, J. D.; Boursalian, G. B.; Borghs, J. C.; Genicot, C.; Jacq, J.; van Gastel, M.; Neese, F.; Ritter, T. Palladium-catalysed electrophilic aromatic C−H fluorination. *Nature* **2018**, *554*, 511-514.

10.   (a) Xie, J., and Zhu, C. (2016). Recent Advances in Non-directed C(sp^3)-H Bond Functionalization. In Sustainable C(sp^3)-H Bond Functionalization (Springer) (b) Hartwig, J. F., and Larsen, M.A. Undirected, homogeneous C-H bond functionalization: challenges and opportunities. *ACS Cent. Sci*. **2016**, *2*, 281–292. (c) Wong, S.-M.K., and F-Y. (2017). Non-directed CH Bond Functionalizations of (Hetero) arenes. In Strategies for Palladium-Catalysed Non-Directed Directed C-H Bond Functionalization, A. R. Kapdi and D. Maiti, eds. (Elsevier), pp. 49–166. (d) Sommer, H., Julia´-Herna´ndez, F., Martin, R., and Marek, I. Walking metals for remote functionalization. *ACS Cent. Sci*. **2018**, *4*, 153–165. (e) Khake, S. M.; Chatani, N. Nickel-Catalysed C–H Functionalization Using A Non-directed Strategy. *Chem.* **2020**, *6*, 1056–1081. (f) Wedi, P.; van Gemmeren, M. Arene-Limited Nondirected C−H Activation of Arenes. *Angew. Chem., Int. Ed.* **2018**, *57*, 13016–13027.

11.   (a) Godula, K.; Sames, D. C-H Bond Functionalization in Complex Organic Synthesis. *Science* **2006**, *312*, 67–72. (b) Yamaguchi, J.; Yamaguchi, A. D.; Itami, K. C-H Bond Functionalization: Emerging synthetic tools for natural products and pharmaceuticals. *Angew. Chem., Int. Ed*. **2012**, *51*, 8960–9009. (c) McMurray, L.; O'Hara, F.; Gaunt, M. J. Recent developments in natural product synthesis using metal-atalysed C–H bond functionalisation. *Chem. Soc. Rev*. **2011**, *40*, 1885. (d) He, R.; Huang, Z.-T.; Zheng, Q.-Y.; Wang, C. Isoquinoline Skeleton Synthesis *via* Chelation-Assisted C−H Activation. *Tetrahedron Lett.* **2014**, *55*, 5705–5713.

12. (a) Gallego. D.; Baquero E. A. Recent Advances on Mechanistic Studies on C–H Activation Catalysed by Base Metals *Open. Chem.* **2018**, *16*, 1001–1058. (b) Balcells, D.; Clot, E.; Eisenstein, O. C-H Bond Activation in Transition Metal Species from a Computational Perspective. *Chem. Rev.* **2010**, *110*, 749–823.

13. (a) Xavier, E. S.; De Alemeida, W. B.; da Silva, J. C. S.; Rocha, W. R. C-H Bond Activation of Methane Promoted by (η^5-Phospholyl)Rh(CO)$_2$: A Theoretical Perspective *Organometallics* **2005**, *24*, 2262. (b) Myers, A. G.; Tanaka, D.; Mannion, M. R. Development of a decarboxylative palladation reaction and its use in a Heck-type olefination of arene carboxylates. *J. Am. Chem. Soc.* **2002**, *124*, 11250–11251. (c) Zhang, C.; Tang, C.; Jiao, N. Recent advances in copper-catalysed dehydrogenative functionalization via a single electron transfer (SET) process. *Chem. Soc. Rev.* **2012**, *41*, 3464-3484. (d) Ruan, Z.; Ghorai, D.; Zanoni, G.; Ackermann, L. Nickel-catalysed C–H activation of purine bases with alkyl halides. *Chem. Commun.* **2017**, *53*, 9113−9116. (e) Jagtap, R. A.; Verma, S. K.; Punji, B. MnBr$_2$-Catalysed Direct and Site-Selective Alkylation of Indoles and Benzo[h]quinoline. *Org. Lett.* **2020**, *22*, 4643–4647. (f) Jagtap, R. A.; Samal, P. P.; Vinod, C. P.; Krishnamurty, S.; Punji, B. Iron-Catalysed C(sp^2)−H Alkylation of Indolines and Benzo[h]quinoline with Unactivated Alkyl Chlorides through Chelation Assistance. *ACS Catal.* **2020**, *10*, 7312–7321. (g) Lafrance, M.; Rowley, C. N.; Woo, T. K.; Fagnou, K. Catalytic Intermolecular Direct Arylation of Perfluorobenzenes. *J. Am. Chem. Soc*. **2006**, *128*, 8754−8756. (h) C. Tirler and L. Ackermann, Ruthenium(II)-catalysed cross-dehydrogenative CeH alkenylations by triazole assistance *Tetrahedron*, **2015**, 71, 4543-4551.

14. (a) Sambiagio, C.; Schönbauer, D.; Blieck, R.; Dao-Huy, T.; Pototschnig, G.; Schaaf, P.; Wiesinger, T.; Zia, M.; Wencel-Delord, J.; Besset, T.; Maes, B.;

Schnürch, M. A comprehensive overview of directing groups applied in metal-catalysed C–H functionalisation chemistry *Chem. Soc. Rev.* **2018**, *47*, 6603–6743. (b) Rej, S.; Ano, Y.; Chatani, N. Bidentate Directing Groups: An Efficient Tool in C–H Bond Functionalization Chemistry for the Expedient Construction of C–C Bonds. *Chem. Rev.* **2020**, *120*, 1788–1887.

15.   (a) Chen, Y.-Q.; Wang, Z.; Wu, Y.; Wisniewski, S. R.; Qiao, J. X.; Ewing, W. R.; Eastgate, M. D.; Yu, J.-Q. Overcoming the Limitations of γ- and δ-C–H Arylation of Amines through Ligand Development. *J. Am. Chem. Soc.* **2018**, *140*, 17884–17894. (b) Gandeepan, P.; Ackermann, L. Transient Directing Groups for Transformative C−H Activation by Synergistic Metal Catalysis. *Chem.* **2018**, *4*, 199−222. (c) St John-Campbell, S.; Bull, J. A. Transient Imines as "next Generation" Directing Groups for the Catalytic Functionalisation of C–H Bonds in a Single Operation. *Org. Biomol. Chem* **2018**, *16*, 4582–4595. (e) Lewis, L.N. Reexamination of the deuteration of phenol catalysed by an ortho-metalated ruthenium complex. *Inorg. Chem.* **1985**, *24*, 4433–4435. (f) Lewis, J. C., Wu, J., Bergman, R. G., and Ellman, J.A. Preagostic Rh-H interactions and C-H bond functionalization: a combined experimental and theoretical investigation of rhodium (I) phosphinite complexes. *Organometallics.* **2005**, *24*, 5737–5746. (g) Jun, C.-H.; Lee, H.; Hong, J.-B. Chelation-Assisted Intermolecular Hydroacylation: Direct Synthesis of Ketone from Aldehyde and 1-Alkene. *J. Org. Chem.* **1997**, *62*, 1200–1201. (h) Zhang, F.-L.; Hong, K.; Li, T.-J.; Park, H.; Yu, J.-Q. Functionalization of $C(sp^3)$–H Bonds Using a Transient Directing Group. *Science* **2016**, *351*, 252–256. (i) Wu, Y.; Chen, Y.-Q.; Liu, T.; Eastgate, M. D.; Yu, J.-Q. Pd-Catalysed γ-$C(sp^3)$–H Arylation of Free Amines Using a Transient Directing Group. *J. Am. Chem. Soc.* **2016**, *138*, 14554–14557. (j) Liu, Y.; Ge, H.

Site-selective C-H arylation of primary aliphatic amines enabled by a catalytic transient directing group. *Nat. Chem*. **2017**, *9*, 26-32.

16.   (a) Huang, H.; Ji, X.; Wu, W.; Jiang, H. Transition metal-catalysed C–H functionalization of N-oxyenamine internal oxidants *Chem. Soc. Rev.* **2015**, *44*, 1155. (b) Yu, X.-L; Chen, K.-H; Guo, S.; Shi, P.-F.; Song, C.; Zhu, J. Direct access to cobaltacycles *via* C-H activation: *N*-chloroamide-enabled room-temperature synthesis of heterocycles. *Org. Lett.* **2017**, *19*, 5348–5351. (c) Mo, J.; Wang, L.; Liu, Y.; Cui, X. Transition-Metal-Catalysed Direct C–H Functionalization under External-Oxidant-Free Conditions *Synthesis* **2015**, *47*, 439-459. (d) Guimond, N.; Fagnou, K. Isoquinoline Synthesis *via* Rhodium-Catalysed Oxidative Cross-Coupling/Cyclization of Aryl Aldimines and Alkynes. *J. Am. Chem. Soc*. **2009,** *131*, 12050–12051. (e) Too, P. C.; Wang, Y.-F.; Chiba, S. Rhodium (III)-Catalysed Synthesis of Isoquinolines from Aryl Ketone O-Acyloxime Derivatives and Internal Alkynes. *Org. Lett*. **2010**, *12*, 5688–5691. (f) Kiran Chinnagolla, R.; Pimparkar, S.; Jeganmohan, M. Ruthenium-Catalysed Highly Regioselective Cyclization of Ketoximes with Alkynes by C-H Bond Activation: A Practical Route to Synthesize Substituted Isoquinolines. *Org. Lett*. **2012**, *14*, 3032–3035. (g) Sen, M.; Kalsi, D.; Sundararaju, B. Cobalt (III)-Catalysed Dehydrative [4+2] Annulation of Oxime with Alkyne by C-H and N-OH Activation. *Chem. - Eur. J.*, **2015**, *21*, 15529–15533.

17.   Rani, G.; Luxami, V.; Paul, K. Traceless directing groups: a novel strategy in regiodivergent C-H functionalization. *Chem. Commun.* **2020**, *56*, 12479–12521. (b) Maehara, A.; Tsurugi, H.; Satoh, T.; Miura, M. Regioselective C–H Functionalization Directed by a Removable Carboxyl Group: Palladium-Catalysed Vinylation at the Unusual Position of Indole and Related

Heteroaromatic Rings. *Org. Lett.* **2008**, *10*, 1159–1162. (c) Liu, X.; Li, X.; Liu, H.; Guo, Q.; Lan, J.; Wang, R.; You, J. Aldehyde as a Traceless Directing Group for Rh(III)-Catalysed C–H Activation: A Facile Access to Diverse Indolo[1,2-*a*]quinolines. *Org. Lett.* **2015**, *17*, 2936–2939. (d) Li, B.; Xu, H.; Wang, H.; Wang, B. Rhodium-Catalysed Annulation of Tertiary Aniline N-Oxides to N-Alkylindoles: Regioselective C–H Activation, Oxygen-Atom Transfer, and N-Dealkylative Cyclization. *ACS Catal.* **2016**, *6*, 3856–3862.

Chapter 2

Hydroxylamine-*O*-Sulfonic Acid (HOSA) as a Redox–Neutral Directing Group: Rhodium Catalysed, Additive Free, One-Pot Synthesis of Isoquinolines from Arylketones

Chapter 2

Hydroxylamine-*O*-Sulfonic Acid (HOSA) as a Redox–Neutral Directing Group: Rhodium-Catalysed, Additive Free, One-Pot Synthesis of Isoquinolines from Arylketones
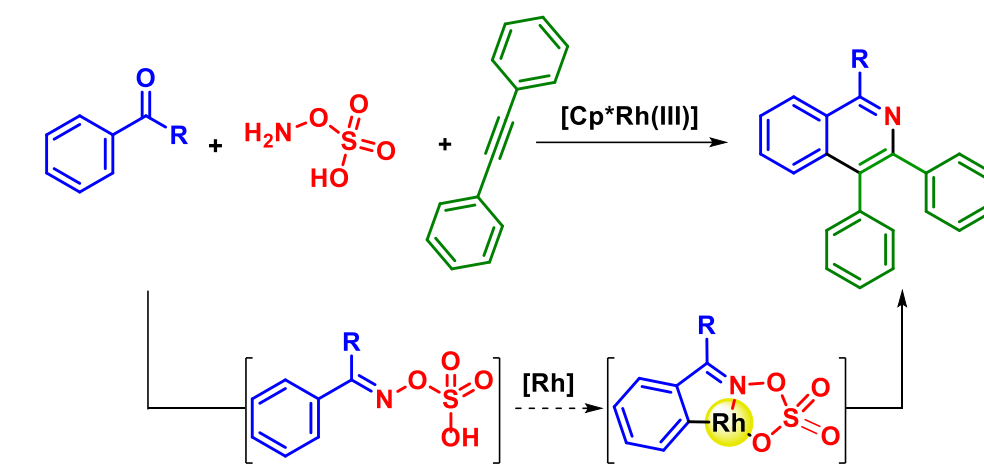
2.1 ABSTRACT: *Herein, a Cp*Rh(III)-catalysed one-pot synthesis of isoquinolines is reported from aryl ketones, alkynes and hydroxylamine-O-sulfonic acid (HOSA). Importantly, an additional application of well-known aminating reagent hydroxylamine-O-sulfonic acid has been discovered as a redox-neutral directing group. This C-H/N-O annulation methodology gives excellent yields even without a silver additive, acid/base or metal oxidant. This is the first report wherein a directing group is simultaneously forming* in situ, *acting as acid additive, and also as an internal oxidant.*

2.2 INTRODUCTION

Transition metal-catalysed C-H bond activation with subsequent functionalization represents a more direct strategy as compared to the traditional synthesis towards the synthesis of pharmaceutically important heterocycles including quinolines and isoquinolines.[1] C-H Bond activation has advantages in terms of atom and step-economical synthetic routes. Nevertheless, it has some limitations, such as the use of stoichiometric

heavy metal oxidants and covalently attached directing groups, which must later be removed, and use of acid or base additives.[2] Hence, there is a need to develop more general and straightforward methods of C-H bond activation in heterocycle synthesis. Discovering a new directing group, which can serve as an effective ligand and in some cases, oxidant, but also balance the required reactivity with selectivity is a challenging task.[3] The Fagnou[4] and Glorius[5] groups have made considerable progress in the development of redox-neutral directing groups (no use of heavy metal oxidant) for the oxidative C-H/N-O annulation of alkynes using Cp*Rh(III) complexes to access isoquinoline/isoquinolone derivatives. Glorius, Sundararaju, Chiba, Jeganmohan and several other groups have independently explored different types of redox neutral directing groups towards the construction of azaheterocycles.[6] However they still needed to use extra acid/base additives and one extra step was required to install the directing group.

In recent years, developing an *in situ*/transient directing group has gained prominence due to step economy. Yu and other groups have explored this *in situ*/transient directing group concept in the Pd(II)-catalysed C-H functionalization by using amino acids as directing groups; however they still needed to use extra acid additive and metal oxidant.[7] Invariably for C-H functionalization reactions involving transient directing groups, acid additives were commonly used to drive the substrate-directing group binding equilibrium.[7] In C-H activation reactions it has been observed that additional acid or base additives are showing positive cooperativity either as a ligand for the cyclometalated intermediate or by making an active catalyst within the reaction.[8] Therefore, discovery of a directing group is needed which can simultaneously act as an *in situ* traceless directing group, substitute for acid additive as well as internal oxidant; this solving all three issues of step economy, use of acid additive, and use of heavy metal oxidant.[9]

Hydroxylamine-*O*-sulfonic acid (HOSA) may correspond to either an electrophilic (NH_2^+ synthon) or a nucleophilic (NH_2^- synthon) reagent depending on the substrates and reaction conditions adopted.[10] Recently, HOSA has been used as a C-H aminating agent for naphthalene and silyl enol ethers in the presence of a transition metal catalyst (Scheme 2.1).[10f, g]

Scheme 2.1 Previous work and our proposals
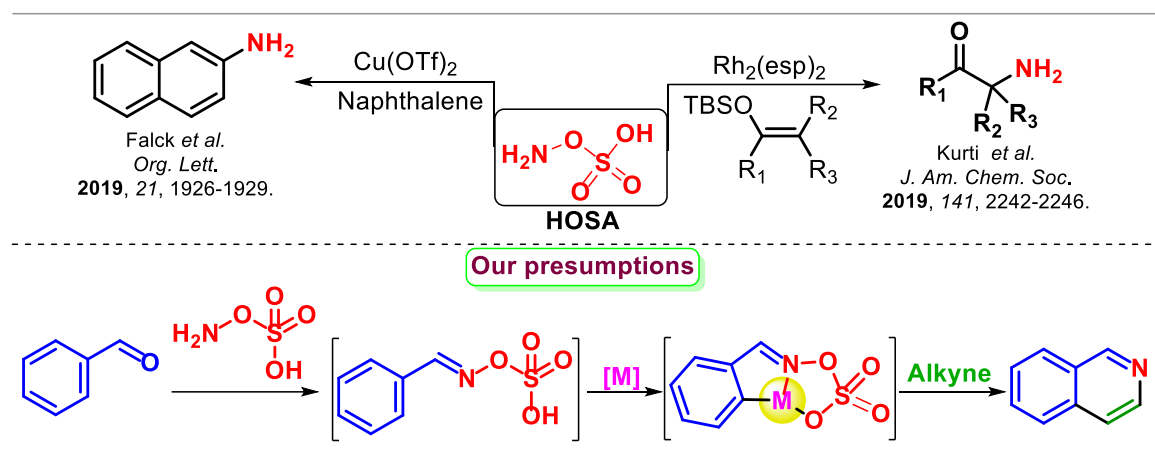
Intrigued by the experimental and computational studies by the Chen group on the importance of neutral and anionic bidentate ligands, as well as weakly coordinating directing groups[11] and the above-mentioned challenges, we hypothesized that HOSA might act as a new redox-neutral directing group for C-H activation. Most importantly, the inherent mild acidity of HOSA might help for *in situ* imination and C-H activation (Scheme 2.1).

2.3 RESULTS AND DISCUSSION

To test our hypothesis, acetophenone **1a** and diphenylacetylene **2a** were investigated as the model substrate and coupling partner respectively. To our satisfaction, when acetophenone **1a** and diphenylacetylene **2a** were treated with HOSA (1.1 equiv) in the presence of 3 mol % of [Cp*RhCl₂]₂ and 1 equivalent of KOAc, the reaction afforded the desired isoquinoline in 30% yield (Table 2.1, entry 1). Hexafluoroisopropanol and

toluene were screened as solvents under the same conditions, but in neither case was any reaction observed (Table 2.1, entries 2-3). Then we changed to various other weak bases such as NaOAc, LiOAc, CsOAc. The use of CsOAc improved the yield up to 61% (Table 2.1, entry 6). Various other catalysts such as [Cp*Co(CO)I$_2$], Co(acac)$_2$, Co(acac)$_3$, and [RuCl$_2$(p-cymene)]$_2$ failed to produce the desired annulated product (Table 2.1, entries 7-

Table 2.1 Optimization for the Cp*Rh-Catalysed One-Pot Synthesis of Isoquinolines[a,b]
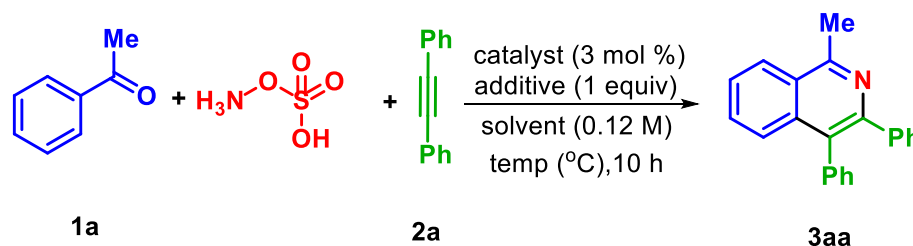
entry	solvent	catalyst	additive	temp (°C)	yield (%)
1	MeOH	[Cp*RhCl$_2$]$_2$	KOAc	100	30
2	HFIP	[Cp*RhCl$_2$]$_2$	KOAc	100	nr
3	Toluene	[Cp*RhCl$_2$]$_2$	KOAc	100	nr
4	MeOH	[Cp*RhCl$_2$]$_2$	NaOAc	100	nr
5	MeOH	[Cp*RhCl$_2$]$_2$	LiOAc	100	13
6	MeOH	[Cp*RhCl$_2$]$_2$	CsOAc	100	61
7	MeOH	[Cp*CoI$_2$]	CsOAc	100	nr
8	MeOH	Co(acac)$_2$	CsOAc	100	nr
9	MeOH	Co(acac)$_3$	CsOAc	100	nr
10	MeOH	[RuCl$_2$ (p-cymene)]$_2$	CsOAc	100	nr
11	MeOH	[Cp*RhL$_3$][SbF$_6$]$_2$	CsOAc	100	80
12	MeOH	[Cp*RhL$_3$][SbF$_6$]$_2$	-	100	90
13	MeOH	[Cp*RhL$_3$][SbF$_6$]$_2$	-	60	63
14	**MeOH**	**[Cp*RhL$_3$][SbF$_6$]$_2$**	**-**	**70**	**92**
15	MeOH	[Cp*RhL$_3$][SbF$_6$]$_2$	-	80	89

[a]Reaction conditions: **1a** (0.10 mmol), **2a** (0.13 mmol), HOSA (0.11 mmol), [Cp*Rh(III)] (3 mol %), additive (1 equiv), solvent (0.1 M), temp (℃), 10 h, L = CH$_3$CN. [b]NMR yield using 1,3,5-trimethoxybenzene as internal standard. nr = no reaction.

10). We presumed that, the use of a reactive cationic Rh-catalyst such as [Cp*Rh(CH₃CN)₃][SbF₆]₂ might enhance the yield. Interestingly, this cationic Rh (III) catalyst afforded the product in 80% yield (Table 2.1, entry 11). To know the influence of extra additive in product yield, we performed a reaction in the absence any additive. Gratifyingly, a considerable improvement of yield was noticed under additive free conditions (Table 2.1, entry 12). For further improvement of product yield, we screened the reaction at different temperatures ranging from 60 °C to 80 °C (Table 2.1, entries 13-15) and achieved excellent yield of 92% at 70 °C. We tested this one-pot protocol using other redox-neutral directing groups but, they gave inferior results, compared with HOSA (Scheme 2.2).

Scheme 2.2 Comparison with reported redox-neutral directing groups[a]
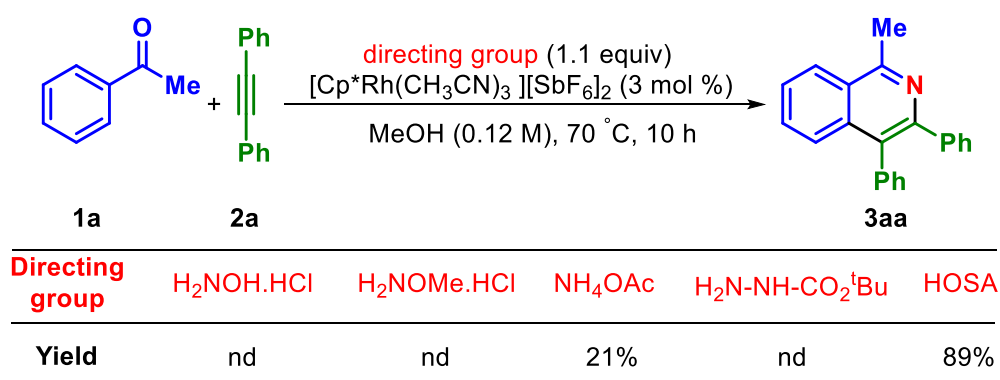
Directing group	H₂NOH.HCl	H₂NOMe.HCl	NH₄OAc	H₂N-NH-CO₂ᵗBu	HOSA
Yield	nd	nd	21%	nd	89%

[a]Reaction conditions: **1a** (0.10 mmol), **2a** (0.13 mmol), HOSA (0.11 mmol), [Cp*Rh(CH₃CN)₃][SbF₆]₂ (3 mol %), MeOH (0.12 M), 70℃, 10 h. nd = not detected.

With the optimized conditions in hand, a variety of electronically different acetophenones was tested using diphenylacetylene as the coupling partner (Scheme 2.3). Except for *ortho*-substituted examples (**3ma**, **3na** and **3oa**), most acetophenones gave isoquinolines in high yield. The poor yields recorded with *ortho*-substituted acetophenones may be due to steric hindrance near to the reaction site. Notably, **1r**, in which the alkoxy- substituent is the part of a dioxolane ring, produced the desired product **3ra** in 71% yield. The cyclic alkoxy- group may be acting as a secondary directing

group.[12] The structure of **3ra** was confirmed by single crystal X-ray analysis. With non-coordinating *meta*-substituents (*m*-Br and *m*-CH₃) the annulated products **3ja** and **3ka** were formed exclusively via the activation from sterically less hindered site. Curiously, with an acetophenone containing the Lewis basic (*m*-OMe) group, a mixture of annulated products **3la** and **3l'a** was obtained in a 53:40 ratio, favouring the formation of the isoquinoline with unfavourable *peri-* interactions between the methoxy- group of the acetophenone and a phenyl substituent of the alkyne. Although the product **3la** suffers from greater steric hindrance than **3l'a** in the intermediate pincer complex, the methoxy-group may act as an additional donor ligand, stabilizing the Rh-complex and favouring activation of the adjacent C-H bond. Halo-substituted acetophenones (**1d-1g** and **1j**) were also compatible with the reaction conditions, producing good to excellent yields of their respective annulated products (**3da-3ja** and **3ga**). Interestingly, the acetophenone **1q**, bearing a free hydroxyl group also reacted efficiently giving **3qa** in 71% yield. Indeed, the optimized conditions worked well with heteroaryl methyl-ketone **3p** giving **3pa** in good yield. Moreover, we have also performed a 1.00 mmol scale reaction, applying the same general procedure, with acetophenone **1a** which resulted in an 87% yield of **3aa**. In addition, the scope of this methodology was evaluated with benzophenones (Scheme 2.3, **3sa-3va**). Both symmetrical and unsymmetrical benzophenones afforded good yields of triaryl-isoquinolines. Especially, in the case of the 4-nitrophenylbenzophenone **3v**, annulation occurred only at the electron-rich phenyl ring of benzophenone, rather than the electron-deficient *para*-nitrophenyl ring, to give **3va** in 70% yield.

To extend the generality of this developed protocol, we further tested the reaction using different alkynes (Scheme 2.4, **3ab-3aj**). Dialkylalkynes (**3ab** and **3ac**), alkyl-aryl alkynes (**3ad-3ah**) and diarylalkynes (**3ai-3aj**) all gave good yields. It is noteworthy that, in the case of alkyl-aryl alkynes, formation of a single regioisomer was observed, where

the aryl ring is oriented towards the heteroatom of isoquinoline.[13] Formation of the

selective

Scheme 2.3 Scope of aryl ketones for one-pot synthesis of isoquinolines[a,b]
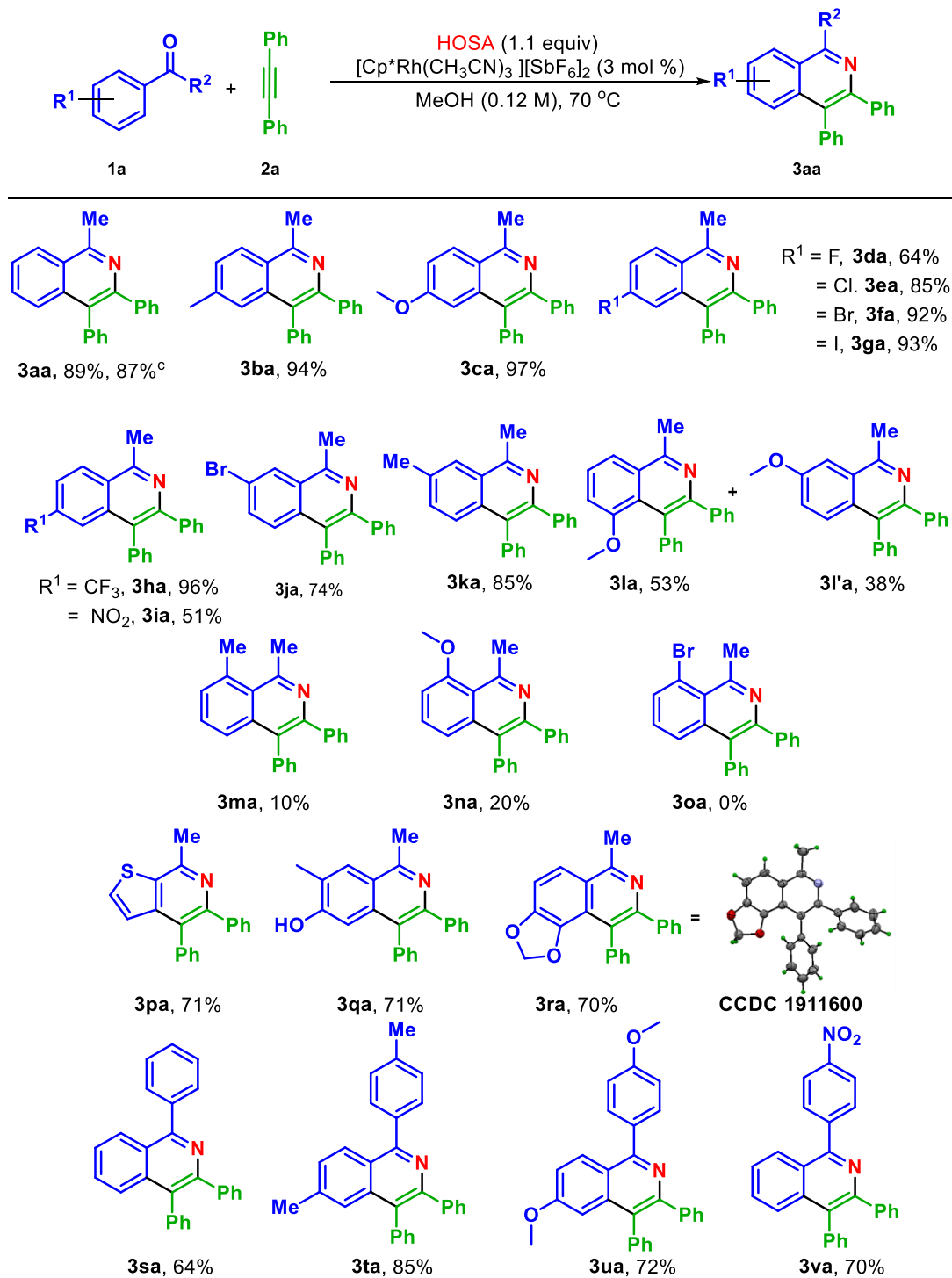
Reaction scheme: 1a + 2a with HOSA (1.1 equiv), [Cp*Rh(CH$_3$CN)$_3$][SbF$_6$]$_2$ (3 mol %), MeOH (0.12 M), 70 °C → 3aa

3aa, 89%, 87%[c]   **3ba,** 94%   **3ca,** 97%   R^1 = F, **3da**, 64%; = Cl. **3ea**, 85%; = Br, **3fa**, 92%; = I, **3ga**, 93%

R^1 = CF$_3$, **3ha**, 96%; = NO$_2$, **3ia**, 51%   **3ja**, 74%   **3ka**, 85%   **3la**, 53%   **3l'a**, 38%

3ma, 10%   **3na**, 20%   **3oa**, 0%

3pa, 71%   **3qa**, 71%   **3ra**, 70%   **CCDC 1911600**

3sa, 64%   **3ta**, 85%   **3ua**, 72%   **3va**, 70%

[a]Reaction conditions: **1a** (0.10 mmol), **2a** (0.13 mmol), HOSA (0.11 mmol), [Cp*Rh(CH$_3$CN)$_3$][SbF$_6$]$_2$ (3 mol %), MeOH (0.12 M), 70°C, 10-20 h. [b]Isolated yield. [c]Isolated yield from 1 mmol scale reaction.

regioisomeric product can be rationalized with the stabilization of the intermediate III (Scheme 2.6) by the phenyl ring through π-interaction with the metal orbitals. Notably, terminal alkynes (trimethylsilylacetylene, phenylacetylene) failed to produce the expected annulated products, possibly due to reaction with Cp*Rh(III) catalyst to produce dimeric alkynes.[14] Similarly, silylalkynes (bis(trimethylsilyl)acetylene, trimethylsilyl phenylacetylene) also failed to produce the expected annulated products, possibly due to reaction with Cp*Rh(III) catalyst to

Scheme 2.4 Coupling partner scope for one-pot synthesis of isoquinolines[a,b]
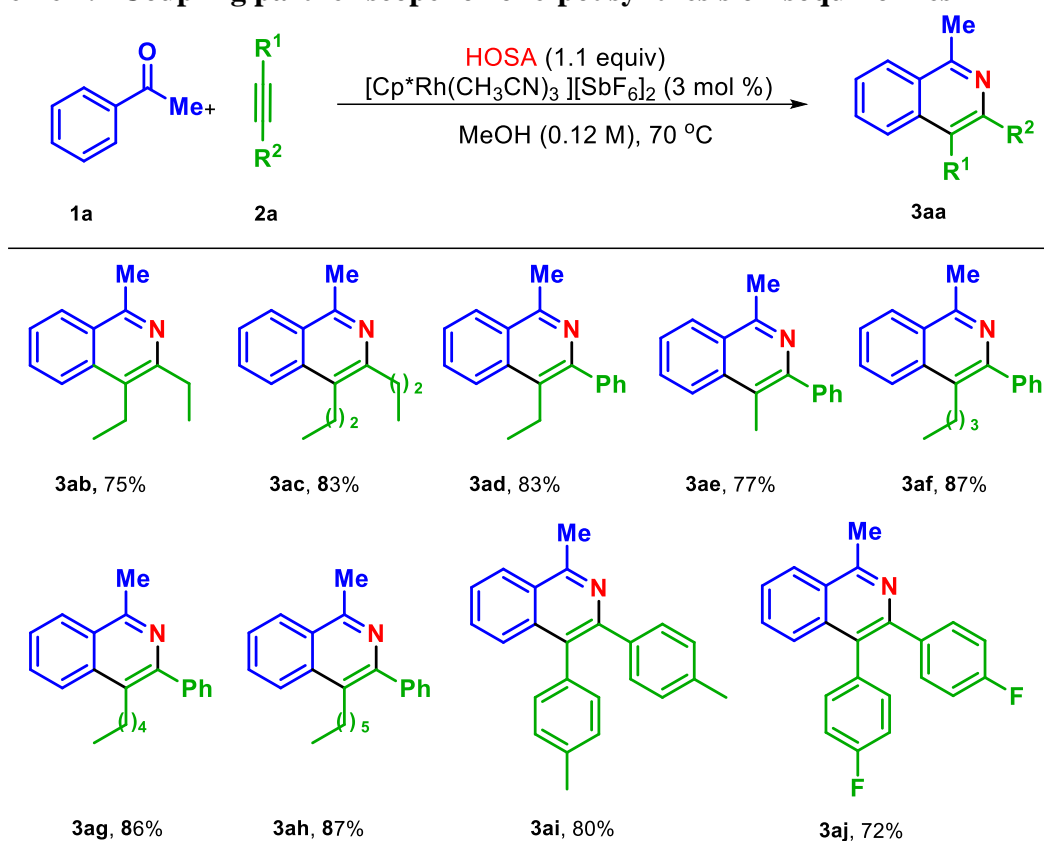
[a]Reaction conditions: **1a** (0.10 mmol), **2a** (0.13 mmol), HOSA (0.11 mmol), [Cp*Rh(CH₃CN)₃][SbF₆]₂ (3 mol %), MeOH (0.12 M), 70 ℃, 10-12 h. [b]Isolated yield.

produce dimeric alkynes.[14] Similarly, silylalkynes (bis(trimethylsilyl)acetylene, trimethylsilyl phenylacetylene) also failed to produce the respective isoquinolines. We presumed that, there may be a protodesilylation pathway operating under the influence of acidic HOSA, which then produces terminal alkynes.

Scheme 2.5 Competitive and mechanistic studies

(a) Intermolecular acetophenone competition:

1c (1 equiv) + 1h (1 equiv)

Ph–≡–Ph 2a (1.3 equiv)

standard conditions

3ca : 3ha = 6.2 : 1

3ca + 3ha
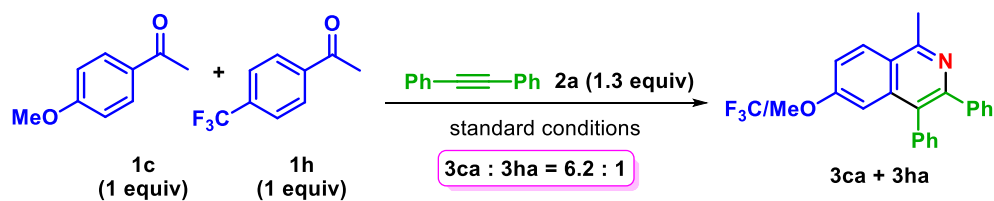
(b) Intramolecular competition (*sp³ vs sp²*):

1w + 2a

standard conditions

3wa, 64%

3w'a, not observed
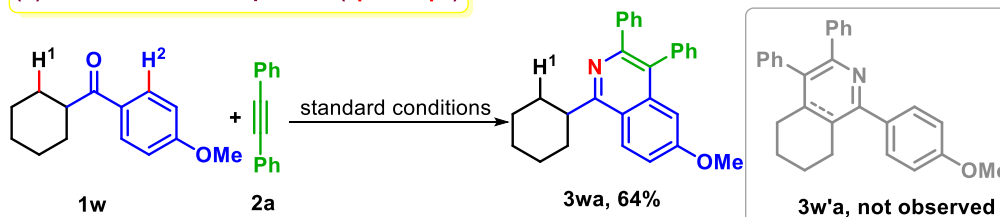
(c) Intermolecular alkyne competition:

1a + 2a + 2b

standard conditions

3aa : 3ab = 1.22 : 1

3aa + 3ab

(d) H/D scrambling experiments:

1a + 2a

HOSA (1.1 equiv)
[Cp*Rh(CH₃CN)₃][SbF₆]₂ (3 mol %)
CD₃OD (10 equiv)
CH₃OH (0.12 M), 70 °C, 30 min

H (100%)

3aa
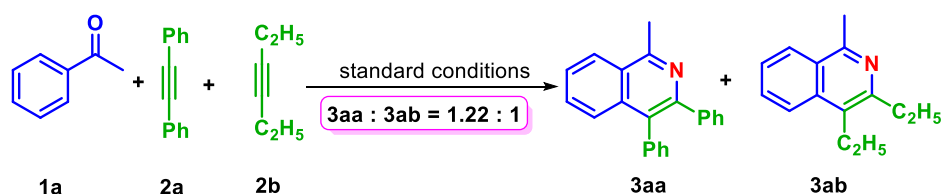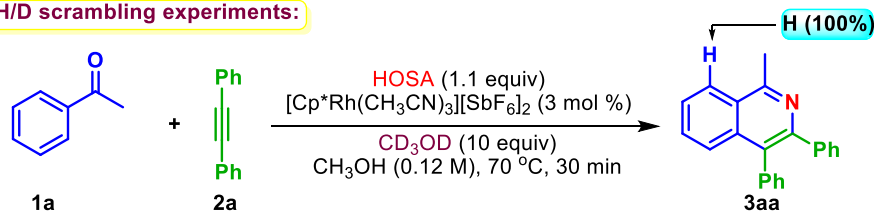
(e) Intramolecular KIE studies:

[D₁]-1a + 2a

HOSA (1.1 equiv)
[Cp*Rh(CH₃CN)₃][SbF₆]₂ (3 mol %)
CH₃OH (0.12 M), 70 °C

KIE = 3.5

D (78%)

[Dn]-3aa, 14%

(f) Intermolecular KIE studies:

1a + [D₅]-1a + 2a

HOSA (1.1 equiv)
[Cp*Rh(CH₃CN)₃][SbF₆]₂ (3 mol %)
CH₃OH (0.12 M), 70 °C

KIE = 5.2

H (84%)

[H₄ + D₄]-3aa, 15%
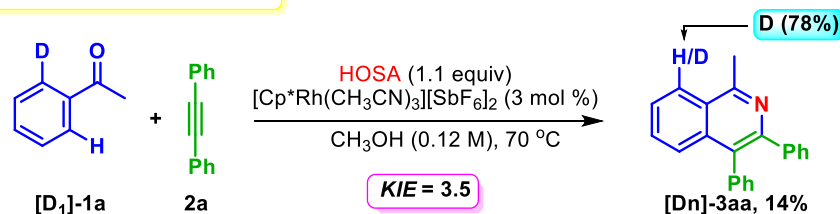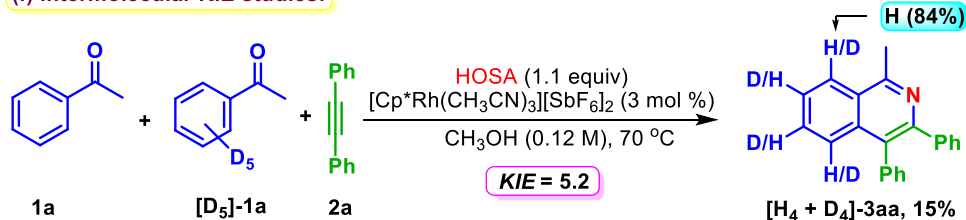
Competitive studies were carried out using a range of acetophenones and alkynes

(Scheme 2.5, a-c) to elucidate how electronics of the substrate influence the reactivity. First, an intermolecular competitive annulation reaction was performed between acetophenones **1c** (*para*-electron donating group) and **1h** (*para*-electron withdrawing group), which produced annulated products **3ca** and **3ha** in a ratio of 6.2:1 (Scheme 2.5, a). This experiment clearly indicates that cyclometallation-deprotonation is faster in electron-rich acetophenone **1c**. This experiment also informs that, under these standard conditions, the substrate is going through an electrophilic substitution mode of C-H activation. Next, an intramolecular competitive study was performed between sp^3-(cyclohexyl) and sp^2-(*para*-methoxyphenyl) C-H bonds, using ketone **1w**. Again, the experiment was conclusive, with **1w** undergoing exclusive sp^2 C-H activation to give **3wa** in 64% yield (Scheme 2.5, b). In an intermolecular competition between diphenylalkyne **2a** and diethylalkyne **2b**, comparable reactivity was observed between the two alkynes, giving their respective annulated products **3aa** and **3ab** in 1.22:1.00 ratio (Scheme 2.5, c).

In order to have a better understanding of the catalytic activity of Cp^*Rh^{2+}, some kinetic experiments were conducted (Scheme 2.5, d-f). Initially, the standard conditions were employed on **1a** with the alkyne **2a** in 10 equiv of methanol-D_4, which showed no *ortho*-deuteriation on **3aa** (Scheme 2.5, d). These results reveal that the C-H activation step is irreversible. Moreover, we observed a kinetic isotope effect for the intra- and intermolecular kinetic experiments to be 3.5 and 5.2 respectively (Scheme 2.5, e and f), suggesting that the initial C-H activation step may be the rate limiting step.[15]

Based on these experimental observations and literature precedents,[6h,11c-d] we proposed a 5-stage catalytic cycle (Scheme 2.6). Initially, the cationic active catalyst, $[Cp^*Rh(MeCN)_3][SbF_6]_2$ undergoes cyclometalation with the *in situ*-generated ketoxime **1a'** to form a five-membered rhodacycle **I**, which after π-complexation with the alkyne

2a, gives intermediate **II**. Next, alkyne insertion occurs to afford the seven-membered rhodacycle **III**, which undergoes subsequent reductive elimination and N-O oxidative insertion to give **IV**. The last step of the catalytic cycle involves regeneration of active catalyst and formation of the desired annulated product **3aa** along with the by-product H_2SO_4. We presume that the acid generated in the final step reacts immediately with the product **3aa** and forms the isoquinolinium salt. Proton NMR spectroscopic analysis of the crude mixture (after filtering through a Celite® pad) showed a downfield shift of the methyl group signal in **3aa**, suggesting the formation of an isoquinolinium salt in the crude mixture.

Scheme 2.6. Proposed catalytic cycle
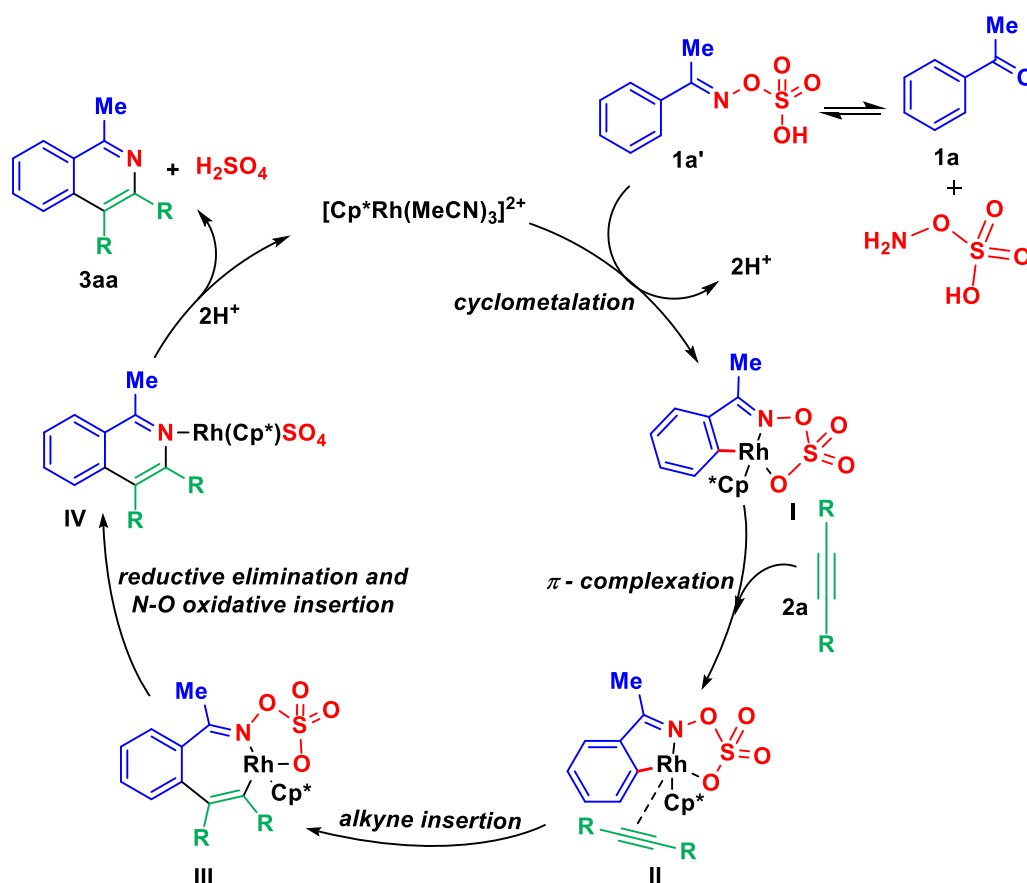
2.4 CONCLUSION

In summary, this is the first time HOSA has ever been used as a redox-neutral directing group for the synthesis of isoquinolines through C-H/N-O annulation from alkynes and the transient ketoxime. Moreover, it is simultaneously acting as an internal oxidant, *in situ* generating a traceless directing group. Owing to these multiple advantages of this reagent, we believe that this reagent has much potential which can be used in various metal-catalysed transformations.

2.5 EXPERIMENTAL SECTION

Acetophenone and benzophenone derivatives were purchased from Sigma Aldrich, Alfa-Aesar, Avra, TCI and Spectrochem and used without further purification. For column chromatography, silica gel (100–200 / 230-400 mesh) from Acme Co. was used. A gradient elution using distilled hexane and ethyl acetate was performed, based on Merck aluminium TLC sheets. All isolated compounds were characterized by ^{1}H NMR, ^{13}C NMR spectroscopy and HRMS. Copies of the ^{1}H NMR, ^{13}C NMR can be found in the Supporting Information. NMR spectra were recorded on Bruker 400 MHz and 700 MHz instruments. All ^{1}H NMR results are reported in parts per million (ppm) relative to the signals for the residual chloroform proton (7.26 ppm) in the deuterated solvent. All ^{13}C NMR spectra are reported in ppm relative to CDCl$_3$ (77.36 ppm).[16] X-ray crystallography was recorded at SCS, NISER, JATNI, BHUBANESWAR, India. [D]$_5$-acetophenone,[6f] [D]$_1$-acetophenone[6f] and [Cp*Rh(CH$_3$CN)$_3$][SbF$_6$]$_2$[17] were prepared by following the literature procedures.

Representative Procedure for the Annulation Reaction:

To an oven-dried 25 mL Schlenk tube charged with a magnetic stirring bar, were added arylketone **1** (0.1 mmol, 1 equiv), dry MeOH (0.1 M, 0.8 mL), hydroxylamine-*O*-Sulfonic acid (0.11 mmol, 1.1 equiv), [Cp*Rh(CH$_3$CN)$_3$][SbF$_6$]$_2$ (0.003 mmol, 0.03 equiv) and alkyne **2** (0.13 mmol, 1.3 equiv) under nitrogen atmosphere sequentially. The reaction mixture was allowed to stir (~500 rpm) at 70 °C in a preheated aluminium block and was monitored by TLC. After completion of the reaction (10-20 h), the reaction mixture was transferred into a 50 mL round bottom flask and the reaction vial was washed twice with ethyl acetate/methanol. The solvent was removed under reduced pressure to give the crude mixture and this was extracted with ethyl acetate (3×10 mL) and washed with saturated NaHCO$_3$. After a brine wash, the organic layer was dried over anhydrous Na$_2$SO$_4$, filtered and then purified by column chromatography using 230-400 mesh silica, giving the product (**3**).

Experimental characterization data of products:

1-Methyl-3,4-diphenylisoquinoline (**3aa**)[6f]:
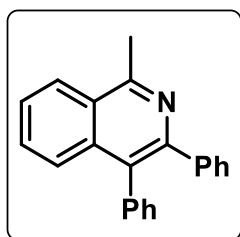
Physical State: White solid (24 mg, 89% yield). **R$_f$** = 0.4 (10% EtOAc/hexane). **mp** 155-157 °C. **^{1}H NMR (CDCl$_3$, 400 MHz):** δ 8.22-8.20 (m, 1H), 7.68-7.66 (m, 1H), 7.61-7.59 (m, 2H), 7.38-7.32 (m, 5H), 7.24-7.17 (m, 5H), 3.09 (s, 3H) ppm.

^{13}C{^{1}H} NMR (CDCl$_3$, 101 MHz): δ 158.1, 149.8, 141.3, 137.9, 136.3, 131.7, 130.6, 130.2, 129.5, 128.5, 127.9, 127.5, 127.3, 126.9, 126.6, 126.5, 125.9, 23.0 ppm. **IR** (KBr, cm^{-1}): 3052, 2957, 2853, 1466. **HRMS (ESI) m/z:** calcd for C$_{22}$H$_{18}$N [M+H]$^+$ 296.1439; found, 296.1439.

1,6-Dimethyl-3,4-diphenylisoquinoline (3ba)[6f]:
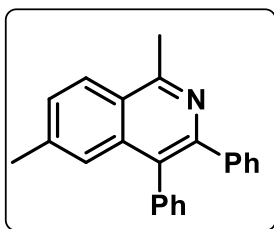
Physical State: White solid (29 mg, 94% yield). R_f = 0.4 (10% EtOAc/hexane). **mp** 168-170 °C. **^{1}H NMR (400 MHz, CDCl$_3$):** δ 8.10 (d, J = 9.2 Hz, 1H), 7.44-7.43 (m, 2H), 7.36-7.34 (m, 5H), 7.23-7.16 (m, 5H), 3.06 (s, 3H), 2.44 (s, 3H) ppm. **^{13}C{^{1}H} NMR (100 MHz, CDCl$_3$):** δ 157.7, 149.8, 141.4, 140.6, 138.0, 136.6, 131.8, 130.6, 129.1, 129.1, 128.5, 127.9, 127.4, 127.2, 125.8, 125.4, 124.9, 22.9, 22.5 ppm. **HRMS (ESI) m/z:** calcd for C$_{23}$H$_{20}$N [M+H]$^+$ 310.1596; found, 310.1595.

6-Methoxy-1-methyl-3,4-diphenylisoquinoline (3ca)[6f]:

Physical State: White solid (32 mg, 98% yield). R_f = 0.6 (20% EtOAc/hexane). **mp** 183-184 °C. **^{1}H NMR (400 MHz, CDCl$_3$):** δ 8.1 (d, J = 9.2 Hz, 1H), 7.36-7.3 (m, 5H), 7.23-7.17 (m, 6H), 6.91 (d, J = 2.8 Hz, 1H), 3.73 (s, 3H), 3.03 (s, 3H) ppm. **^{13}C{^{1}H} NMR (100 MHz, CDCl$_3$):** δ 160.8, 157.3, 150.4, 141.5, 138.3, 138.1, 131.6, 130.5, 128.6, 127.9, 127.7, 127.4, 127.2, 122.2, 119.0, 104.7, 55.5, 22.9 ppm. **HRMS (ESI) m/z:** calcd for C$_{23}$H$_{20}$NO [M+H]$^+$ 326.1545; found, 326.1545.

6-Fluoro-1-methyl-3,4-diphenylisoquinoline (3da)[6f]:
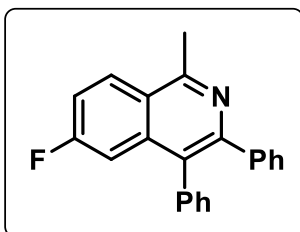
Physical State: White solid (20 mg, 64% yield). R_f = 0.6 (10% EtOAc/hexane). **mp** 140-142 °C. **^{1}H NMR (400 MHz, CDCl$_3$):** δ 8.20 (dd, J = 9.2 Hz, 5.6 Hz, 1H), 7.39-7.32 (m, 6H), 7.29-7.26 (m, 1H), 7.23-7.20 (m, 5H), 3.07 (s, 3H) ppm. **^{13}C{^{1}H} NMR (100 MHz, CDCl$_3$):** δ 164.8, 162.3, 157.8, 150.7, 140.9, 138.4 (d, J = 9.6 Hz), 137.4, 131.5, 130.5, 129.3 (d, J = 5.2 Hz), 128.9 (d, J = 9.5 Hz), 128.7,

128.0, 127.7, 127.5, 123.7, 117.0 (d, J = 25.0 Hz), 110.2 (d, J = 22.1 Hz), 23.1 ppm.

**HRMS (ESI) m/z**: calcd for $C_{22}H_{17}FN$ [M+H]$^+$ 314.1345; found, 314.1347.

6-Chloro-1-methyl-3,4-diphenylisoquinoline (**3ea**)[6f]:
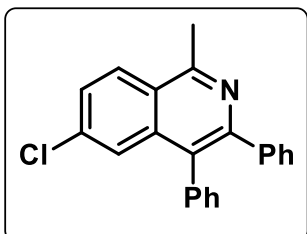
Physical State: White solid (28 mg, 85% yield). R_f = 0.5 (10% EtOAc/hexane). **mp** 179-181°C. **^{1}H NMR (400 MHz, CDCl$_3$)**: δ 8.14 (d, J = 9.2 Hz, 1H), 7.63 (d, J = 2.0 Hz, 1H), 7.53 (dd, J = 8.8 Hz, 2.0 Hz, 1H), 7.38-7.34 (m, 5H), 7.22-7.17 (m, 5H), 3.06 (s, 3H) ppm. **^{13}C{^{1}H} NMR (100 MHz, CDCl$_3$)**: δ 158.0, 150.9, 140.9, 137.5, 137.2, 136.7, 131.6, 130.5, 128.8, 128.7, 128.0, 127.8, 127.78, 127.7, 127.5, 125.5, 124.7, 23.0 ppm. **HRMS (ESI) m/z**: calcd for $C_{22}H_{17}ClN$ [M+H]$^+$ 330.1044; found, 330.1037.
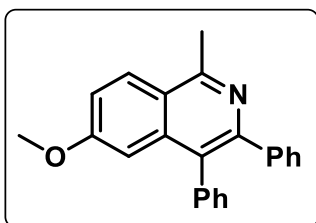
6-Bromo-1-methyl-3,4-diphenylisoquinoline (**3fa**)[6f]:
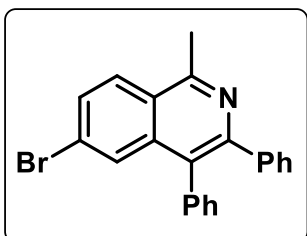
Physical State: White solid (36 mg, 96% yield). R_f = 0.4 (10% EtOAc/hexane). **mp:** 183-185 °C. **^{1}H NMR (400 MHz, CDCl$_3$)**: δ 8.06 (d, J = 4.8 Hz, 1H), 7.8 (s, 1H), 7.66 (dd, J = 5.2 Hz, 2.0 Hz, 1H), 7.37-7.34 (m, 5H), 7.21-7.18 (m, 5H), 3.06 (s, 3H) ppm. **^{13}C{^{1}H} NMR (100 MHz, CDCl$_3$)**: δ 158.1, 150.9, 140.9, 137.7, 137.1, 131.6, 130.5, 130.3, 128.74, 128.7, 128.6, 128.0, 127.8, 127.6, 127.5, 125.4, 124.9, 23.0 ppm. **HRMS (ESI) m/z**: calcd for $C_{22}H_{17}BrN$ [M+H]$^+$ 374.0544; found, 374.0552. **m/z**: [M+H]$^+$ calcd for $C_{22}H_{17}Br^{81}N$ 376.0521; found, 376.0533.

6-Iodo-1-methyl-3,4-diphenylisoquinoline (**3ga**):

Physical State: White solid (39 mg, 93% yield). R_f = 0.5 (10% EtOAc/hexane).

mp 189-191°C. **^{1}H NMR (400 MHz, CDCl$_3$)**: δ 8.04 (s, 1H), 7.90 (d, J = 8.8 Hz, 1H), 7.85 (d, J = 8.8 Hz, 1H), 7.36-7.33 (m, 6H), 7.21-7.18 (m, 5H), 3.04 (s, 3H) ppm. **^{13}C{^{1}H} NMR (100 MHz, CDCl$_3$)**: δ 158.2, 150.8, 140.9, 137.8, 137.1, 135.7, 135.4, 131.6, 130.5, 128.7, 128.3, 128.0, 127.8, 127.5, 127.3, 125.2, 98.0, 23.9 ppm. **HRMS (ESI) m/z**: calcd for C$_{22}$H$_{17}$IN [M+H]$^+$ 422.0400; found, 422.0405.

6-(Trifluoromethyl)-1-methyl-3,4-diphenylisoquinoline (**3ha**)[6f]:
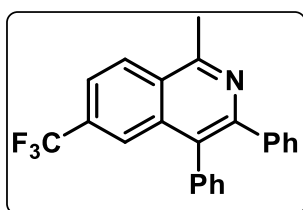
Physical State: White solid (35 mg, 96% yield). **R$_f$** = 0.6 (10% EtOAc/hexane)**. mp** 114-116 °C. **^{1}H NMR (400 MHz, CDCl$_3$)**: δ 8.33 (d, J = 8.8 Hz, 1H), 7.99 (s, 1H), 7.77 (dd, J = 8.4 Hz, 1.2 Hz, 1H), 7.39-7.37 (m, 5H), 7.24-7.21 (m, 5H), 3.12 (s, 3H) ppm. **^{13}C{^{1}H} NMR (100 MHz, CDCl$_3$)**: δ 158.2, 151.2, 140.7, 136.8, 135.8, 132.0, 131.7, 131.6, 130.6, 130.1, 128.8, 128.1, 128.0, 127.7, 127.3, 127.2, 124.2 (q, J = 4.5 Hz), 122.8, 122.5 (q, J = 2.8 Hz), 23.1 ppm. **HRMS (ESI) m/z**: calcd for C$_{23}$H$_{17}$F$_3$N [M+H]$^+$ 364.1308; found, 364.1305.

6-Nitro-1-methyl-3,4-diphenylisoquinoline (**3ia**)[6f]:
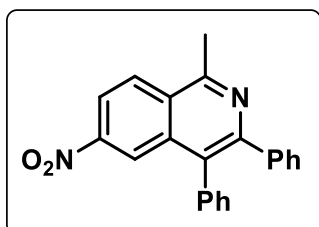
Physical State: Yellow solid (17 mg, 51% yield). **R$_f$** = 0.4 (10% EtOAc/hexane)**. mp** 173-176 °C. **^{1}H NMR (400 MHz, CDCl$_3$)**: δ δ 8.59 (s, 1H), 8.37-8.31 (m, 2H), 7.41-7.37 (m, 5H), 7.23-7.22 (m, 5H), 3.14 (s, 3H) ppm.

^{13}C{^{1}H} NMR (100 MHz, CDCl$_3$): δ 158.4, 151.9, 148.6, 140.2, 136.3, 136.2, 131.5,

130.8, 130.5, 129.1, 128.4, 128.15, 128.1, 128.0, 123.1, 120.3, 23.2 ppm. **HRMS (ESI)**

m/z: calcd for $C_{22}H_{17}N_2O_2$ [M+H]$^+$ is 341.1285; found, 341.1293.

7-Bromo-1-methyl-3,4-diphenylisoquinoline (**3ja**)[6f]:
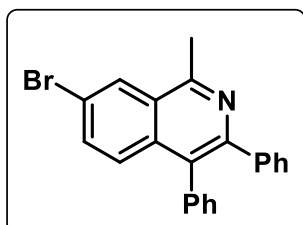
Physical State: White solid (28mg, 74% yield). R_f = 0.55 (10% EtOAc/hexane**). mp:** 132-135 °C. **¹H NMR (400 MHz, CDCl₃):** δ 8.62 (d, J = 1.6 Hz, 1H), 7.55 (dd, J = 9.0 Hz, 1.7 Hz, 1H), 7.45 (d, J = 9.0 Hz, 1H), 7.28-7.25 (m, 5H), 7.12-7.09 (m, 5H), 3.09 (s, 3H) ppm. **¹³C{¹H} NMR (100 MHz, CDCl₃):** δ 157.1, 150.2, 140.9, 137.3, 135.0, 133.6, 131.6, 130.5, 129.4, 128.7, 128.6, 128.2, 127.7, 127.6, 127.5, 120.8, 23.0 ppm. **HRMS (ESI) m/z:** calcd for $C_{22}H_{17}BrN$ [M+H]$^+$ 374.0544; found, 374.0545.
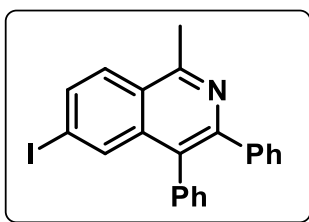
1,7-Dimethyl-3,4-diphenylisoquinoline (**3ka**)[6f]:
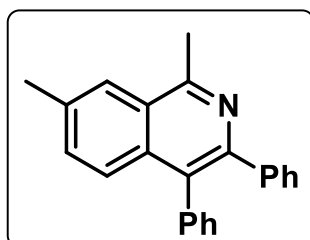
Physical State: White solid (28mg, 90% yield). R_f = 0.4 (10% EtOAc/hexane**). mp** 132-134 °C. **¹H NMR (400 MHz, CDCl₃):** δ 7.89 (s, 1H), 7.48 (d, J = 4.8 Hz, 1H), 7.35 (dd, J = 4.8 Hz, 0.5 Hz, 1H), 7.28-7.22 (m, 5H), 7.14-7.07 (m, 5H), 2.99 (s, 3H), 2.50 (s, 3H) ppm. **¹³C{¹H} NMR (100 MHz, CDCl₃):** δ 157.4, 148.8, 141.1, 138.0, 136.9, 134.6, 132.6, 131.7, 130.6, 129.6, 128.5, 127.9, 127.4, 127.2, 126.7, 126.5, 124.9, 22.9, 22.2 ppm. **HRMS (ESI) m/z:** calcd for $C_{23}H_{20}N$ [M+H]$^+$ 310.1590; found, 310.1583.

5-Methoxy-1-methyl-3,4-diphenylisoquinoline (**3la**)[6a]:

Physical State: White solid (17mg, 53% yield). R_f = 0.6 (20% EtOAc/hexane).

mp 151-153 °C. **^{1}H NMR (400 MHz, CDCl$_3$):** δ 7.8 (d, J = 8.4 Hz, 1H), 7.54 (t, J = 8.0 Hz, 1H), 7.25 (d, J = 6.8 Hz, 2H), 7.19-7.12 (m, 8H), 6.97 (d, J = 7.6 Hz, 1H), 3.4 (s, 3H), 3.06 (s, 3H) ppm. **^{13}C{^{1}H} NMR (100 MHz, CDCl$_3$):** δ 157.4, 157.2, 151.4, 141.9, 141.7, 130.7, 130.6, 128.2, 128.1, 127.8, 127.6, 127.4, 126.8, 125.9, 118.4, 110.4, 55.8, 23.7 ppm. **HRMS (ESI) m/z:** calcd for C$_{23}$H$_{20}$NO [M+H]$^+$ 326.1545; found, 326.1518.

7-Methoxy-1-methyl-3,4-diphenylisoquinoline (**3l'a**)[6a]:

Physical State: White solid (12mg, 38% yield). **R$_f$** = 0.5 (20% EtOAc/hexane). **mp** 116-118 °C. **^{1}H NMR (400 MHz, CDCl$_3$):** δ 7.58 (d, J = 9.2 Hz, 1H), 7.4 (d, J = 2.4 Hz, 1H), 7.37-7.33 (m, 5H), 7.24-7.15 (m, 6H), 3.99 (s, 3H), 3.04 (s, 3H) ppm. **^{13}C{^{1}H} NMR (100 MHz, CDCl$_3$):** δ 158.2, 156.3, 148.1, 148.06, 141.3, 138.0, 131.7, 130.6, 129.5, 128.5, 128.4, 127.9, 127.7, 127.4, 127.1, 122.6, 103.8, 55.8, 23.2 ppm. **HRMS (ESI) m/z:** calcd for C$_{23}$H$_{20}$NO [M+H]$^+$ 326.1545; found, 326.1548.

1,8-Dimethyl-3,4-diphenylisoquinoline (**3ma**):

Physical State: White solid (6mg, 10% yield). **R$_f$** = 0.6 (10% EtOAc/hexane). **mp** 121-123 °C. **^{1}H NMR (400 MHz, CDCl$_3$):** δ 7.49 (d, J = 7.2 Hz, 1H), 7.38-7.30 (m, 7H), 7.20-7.10 (m, 5H), 3.24 (s, 3H), 3.0 (s, 3H) ppm. **^{13}C{^{1}H} NMR (100 MHz, CDCl$_3$):** δ 158.0, 148.9, 141.2, 138.6, 138.4, 136.3, 131.8, 130.52, 130.5, 129.8, 129.5, 128.5, 127.9, 127.5, 127.4, 127.3, 125.4, 30.0, 26.3 ppm. **HRMS (ESI) m/z:** calcd for C$_{23}$H$_{20}$N [M+H]$^+$ 310.1590; found, 310.1582.
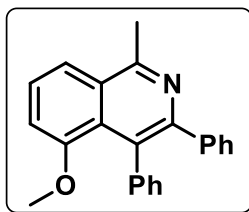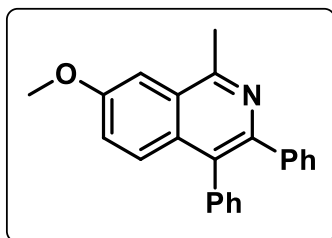
8-Methoxy-1-methyl-3,4-diphenylisoquinoline (3na)[6a]:

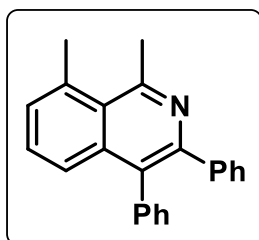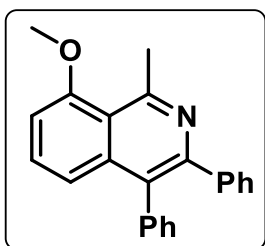**Physical State:** White solid (7mg, 20% yield). R_f = 0.5 (10% EtOAc/hexane). **mp** 149-151 °C. **^{1}H NMR (400 MHz, CDCl$_3$):** δ 7.44 (t, J = 8.0 Hz, 1H), 7.37-7.3 (m, 5H), 7.22-7.16 (m, 6H), 6.90 (d, J = 7.6 Hz, 1H), 4.02 (s, 3H), 3.22 (s, 3H) ppm. **^{13}C{^{1}H} NMR (100 MHz, CDCl$_3$):** δ 158.5, 157.8, 149.8, 141.3, 139.2, 138.5, 131.8, 130.5, 130.4, 128.7, 128.5, 127.9, 127.3, 127.2, 119.4, 118.7, 106.7, 55.9, 29.6 ppm. **HRMS (ESI) m/z:** calcd for C$_{23}$H$_{20}$NO [M+H]$^+$ is 326.1539; found, 326.1541.

7-Methyl-4,5-diphenylthieno[2,3-c]pyridine (3pa)[6e]:
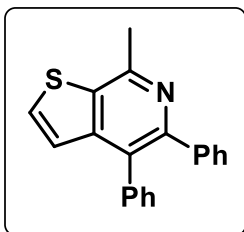
Physical State: White solid (21 mg, 71% yield). R_f = 0.6 (10% EtOAc/hexane). **mp:** 153-155 °C. **^{1}H NMR (400 MHz, CDCl$_3$):** δ 7.53 (d, J = 5.4 Hz, 1H), 7.29-7.26 (m, 5H), 7.17-7.11 (m, 6H), 3.84 (s, 3H) ppm. **^{13}C{^{1}H} NMR (100 MHz, CDCl$_3$):** δ 151.7, 151.2, 146.1, 140.6, 138.5, 134.6, 131.4, 130.9, 130.7, 128.6, 128.6, 128.1, 127.5, 127.46, 124.6, 23.9 ppm. **HRMS (ESI) m/z:** calcd for C$_{20}$H$_{16}$NS [M+H]$^+$ 302.0998; found, 302.0996.

1,7-Dimethyl-3,4-diphenylisoquinolin-6-ol (3qa):
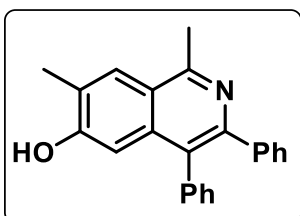
Physical State: White solid (23 mg, 71% yield). R_f = 0.7 (30% EtOAc/hexane). **mp** 157-159 °C. **^{1}H NMR (400 MHz, CDCl$_3$ + DMSO-d$_6$):** δ 9.1 (br, 1H), 7.90 (s, 1H), 7.29-7.25 (m, 4H), 7.23-7.18 (m, 3H), 7.1-7.16 (m, 3H), 6.90 (s, 1H), 2.96 (s, 3H), 2.43 (s, 3H) ppm. **^{13}C{^{1}H} NMR (175 MHz, CDCl$_3$ + DMSO-d$_6$):** δ 158.3, 156.4, 149.0, 141.5, 138.8, 137.1, 131.7, 130.5, 128.7, 128.3, 128.0, 127.7, 127.3, 126.9,

121.7, 107.2, 22.6, 17.2 ppm. **IR (neat)**: 3439, 3054, 2989, 2924, 2855, 2305, 1613, 1554, 1516, 1384, 1263, 1165, 898, 741,700 cm^{-1}. **HRMS (ESI) m/z**: calcd for C$_{23}$H$_{20}$NO [M+H]$^+$ 326.1539; found, 326.1534.

6-Methyl-8,9-diphenyl-[1,3]dioxolo[4,5-f]isoquinoline (**3ra**)[6f]:
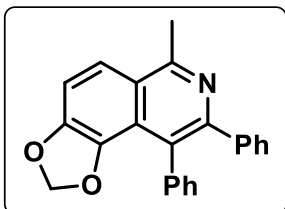
Physical State: White solid (25 mg, 74% yield). **R$_f$** = 0.2 (10% EtOAc/hexane). **mp** 248-249 °C. **^{1}H NMR (400 MHz, CDCl$_3$)**: δ 7.75 (d, *J* = 8.7 Hz, 1H), 7.21-7.07 (m, 11H), 7.23 (s, 2H), 2.92 (s, 3H) ppm. **^{13}C{^{1}H} NMR (100 MHz, CDCl$_3$)**: δ 158.1, 150.2, 148.2, 142.1, 140.7, 138.6, 131.5, 130.6, 127.8, 127.4, 127.3, 127.2, 125.3, 123.5, 122.8, 121.4, 111.3, 101.8, 23.5 ppm. **HRMS (ESI) m/z**: calcd for C$_{23}$H$_{18}$NO$_2$ [M+H]$^+$ 340.1338; found, 340.1340. It was crystallized from dichloromethane.

1,3,4-Triphenylisoquinoline (**3sa**)[6g]:
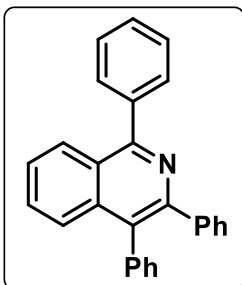
Physical State: White solid (23 mg, 64% yield). **R$_f$** = 0.58 (10% EtOAc/hexane). **mp** 181-183 °C. **^{1}H NMR (400 MHz, CDCl$_3$)**: δ 8.18 (d, *J* = 8.3 Hz, 1H), 7.82 (d, *J* = 6.8 Hz, 2H), 7.72 (d, *J* = 8.4 Hz, 1H), 7.61-7.49 (m, 5H), 7.43-7.29 (m, 7H), 7.19-7.15 (m, 3H) ppm. **^{13}C{^{1}H} NMR (100 MHz, CDCl$_3$)**: δ 160.1, 150.0, 141.2, 140.1, 137.9, 137.3, 131.7, 130.8, 130.5, 130.3, 130.1, 128.9, 128.6, 127.9, 127.6, 127.3, 126.9, 126.3, 125.7 ppm. **HRMS (ESI) m/z**: calcd for C$_{27}$H$_{20}$N [M+H]$^+$ 358.1596; found, 358.1598.

6-Methyl-3,4-diphenyl-1-(p-tolyl)isoquinoline (**3ta**)[18]:

Physical State: White solid (33 mg, 85% yield). **R$_f$** = 0.5 (20% DCM/hexane). **mp** 171-173°C. **^{1}H NMR (400 MHz, CDCl$_3$)**: δ 8.14 (dd, *J* = 8.4 Hz, 0.8 Hz, 1H), 7.75 (dd,
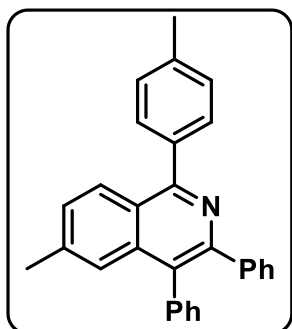
J = 8.4 Hz, 1.2 Hz, 1H), 7.5 (s, 1H), 7.46-7.31 (m, 10H), 7.20-7.18 (m, 3H), 2.49 (s, 3H), 2.45 (s, 3H) ppm. **¹³C{¹H} NMR (100 MHz, CDCl₃):** δ 159.8, 150.1, 141.4, 140.5, 138.6, 138.1, 137.5, 137.4, 131.7, 130.8, 130.5, 129.4, 129.3, 129.0, 128.6, 127.8, 127.8, 127.5, 127.2, 125.1, 124.2, 22.4, 21.7

ppm. **HRMS (ESI) m/z:** calcd for $C_{29}H_{24}N$ [M+H]⁺ 386.1909; found, 386.1918.

6-Methoxy-1-(4-methoxyphenyl)-3,4-diphenylisoquinoline (**3ua**)[6g]:
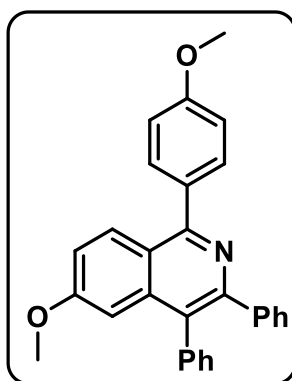
Physical State: White solid (30 mg, 72% yield). **R$_f$** = 0.4 (10% DCM/hexane)**. mp** 174-176 °C. **¹H NMR (400 MHz, CDCl₃):** δ 8.03 (d, J = 9.2 Hz, 1H), 7.67 (d, J = 8.4 Hz, 2H), 7.33-7.19 (m, 7H), 7.11-7.03 (m, 4H), 6.98 (d, J = 8.4 Hz, 2H), 6.87 (d, J = 2.2 Hz, 1H) ppm. **¹³C{¹H} NMR (100 MHz, CDCl₃):** δ 160.8, 160.3, 159.1, 150.6, 141.5, 139.4, 138.3, 132.8, 131.8, 131.6, 130.7, 129.8, 129.0, 128.7, 127.8, 127.5, 127.2, 121.5, 119.1, 114.1, 104.5, 55.7, 55.5 ppm. **HRMS (ESI) m/z**: calcd for $C_{29}H_{24}NO_2$ [M+H]⁺ is 418.1807; found, 418.1812.

1-(4-Nitrophenyl)-3,4-diphenylisoquinoline (**3va**):
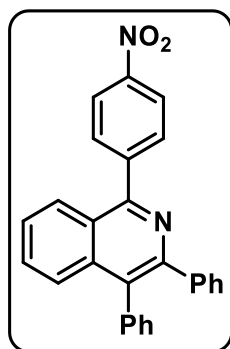
Physical State: Pale yellow solid (32 mg, 80% yield). **R$_f$** = 0.5 (60% DCM/hexane)**. mp** 179-181 °C. **¹H NMR (400 MHz, CDCl₃):** δ 8.34 (d, J = 8.5 Hz, 2H), 7.99 (d, J = 8.3 Hz, 1H), 7.94 (d, J = 8.5 Hz, 2H), 7.69 (d, J = 8.5 Hz, 1H), 7.57 (t, J = 15.0 Hz, 1H), 7.49 (t, J = 15.0 Hz, 1H), 7.34-7.31 (m, 5H), 7.23-7.21 (m, 2H), 7.13-7.11 (m, 3H) ppm. **¹³C{¹H} NMR (100 MHz, CDCl₃):** δ 157.5, 150.3, 148.3, 146.4, 140.7, 137.4, 137.4, 131.6, 131.5, 131.3, 130.7, 130.7, 128.8, 128.0, 127.9, 127.7,

127.6, 126.8, 126.8, 125.5, 123.9 ppm. **HRMS (ESI) m/z:** calcd for $C_{27}H_{19}N_2O_2$ $[M+H]^+$ 403.1447; found, 403.1431.

1-Methyl-diethylisoquinoline (**3ab**):
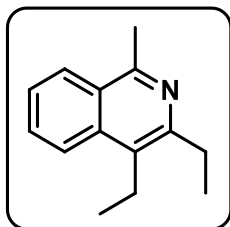
Physical State: Pale yellow solid (15 mg, 75% yield). R_f = 0.4 (10% EtOAc/hexane**). mp** 57-59 °C. **^{1}H NMR (400 MHz, CDCl$_3$):** δ 8.08 (d, J = 4 Hz, 1H), 7.98 (d, J = 8.4 Hz, 1H), 7.66 (t, J = 7.2 Hz, 1H), 7.5 (t, J = 7.2 Hz, 1H), 3.05 (q, J = 7.2 Hz, 2H), 2.97 (q, J = 7.2 Hz, 2H), 2.92 (s, 3H), 1.34 (t, J = 7.2 Hz, 3H), 1.29 (t, J = 7.2 Hz, 3H) ppm. **^{13}C{^{1}H} NMR (100 MHz, CDCl$_3$):** δ 156.1, 152.8, 135.5, 129.9, 127.6, 126.5, 126.4, 125.6, 123.7, 28.8, 22.6, 21.0, 15.6, 15.3 ppm. **HRMS (ESI) m/z:** calcd for $C_{14}H_{18}N$ $[M+H]^+$ 200.1439; found, 200.1440.

1-Methyl-dipropylisoquinoline (**3ac**)[6e]:
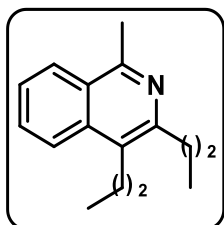
Physical State: Colorless liquid (15 mg, 75% yield). R_f = 0.6 (10% EtOAc/hexane**). ^{1}H NMR (400 MHz, CDCl$_3$):** δ 8.08 (d, J = 8.4 Hz, 1H), 7.96 (d, J = 8.4 Hz, 1H), 7.65 (td, J = 8.0 Hz, 1.2 Hz, 1H), 7.5 (td, J = 8.0 Hz, 0.8 Hz, 1H), 2.98 (t, J = 7.6 Hz, 2H), 2.93-2.89 (m, 5H), 1.80 (sext, J = 8 Hz, 2H), 1.67 (sext, J = 8.0 Hz, 2H), 1.09 (t, J = 7.2 Hz, 3H), 1.05 (t, J = 7.2 Hz, 3H) ppm. **^{13}C{^{1}H} NMR (100 MHz, CDCl$_3$):** δ 155.9, 151.9, 135.8, 129.8, 126.6, 126.4, 126.3, 125.6, 123.9, 37.7, 30.1, 24.5, 24.2, 22.6, 14.9, 14.7 ppm. **HRMS (ESI) m/z:** calcd for $C_{16}H_{22}N$ $[M+H]^+$ 228.1747; found, 228.1745.


1-Methyl-4-ethyl-3-phenylisoquinoline (**3ad**)[6e]:

Physical State: White solid (21 mg, 83% yield). R_f = 0.5 (10% EtOAc/hexane**).**
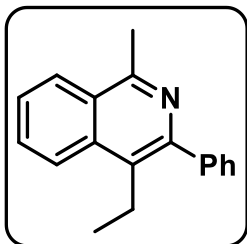
mp 122-123 °C. **¹H NMR (400 MHz, CDCl₃)**: δ 8.18 (d, *J* = 7.6 Hz, 1H), 8.90 (d, *J* = 8.8 Hz, 1H), 7.75 (t, *J* = 7.6 Hz, 1H), 7.61 (t, *J* = 7.6 Hz, 1H), 7.52 (d, *J* = 7.2 Hz, 2H), 7.47 (t, *J* = 7.2 Hz, 2H), 7.4 (t, *J* = 7.2 Hz, 1H), 3.03-2.98 (m, 5H), 1.27 (t, *J* = 7.6 Hz, 3H) ppm. **¹³C{¹H} NMR (100 MHz, CDCl₃)**: δ 157.9, 153.0, 138.2, 136.5, 130.7, 130.0, 129.1, 128.8, 127.7, 126.2, 126.1, 125.8, 125.7, 29.3, 22.8, 15.3 ppm. **HRMS (ESI) m/z**: calcd for $C_{18}H_{18}N$ $[M+H]^+$ 248.1424; found, 248.1427.

1,4-Dimethyl-3-phenylisoquinoline (**3ae**)[6f]:
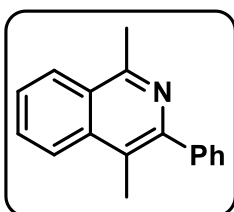
Physical State: Pale yellow solid (29 mg, 75% yield). R_f = 0.5 (10% EtOAc/hexane). **mp** 100-103 °C. **¹H NMR (400 MHz, CDCl₃)**: δ 8.17 (d, *J* = 8.4 Hz, 1H), 8.06 (d, *J* = 8.8 Hz, 1H), 7.75 (t, *J* = 7.6 Hz, 1H), 7.61-7.58 (m, 3H), 7.48 (t, *J* = 7.6 Hz, 2H), 7.40 (t, *J* = 7.6 Hz, 1H), 3.00 (s, 3H), 2.61 (s, 3H) ppm. **¹³C{¹H} NMR (100 MHz, CDCl₃)**: δ 156.2, 151.0, 142.0, 136.6, 130.2, 128.4, 127.7, 126.6, 126.5, 126.4, 124.4, 122.5, 22.8, 15.7 ppm. **HRMS (ESI) m/z**: calcd for $C_{17}H_{18}N$ $[M+H]^+$ 234.1277; found, 234.1289.

4-Butyl-1-methyl-3-phenylisoquinoline (**3af**):
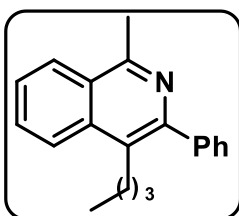
Physical State: Oily liquid (28 mg, 83% yield). R_f = 0.3 (10% EtOAc/hexane). **¹H NMR (400 MHz, CDCl₃)**: δ 8.17 (d, *J* = 8.0 Hz, 1H), 8.06 (d, *J* = 8.0 Hz, 1H), 7.74 (t, *J* = 8.0 Hz, 1H), 7.61 (t, *J* = 8.0 Hz, 3H), 7.52-7.44 (m, 4H), 7.40 (t, *J* = 7.2 Hz, 1H), 2.98-2.95 (m, 5H), 1.65-1.59 (m, 2H), 1.36-1.31 (m, 2H), 0.85 (t, *J* = 7.6 Hz, 3H) ppm. **¹³C{¹H} NMR (100 MHz, CDCl₃)**: δ 156.1, 151.2, 142.1, 135.7, 130.1, 129.7, 128.4, 127.8, 127.7, 127.0, 126.6, 126.5, 124.6, 33.7, 28.6, 23.3, 22.8, 14.1 ppm. **IR (neat)**: 3424, 3067, 3026, 2956, 2926,

2869, 2359, 1723, 1614, 1563, 1503, 1463, 1439, 1391, 1333, 1274, 1155, 1101, 1072, 1029, 853, 792, 758, 701, 616 cm^{-1}. **HRMS (ESI) m/z:** calcd for C$_{20}$H$_{22}$N [M+H]$^+$ 276.1747; found, 276.1743.

1-Methyl-4-pentyl-3-phenylisoquinoline (**3ag**):
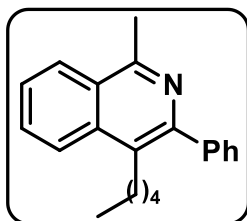
Physical State: Oily liquid (29 mg, 85% yield). **R$_f$** = 0.4 (10% EtOAc/hexane). **^{1}H NMR (400 MHz, CDCl$_3$):** δ 8.17 (d, *J* = 8.4 Hz, 1H), 8.06 (d, *J* = 8.4 Hz, 1H), 7.74 (t, *J* = 8.4 Hz, 1H), 7.59 (t, *J* = 8 Hz, 3H), 7.52-7.45 (m, 4H), 7.39 (t, *J* = 7.2 Hz, 1H), 2.98-2.94 (m, 5H), 1.69-1.61 (m, 2H), 1.34-1.21 (m, 4H), 0.85 (t, *J* = 7.2 Hz, 3H) ppm. **^{13}C{^{1}H} NMR (100 MHz, CDCl$_3$):** δ 156.1, 151.2, 142.2, 135.7, 130.1, 129.6, 128.4, 127.8, 127.7, 127.0, 126.6, 126.5, 124.5, 32.4, 31.2, 28.8, 22.8, 22.6, 14.3 ppm. **IR (neat):** 3424, 3067, 2955, 2926, 2868, 1726, 1614, 1563, 1503, 1440, 1391, 1333, 1266, 1122, 1072, 1050, 1029, 982, 962, 869, 805, 789, 758, 736, 701, 618, 592 cm^{-1}. **HRMS (ESI) m/z:** calcd for C$_{21}$H$_{24}$N [M+H]$^+$ 290.1903; found, 290.1899.

4-Hexyl-1-methyl-3-phenylisoquinoline (**3ah**):
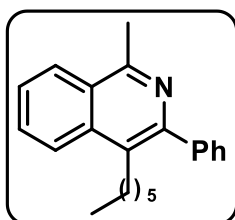
Physical State: Oily liquid (26 mg, 87% yield). **R$_f$** = 0.4 (10% EtOAc/hexane). **^{1}H NMR (400 MHz, CDCl$_3$):** δ 8.16 (d, *J* = 8.4 Hz, 1H), 8.05 (d, *J* = 8.4 Hz, 1H), 7.72 (t, *J* = 7.6 Hz, 1H), 7.58 (t, *J* = 7.6 Hz, 1H), 7.51-7.36 (m, 5H), 2.97-2.93 (m, 5H), 1.67-1.59 (m, 2H), 1.34-1.18 (m, 6H), 0.86-0.82 (m, 3H) ppm. **^{13}C{^{1}H} NMR (100 MHz, CDCl$_3$):** δ 155.7, 150.9, 141.8, 135.3, 129.7, 129.3, 128.1, 127.4, 127.3, 126.6, 126.2, 126.1, 124.2, 31.3, 31.2, 29.5, 28.5, 22.5, 22.4, 14.0 ppm. **HRMS (ESI) m/z:** calcd for C$_{22}$H$_{26}$N [M+H]$^+$ 304.2050; found, 304.2060.

1-Methyl-3,4-di-p-tolylisoquinoline (**3ai**)[6f]:
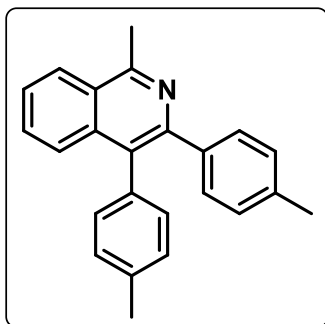
Physical State: Pale yellow solid (31 mg, 80% yield). $\mathbf{R}_f$ = 0.5 (10% EtOAc/hexane). **mp** 151-154 °C. **^{1}H NMR (400 MHz, CDCl$_3$):** δ 8.19-8.17 (m, 1H), 7.68-7.66 (m, 1H), 7.78-7.55 (m, 2H), 7.3 (d, J = 8.0 Hz, 2H), 7.17 (d, J = 7.6 Hz, 2H), 7.12 (d, J = 8.0 Hz, 2H), 7.02 (d, J = 7.6 Hz, 2H), 3.07 (s, 3H), 2.40 (s, 3H), 2.29 (s, 3H) ppm. **^{13}C{^{1}H} NMR (100 MHz, CDCl$_3$):** δ 157.7, 149.7, 138.6, 136.9, 136.8, 136.6, 135.0, 131.5, 130.5, 130.0, 129.3, 129.2, 128.7, 126.6, 126.4, 125.8, 23.0, 21.6, 21.5 ppm. **HRMS (ESI) m/z**: calcd for C$_{24}$H$_{22}$N [M+H]$^+$ 324.1747; found, 324.1761.

3,4-Bis(4-fluorophenyl)-1-methylisoquinoline (**3aj**)[6f]:
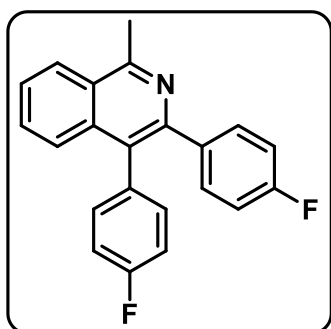
Physical State: Pale yellow solid (28 mg, 72% yield). $\mathbf{R}_f$ = 0.5 (10% EtOAc/hexane). **mp** 143-145 °C. **^{1}H NMR (400 MHz, CDCl$_3$):** δ 8.22-8.20 (m, 1H), 7.62-7.61 (m, 3H), 7.35-7.31 (m, 2H), 7.20-7.17 (m, 2H), 7.10 (t, J = 8.8 Hz, 2H), 6.91 (t, J = 8.8 Hz, 2H), 3.10 (s, 3H) ppm.

^{13}C{^{1}H} NMR (100 MHz, CDCl$_3$): δ 163.6 (d, J = 8.0 Hz), 161.1 (d, J = 7.7 Hz), 158.4, 148.9, 137.2 (d, J = 3.3 Hz), 137.3, 133.6 (d, J = 3.5 Hz), 133.2 (d, J = 7.9 Hz), 132.3 (d, J = 8.1 Hz), 130.5, 128.4, 127.1, 126.5, 126.2, 126.0, 115.8 (d, J = 21.0 Hz), 115.0 (d, J = 21.0 Hz), 23.0 ppm. **HRMS (ESI) m/z**: calcd for C$_{22}$H$_{16}$F$_2$N [M+H]$^+$ 332,1245; found, 333.1244.

1-Cyclohexyl-6-methoxy-3,4-diphenylisoquinoline (**3wa**):

Physical State: Colourless oily liquid (32 mg, 64% yield). $\mathbf{R}_f$ = 0.45 (5% EtOAc/hexane).

^{1}H NMR (700 MHz, CDCl$_3$): δ 8.20 (d, *J* = 9.1 Hz, 1H), 7.42 (d, *J* = 6.3 Hz, 2H), 7.36 (t, *J* = 7.0 Hz, 2H), 7.33 (t, *J* = 7.0 Hz, 1H), 7.23 (d, *J* = 7.0 Hz, 2H), 7.20-7.16 (m, 4H), 6.93 (d, *J* = 2.1 Hz, 1H), 3.7 (s, 3H), 3.58-3.55 (m, 1H), 2.05 (d, *J* = 12.6 Hz, 2H), 2.00-1.94 (m, 4H), 1.82 (d, *J* = 12.6 Hz, 1H), 1.56 (q, *J* = 13.3 Hz, 3H) ppm. **^{13}C{^{1}H} NMR (175 MHz, CDCl$_3$)**: δ 164.2, 160.4, 149.7, 141.8, 138.9, 138.7, 131.7, 130.9, 128.7, 128.0, 127.7, 127.4, 127.1, 126.8, 120.9, 118.7, 105.1, 55.5, 42.2, 32.8, 27.3, 26.6 ppm. **IR (neat)**: 3427, 2925, 2852, 1617, 1574, 1502, 1410, 1373, 1264, 1235, 1030, 738, 700 cm^{-1}. **^{1}HRMS (ESI) m/z**: calcd: for C$_{28}$H$_{28}$NO [M+H]$^+$ 394.2171, found: 394.2153.
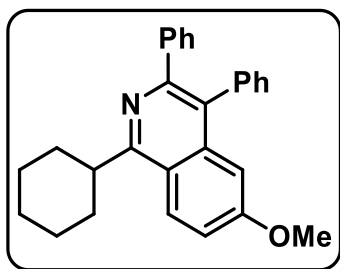
NMR spectra of 1-Methyl-3,4-diphenylisoquinoline (3aa):

3aa, ^{1}H NMR (CDCl$_3$, 400 MHz)

3aa, ^{13}C{^{1}H} NMR (CDCl$_3$, 100 MHz)
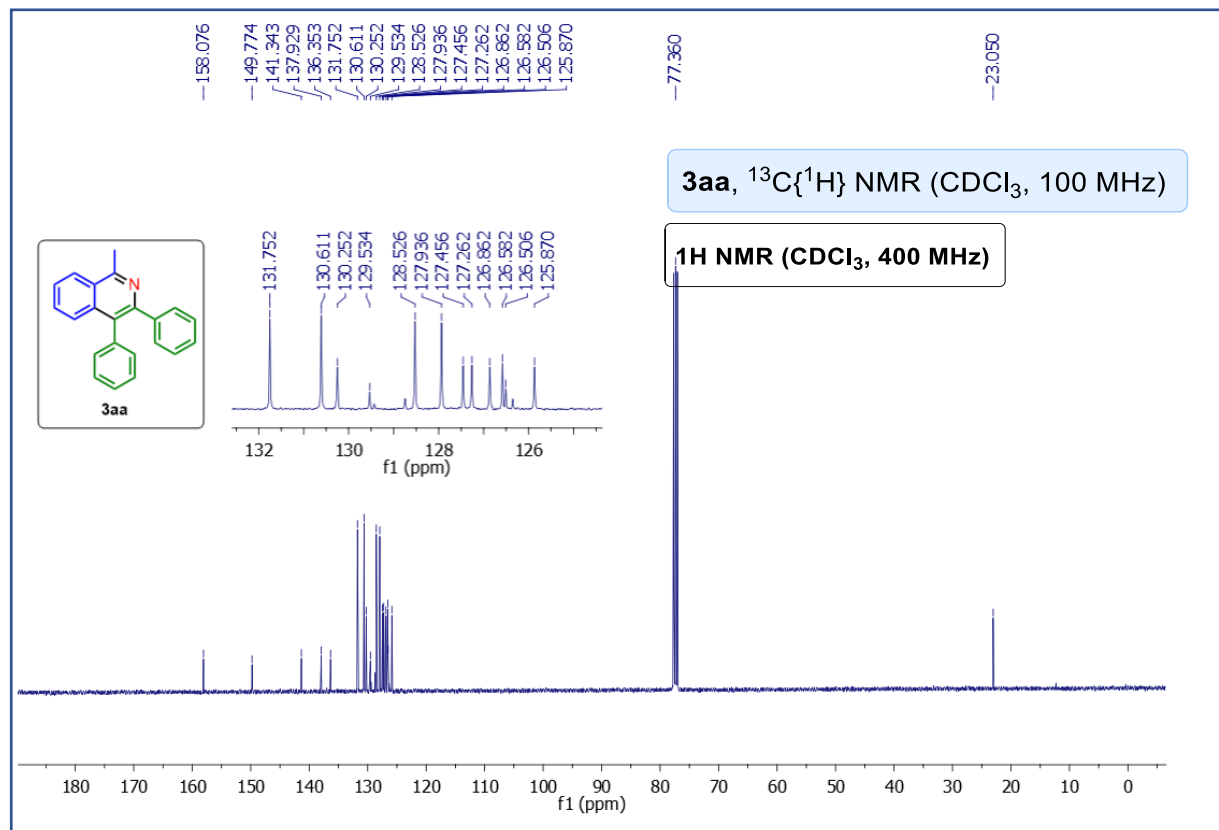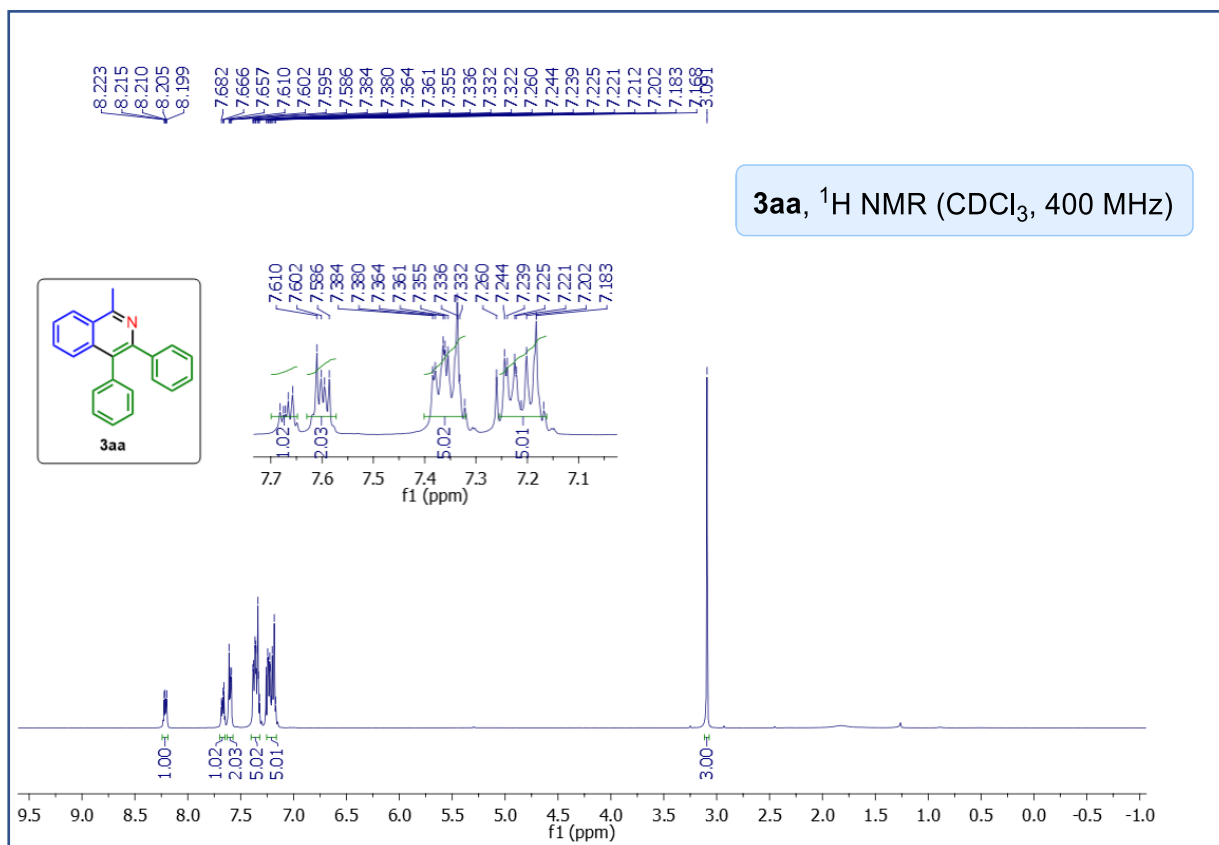
1H NMR (CDCl$_3$, 400 MHz)

NMR spectra of 1-Methyl-4-ethyl-3-phenylisoquinoline (3ad):

3ad, ^{1}H NMR (CDCl$_3$, 400 MHz)

3ad, ^{13}C{^{1}H} NMR (CDCl$_3$, 100 MHz)
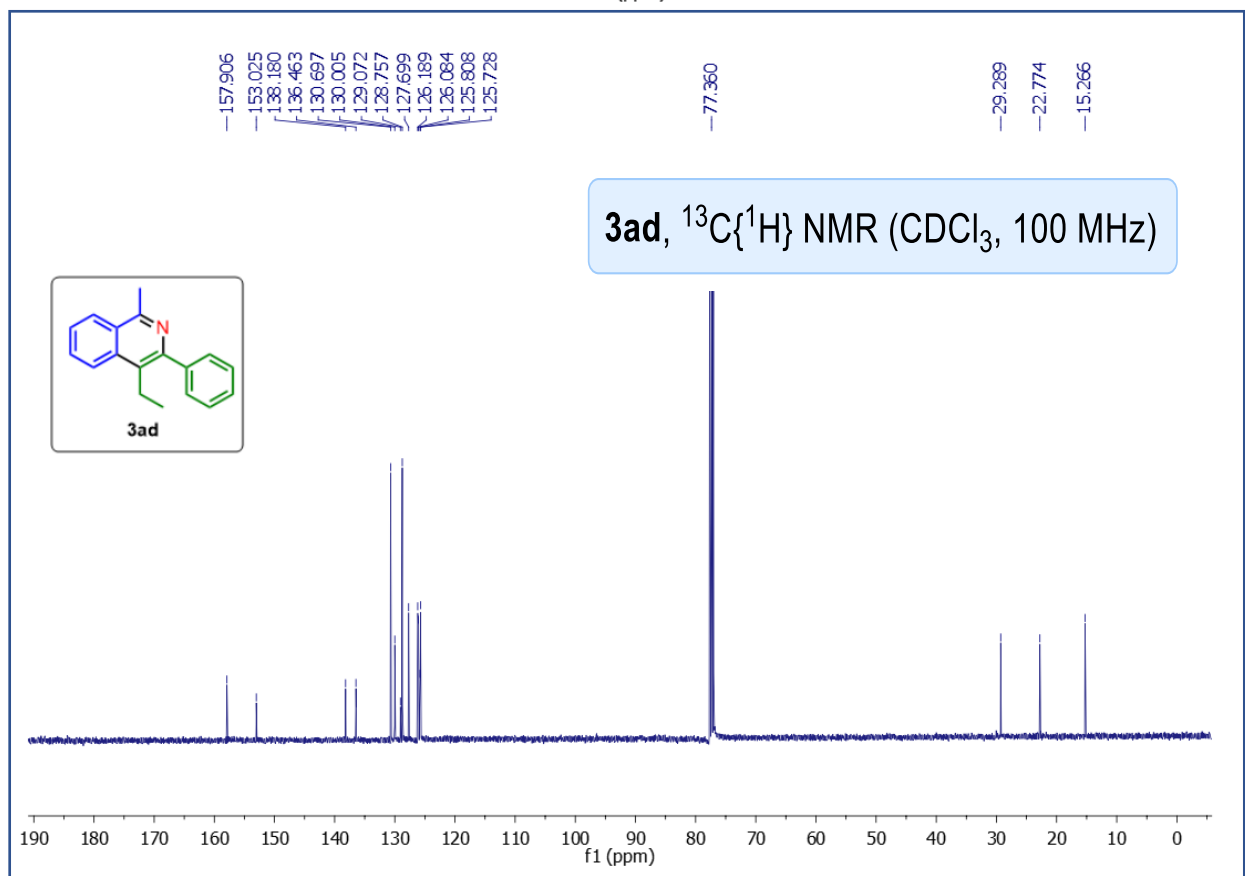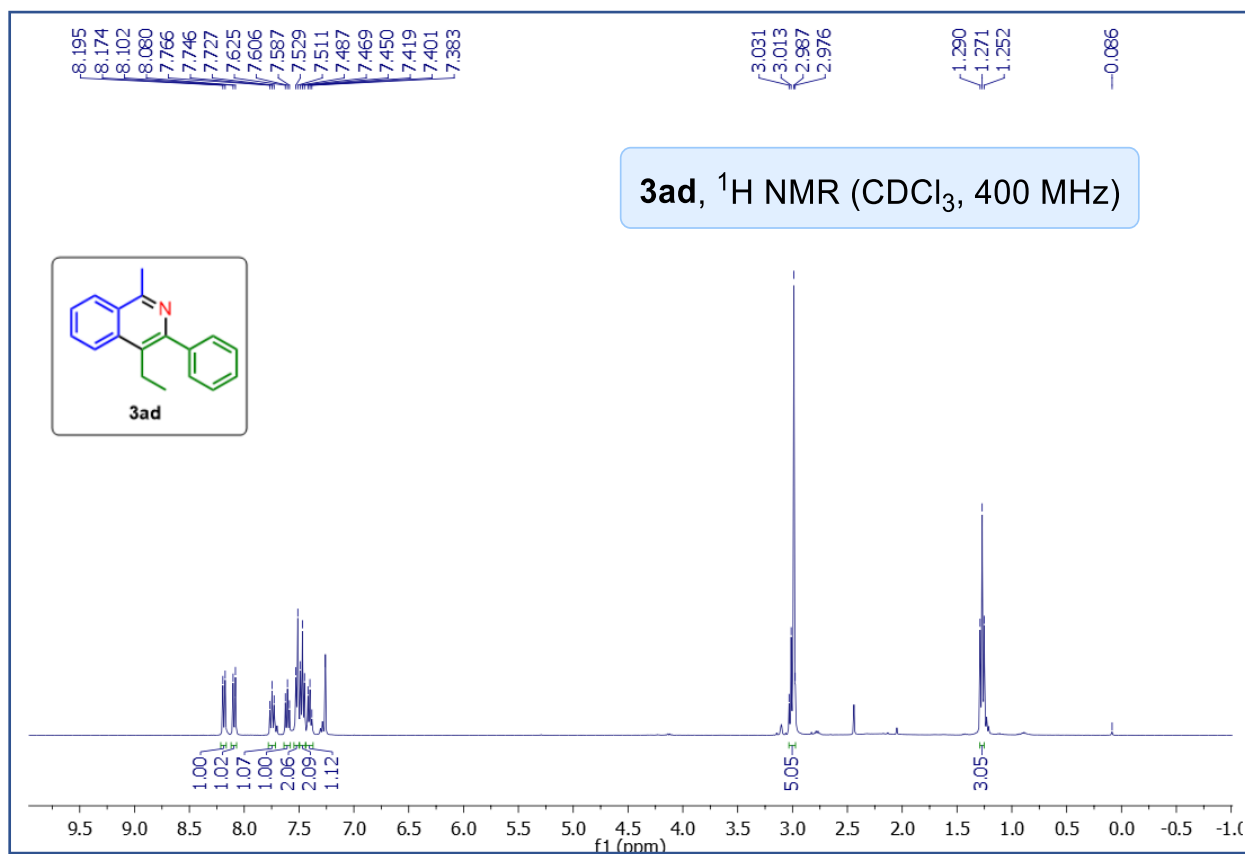
^{1}H-^{13}C HMBC confirms the product 3ad.

3ad
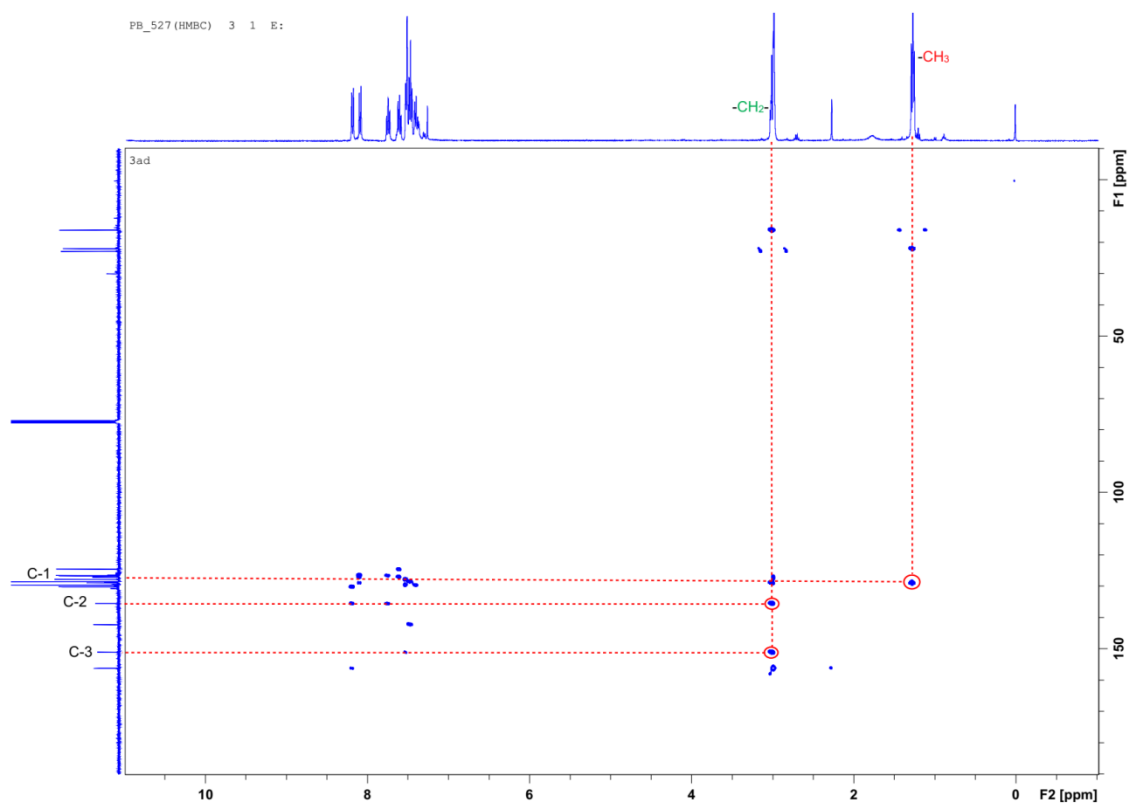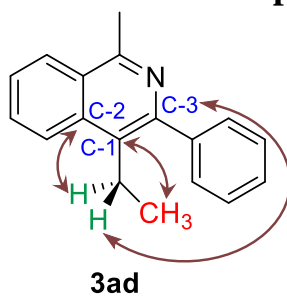
Crystal structure of 3ra

3ra = CCDC 1911600
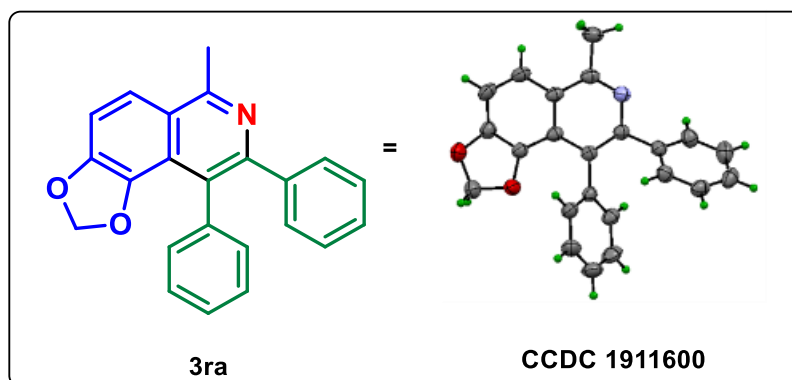
Datablock pcr-pb-bridge - ellipsoid plot
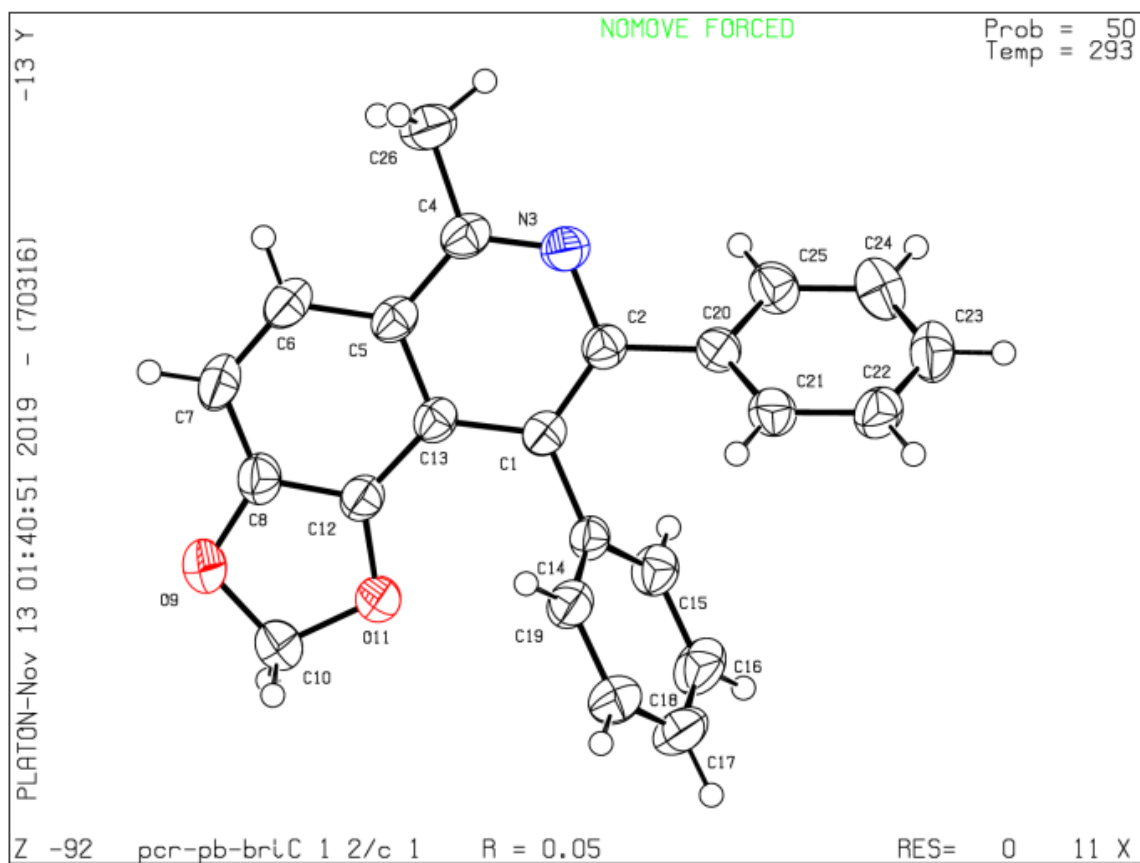
2.6 REFERENCES

1. (a) McMurray, L.; O'Hara, F.; Gaunt, M. J. Recent Developments in Natural Product Synthesis Using Metal-Catalysed C–H Bond Functionalisation. *Chem. Soc. Rev*. **2011**, *40*, 1885. (b) Godula, K.; Sames, D. C-H Bond Functionalization in Complex Organic Synthesis. *Science* **2006**, *312*, 67–72. (c) Yamaguchi, J.; Yamaguchi, A. D.; Itami, K. C-H Bond Functionalization: Emerging Synthetic Tools for Natural Products and Pharmaceuticals. *Angew. Chem., Int. Ed*. **2012**, *51*, 8960–9009. (d) He, R.; Huang, Z.-T.; Zheng, Q.-Y.; Wang, C. Isoquinoline Skeleton Synthesis via Chelation-Assisted C−H Activation. *Tetrahedron Lett.* **2014**, *55*, 5705–5713.

2. T Gensch, T.; Hopkinson, M. N.; Glorius, F.; Wencel-Delord, J. Mild Metal-Catalysed C–H Activation: Examples and Concepts. *Chem. Soc. Rev*. **2016**, *45*, 2900–2936.

3. (a) Colby, D. A.; Tsai, A. S.; Bergman, R. G.; Ellman, J. A. Rhodium-Catalysed Chelation-Assisted C–H Bond Functionalization Reactions. *Acc. Chem. Res*. **2012**, *45*, 814–825. (b) Rouquet, G.; Chatani, N. Catalytic Functionalization of C(sp^2)-H and C(sp^3)-H Bonds by Using Bidentate Directing Groups. *Angew. Chem., Int. Ed*. **2013**, *52*, 11726–11743. (c) Zhu, R.-Y.; Farmer, M. E.; Chen, Y.-Q.; Yu, J.-Q. A Simple and Versatile Amide Directing Group for C−H Functionalizations. *Angew. Chem., Int. Ed*. **2016**, *55*, 10578–10599.

4. (a) Guimond, N.; Gouliaras, C.; Fagnou, K. Rhodium(III)-Catalysed Isoquinolone Synthesis: The N−O Bond as a Handle for C−N Bond Formation and Catalyst Turnover. *J. Am. Chem. Soc*. **2010**, *132*, 6908–6909. (b) Guimond, N.; Gorelsky, S. I.; Fagnou, K. Rhodium(III)-Catalysed Heterocycle Synthesis Using an Internal

Oxidant: Improved Reactivity and Mechanistic Studies. *J. Am. Chem. Soc*. **2011**, *133*, 6449–6457.

5. (a) Wang, H.; Grohmann, C.; Nimphius, C.; Glorius, F. Mild Rh(III)-Catalysed C–H Activation and Annulation with Alkyne MIDA Boronates: Short, Efficient Synthesis of Heterocyclic Boronic Acid Derivatives. *J. Am. Chem. Soc*. **2012**, *134*, 19592–19595. (b) Shi, Z.; Boultadakis-Arapinis, M.; Koester, D. C.; Glorius, F. Rh(III)-Catalysed Intramolecular Redox-Neutral Cyclization of Alkenes via C–H Activation. *Chem. Commun*. **2014**, *50*, 2650. (c) Zhao, D.; Lied, F.; Glorius, F. Rh(iii)-Catalysed C–H Functionalization/Aromatization Cascade with 1,3-Dienes: A Redox-Neutral and Regioselective Access to Isoquinolines. *Chem. Sci*. **2014**, *5*, 2869.

6. (a) Too, P. C.; Wang, Y.-F.; Chiba, S. Rhodium(III)-Catalysed Synthesis of Isoquinolines from Aryl Ketone *O*-Acyloxime Derivatives and Internal Alkynes. *Org. Lett*. **2010**, *12*, 5688–5691. (b) Kiran Chinnagolla, R.; Pimparkar, S.; Jeganmohan, M. Ruthenium-Catalysed Highly Regioselective Cyclization of Ketoximes with Alkynes by C-H Bond Activation: A Practical Route to Synthesize Substituted Isoquinolines. *Org. Lett*. **2012**, *14*, 3032–3035. (c) Shi, Z.; Boultadakis-Arapinis, M.; Koester, D. C.; Glorius, F. Rh(III)-Catalysed Intramolecular Redox-Neutral Cyclization of Alkenes via C–H Activation. *Chem. Commun*. **2014**, *50*, 2650. (d) Sen, M.; Kalsi, D.; Sundararaju, B. Cobalt(III)-Catalysed Dehydrative [4+2] Annulation of Oxime with Alkyne by C-H and N-OH Activation. *Chem. - Eur. J.*, **2015**, *21*, 15529–15533. (e) Wang, H.; Koeller, J.; Liu, W.; Ackermann, L. Cobalt(III)-Catalysed C-H/N-O Functionalizations: Isohypsic Access to Isoquinolines. *Chem. - Eur. J.* **2015**, *21*, 15525–15528. (f) Pawar, A. B.; Agarwal, D.; Lade, D. M. Cp*Co(III)-Catalysed C–H/N–N Functionalization of

Arylhydrazones for the Synthesis of Isoquinolines. *J. Org. Chem*. **2016**, *81*, 11409–11415. (g) Li, X.-C.; Du, C.; Zhang, H.; Niu, J.-L.; Song, M.-P. Cp*-Free Cobalt-Catalysed C–H Activation/Annulations by Traceless *N, O*-Bidentate Directing Group: Access to Isoquinolines. *Org. Lett.* **2019**, *21*, 2863–2866. and references cited therein.

7. (a) Park, H.; Verma, P.; Hong, K.; Yu, J.-Q. Controlling Pd(IV) Reductive Elimination Pathways Enables Pd(II)-Catalysed Enantioselective $C(sp^3)$−H Fluorination. *Nat. Chem*. **2018**, *10*, 755–762. (b) Guan, Z.; Chen, S.; Huang, Y.; Yao, H. Rhodium(III)-Catalysed Intramolecular Olefin Hydroarylation of Aromatic Aldehydes Using a Transient Directing Group. *Org. Lett.* **2019**, *21*, 3959–3962.

8. (a) Chuang, S.-C.; Gandeepan, P.; Cheng, C.-H. Synthesis of Isoquinolines via Rh(III)-Catalysed C–H Activation Using Hydrazone as a New Oxidizing Directing Group. *Org. Lett*. **2013**, *15*, 5750–5753. (b) Luo, C.-Z.; Gandeepan, P.; Wu, Y.-C.; Tsai, C.-H.; Cheng, C.-H. Cooperative $C(sp^3)$–H and $C(sp^2)$–H Activation of 2-Ethylpyridines by Copper and Rhodium: A Route toward Quinolizinium Salts. *ACS Catal.* **2015**, *5*, 4837–4841. (c) Váňa, J.; Bartáček, J.; Hanusek, J.; Roithová, J.; Sedlák, M. C-H Functionalizations by Palladium Carboxylates: The Acid Effect. *J. Org. Chem.* **2019**, *84*, 12746–12754.

9. A Scifinder search (key word such as additive free, redox-neutral and transient directing group, C-H activation) did not retrieve any report regarding an additive-free redox-neutral traceless directing group.

10. (a) Wallace, R. G.; Barker, J. M.; Wood, M. L. Migration to Electron-Deficient Nitrogen. A One Pot Synthesis of Aromatic and Heteroaromatic Amines from Carboxylic Acids. *Synthesis*. **1990**, 1143–1144. (b) Evans, L. E.; Cheeseman, M.

D.; Jones, K. N–N Bond-Forming Cyclization for the One-Pot Synthesis of N -Aryl[3,4- d]Pyrazolopyrimidines. *Org. Lett*. **2012**, *14*, 3546–3549. (c) Strom, A. E.; Hartwig, J. F. One-Pot Anti-Markovnikov Hydroamination of Unactivated Alkenes by Hydrozirconation and Amination. *J. Org. Chem.* **2013**, *78*, 8909–8914 (d) Voth, S.; Hollett, J. W.; Mccubbin, J. A. Transition-Metal-Free Access to Primary Anilines from Boronic Acids and a Common +NH2 Equivalent. *J. Org. Chem.* **2015**, *80,* 2545–2553 (e) Ma, Z.; Zhou, Z.; Kürti, L. Direct and Stereospecific Synthesis of N-H and N-Alkyl Aziridines from Unactivated Olefins Using Hydroxylamine- O -Sulfonic Acids. *Angew. Chem., Int. Ed*. **2017**, *56*, 9886–9890. (f) Zhou, Z.; Cheng, Q.-Q.; Kürti, L. Aza-Rubottom Oxidation: Synthetic Access to Primary α-Aminoketones. *J. Am. Chem. Soc.* **2019**, *141*, 2242–2246. (g) Munnuri, S.; Anugu, R. R.; Falck, J. R. Cu(II)-Mediated N –H and N-Alkyl Aryl Amination and Olefin Aziridination. *Org. Lett*. **2019**, *21*, 1926–1929. (h) Yi, J.-C.; Wu, Z.-J.; You, S.-L. Rh-Catalysed Aminative Dearomatization of Naphthols with Hydroxylamine-*O*-Sulfonic Acid (HOSA). *Eur. J. Org. Chem.* **2019**, *2019*, 5736–5739. (i) Munnuri, S.; Verma, S.; Chandra, D.; Anugu, R. R.; Falck, J. R.; Jat, J. L. Cu(OTf)2 -Catalysed Beckmann Rearrangement of Ketones Using Hydroxylamine- O -Sulfonic Acid (HOSA). *Synthesis* **2019**, *51*, 3709–3714.

11. (a) Tan, Y.; Hartwig, J. F. Palladium-Catalysed Amination of Aromatic C-H Bonds with Oxime Esters. *J. Am. Chem. Soc*., **2010**, *132*, 3676–3677. (b) Xu, L.; Zhu, Q.; Huang, G.; Cheng, B.; Xia, Y. Computational Elucidation of the Internal Oxidant-Controlled Reaction Pathways in Rh(III)-Catalysed Aromatic C–H Functionalization. *J. Org. Chem.* **2012**, *77*, 3017–3024. (c) Tang, H.; Zhou, B.; Huang, X.-R.; Wang, C.; Yao, J.; Chen, H. Origins of Selective C(sp^2)–H Activation Using Transition Metal Complexes with *N, N*-Bidentate Directing

Groups: A Combined Theoretical–Experimental Study. *ACS Catal*. **2014**, *4*, 649–656. (d) Tang, H.; Huang, X.-R.; Yao, J.; Chen, H. Understanding the Effects of Bidentate Directing Groups: A Unified Rationale for *sp^2* and *sp^3* C–H Bond Activations. *J. Org. Chem*. **2015**, *80*, 4672–4682.

12. Punji, B.; Song, W.; Shevchenko, G. A.; Ackermann, L. Cobalt-Catalysed C-H Bond Functionalizations with Aryl and Alkyl Chlorides. *Chem. - Eur. J.* **2013**, *19*, 10605–10610.

13. (a) Wang, H.; Koeller, J.; Liu, W.; Ackermann, L. Cobalt(III)-Catalysed C-H/N-O Functionalizations: Isohypsic Access to Isoquinolines. *Chem. - Eur. J.* **2015**, *21*, 15525–15528. (b) Ackermann, L.; Lygin, A. V.; Hofmann, N. Ruthenium-Catalysed Oxidative Annulation by Cleavage of C-H/N-H Bonds. *Angew. Chem., Int. Ed.* **2011**, *50*, 6379–6382. (c) Shiota, H.; Ano, Y.; Aihara, Y.; Fukumoto, Y.; Chatani, N. Nickel-Catalysed Chelation-Assisted Transformations Involving Ortho C–H Bond Activation: Regioselective Oxidative Cycloaddition of Aromatic Amides to Alkynes. *J. Am. Chem. Soc.* **2011**, *133*, 14952–14955.

14. Lee, C.-C.; Lin, Y.-C.; Liu, Y.-H.; Wang, Y. Rhodium-Catalysed Dimerization of Terminal Alkynes Assisted by MeI. *Organometallics* **2005**, *24*, 136–143.

15. Simmons, E. M.; Hartwig, J. F. On the Interpretation of Deuterium Kinetic Isotope Effects in C-H Bond Functionalizations by Transition-Metal Complexes. *Angew. Chem., Int. Ed*. **2012**, *51*, 3066–3072.

16. Gottlieb, H. E.; Kotlyar, V.; Nudelman, A. NMR Chemical Shifts of Common Laboratory Solvents as Trace Impurities. *J. Org. Chem*. **1997**, *62*, 7512−7515.

17. White, C.; Thompson, S. J; Maitlis, P. M. Pentamethylcyclopentadienyl-rhodium and -iridium complexes. Part XII. Tris(solvent) complexes and complexes of η^6-

benzene, -naphthalene, -phenanthrene, -indene, -indole, and -fluorene and η^5-lndenyl and -indolyl. *J. Chem. Soc. Dalt. Trans.* **1977**, 1654–1661.

18. Qiu, L.; Huang, D.; Xu, G.; Dai, Z.; Sun, J. Realized C-H functionalization of aryldiazo compounds via rhodium relay catalysis. *Org. Lett.* **2015**, *17*, 1810–1813.

Chapter 3

Rhodium-Catalysed One-Pot Access to *N*-Polycyclic Aromatic Hydrocarbons from Aryl Ketones through Triple C-H Bond Activations

3.1 Abstract

3.2 Introduction

3.3 Results and Discussions

3.4 Conclusions

3.5 Experimental Section

3.6 References

Chapter 3

Rhodium-Catalysed One-Pot Access to *N*-Polycyclic Aromatic Hydrocarbons from Aryl Ketones through Triple C-H Bond Activations
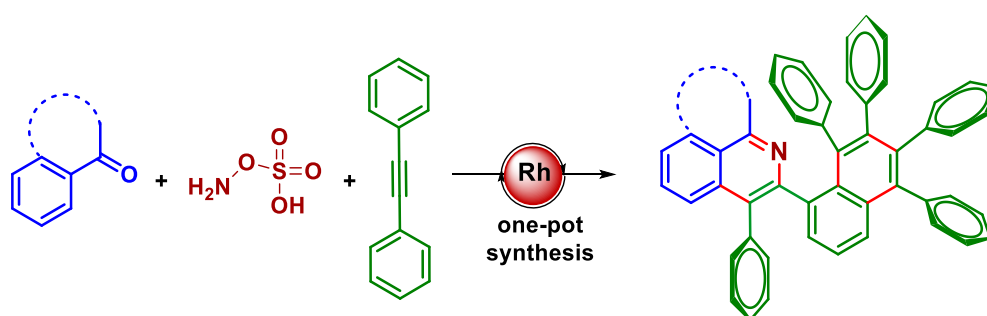
● **HOSA as N-transfer reagent**   ● **cascade triple C-H bond activation**

● **4 C-C & 2 C-N bonds formation in a single operation**

3.1 ABSTRACT: *The synthesis of hetero-polycyclic aromatic hydrocarbons has been explored from readily available aryl-alkyl ketones and alkynes in a pot and step economic protocol* via *rhodium catalysis. Multiple bond formation in a single operation through a cascade of triple C-H bond activations is a key feature of this protocol. Additionally, a novel synthetic application of the well-known aminating reagent hydroxylamine-O-sulfonic acid (HOSA) has been explored as an in situ redox-neutral directing group for the formation of N-PAHs via isoquinoline. The challenging annulations of two different alkynes in a regioselective fashion have been demonstrated effectively. Mechanistic studies reveal that, 3,4-diphenyl-1-methylisoquinoline as an active intermediate for this one- pot transformation.*

3.2 INTRODUCTION

In recent decades, synthesis of polycyclic aromatic hydrocarbons (PAHs) has gained significant attention among synthetic and material chemists. These compounds

have been extensively employed in optoelectronics and advanced organic materials, which can be attributed to their structural features.[1] It has been observed that incorporation of heteroatoms such as boron (B), nitrogen (N), and sulfur (S) into the aromatic frameworks of PAHs could modulate their electronic properties.[2] Particularly, nitrogen-containing PAHs (*N*-PAHs) have a key significance in organic electronics because of nitrogen's influence on electronic modulation and its role in stabilizing the PAHs.[3] Moreover, nitrogen-atom containing π-extended organic compounds are of prominent interest in organic light-emitting diodes (OLEDs) and organic field-effect transistors (OFETs).[4] Because of the unique electronic properties of the nitrogen-atom, *N*-containing compounds are being used as model synthetic equivalents for nitrogen-doped graphene in current studies.[4d,e] Hence, the presence of heterocyclic rings in PAHs has a dramatic impact on organic solar cells, sensors, field-effect transistors and the photophysical properties. Despite much exploration and advancement in this field, the common issue in this field is the complicated multistep syntheses of *N*-PAHs. Consequently, developing a straightforward methodology for the construction of highly conjugated PAHs is highly desirable.

During the past few decades, transition metal-catalysed directed C-H bond functionalization has greatly improved the arsenal of synthetic chemistry by creating an attractive transformative platform for the construction of complex organic scaffolds.[5] The Miura research group has reported the Rh-catalysed synthesis of polyarylated naphthyl- and anthrylazoles en route to the cleavage of multiple C-H bonds by taking *N*-phenylazoles and diarylalkynes as reacting partners.[6a] Likewise, Jioa and co-workers have disclosed the synthesis of polyarylated naphthylamides and isoquinolinone derivatives from benzamides and alkynes.[6b] Very recently, the Dong research group has addressed the synthesis of azahelicenes from *N*-phenyl-7-azaindole, which has significant

applications in photophysics.[6c] Moreover, the Ackermann group has developed a rhoda-electrocatalysed synthesis of *N*-PAHs enabled by a cascade of C-H activations.[6d] In addition, the use of redox-neutral directing groups is of current interest in the synthetic community. Such methodologies contribute greatly toward green synthesis as it obviates the use of extra metal oxidants.[7]

Figure 3.1 Transition metal-catalysed oxidative annulation reactions with alkyne
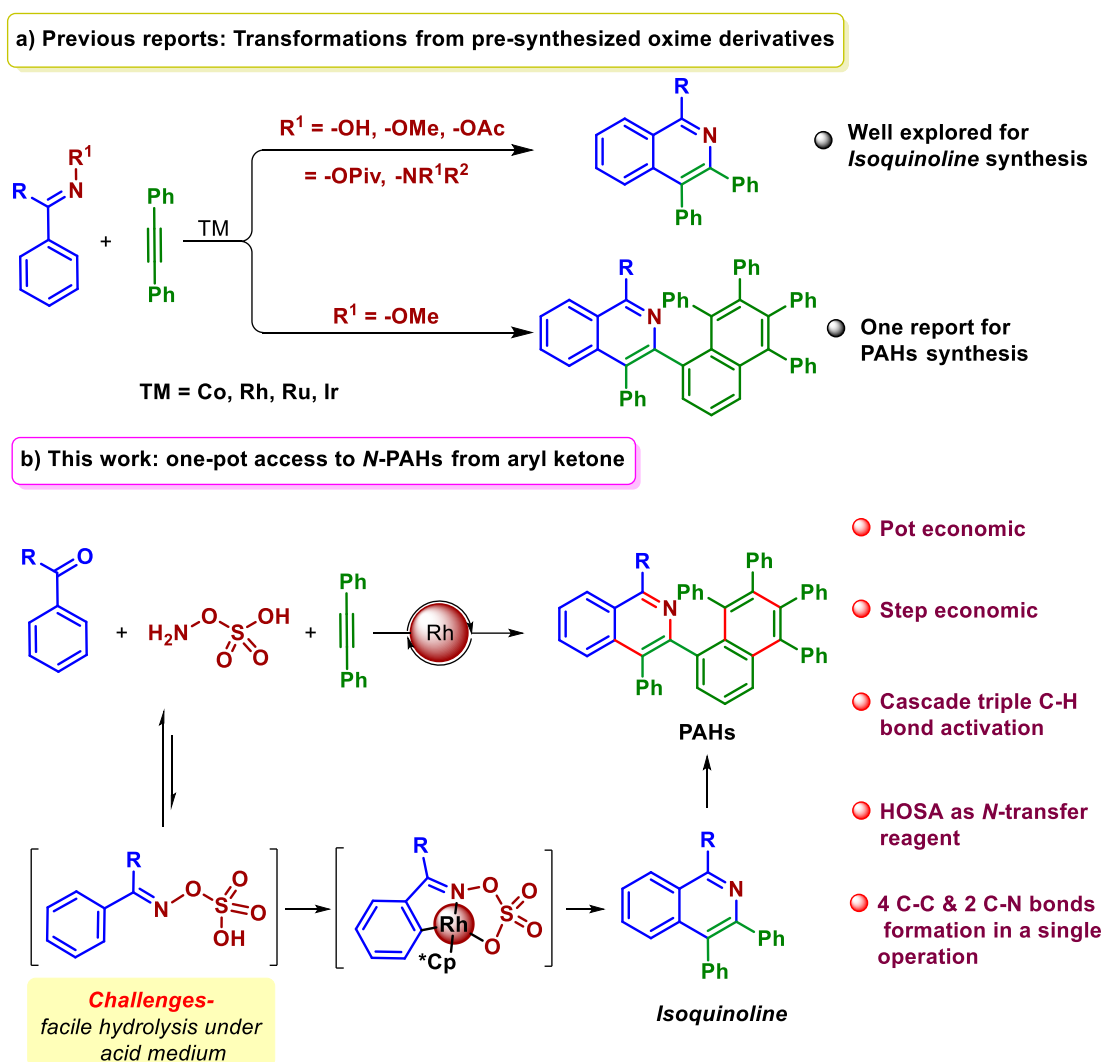
In transition metal-catalysed C-H bond activation, various types of redox-neutral directing groups have been well documented for different transformations.[8] In this context, isoquinoline synthesis has been depicted by taking different preinstalled redox-neutral directing groups with Rh, Co, Ru and Ir catalyst (Figure 3.1, a).[9] Although there are several reports on the synthesis of isoquinoline employing redox-neutral strategy with

preformed imines, the synthesis of *aza*-PAHs is limited to only one report (Figure 3.1, a).[10] Thus, development of a simpler protocol to achieve complex value added scaffolds is highly desirable in synthetic organic chemistry. In this context, a pot-economic protocol is being considered as an efficient approach in synthetic organic chemistry. One-pot synthesis is a promising green approach to contemporary synthesis because it minimizes the steps, pursues multiple new bond formations in a single operation, addresses the waste of chemicals, and more importantly minimizes wasteful effort.[11]

In our previous work, we documented the synthetic application of the well-known aminating reagent hydroxylamine-*O*-sulfonic acid (HOSA) as a new redox-neutral directing group for the one-pot synthesis of isoquinoline from readily available aryl ketones.[8f] In our continuous pursuit to expand our stockpile of new synthetic applications of HOSA, we envisaged the possibility of using acetophenone and alkyne for the synthesis of poly-arylated aromatic hydrocarbons in a one-pot strategy through a cascade of triple C-H bond activations (Figure 3.1, b). Salient features of this methodology include (i) pot as well as step economic synthesis, (ii) a novel application of obscure redox-neutral directing group HOSA, (iii) cascade triple C-H bond functionalization, and (iv) four C-C and two C-N bond formations in a single operation.

3.3 RESULTS AND DISCUSSION

We commenced our investigation by taking acetophenone (**1a**), diphenylacetylene (**2a**) as model substrates, and HOSA as *N*-transfer reagent (Table 3.1). To our satisfaction, a preliminary attempt with 5 mol % of [Cp*RhCl$_2$]$_2$, 50 mol % of AgOAc as additive, and 2 equiv of Cu(OAc)$_2$ as oxidant in 1 mL of MeOH at 70 °C afforded a 30% isolated yield of the desired product **3aa** along with 12% of **4aa** (Table 3.1, entry 1). Addition of 1 equiv of AgOAc lowered the overall yields. As addition of extra additive gave a lower yield of

3aa (entry 2), we presumed that lowering the additive loading for the first annulation step could improve the yields.

Table 3.1 Optimization for One-pot synthesis of *N*-PAHs[a,b]
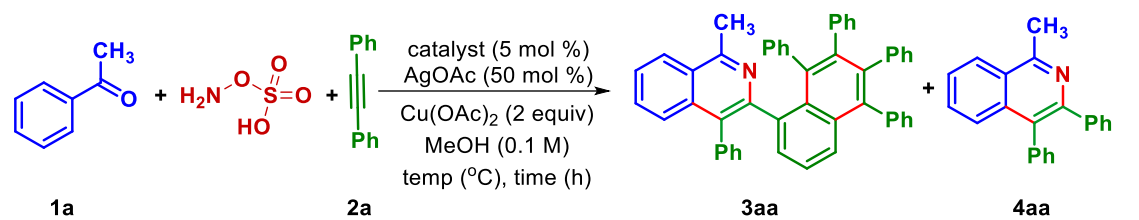
entry	catalyst	additive	oxidant	temp & time	(3aa/4aa)[b]
1	[Cp*Rh(Cl)₂]₂	AgOAc	Cu(OAc)₂	70°C, 12 h	30/12
2	[Cp*Rh(Cl)₂]₂	AgOAc (100 mol %)	Cu(OAc)₂	70°C, 12 h	25/14
3[c]	[Cp*Rh(Cl)₂]₂	AgOAc	Cu(OAc)₂	70°C, 12 h	21/57
4[c]	[Cp*Rh(Cl)₂]₂	AgOAc	Cu(OAc)₂	100°C, 12 h	27/22
5[c]	[Cp*Rh(Cl)₂]₂	AgOAc	Cu(OAc)₂	110°C, 12 h	61/11
6[c]	[Cp*Rh(Cl)₂]₂	AgOAc	Cu(OAc)₂	120°C, 12 h	34/18
7[c]	[Cp*Rh(Cl)₂]₂	AgOAc	Cu(OAc)₂ (1)	110°C, 12 h	23/60
8[c]	[Cp*Rh(Cl)₂]₂	AgOAc	Cu(OAc)₂ (1.5)	110°C, 12 h	46/37
9[c]	[Cp*Rh(Cl)₂]₂	AgOAc	Cu(OAc)₂ (2.5)	110°C, 12 h	55/trace
10[c,d]	**[Cp*Rh(Cl)₂]₂**	**AgOAc**	**Cu(OAc)₂**	**110°C, 18 h**	**71**/trace
11[c,e]	[Cp*Rh(Cl)₂]₂	AgOAc	Cu(OAc)₂	110°C, 18 h	21/nd
12[c,f]	[Cp*Rh(Cl)₂]₂	AgOAc	Cu(OAc)₂	110°C, 18 h	nd/50
13[c,g]	[Cp*Rh(Cl)₂]₂	AgOAc	Cu(OAc)₂	110°C, 18 h	nd/nd
14[c]	[Cp*Rh(CH₃CN)₃][SbF₆]₂	-	Cu(OAc)₂	110°C, 18 h	11/67
15[c]	[Cp*Co(CO)I₂	AgOAc	Cu(OAc)₂	110°C, 18 h	nd/nd
16[c]	[RuCl₂(*p*-cymene)]₂	AgOAc	Cu(OAc)₂	110°C, 18 h	nd/nd
17[c]	[Cp*Rh(Cl)₂]₂	-	Cu(OAc)₂	110°C, 18 h	nd/nd
18[c]	[Cp*Rh(Cl)₂]₂	AgOAc	-	110°C, 18 h	trace/85
19[c]	-	AgOAc	Cu(OAc)₂	110°C, 18 h	nd/nd

[a]Reaction conditions: **1a** (0.10 mmol), **2a** (0.45 mmol), HOSA (0.11 mmol), catalyst (5 mol %), AgOAc (50 mol %), solvent (0.1 M), temp (°C), 12 h. [b]NMR yields using 1,3,5-trimethoxybenzene as internal standard. [c]Reactions were heated at 70 °C for 5 h without Cu(OAc)₂, and then Cu(OAc)₂ was added followed by stirring. [d]Isolated yield. [e]DCE as the solvent. [f]CH₃CN as the solvent. [g]TFE as the solvent. nd = not detected.

To our satisfaction, when the oxidant, Cu(OAc)$_2$ was added after the complete conversion of acetophenone (5 h) to isoquinoline (**4aa**), we obtained 21% of **3aa** along with an improved yield of isoquinoline **4aa** to 57%, which is the active starting material for second and third C-H bond activations (Table 3.1, entry 3). Next, we moved to screen the reaction at different temperatures (Table 3.1, entries 4-6). From these screenings, 110 °C was found to be the optimal temperature (Table 3.1, entry 5). Several trials were performed to assess the influence of oxidant equivalents (Table 3.1, entries 7-9). It was observed that increasing or lowering the equivalents of oxidant did not improve the yield of **3aa**. A better yield of **3aa** was observed on increasing the reaction time to 18 h with almost total consumption of the starting material (entry 10). The reaction failed to produce better results when we attempted to replace MeOH by DCE, CH$_3$CN, and TFE (Table 3.1, entries 11-13). The replacement of the catalytic system [Cp*RhCl$_2$]$_2$ and AgOAc with the cationic rhodium catalyst [Cp*Rh(CH$_3$CN)$_3$][SbF$_6$]$_2$ had a deleterious impact on the reaction, resulting in only 11% of **3aa** (Table 3.1, entry 14). Similarly, attempts to replace the catalyst [Cp*RhCl$_2$]$_2$ by [Cp*Co(CO)I$_2$] and [RuCl$_2$(*p*-cymene)]$_2$ resulted in complete loss of reactivity (Table 3.1, entries 15 and 16). Next, to check the influence of [Cp*RhCl$_2$]$_2$, AgOAc and Cu(OAc)$_2$ on the reaction, three control experiments were carried out (Table 3.1, entries 17-19). The reaction did not furnish isoquinoline **4aa** in the absence of silver additive (Table 3.1, entry 17). This indicates that AgOAc is playing a major role to make the active catalyst Cp*Rh(OAc)$_2$. Moreover, the presence of Cu(OAc)$_2$ is also essential as oxidant to regenerate the catalyst (Table 3.1, entry 18). Similarly, we did not observe the formation of **3aa** in absence the of [Cp*RhCl$_2$]$_2$ (Table 3.1, entry 19).

With the obtained optimized reaction conditions, we began examining various substituted acetophenones. We were pleased to see that this protocol is quite general with many

structurally and electronically diverse compounds.

Scheme 3.1 Evaluation of Arylketones for One-Pot Synthesis of *N*-PAHs[a,b]

3aa, 71%
1 mmol scale: 65%

R = Me, 3ba, 60%
= OMe, 3ca, 95%
= SMe, 3da, 57%

3ea, 57%

R[2] = F, 3fa, 45%
= Br, 3ga, 67%
= I, 3ha, 62%

R = Me, 3ia, 80%
= Br, 3ja, 14%

3ka, 66%

3la, 78%

3ma, 63%

3na, 64%

3oa, 31%

X = O, 3pa, 50%
= S, 3qa, 61%

3ra, 75%

3sa, 55%

R[1] = H, 3ta, nr. R[1] = C$_2$H$_5$, 3ua, 53%
= CH(Me)$_2$, 3va, trace
= Ph, 3wa, nr. R[1] = CF$_3$, 3xa, nr

3cb, 30%
CCDC 2036625

R = OMe, 3ac, trace
= Me, 3ad, trace

3ae, 50%

3af, 53%

3cf, 43%
CCDC 2036544

R = H, 3ag, nr
= Ph, 3ah, nr

[a]Reaction conditions: **1a** (0.10 mmol), **2a** (0.45 mmol), HOSA (0.11 mmol), [Cp*RhCl$_2$]$_2$ (5 mol %), AgOAc (50 mol %), MeOH (0.1 M), 70-110 °C, 17-20 h. [b]Isolated yields.

Acetophenones bearing electron donating groups such as *p*-Me, *p*-OMe, *m*-Me, and *o*-OMe afforded good to excellent yields of the respective annulated products (Scheme 3.1, **3ba**, **3ca**, **3ia**, **3ka**). The protocol also worked smoothly with substrates bearing -thiomethyl, and -trifluoromethyl groups delivering 57% of yields of **3da,** and **3ea** respectively. Gratifyingly, substrates with readily transformable halogen substituents F, Br, I also behaved smoothly under the reaction conditions giving moderate to good yields of **3fa**, **3ga**, and **3ha**. This protocol was found compatible with a free hydroxy-substituent, affording 78% of **3la**. To make more conjugated molecules, we examined this protocol with 4-phenylacetophenone and 1-acetylnaphthalene which delivered their respective products **3ma** and **3na** in good yields. An acetophenone having a dioxolane ring reacted in a completely regioselective fashion yielding **3oa** in 31% yield. It is noteworthy that heteroaromatic aryl ketones such as furan, thiophene, and indole derivatives delivered their respective products **3pa**, **3qa**, and **3ra** in moderate to very good yields. It is worth mentioning that the unsymmetrical ketones **1i**, **1j**, **1l** and **1o** underwent annulation in a regioselective manner delivering their respective products **3ia**, **3ja**, **3la**, and **3oa**. Pleasingly, when 1-tetralone was subjected to the standard reaction conditions, a 55% yield of the corresponding *N*-PAH (**3sa**) was isolated. A variety of carbonyl compounds obtained by the replacement of the methyl group of acetophenone (**1t**, **1u**, **1v**, **1w,** and **1x**) was also investigated for the formation of *N*-PAHs under the standard reaction conditions. Of these carbonyl compounds, propiophenone (**1u**) was only successful in providing the desired *N*-PAHs (**3ua**).

To extend the generality of this protocol, various disubstituted alkynes were investigated. Diaryl alkynes such as 4,4'-dichlorodiphenylacetylene (**2b**) afforded the corresponding annulated product **3cb** in moderate yield. In contrast, alkynes having electron donating groups such as Me and OMe are very less reactive and produced **3ac**

and **3ad,** respectively in trace amounts. Taking advantage of the sequential addition of different alkynes, we proposed constructing unsymmetrical annulated products by using two different types of alkynes (alk-1 and alk-2). Gratifyingly, when **1a** was reacted with **2b** and **2a**, it delivered 50% of **3ae**. In similar vein, we were able to construct **3af** and **3cf**

Scheme 3.2 Mechanistic and Kinetic Experiments

a) Reaction of 1-methyl-3,4-diphenylisoquinoline in standard condition:

b) H/D scrambling experiment w/o alkyne:

c) H/D scrambling experiment in presence of alkyne:

d) Intermolecular kinetic isotope study:
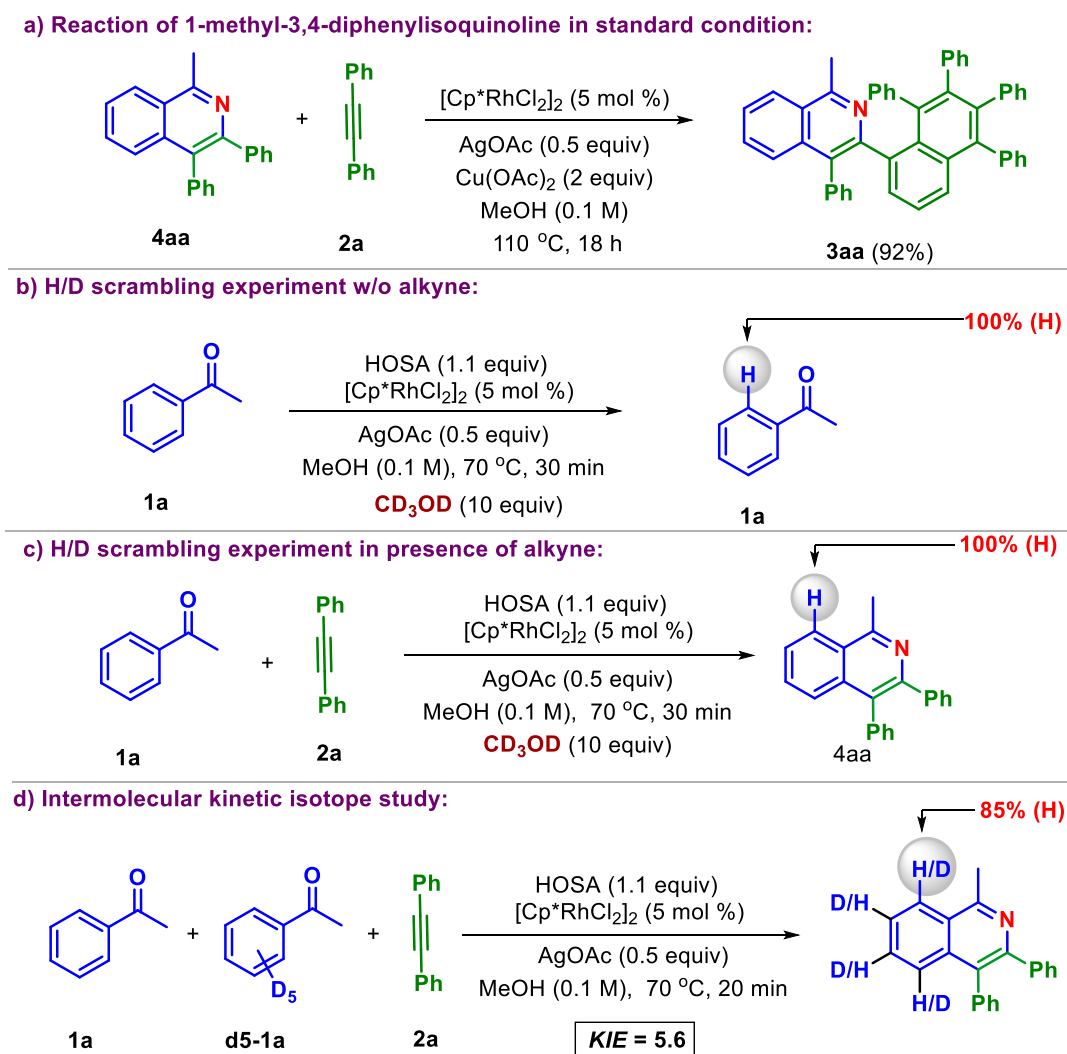
in 53% and 43% yields respectively. Unfortunately, terminal alkynes failed to produce **3ag** and **3ah** under the standard reaction conditions. To show the synthetic utility of this protocol further, a 1 mmol scale reaction was performed, which gave 65% of **3aa** (Scheme 3.1).

To gain mechanistic insight, we have performed a range of experiments (Scheme 3.2). When 1-methyl-3,4-diphenylisoquinoline (**4aa**) was subjected to the standard reaction conditions, it afforded 92% of **3aa** (Scheme 3.2, a). This indicates that formation of **3aa** is proceeding through intermediate **4aa**. To understand the catalytic activity, further experiments were conducted (Scheme 3.2, b-d). No H/D scrambling could be confirmed at the *o*-position of acetophenone **1a** when the standard reaction was carried out with CD₃OD in the absence or presence of a coupling partner (Scheme 3.2, b-c). A kinetic isotope effect value of 5.6 was obtained for the intermolecular kinetic experiment (Scheme 3.2, d). All these experiments indicate that the Rh-catalysed C-H activation step is involved in the rate-limiting step.[12]

Scheme 3.3 Proposed Catalytic Cycle
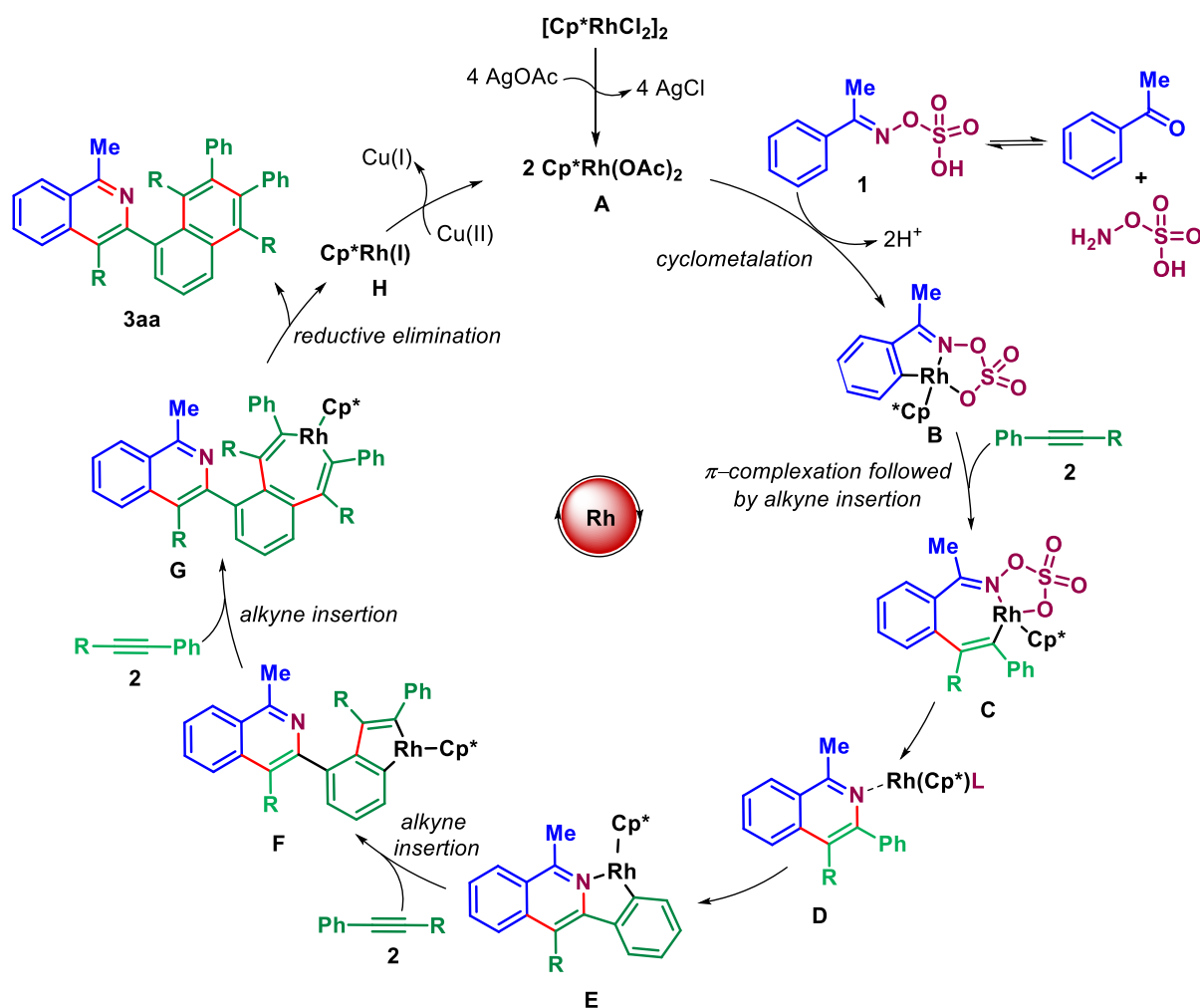
A plausible mechanism can be proposed for the formation of **3aa** based on the performed mechanistic experiments and previous literature reports (Scheme 3.3).[8f,10] At first, active rhodium catalyst **A** is generated from [Cp*RhCl$_2$]$_2$ and AgOAc, which then undergoes cyclometalation irreversibly with *in situ* generated imine **1,** giving the cyclometalated species **B**. Then coordination and insertion of alkyne into the C-Rh bond of **B** gives **C**, followed by cyclization in a redox-neutral manner to give the annulated product **D**. The catalyst activates the second C-H bond directed by the coordinating *N*-atom from isoquinoline. Subsequent insertion of 2 equiv. of alkyne leads to intermediates **F** and **G**. Intermediate **G** undergoes reductive elimination, affording **3aa** and Cp*Rh(I) catalyst, which is again reoxidized by Cu(II) salt, to participate in the next catalytic cycle.

3.4 CONCLUSION

In summary, we have presented a rhodium-catalysed one-pot synthesis of hetero-polycyclic aromatic hydrocarbons (N-PAHs) directly from various aryl-alkyl ketones and internal alkynes. Control experiments and mechanistic studies clarify the role of each reagent and details of the mechanism. This methodology tolerates a wide range of functional groups including a free hydroxy(-OH) group. The well-known amination reagent HOSA has been used here as *N*-transfer reagent, *in situ* directing group, traceless directing group and *in situ* oxidant. Moreover, the easily synthesizable highly arylated *N*-PAH products could be applicable in optoelectronics. We expect that this synthetic protocol could gain the attention of synthetic and material chemists significantly.

3.5 EXPERIMENTAL SECTION

Acetophenone derivatives were bought from Sigma Aldrich, Alfa-Aesar, Avra, TCI and Spectrochem, and used without any further purification. For column chromatography, silica gel (230-400 mesh) from Acme Co. was used. A gradient elution using distilled

hexane and ethyl acetate was performed, based on Merck aluminum TLC sheets. All isolated compounds were characterized by ^{1}H NMR, and ^{13}C NMR spectroscopy (Bruker-400 MHz) and HRMS. Copies of the ^{1}H NMR, ^{13}C NMR, and ^{19}F NMR can be found in Supporting Information. Nuclear magnetic resonance spectra were recorded on a Bruker 400 MHz instrument. HRMS signal analysis was performed using micro TOF Q-II mass spectrometer. X-ray analysis was conducted using Rigaku Smartlab X-ray diffractometer in our institute. All ^{1}H NMR experiments were reported in parts per million (ppm), and were measured relative to the signals for residual chloroform (7.26 ppm) in the deuterated solvent. All ^{13}C NMR spectra were reported in ppm relative to CDCl$_3$ (77.36 ppm). The starting materials 2b,[13] 2c,[13] 2d,[13] acetophenone-d_5,[14] and 4aa[8f] were prepared by following the reported procedure.

General procedure for Rhodium-Catalysed Annulation reaction (A):

To an oven-dried 25 mL Schlenk tube, charged with a magnetic stirring bar, were added dry MeOH (0.1 M, 1 mL), aryl ketone **1** (0.1 mmol, 1 equiv), and HOSA (0.11 mmol, 1.1 equiv) sequentially under a nitrogen atmosphere. To this solution, were added alkyne **2** (0.45 mmol, 4.5 equiv), [Cp*RhCl$_2$]$_2$ (0.005 mmol, 0.05 equiv), and AgOAc (0.05 mmol, 0.5 equiv). Then the reaction mixture was stirred (500 rpm) at 70 $^\circ$C in a pre-heated aluminum block for 5-7 h and the reaction was monitored by TLC. After complete conversion of the aryl ketone to the corresponding isoquinoline, the reaction mixture was allowed to attain ambient temperature. To the reaction mixture, was added Cu(OAc)$_2$ (0.2 mmol, 2 equiv) under nitrogen atmosphere and the mixture again heated at 110 °C in a preheated aluminum block for 12-20 h, monitoring by TLC. After complete conversion, the reaction mixture was transferred into a 50 mL round-bottom flask. The reaction vial was washed twice or three times with ethyl acetate (10-15 mL). The solvent was removed under reduced pressure to obtain a crude residue that was triturated with ethyl acetate

(3×10 mL) and the extracts washed with saturated aqueous sodium bicarbonate (10 mL). After separation, the organic layer was dried over anhydrous Na_2SO_4, filtered, the solvent evaporated uder reduced pressure and the residue purified by column chromatography using 230-400 mesh silica, giving 46 mg (71%) of **3**.

General procedure for Rhodium-catalysed annulation reaction (B):

To an oven-dried 25 mL Schlenk tube, charged with a magnetic stirring bar, were added dry MeOH (0.1 M, 1 mL), aryl ketone **1** (0.11 mmol, 1.1 equiv), and HOSA (0.12 mmol, 1.2 equiv) sequentially under a nitrogen atmosphere. To this solution, were added the first alkyne **alk-1** (0.1 mmol, 1 equiv), [Cp*RhCl$_2$]$_2$ (0.005 mmol, 0.05 equiv), and AgOAc (0.05 mmol, 0.5 equiv). Then the reaction mixture was stirred (500 rpm) at 70 °C in a pre-heated aluminum block for 5-7 h and the reaction was monitored by TLC. After complete conversion of the aryl ketone to the corresponding isoquinoline, the reaction mixture was allowed to attain ambient temperature. To the above reaction mixture, were added the second alkyne **alk-2** (0.35 mmol, 3.5 equiv), Cu(OAc)$_2$ (0.2 mmol, 2 equiv) under a nitrogen atmosphere and the mixture was again heated at 110 °C in a preheated aluminum block for 12-20 h and monitored by TLC. After complete conversion, the reaction mixture was transferred into a 50 mL round-bottom flask and the reaction vial was washed twice or three times with ethyl acetate (10-15 mL). The solvent was removed under reduced pressure to afford a crude residue that was extracted with ethyl acetate (3×10 mL) and washed with saturated aqueous sodium bicarbonate (10 mL). The organic layer was separated, dried over anhydrous Na_2SO_4, filtered, the solvent was removed and the residue purified by column chromatography using 230-400 mesh silica, giving the corresponding *N*-PAH (**3ae**, **3af**, and **3cf**).

General procedure for 1 mmol scale reaction for the synthesis of 3aa:

To an oven-dried 25 mL Schlenk tube, charged with a magnetic stirring bar, were added dry MeOH (0.1 M, 10 mL), arylketone (1 mmol, 1 equiv), and hydroxylamine-O-sulfonic acid (1.1 mmol, 1.1 equiv) sequentially under a nitrogen atmosphere. To this solution, were added the alkyne (4.5 mmol, 4.5 equiv), [Cp*RhCl$_2$]$_2$ (0.05 mmol, 0.05 equiv), and AgOAc (0.5 mmol, 0.5 equiv). Then the reaction mixture was stirred (500 rpm) at 70 °C in a preheated aluminum block for 5 h and monitored by TLC. After complete conversion of the aryl ketone to the corresponding isoquinoline, the reaction mixture was allowed to attain ambient temperature. To the above reaction mixture, was added Cu(OAc)$_2$ (2 mmol, 2 equiv) under a nitrogen atmosphere and the mixture again heated at 110 °C in a preheated aluminum block for 18 h, monitoring by TLC. After complete conversion, the reaction mixture was transferred into a 50 mL round-bottom flask. The reaction vial was washed twoce or three times with ethyl acetate (20-30 mL) and the solvent was removed under reduced pressure to give a crude residue that was extracted with ethyl acetate (3×10 mL) and the extrtact washed with saturated aqueous sodium bicarbonate (10 mL). The organic layer was separated, dried over anhydrous Na$_2$SO$_4$, filtered, the solvent removed and the residue purified by column chromatography using 230-400 mesh silica, giving 422 mg (65%) of **3aa**.

Experimental characterization data of products:

1-Methyl-4-phenyl-3-(5,6,7,8-tetraphenylnaphthalen-1-yl)isoquinoline (**3aa**)[10]:
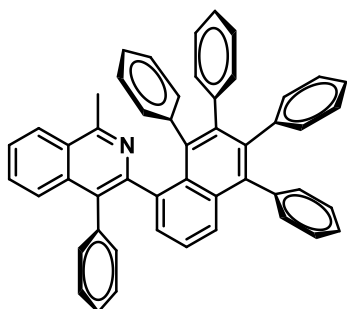
Prepared according to the general procedure A. **Physical State:** Pale brown solid (45 mg, 71% yield). R_f = 0.2 (10% EtOAc/hexane). **mp** 143–145°C. **^{1}H NMR (CDCl$_3$, 400 MHz):** δ 7.92–7.90 (m, 1H), 7.45–7.38 (m, 6H), 7.26–7.20 (m, 4H), 7.17–7.11 (m, 4H), 7.02 (t, J = 8.0 Hz, 2H), 6.91–6.88 (m, 1H), 6.85–6.82 (m, 1H), 6.79–6.66 (m, 9H), 6.54 (d, J = 4.0 Hz, 2H), 6.47 (t, J = 8.0 Hz, 1H), 6.12 (t, J = 8.0 Hz, 1H), 2.76 (s, 3H) ppm. **^{13}C{^{1}H} NMR (CDCl$_3$, 100 MHz):** δ 156.3, 141.1, 141.0, 140.9, 140.3 (2C), 138.5, 138.4, 137.9, 135.4, 133.6, 133.5, 132.2, 131.7, 131.6 (2C), 131.5, 131.4 (2C), 131.3, 131.2, 130.6, 130.4, 127.7, 127.6, 127.5, 127.4, 126.7 (2C), 126.6, 126.4, 126.3, 126.1, 126.0, 125.9, 125.5, 125.4, 125.3, 125.2, 124.8, 124.6, 22.3 ppm. **IR (KBr, cm^{-1}):** 3056, 2870, 1602, 1441. **HRMS (ESI) m/z:** [M+H]$^+$ calcd for C$_{50}$H$_{36}$N 650.2842; found 650.2878.

1,6-Dimethyl-4-phenyl-3-(5,6,7,8-tetraphenylnaphthalen-1-yl)isoquinoline (**3ba**)[10]:
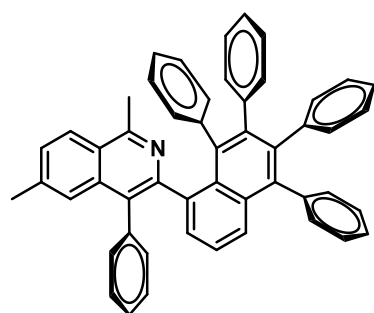
was prepared according to the general procedure A. **Physical State:** Brown solid (40 mg, 60% yield). R_f = 0.3 (10% EtOAc/hexane). **mp** 173–175 °C. **^{1}H NMR (CDCl$_3$, 400 MHz):** δ 7.80 (d, J = 8.0 Hz, 1H), 7.41–7.38 (m, 3H), 7.27 (d, J = 8.0 Hz, 2H), 7.23–7.19 (m, 4H), 7.16–7.10 (m, 4H), 7.02 (t, J = 8.0 Hz, 2H), 6.92 (t, J = 8.0 Hz, 1H), 6.85–6.83 (m, 1H), 6.79–6.77 (m, 3H), 6.74–6.67 (m, 6H), 6.53–6.48 (m, 3H), 6.13 (t, J = 8.0 Hz, 1H), 2.72 (s, 3H), 2.36 (s, 3H) ppm. **^{13}C{^{1}H} NMR (CDCl$_3$, 100 MHz):** δ 156.0, 141.1 (2C), 141.0, 140.3, 140.2, 138.5, 138.3, 137.9, 135.6, 133.6, 133.4, 132.3, 131.7,

131.6 (2C), 131.5, 131.4, 131.3, 131.2, 130.6, 130.4, 128.5, 127.8, 127.5, 127.3, 127.2, 126.7 (2C), 126.6, 126.5, 126.4, 126.1, 125.5, 125.4, 125.2 (2C), 124.9, 124.8, 124.6, 124.3, 22.3, 22.1 ppm. **IR (KBr, cm^{-1})**: 3054, 2868, 1600, 1440.

6-Methoxy-1-methyl-4-phenyl-3-(5,6,7,8-tetraphenylnaphthalen-1-yl)isoquinoline
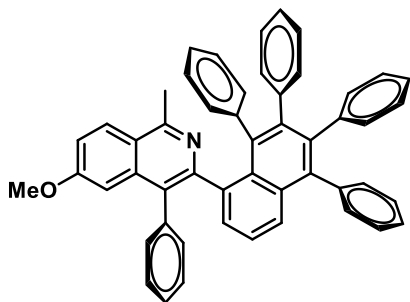
(**3ca**)[10]: was prepared according to the general procedure A. **Physical State:** Pale yellow solid (65 mg, 95% yield). R_f = 0.2 (20% EtOAc/hexane). **mp** 144–146 °C. **^{1}H NMR (CDCl$_3$, 400 MHz)**: δ 7.77 (d, J = 8.0 Hz, 1H), 7.39–7.34 (m, 3H), 7.21–7.16 (m, 4H), 7.10 (q, J = 8.0 Hz, 4H), 7.03–6.99 (m, 3H), 6.91–6.87 (m, 1H), 6.83–6.79 (m, 1H), 6.75–6.73 (m, 3H), 6.70–6.62 (m, 7H), 6.53–6.48 (m, 3H), 6.16 (t, J = 8.0 Hz, 1H), 3.64 (s, 3H), 2.67 (s, 3H) ppm. **^{13}C{^{1}H} NMR (CDCl$_3$, 100 MHz)**: δ 160.4, 155.6, 141.0 (2C), 140.9, 140.3, 140.2, 138.5, 138.2, 137.9, 137.8, 137.3, 133.6, 133.4, 132.2, 131.6, 131.4 (2C), 131.3 (2C), 131.1, 130.6, 130.2, 127.7, 127.6, 127.5, 127.4, 127.2, 126.7, 126.6 (2C), 126.4, 126.0, 125.4 (2C), 125.1, 124.9, 124.6, 121.6, 118.3, 104.4, 55.4, 22.2 ppm. **IR (KBr, cm^{-1})**: 3055, 2868, 1618, 1441, 1028.
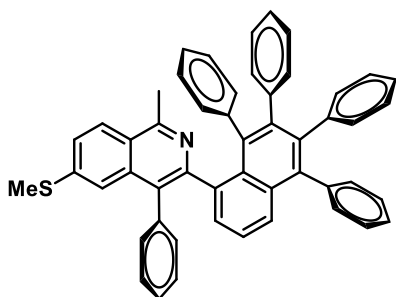
1-Methyl-6-(methylthio)-4-phenyl-3-(5,6,7,8-tetraphenylnaphthalen-1-yl)isoquinoline

(**3da**): was prepared according to the general procedure A. **Physical State:** Pale yellow solid (40 mg, 57% yield). R_f=: 0.2 (10% EtOAc/hexane). **mp** 145–147 °C. **^{1}H NMR (CDCl$_3$, 400 MHz)**: δ 7.78 (d, J = 8.0 Hz, 1H), 7.43–7.38 (m, 3H), 7.29 (dd, J = 8.0 Hz, 4 Hz, 1H), 7.25–7.21 (m, 4H), 7.17–7.10 (m, 5H), 7.03–6.98 (m, 2H), 6.91 (t, J = 8.0 Hz, 1H), 6.87–6.83 (m, 1H), 6.79–6.67 (m, 9H), 6.56–6.50 (m, 3H), 6.18 (t, J = 8.0 Hz, 1H), 2,69 (s, 3H), 2.32 (s, 3H) ppm. **^{13}C{^{1}H} NMR**

(CDCl₃, 100 MHz): δ 156.0, 152.7, 141.1, 141.0, 140.9, 140.2 (2C), 139.2, 138.5, 138.3, 137.8, 137.4, 135.7, 133.6, 133.4, 132.2, 131.6, 131.5, 131.4 (2C), 131.3 (2C), 131.1, 130.6, 130.3, 128.4, 127.7, 127.6, 127.5, 127.3, 127.2, 126.7 (2C), 126.5, 126.4, 126.0, 125.6, 125.5, 125.4, 125.2, 125.0, 124.9, 124.6, 123.5, 120.3, 22.2, 15.1 ppm. **IR (KBr, cm⁻¹)**: 3055, 2837, 1601, 1440. **HRMS (ESI) m/z**: [M+H]⁺ calcd for $C_{51}H_{38}NS$ 696.2719; found 696.2690.

1-Methyl-4-phenyl-3-(5,6,7,8-tetraphenylnaphthalen-1-yl)-6-(trifluoromethyl)
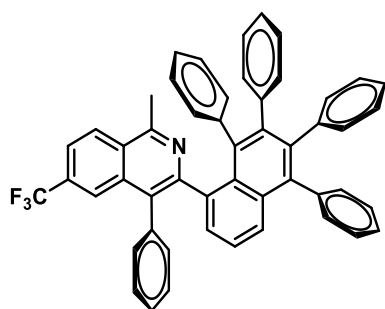
isoquinoline (**3ea**)[10]: was prepared according to the general procedure A. **Physical State:** Pale yellow solid (25 mg, 57% yield). **R**$_f$ = 0.3 (10% EtOAc/hexane). **mp** 119–121 °C. **¹H NMR (CDCl₃, 400 MHz)**: δ 8.02 (d, *J* = 8.8 Hz, 1H), 7.76 (s, 1H), 7.62 (dd, *J* = 8.4 Hz, 1.2 Hz, 1H), 7.45 (dd, *J* = 8.4 Hz, 1.2 Hz, 1H), 7.40–7.36 (m, 2H), 7.30–7.11 (m, 9H), 7.04 (d, *J* = 7.2 Hz, 1H), 6.99 (d, *J* = 7.6 Hz, 1H), 6.89 (t, *J* = 7.6 Hz, 1H), 6.85–6.82 (m, 1H), 6.78–6.76 (m, 2H), 6.74–6.66 (m, 6H), 6.56–6.52 (m, 2H), 6.47 (t, *J* = 7.6 Hz, 1H), 6.13 (t, *J* = 7.6 Hz, 1H), 2.78 (s, 3H) ppm. **¹³C{¹H} NMR (CDCl₃, 100 MHz)**: δ 156.5, 153.6, 141.1, 141.0, 140.8, 140.6, 140.2, 138.8, 138.7, 138.6, 137.7, 136.5, 134.7, 133.8, 133.6, 132.1, 131.6 (2C), 131.5, 131.4, 131.3, 131.1, 131.0, 130.7, 130.3, 130.0, 127.9, 127.8, 127.7, 127.6 (2C), 127.2, 126.9 (q, $J_{C\text{-}F}$ = 270.8 Hz), 126.8, 126.6 (2C), 126.5, 126.1, 125.6, 125.5, 125.3, 125.0, 124.6, 123.8 (q, $J_{C\text{-}F}$ = 4.0 Hz), 121.9 (q, $J_{C\text{-}F}$ = 2.9 Hz), 22.5 ppm. **¹⁹F NMR (CDCl₃, 376 MHz)**: δ -62.7 ppm. **IR (KBr, cm⁻¹)**: 3057, 2852, 1601, 1441, 1311.

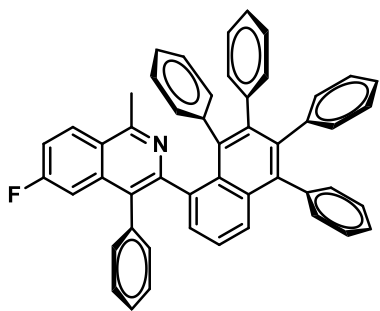*6-Fluoro-1-methyl-4-phenyl-3-(5,6,7,8-tetraphenylnaphthalen-1-yl)isoquinoline*

(**3fa**)[10]: was prepared according to the general procedure A. **Physical State:** Brown

solid (30 mg, 45% yield). **R$_f$ =** 0.3 (10% EtOAc/hexane)**. mp** 135–137 °C. **^{1}H NMR (CDCl$_3$, 400 MHz)**: δ 7.94–7.90 (m, 1H), 7.44–7.36 (m, 3H), 7.28 (d, J = 8.0 Hz, 1H), 7.23–7.19 (m, 3H), 7.17–7.12 (m, 5H), 7.06–6.97 (m, 3H), 6.89–6.82 (m, 2H), 6.79–6.70 (m, 8H), 6.66 (d, J = 8.0 Hz, 1H), 6.59–6.54 (m, 2H), 6.48 (t, J = 8.0 Hz, 1H), 6.19–6.16 (m, 1H), 2.73 (s, 3H) ppm. **^{13}C{^{1}H} NMR (CDCl$_3$, 100 MHz)**: δ 163.1 (d, J_{C-F} = 248.0 Hz), 156.2, 153.0, 141.1, 141.0, 140.9, 140.4, 140.2, 139.9, 138.6, 138.4, 137.8, 137.3 (d, J_{C-F} = 10.0 Hz), 137.2, 133.7, 133.5, 132.0, 131.6 (2C), 131.5, 131.4 (d, J_{C-F} = 3 Hz), 131.3, 131.2, 130.7, 130.2, 128.3 (2C), 127.8, 127.6 (d, J_{C-F} = 3.0 Hz), 127.5, 126.9, 126.7 (d, J_{C-F} = 3.0 Hz), 126.6 (2C), 126.5, 126.0, 125.5, 125.4, 125.2, 124.9, 124.6, 123.2, 116.3 (d, J_{C-F} = 25 Hz), 109.7 (d, J_{C-F} = 22 Hz), 22.5 ppm. **^{19}F NMR (CDCl$_3$, 376 MHz)**: δ -108.6 ppm. **IR (KBr, cm^{-1})**: 3055, 2852, 1601, 1400, 1188.

6-Bromo-1-methyl-4-phenyl-3-(5,6,7,8-tetraphenylnaphthalen-1-yl)isoquinoline **(3ga)***:*

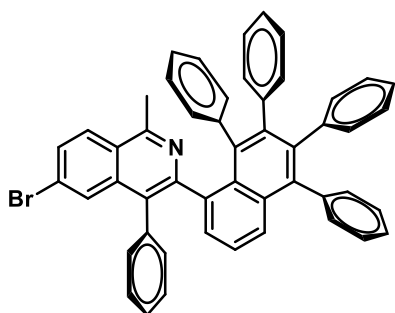was prepared according to the general procedure A. **Physical State:** Pale yellow solid (49 mg, 67% yield). **R$_f$ =** 0.3 (10% EtOAc/hexane)**.mp** 113–115 °C. **^{1}H NMR (CDCl$_3$, 400 MHz)**: δ 7.74 (d, J = 8.0 Hz, 1H), 7.55 (d, J = 4.0 Hz, 1H), 7.49 (dd, J = 8.8 Hz, 0.8 Hz, 1H), 7.41–7.36 (m, 2H), 7.35 (dd, J = 6.8 Hz, 0.8 Hz, 1H), 7.28 (d, J = 8 Hz, 1H), 7.20 (dt, J = 7.2 Hz, 2.4 Hz, 3H), 7.13–7.12 (m, 3H), 7.09–7.07 (m, 1H), 7.01–6.96 (m, 2H), 6.89 (t, J = 8.0 Hz, 1H), 6.84–6.80 (m, 1H), 6.76–6.71 (m, 3H), 6.69–6.65 (m, 5H), 6.61 (d, J = 4.0 Hz, 1H), 6.54–6.47 (m, 3H), 6.16 (t, J = 8.0 Hz, 1H), 2.70 (s, 3H) ppm. **^{13}C{^{1}H}**

NMR (CDCl$_3$, 100 MHz): δ 156.4, 153.2, 141.1, 141.0, 140.8, 140.4, 140.2, 138.8, 138.6, 138.4, 137.7, 136.8, 136.7, 133.7, 133.5, 132.1, 131.6, 131.5, 131.4 (2C), 131.3 (2C), 131.1, 130.6, 130.3, 129.7, 128.2, 127.8, 127.6 (2C), 127.5, 127.1, 127.0, 126.7 (2C), 126.6 (2C), 126.5, 126.1, 125.7, 125.5, 125.2, 125.0, 124.6, 124.3, 22.4 ppm. **IR (KBr, cm^{-1})**: 3056, 2852, 1599, 1441, 652. **HRMS (ESI) m/z**: [M+H]$^+$ calcd for C$_{50}$H$_{35}$BrN 728.1947; found 728.1949. **m/z**: [M+H]$^+$ calcd for C$_{50}$H$_{35}$Br^{81}N 730.1931; found, 730.1943.

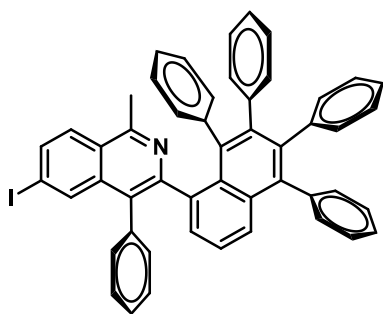*6-Iodo-1-methyl-4-phenyl-3-(5,6,7,8-tetraphenylnaphthalen-1-yl)isoquinoline* **(3ha):** was prepared according to the general procedure A. **Physical State:** Pale yellow solid (48 mg, 62% yield). **R$_f$** = 0.3 (10% EtOAc/hexane). **mp** 117–119 °C. **^{1}H NMR (CDCl$_3$, 400 MHz)**: δ 7.82 (d, J = 1.6 Hz, 1H), 7.72 (dd, J = 8.8 Hz, 1.6 Hz, 1H), 7.61 (d, J = 8.8 Hz, 1H), 7.42 (dd, J = 8.4 Hz, 1.2 Hz, 1H), 7.36 (dd, J = 6.8 Hz, 1.6 Hz, 1H), 7.30–7.28 (m, 1H), 7.23–7.22 (m, 1H), 7.21–7.20 (m, 1H), 7.17–7.14 (m, 2H), 7.13–7.10 (m, 2H), 7.02 (d, J = 7.6 Hz, 1H), 6.98 (td, J = 7.6 Hz, 1.2 Hz, 1H), 6.92–6.88 (m, 1H), 6.86–6.83 (m, 1H), 6.79–6.75 (m, 4H), 6.73–6.66 (m, 7H), 6.54–6.49 (m, 3H), 6.18–6.14 (m, 1H), 2.70 (s, 3H) ppm. **^{13}C{^{1}H} NMR (CDCl$_3$, 100 MHz)**: δ 156.5, 141.1, 141.0, 140.8, 140.4, 140.2, 138.6, 138.4, 137.7, 136.8 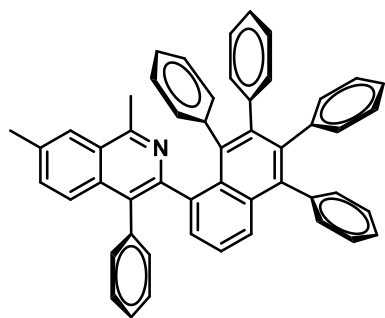(2C), 135.1, 134.8, 133.6, 133.4, 132.1, 131.6 (2C), 131.5 (2C), 131.4, 131.3 (2C), 131.1, 130.6, 130.3, 127.8, 127.7, 127.6, 127.4, 126.9, 126.8, 126.7(2C), 126.6, 126.5, 126.1, 125.7, 125.4, 125.2, 125.0, 124.6, 97.2, 22.2 ppm. **IR (KBr, cm^{-1})**: 3056, 2856, 1592, 1440, 583. **HRMS (ESI) m/z**: [M+H]$^+$ calcd for C$_{50}$H$_{35}$IN 776.1809; found 776.1793.

1,7-Dimethyl-4-phenyl-3-(5,6,7,8-tetraphenylnaphthalen-1-yl)isoquinoline (**3ia**):[10] was
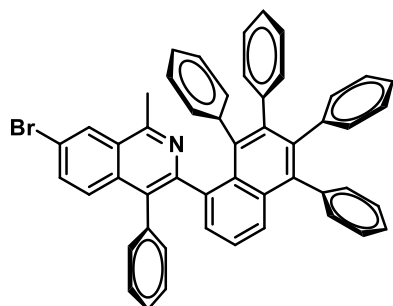
prepared according to the general procedure A. **Physical State:** Pale yellow solid (53 mg, 80% yield). R_f = 0.2 (10% EtOAc/hexane). **mp** 152–154 °C. **^{1}H NMR (CDCl$_3$, 400 MHz)**: δ 7.66 (s, 1H), 7.42–7.32 (m, 4H), 7.28–7.25 (m, 2H), 7.22–7.18 (m, 3H), 7.15–7.10 (m, 4H), 7.01 (dd, J = 16.0 Hz, 8.0 Hz, 2H), 6.88 (t, J = 8.0 Hz, 1H), 6.84–6.82 (m, 1H), 6.79–6.70 (m, 8H), 6.66 (d, J = 4.0 Hz, 1H), 6.55 (d, J = 8.0 Hz, 2H), 6.48 (t, J = 8.0 Hz, 1H), 6.16–6.13 (m, 1H), 2.71 (s, 3H), 2.49 (s, 3H) ppm. **^{13}C{^{1}H} NMR (CDCl$_3$, 100 MHz)**: δ 155.6, 151.1, 141.1, 141.0, 140.3, 140.2, 139.4, 138.5, 138.3, 137.9, 137.8, 135.9, 133.6, 133.5, 132.3, 131.7 (2C), 131.6 (2C), 131.5 (2C), 131.4, 131.3, 131.2, 130.6, 130.4, 129.2, 127.7, 127.5, 127.3, 127.2, 126.7 (2C), 126.5, 126.4, 126.1, 125.9, 125.5, 125.4, 125.1, 124.8, 124.6, 124.2, 22.4, 22.1 ppm. **IR (KBr, cm^{-1})**: 3055, 2917, 1601, 1410.

7-Bromo-1-methyl-4-phenyl-3-(5,6,7,8-tetraphenylnaphthalen-1-yl)isoquinoline (**3ja**):

was prepared according to the general procedure A. **Physical State:** Brown solid (10 mg, 14% yield). R_f = 0.2 (10% EtOAc/hexane). **mp** 140–142 °C. **^{1}H NMR (CDCl$_3$, 400 MHz)**: δ 8.05 (s, 1H), 7.50 (d, J = 8.8 Hz, 1H), 7.43 (d, J = 8.4 Hz, 1H), 7.39–7.31 (m, 4H), 7.23–7.21 (m, 3H), 7.18–7.12 (m, 5H), 7.03 (d, J = 7.6 Hz, 1H), 6.98 (d, J = 7.6 Hz, 1H), 6.90 (t, J = 7.6 Hz, 1H), 6.84–6.82 (m, 1H), 6.80–6.79 (m, 2H), 6.74–6.69 (m, 5H), 6.65 (d, J = 7.2 Hz, 1H), 6.56–6.50 (m, 3H), 6.20–6.18 (m, 1H), 2.70 (s, 1H) ppm. **^{13}C{^{1}H} NMR (CDCl$_3$, 100 MHz)**: δ 155.4, 152.5, 141.1, 141.0, 140.9, 140.4, 140.2, 138.8, 138.7,

138.4, 137.0, 134.0, 133.7, 133.5, 132.9, 132.0, 131.6 (2C), 131.4, 131.3, 131.2, 130.6, 130.3, 128.1, 127.8, 127.7, 127.6, 127.5 (2C), 127.0, 126.9, 126.8, 126.7, 126.6, 126.5, 126.1, 125.6, 125.5, 125.2, 125.1, 124.6, 120.2, 22.4 ppm. **IR (KBr, cm⁻¹)**: 3055, 2852, 1601, 1408, 651. **HRMS (ESI) m/z**: [M+H]⁺ calcd for $C_{50}H_{35}BrN$ 728.1947; found 728.1987. **m/z**: [M+H]⁺ calcd for $C_{50}H_{35}Br^{81}N$ 730.1931; found, 730.1980.

8-Methoxy-1-methyl-4-phenyl-3-(5,6,7,8-tetraphenylnaphthalen-1-yl)isoquinoline
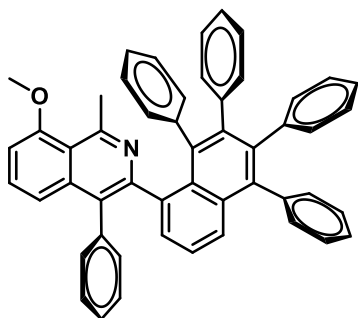
(**3ka**): was prepared according to the general procedure A. **Physical State:** Pale yellow solid (45 mg, 66% yield). R_f = 0.2 (10% EtOAc/hexane). **mp** 273–275 °C. **¹H NMR (CDCl₃, 400 MHz)**: δ 7.41–7.34 (m, 3H), 7.28 (t, J = 8.0 Hz, 1H), 7.22–7.09 (m, 8H), 7.01 (dd, J = 16.0 Hz, 8.0 Hz, 2H), 6.91 (dd, J = 16.0 Hz, 8.0 Hz, 2H), 6.85–6.81 (m, 1H), 6.78–6.66 (m, 10H), 6.58–6.55 (m, 2H), 6.51 (t, J = 8.0 Hz, 1H), 6.22–6.19 (m, 1H), 3.92 (s, 3H), 2.89 (s, 3H) ppm. **¹³C{¹H} NMR (CDCl₃, 100 MHz)**: δ 158.1, 156.1, 152.0, 141.1, 141.0, 140.9, 140.3, 140.2, 139.3, 138.5, 138.3, 138.2, 138.0, 133.6, 133.4, 132.1, 131.7, 131.6 (2C), 131.5, 131.4 (2C), 131.3, 131.2, 130.6, 130.3, 129.5, 128.5, 127.7, 127.5, 127.3, 127.2, 126.7, 126.6, 126.5 (2C), 126.4, 126.0, 125.4 (2C), 125.1, 124.9, 124.6, 118.9, 118.3, 105.8, 55.8, 28.9 ppm. **IR (KBr, cm⁻¹)**: 3055, 2877, 2837, 1611, 1440, 1027. **HRMS (ESI) m/z**: [M+H]⁺ calcd for $C_{51}H_{38}NO$ 680.2948; found 680.2932.

1,7-Dimethyl-4-phenyl-3-(5,6,7,8-tetraphenylnaphthalen-1-yl)isoquinolin-6-ol (**3la**):

was prepared according to the general procedure A. **Physical State:** Pale brown solid (53 mg, 78% yield). R_f =: 0.2 (30% EtOAc/hexane). **mp** 242–244 °C. **¹H NMR (CDCl₃, 400**
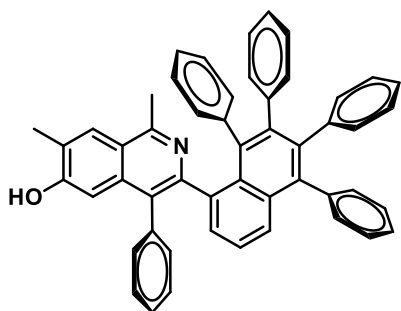
MHz): δ 7.55 (s, 1H), 7.27 (d, J = 8.4 Hz, 1H), 7.17–7.09 (m, 4H), 7.05 (d, J = 6.8 Hz, 1H), 7.02–7.00 (m, 1H), 6.98–6.91 (m, 3H), 6.89–6.85 (m, 1H), 6.81–6.75 (m, 6H), 6.71–6.65 (m, 5H), 6.63–6.60 (m, 1H), 6.59 (s, 1H), 6.54–6.49 (m, 3H), 6.45 (d, J = 7.6 Hz, 1H), 6.16–6.13 (m, 1H), 2.50 (s, 3H), 2.31 (s, 3H) ppm. **¹³C{¹H} NMR (CDCl₃, 100 MHz)**: δ 154.4, 141.0 (2C), 140.9, 140.2, 140.1, 138.3, 138.1, 137.9, 137.8, 136.4, 133.6, 133.2, 132.5, 131.6, 131.4 (2C), 131.3, 131.2, 130.5, 129.8, 128.5, 127.7, 127.5 (2C), 127.2, 127.0, 126.9, 126.7 (2C), 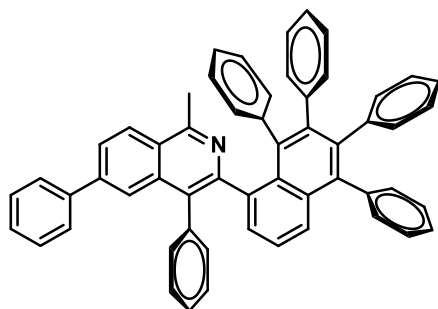126.6, 126.5, 126.4, 126.1 (2C), 125.5, 125.4, 125.2, 124.9, 124.2, 121.3, 107.3, 21.0, 17.2 ppm. **IR (KBr, cm⁻¹)**: 3443, 3056, 2868, 1440. **HRMS (ESI) m/z**: [M+H]⁺ calcd for C₅₁H₃₈NO 680.2948; found 680.2906.

1-Methyl-4,6-diphenyl-3-(5,6,7,8-tetraphenylnaphthalen-1-yl)isoquinoline (**3ma**): was prepared according to the general procedure A. **Physical State:** Pale yellow solid (45 mg, 63% yield). **R**$_f$ = 0.2 (10% EtOAc/hexane). **mp** 155–157 °C. **¹H NMR (CDCl₃, 400 MHz)**: δ 8.03 (d, J = 8.0 Hz, 1H), 7.76 (s, 1H), 7.62 (dd, J = 12.0 Hz, 4.0 Hz, 1H), 7.45 (dd, J = 12.0 Hz, 4.0 Hz, 1H),7.40–7.36 (m, 2H), 7.29–7.13 (m, 11H), 7.04 (d, J = 8.0 Hz, 1H), 6.99 (d, J = 8.0 Hz, 1H), 6.90 (t, J = 8.0 Hz, 1H), 6.86–6.83 (m, 1H), 6.80–6.66 (m, 11H), 6.55–6.52 (m, 2H), 6.48 (t, J = 8.0 Hz, 1H), 6.13 (t, J = 8.0 Hz, 1H), 2.78 (s, 3H) ppm. **¹³C{¹H} NMR (CDCl₃, 100 MHz)**: δ 156.2, 153.2, 140.8, 140.6, 140.5, 140.2, 139.8, 138.4, 138.3, 138.2, 137.3, 136.1, 134.3, 133.4, 133.2, 131.7, 131.3, 131.2, 131.1 (2C), 131.0, 130.8, 130.3, 130.0, 129.6, 127.5 (2C), 127.4, 127.3 (2C), 126.9, 126.4 (2C), 126.3 (2C), 126.2, 125.8, 125.3, 125.2, 125.0, 124.7, 124.3, 123.4 (2C), 121.6

(2C), 22.2 ppm. **IR (KBr, cm^{-1})**: 3056, 2857, 1600, 1441. **HRMS (ESI) m/z**: [M+H]$^+$ calcd for C$_{56}$H$_{40}$N 726.3155; found 726.3129.
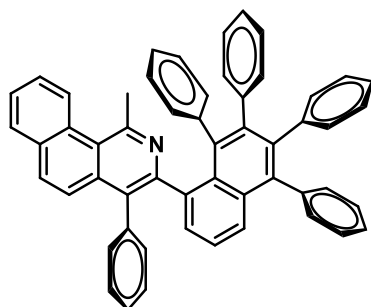
1-Methyl-4-phenyl-3-(5,6,7,8-tetraphenylnaphthalen-1-yl)benzo[h]isoquinoline (**3na**): was prepared according to the general procedure A. **Physical State:** Brown solid (45 mg, 64% yield). **R$_f$** = 0.2 (10% EtOAc/hexane)**. mp** 258–259 °C. **^{1}H NMR (CDCl$_3$, 400 MHz)**: δ 8.62 (d, J = 12.0 Hz, 1H), 7.84 (d, J = 8.0 Hz, 1H), 7.69 (t, J = 8.0 Hz, 1H), 7.65–7.58 (m, 2H), 7.53 (d, J = 8.0 Hz, 1H), 7.42 (d, J = 8.0 Hz, 1H), 7.35 (d, J = 8.0 Hz, 1H), 7.33–7.25 (m, 3H), 7.24–7.20 (m, 2H), 7.16–7.09 (m, 4H), 7.03 (d, J = 8.0 Hz, 1H), 7.00–6.95 (m, 2H), 6.87–6.83 (m, 1H), 6.78–6.65 (m, 9H), 6.56–6.44 (m, 2H), 6.39 (d, J = 8.0 Hz, 1H), 5.95 (t, J = 8.0 Hz, 1H), 3.08 (s, 3H) ppm. **^{13}C{^{1}H} NMR (CDCl$_3$, 100 MHz)**: δ 154.1, 153.5, 141.0 (2C), 140.8, 140.2, 138.5, 138.3, 137.8 (2C), 136.1, 133.4 (2C), 133.0, 132.3, 131.6 (2C), 131.5 (2C), 131.4, 131.3 (2C), 131.0, 130.9, 130.7, 130.5, 130.4, 129.9, 128.8, 127.8, 127.6, 127.5, 127.4, 127.3, 126.7 (3C), 126.6 (3C), 126.5, 126.4, 126.2, 125.8, 125.4, 125.2, 124.6 (2C), 124.3, 123.8, 29.9 ppm. **IR (KBr, cm^{-1})**: 3054, 2856, 1601, 1440. **HRMS (ESI) m/z**: [M+H]$^+$ calcd for C$_{54}$H$_{38}$N 700.2999; found 700.2983.

6-Methyl-9-phenyl-8-(5,6,7,8-tetraphenylnaphthalen-1-yl)-[1,3]dioxolo[4,5-
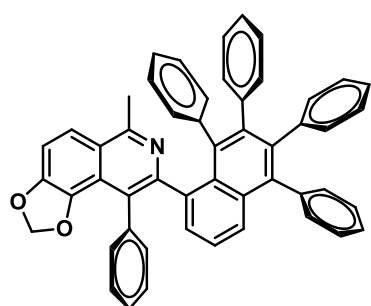
f]isoquinoline (**3oa**): was prepared according to the general procedure A. **Physical State:** Brown solid (21 mg, 31% yield). **R$_f$** = 0.5 (30% EtOAc/hexane)**. mp** 155–157 °C. **^{1}H NMR (CDCl$_3$, 400 MHz)**: δ 7.54 (d, J = 8.0 Hz, 1H), 7.39 (dd, J = 8.0 Hz, 4.0 Hz, 1H), 7.36–

7.33 (m, 1H), 7.31 (dd, J = 7.2 Hz, 1.2 Hz, 1H), 7.23–7.19 (m, 2H), 7.17–7.10 (m, 6H), 7.05–7.00 (m, 2H), 6.98 (d, J = 8.0 Hz, 1H), 6.91 (t, J = 8.0 Hz, 1H), 6.87–6.83 (m, 1H), 6.79–6.68 (m, 9H), 6.64 (d, J = 8.0 Hz, 1H), 6.55–6.51 (m, 2H), 6.22 (t, J = 8.0 Hz, 1H), 5.83 (d, J = 1.2 Hz, 1H), 5.73 (d, J = 1.2 Hz, 1H), 2.67 (s, 3H) ppm. **^{13}C{^{1}H} NMR (CDCl$_3$, 100 MHz)**: δ 156.4, 152.6, 147.4, 141.1, 141.0 (2C), 140.3, 140.2, 138.5, 138.4, 138.3, 137.9, 133.7, 133.4,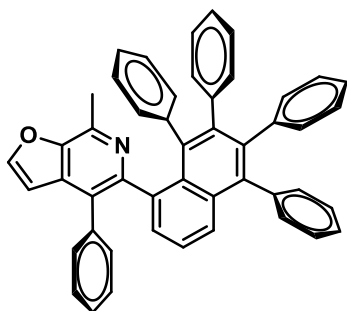 132.3, 131.6 (2C), 131.5, 131.4, 131.3 (2C), 131.1 (2C), 130.7, 130.3, 127.7, 127.5, 127.2, 126.7 (2C), 126.6, 126.5, 126.4, 126.3, 126.2, 126.0, 125.6, 125.4, 125.2, 124.9, 124.5, 123.2, 121.9, 120.7, 110.5, 101.5, 23.1 ppm. **IR (KBr, cm^{-1})**: 3054, 2873, 1600, 1441, 1278. **HRMS (ESI) m/z**: [M+H]$^+$ calcd for C$_{51}$H$_{36}$NO$_2$ 694.2741; found 694.2727.

7-Methyl-4-phenyl-5-(5,6,7,8-tetraphenylnaphthalen-1-yl)furo[2,3-c]pyridine (**3pa**): was prepared according to the general procedure A. **Physical State:** Pale yellow solid (32 mg, 50% yield). **R$_f$** = 0.3 (10% EtOAc/hexane)**. mp** 239–241 °C. **^{1}H NMR (CDCl$_3$, 400 MHz)**: δ 7.58 (d, J = 2.0 Hz, 1H), 7.54 (d, J = 8.0 Hz, 1H), 7.38 (d, J = 8.0 Hz, 1H), 7.29 (t, J = 8.0 Hz, 1H), 7.23–7.11 (m, 8H), 7.07–7.04 (m, 2H), 6.92 (d, J = 4.0 Hz, 1H), 6.83 (d, J = 8.0 Hz, 2H), 6.78–6.63 (m, 8H), 6.57–6.50 (m, 4H), 6.34 (t, J = 8.0 Hz, 1H), 2.56 (s, 3H) ppm. **^{13}C{^{1}H} NMR (CDCl$_3$, 100 MHz)**: δ 151.4, 149.4, 147.2, 141.0 (2C), 140.9, 140.6, 140.3, 140.1, 139.0, 138.7, 138.5, 137.6, 137.5, 133.8, 133.5, 133.0, 131.9, 131.7, 131.6 (2C), 131.5, 131.4, 131.2 (2C), 130.4, 130.1, 127.8 (2C), 127.6 (2C), 126.9, 126.8, 126.7, 126.6 (2C), 126.5, 126.3, 125.7, 125.4, 125.2, 125.1, 124.8 (2C), 106.6, 18.5 ppm. **IR (KBr, cm^{-1})**: 3056, 2853, 1601, 1441. **HRMS (ESI) m/z**: [M+H]$^+$ calcd for C$_{48}$H$_{34}$NO 640.2635; found 640.2646.

7-Methyl-4-phenyl-5-(5,6,7,8-tetraphenylnaphthalen-1-yl)thieno[2,3-c]pyridine
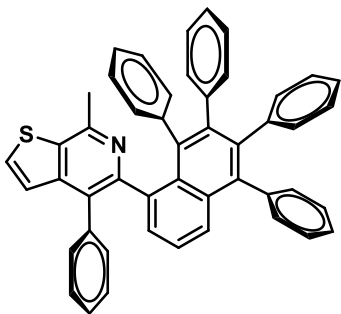
(3qa)[10]: was prepared according to the general procedure A. **Physical State:** Brown solid (43 mg, 61% yield). R_f = 0.3 (10% EtOAc/hexane). **mp** 110–112 °C. **^{1}H NMR (CDCl3, 400 MHz)**: δ 7.49 (d, J = 8.0 Hz, 1H), 7.45 (d, J = 5.2 Hz, 1H), 7.37 (d, J = 6.0 Hz, 1H), 7.28–7.13 (m, 10H), 7.09–7.04 (m, 2H), 6.93 (d, J = 4.0 Hz, 1H), 6.86–6.80 (m, 2H), 6.78–6.67 (m, 7H), 6.62–6.61 (m, 2H), 6.55–6.50 (m, 2H), 6.25 (t, J = 8.0 Hz, 1H), 2.59 (s, 3H) ppm. **^{13}C{^{1}H} NMR (CDCl3, 100 MHz)**: δ 152.9, 150.1, 144.6, 141.0 (3C), 140.5, 140.3, 138.8, 138.7, 138.5, 138.1, 137.7, 133.9, 133.7, 133.5, 132.1, 131.6 (2C), 131.5, 131.4, 131.3, 131.2, 130.5, 130.2, 128.3, 127.8, 127.7, 127.6, 126.8, 126.7, 126.6 (2C), 126.5, 126.4, 125.7, 125.4, 125.2 (2C), 124.7, 124.6, 124.3, 23.4 ppm. **IR (KBr, cm[-1])**: 3054, 2855, 1600, 1440.

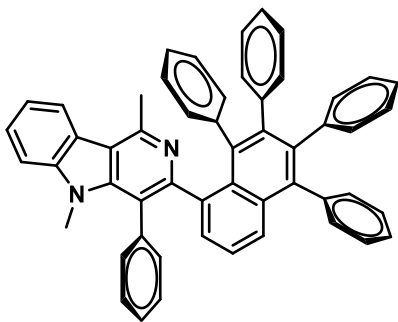## 1,5-Dimethyl-4-phenyl-3-(5,6,7,8-tetraphenylnaphthalen-1-yl)-5H-pyrido[4,3-b]indole

(3ra)[10]: was prepared according to the general procedure A. **Physical State:** Brown solid (53 mg, 75% yield). R_f = 0.5 (50% EtOAc/hexane). **mp** 124–126 °C. **^{1}H NMR (CDCl3, 400 MHz)**: δ 8.08 (d, J = 8.0 Hz, 1H), 7.47 (t, J = 8.0 Hz, 1H), 7.43–7.40 (m, 2H), 7.34–7.28 (m, 3H), 7.23–7.20 (m, 4H), 7.17–7.12 (m, 4H), 7.06 (d, J = 8.0 Hz, 1H), 7.01 (d, J = 8.0 Hz, 1H), 6.85–6.77 (m, 5H), 6.74–6.68 (m, 5H), 6.63 (d, J = 8.0 Hz, 1H), 6.59–6.57 (m, 1H), 6.44 (t, J = 8.0 Hz, 1H), 6.22 (t, J = 8.0 Hz, 1H), 3.12 (s, 3H), 2.86 (s, 3H) ppm. **^{13}C{^{1}H} NMR (CDCl3, 100 MHz)**: δ 154.9, 150.6, 143.3, 142.3, 141.1, 141.0, 140.9, 140.4, 140.3, 138.5, 138.4, 138.1, 133.8, 133.4, 132.4, 132.0, 131.6 (2C), 131.5, 131.4, 131.3, 131.2, 131.1, 130.6, 130.5, 127.8, 127.5 (2C), 127.2, 126.9, 126.8, 126.6

(2C), 126.5, 126.4, 126.0, 125.9, 125.4, 125.2, 124.7, 124.5, 122.4, 122.1, 120.6, 117.7, 116.8, 109.1, 32.4, 23.5 ppm. **IR (KBr, cm^{-1})**: 3055, 2852, 1601, 1441.

3-Phenyl-2-(5,6,7,8-tetraphenylnaphthalen-1-yl)-8,9-dihydro-7H-benzo[de]quinoline

(**3sa**)[10]: was prepared according to the general procedure A. **Physical State:** Brown solid (37 mg, 55% yield). **R$_f$** = 0.3 (50% EtOAc/hexane). **mp** 125–127°C. **^{1}H NMR (CDCl$_3$, 400 MHz)**: δ 7.43–7.39 (m, 3H), 7.36–7.32 (m, 1H), 7.28–7.24 (m, 4H), 7.22–7.19 (m, 2H), 7.17–7.14 (m, 2H), 7.12–7.09 (m, 2H), 7.04–6.99 (m, 2H), 6.92 (t, J = 7.6 Hz, 1H), 6.88–6.83 (m, 1H), 6.79–6.75 (m, 3H), 6.71–6.67 (m, 6H), 6.57–6.51 (m, 3H), 6.17 (t, J = 7.6 Hz, 1H), 3.09–3.00 (m, 4H), 2.14–2.10 (m, 2H) ppm. **^{13}C{^{1}H} NMR (CDCl$_3$, 100 MHz)**: δ 157.6, 141.2, 141.0, 140.9, 140.3, 140.2, 138.5, 138.3, 138.2, 137.8, 135.6, 133.5, 133.4, 132.3, 131.6, 131.5(2C), 131.4(2C), 131.3, 131.1, 130.7, 130.4, 127.7, 127.5, 127.3, 127.2, 126.7(2C), 126.5(2C), 126.4, 126.1, 125.5, 125.4, 125.2, 124.8, 124.6, 124.3, 123.6, 123.3, 34.3, 30.9, 23.5 ppm. **IR (KBr, cm^{-1})**: 3056, 2867, 1601, 1441.

1-Ethyl-4-phenyl-3-(5,6,7,8-tetraphenylnaphthalen-1-yl)isoquinoline
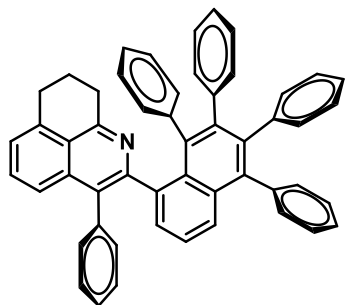
(**3ua**): was prepared according to the general procedure A. **Physical State:** Pale yellow solid (35mg, 53% yield). **R$_f$** = 0.2 (5% EtOAc/hexane). **mp:** 106–108 °C. **^{1}H NMR (CDCl$_3$, 400 MHz)**: δ 7.98–7.95 (m, 1H), 7.48–7.40 (m, 6H), 7.28–7.25 (m, 2H), 7.23–7.20 (m, 2H), 7.16–7.14 (m, 2H), 7.12–7.09 (m, 2H), 7.05 (t, J = 7.6 Hz, 1H), 6.98 (d, J = 7.6 Hz, 1H), 6.90–7.83 (m, 2H), 6.78–6.75 (m, 3H), 6.72–6.64 (m, 6H), 6.50–6.45 (m, 3H), 6.11 (t, J = 7.6 Hz, 1H),

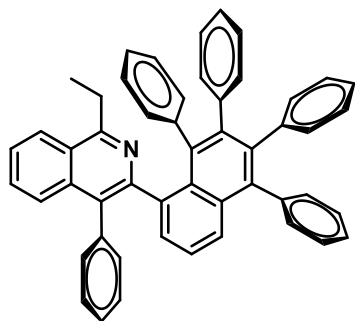3.29–3.20 (m, 1H), 3.03–2.94 (m, 1H), 1.38 (t, J = 7.6 Hz, 3H) ppm. ^{13}C{^{1}H} NMR (CDCl$_3$, 100 MHz): δ 161.0, 152.1, 141.1(2C), 141.0, 140.3, 140.1, 139.6, 138.4, 138.2, 137.8, 137.6, 135.6, 133.4, 132.3, 131.6, 131.5(2C), 131.4(2C), 131.3, 131.1, 130.6, 130.5, 129.3, 127.8, 127.5(2C), 127.2, 127.1, 126.7(2C), 126.6, 126.5(2C), 126.4(2C), 126.2, 126.1, 125.5, 125.4, 125.2, 125.1, 125.0, 124.6, 29.2, 14.3 ppm. IR (KBr, cm^{-1}): 3055, 2930, 1601, 1441. HRMS (ESI) m/z: [M+H]$^+$ calcd for C$_{51}$H$_{38}$N 664.2999; found 664.3055.

3-(4-Chloro-5,6,7,8-tetrakis(4-chlorophenyl)naphthalen-1-yl)-4-(4-chlorophenyl)-6-
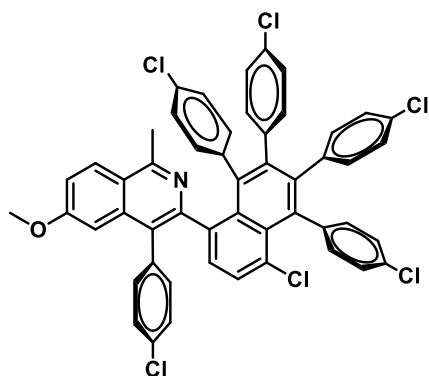
methoxy-1-methylisoquinoline (**3cb**): was prepared according to the general procedure A. **Physical State:** Pale yellow solid (26mg, 30% yield). **R$_f$** = 0.3 (20% EtOAc/hexane)**. mp** 128–130 °C. **^{1}H NMR (CDCl$_3$, 400 MHz)**: δ 7.94 (d, J = 9.2 Hz, 1H), 7.51–7.47 (m, 2H), 7.24 (d, J = 2.4 Hz, 1H), 7.19 (s, 2H), 7.15 (dd, J = 8.8 Hz, 2.4 Hz, 2H), 7.08 (d, J = 8.4 Hz, 1H), 6.99–6.94 (m, 2H), 6.86–6.79 (m, 4H), 6.77–6.73 (m, 2H), 6.67 (d, J = 2.4 Hz, 1H), 6.51–6.45 (m, 3H), 6.39 (d, J = 8.4 Hz, 1H), 6.25 (dd, J = 8.0 Hz, 2 Hz, 1H), 6.04–5.98 (m, 2H), 3.70 (s, 3H), 2.75 (s, 3H) ppm. ^{13}C{^{1}H} NMR (CDCl$_3$, 100 MHz): δ 161.0, 157.3, 139.2, 138.6, 138.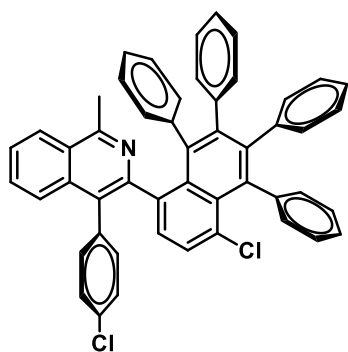2, 138.1, 137.7, 137.3, 136.4, 136.0, 135.6 (2C), 134.6, 132.9 (2C), 132.7, 132.5, 132.4, 132.3, 132.2, 132.1, 132.0, 131.9, 131.6, 131.4, 130.9, 130.4, 130.1, 129.1, 128.3, 128.1, 127.8 (2C), 127.7 (3C), 127.5 (2C), 127.2, 126.8, 121.5, 119.1, 103.6, 55.5, 22.1 ppm. IR (KBr, cm^{-1}): 2855, 1412, 1027, 771. HRMS (ESI) m/z: [M+H]$^+$ calcd for C$_{51}$H$_{32}$Cl$_6$NO 884.0610; found 884.0593.

3-(4-Chloro-5,6,7,8-tetraphenylnaphthalen-1-yl)-4-(4-chlorophenyl)-1-

methylisoquinoline (**3ae**): was prepared according to the general procedure B. **Physical State:** Pale yellow solid (36mg, 50% yield). R_f = 0.3 (20% EtOAc/hexane). **mp** 274–276 °C. **¹H NMR (CDCl₃, 400 MHz)**: δ 7.96–7.92 (m, 1H), 7.49–7.42 (m, 5H), 7.32–7.23 (m, 3H), 7.16–7.07 (m, 3H), 6.96–6.91 (m, 3H), 6.89–6.83 (m, 2H), 6.78–6.73 (m, 4H), 6.72–6.66 (m, 2H), 6.63–6.56 (m, 3H), 6.42 (dd, *J* = 8.0 Hz, 4Hz, 1H), 6.33 (d, *J* = 8.0 Hz, 1H), 6.07 (d, *J* = 8.0 Hz, 1H), 5.94 (t, *J* = 8.0 Hz, 1H), 2.69 (s, 3H) ppm. **¹³C{¹H} NMR (CDCl₃, 100 MHz)**: δ 157.2, 151.3, 141.3, 140.8, 140.6, 140.3, 140.0, 139.8, 138.9, 138.0, 136.3, 135.8, 135.7, 134.6, 133.4, 133.0, 132.2, 132.0, 131.8, 131.6 (2C), 131.4, 131.0, 130.5, 130.2, 130.0 (2C), 129.8, 128.9, 128.5, 128.1, 127.3, 127.2, 127.0, 126.9, 126.8, 126.7, 126.6, 126.3, 126.0, 125.8, 125.6, 125.5, 125.4, 125.2, 22.2 ppm. **IR (KBr, cm⁻¹)**: 3066, 2852, 1441, 696. **HRMS (ESI) m/z**: [M+H]⁺ calcd for $C_{50}H_{34}Cl_2N$ 718.2063; found 718.2028.

4-Ethyl-1-methyl-3-(5,6,7,8-tetraphenylnaphthalen-1-yl)isoquinoline (**3af**): was prepared according to the general procedure B. **Physical State:** Pale yellow solid (32mg, 53% yield). R_f = 0.2 (10% EtOAc/hexane). **mp** 240–242 °C. **¹H NMR (CDCl₃, 400 MHz)**: δ 7.91 (d, *J* = 8.0 Hz, 1H), 7.74 (d, *J* = 8.0 Hz, 1H), 7.68 (d, *J* = 8.0 Hz, 1H), 7.55–7.52 (m, 1H), 7.46–7.39 (m, 3H), 7.28–7.24 (m, 4H), 7.20–7.16 (m, 1H), 6.81–6.74 (m, 6H), 6.68–6.57 (m, 6H), 6.35–6.32 (m, 1H), 6.20 (t, *J* = 8.0 Hz, 1H), 5.95 (t, *J* = 8.0 Hz, 1H), 2.79 (s, 3H), 2.72 (q, *J* = 8.0 Hz, 1H), 2.62 (q, *J* = 8.0 Hz, 1H), 1.17 (t, *J* = 8.0 Hz, 3H) ppm. **¹³C{¹H} NMR (CDCl₃,**
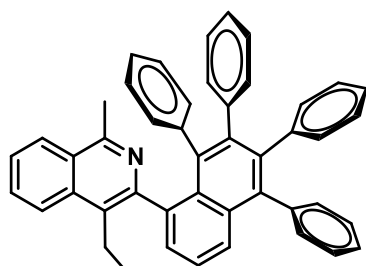
100 MHz): δ 154.9, 152.4, 141.3, 141.0 (2C), 140.6, 140.5, 140.1, 139.1, 138.6, 134.8, 133.9, 131.9, 131.8, 131.5 (2C), 131.4, 131.3 (2C), 130.5, 130.2 (2C), 129.4, 128.9, 128.2, 127.8, 127.7, 126.7, 126.6, 126.3, 126.2, 125.9, 125.8, 125.4, 125.1 (2C), 125.0, 124.6, 124.5, 123.8, 23.8, 22.4, 15.2 ppm. **IR (KBr, cm^{-1})**: 3056, 2873, 1601, 1441. **HRMS (ESI) m/z**: [M+H]$^+$ calcd for C$_{46}$H$_{36}$N 602.2842; found 602.2804.

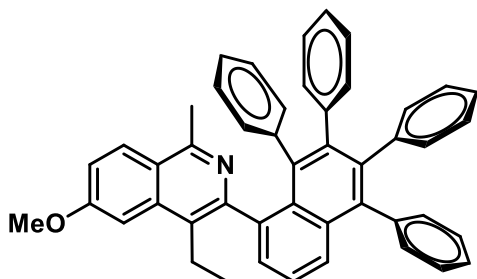***4-Ethyl-6-methoxy-1-methyl-3-(5,6,7,8-tetraphenylnaphthalen-1-yl)isoquinoline*** (**3cf**):

was prepared according to the general procedure B. **Physical State:** Brown solid (27 mg, 43% yield). **R$_f$** = 0.3 (20% EtOAc/hexane). **mp** 147–149 °C. **^{1}H NMR (CDCl$_3$, 400 MHz)**:

δ 7.82 (d, J = 8.0 Hz, 1H), 7.43 (dd, J = 8.4 Hz, 1.2 Hz, 1H), 7.45–7.41 (m, 1H), 7.38 (dd, J = 6.8 Hz, 1.2 Hz, 1H), 7.29–7.22 (m, 4H), 7.20–7.16 (m, 1H), 7.09 (dd, J = 9.2 Hz, 2.4 Hz, 1H), 6.92 (d, J = 2.4 Hz, 1H), 6.83–6.74 (m, 6H), 6.70–6.63 (m, 5H), 6.60–6.58 (m, 1H), 6.39–6.36 (m, 1H), 6.23 (t, J = 8.0 Hz, 1H), 6.01 (t, J = 7.6 Hz, 1H), 3.91 (s, 3H), 2.74 (s, 3H), 2.61 (q, J = 8.0 Hz, 2H), 1.17 (t, J = 8.0 Hz, 3H) ppm. **^{13}C{^{1}H} NMR (CDCl$_3$, 100 MHz)**: δ 160.3, 154.2, 141.3, 141.1, 141.0, 140.5, 139.1 (2C), 138.6, 136.7, 133.9, 131.9, 131.8, 131.6, 131.5, 131.4, 131.3, 131.2, 130.5, 130.2, 130.1, 128.2, 128.1, 127.9, 127.8, 127.7, 126.7, 126.6, 126.3, 126.2, 125.4, 125.1, 125.0, 124.8, 124.6 (2C), 122.4, 117.7, 102.4, 55.6, 23.9, 22.2, 14.6 ppm. **IR (KBr, cm^{-1})**: 3055, 2871, 1440, 1027. **HRMS (ESI) m/z**: [M+H]$^+$ calcd for C$_{47}$H$_{38}$NO 632.2948; found 632.2921.

NMR spectra of 1-methyl-4-phenyl-3-(5,6,7,8-tetraphenylnaphthalen-1-yl)isoquinoline (3aa):

3aa, ¹H NMR (CDCl₃, 400 MHz)

3aa, ¹³C{¹H} NMR (CDCl₃, 100 MHz)
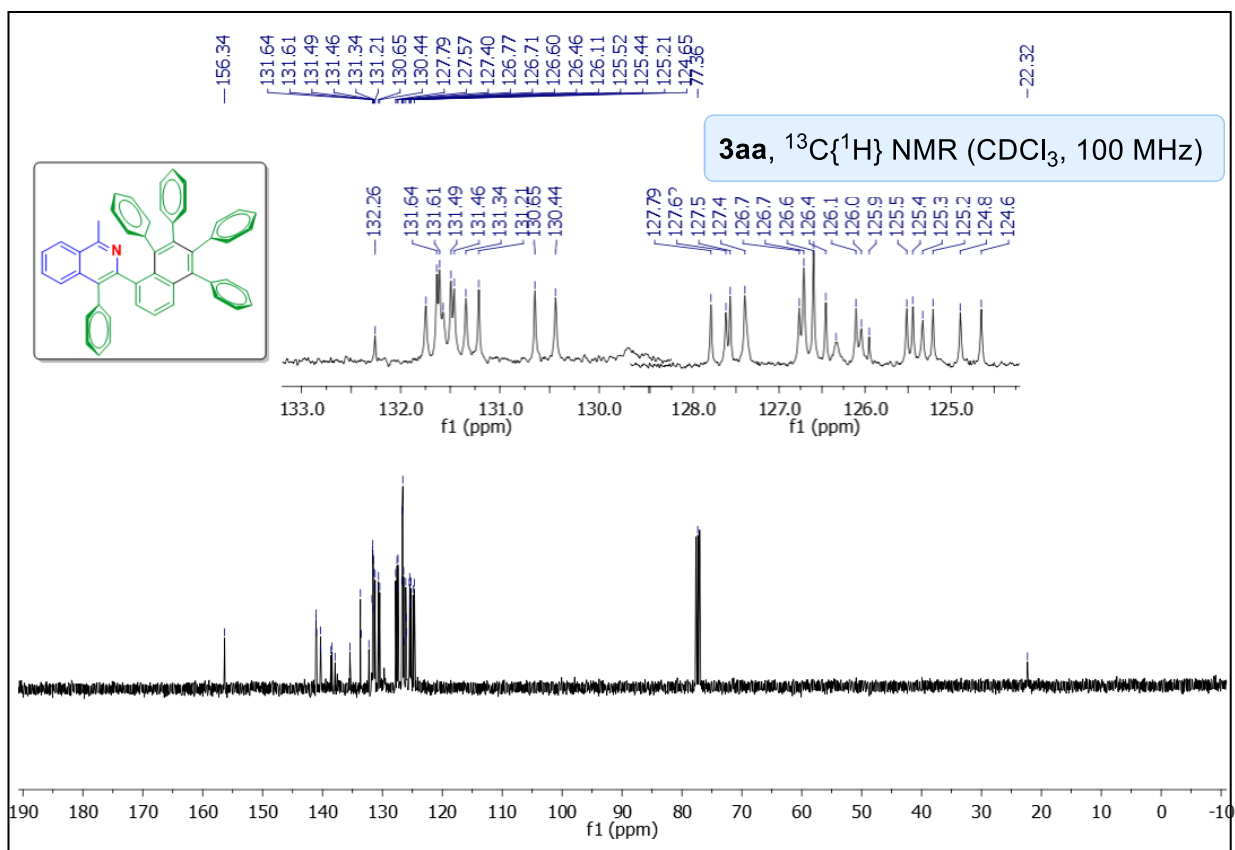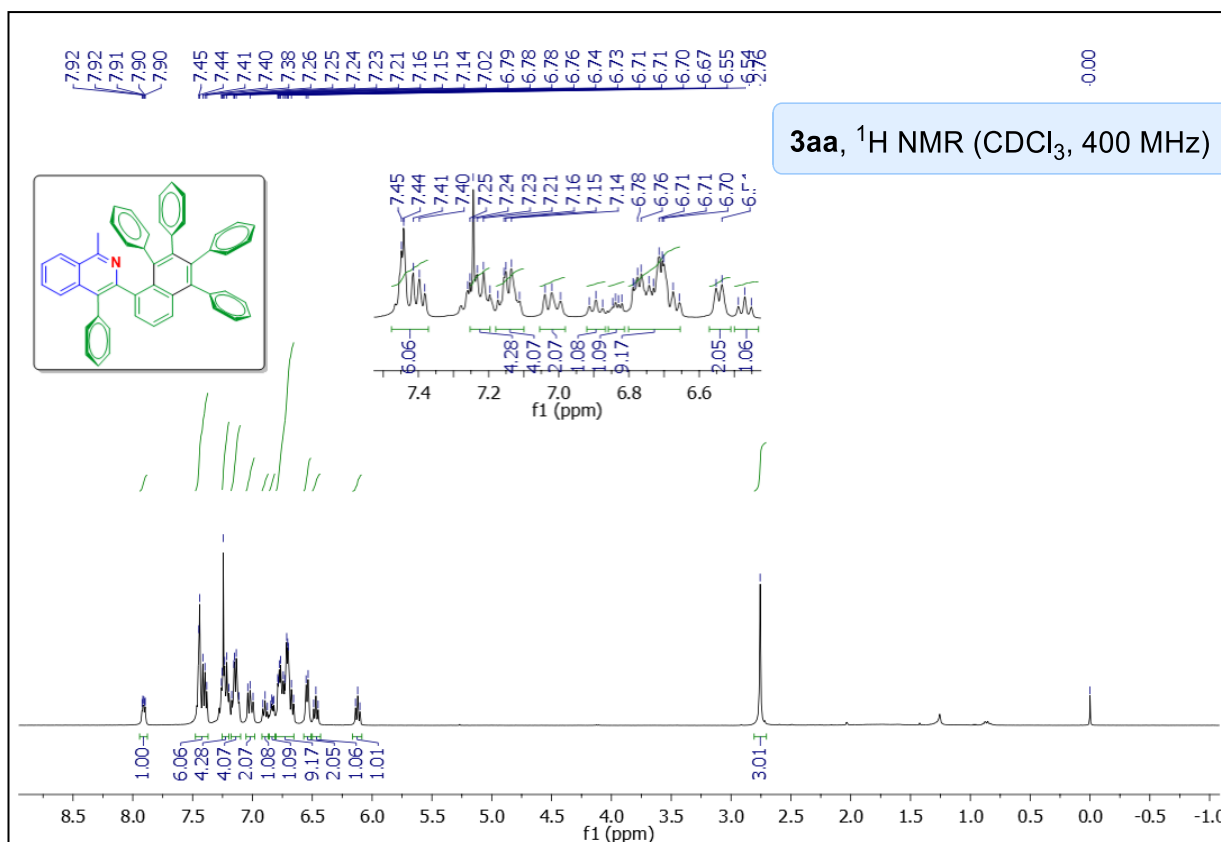
Single x-ray Crystal structure of 3pa

3pa ≡ **CCDC 2038561**
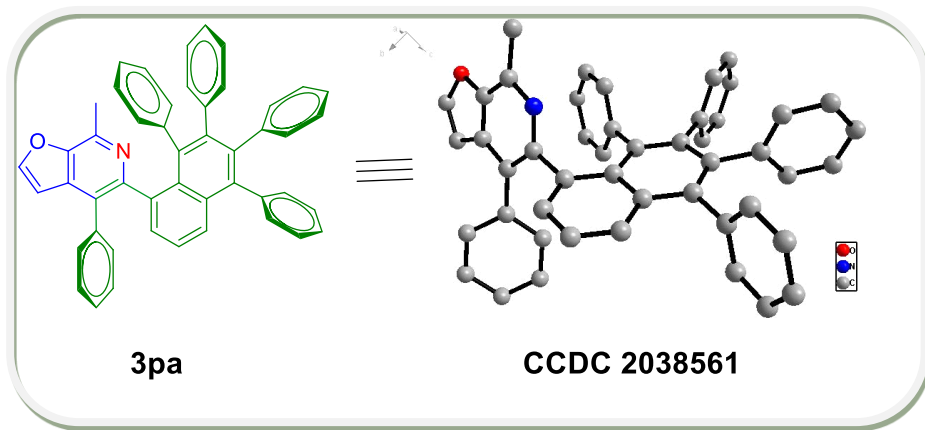
Datablock pcr-pb-1290 - ellipsoid plot

NOMOVE FORCED Prob = 50 Temp = 100

Z -100 pcr-pb-1290 P 1 21/n 1 R = 0.05 RES= 0 140 X
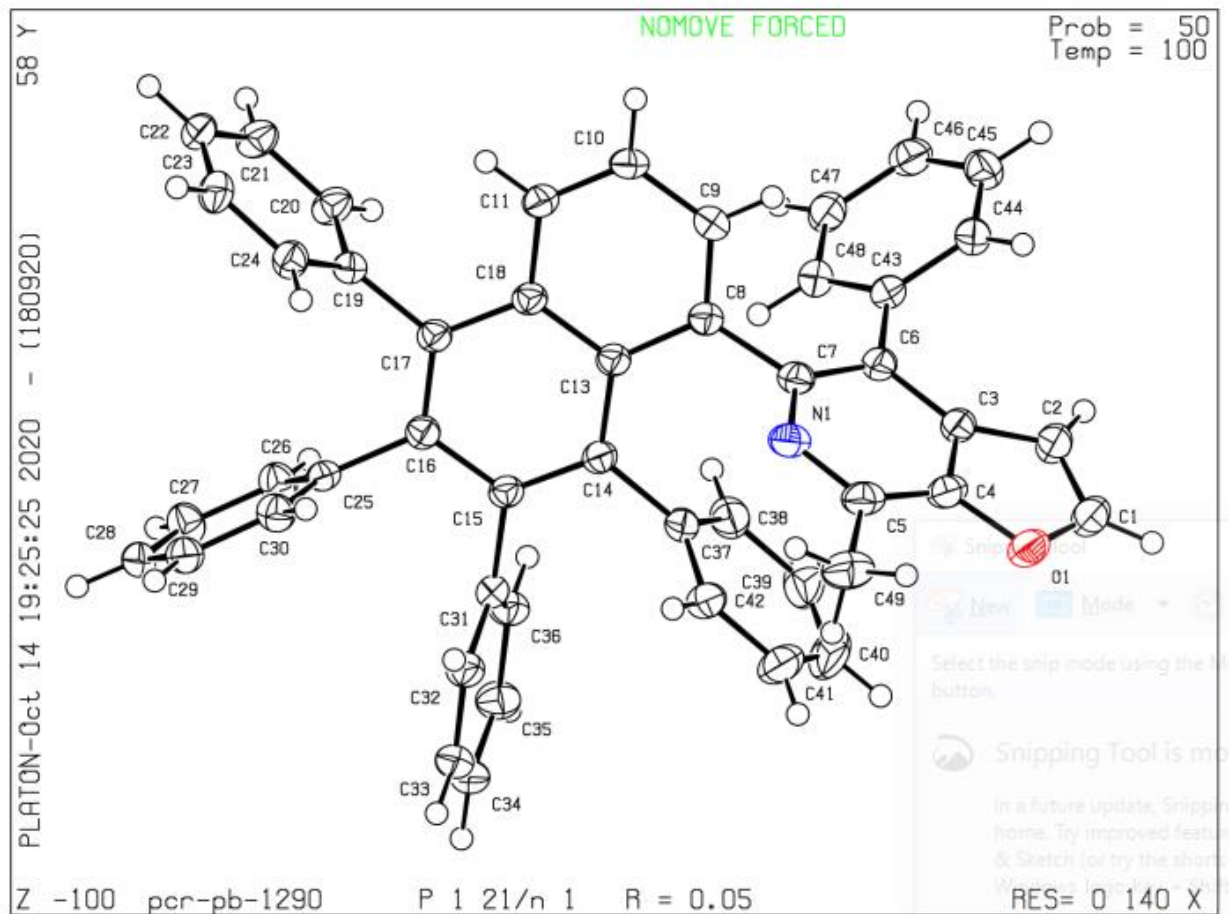
Single x-ray Crystal structure of 3cb

3cb

CCDC 2036625
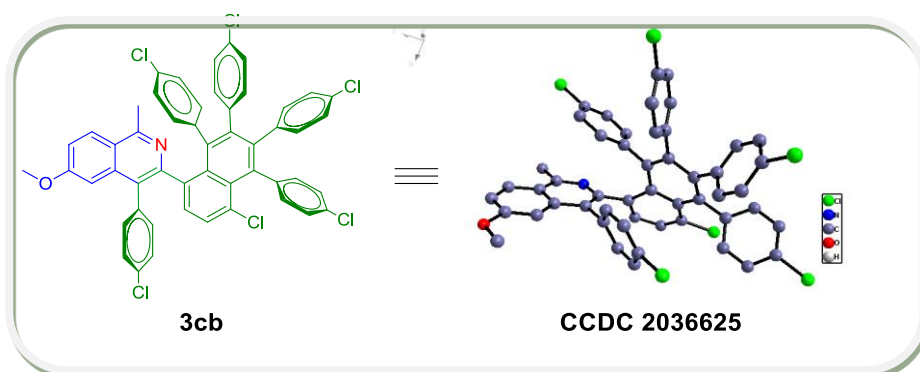
Datablock pcr-pb-1152-repeat - ellipsoid plot
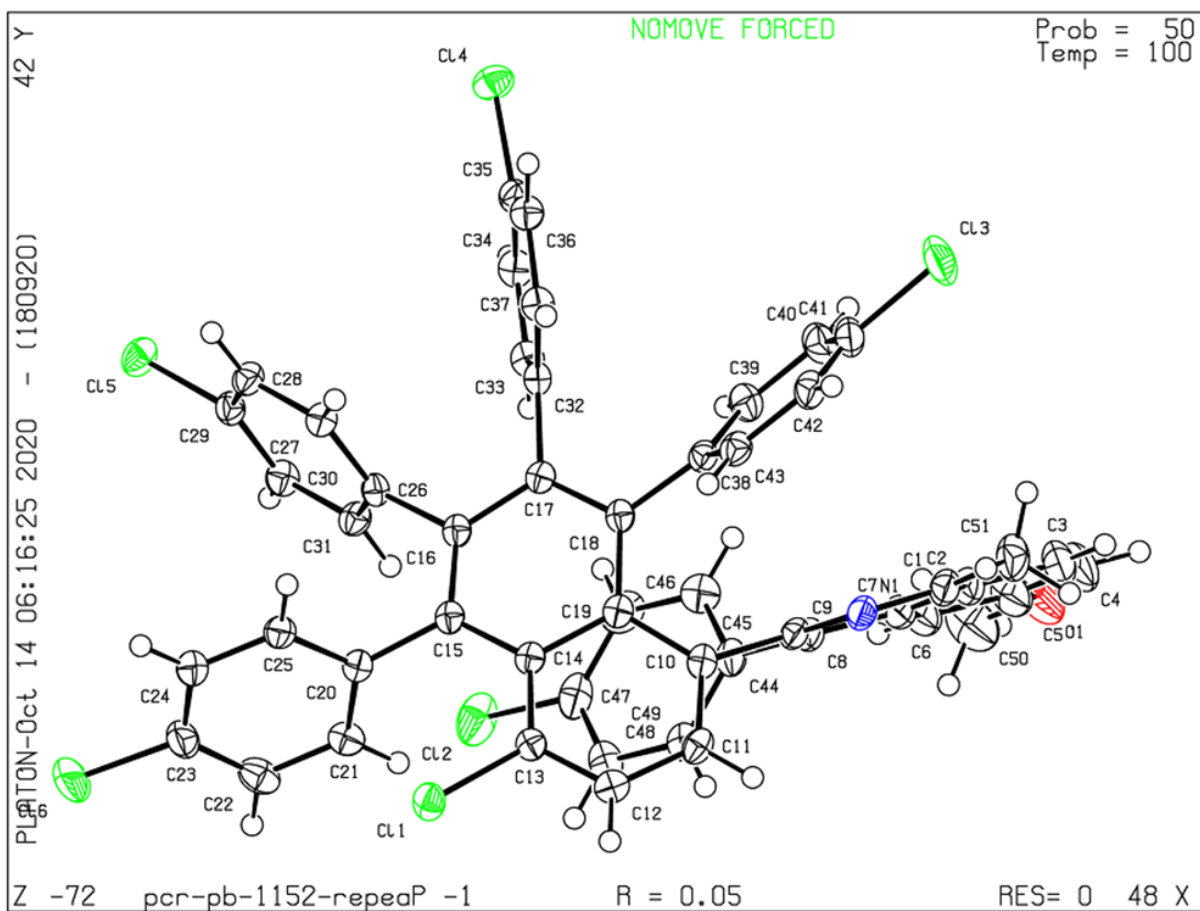
Single x-ray Crystal structure of 3cf

3cf   CCDC 2036544
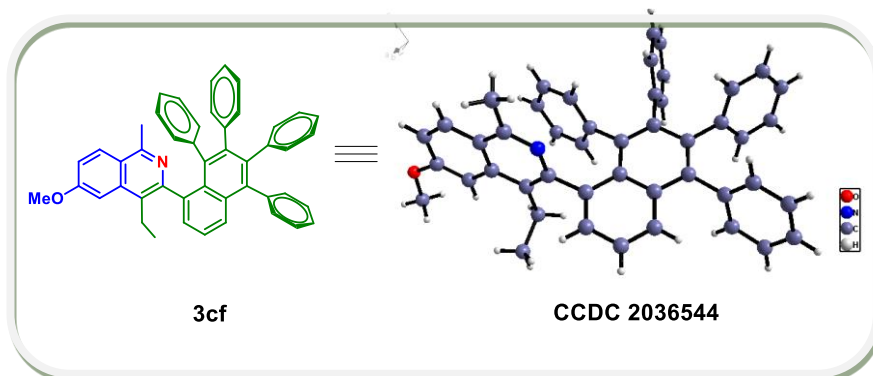
Datablock pcr-pb-1158 - ellipsoid plot
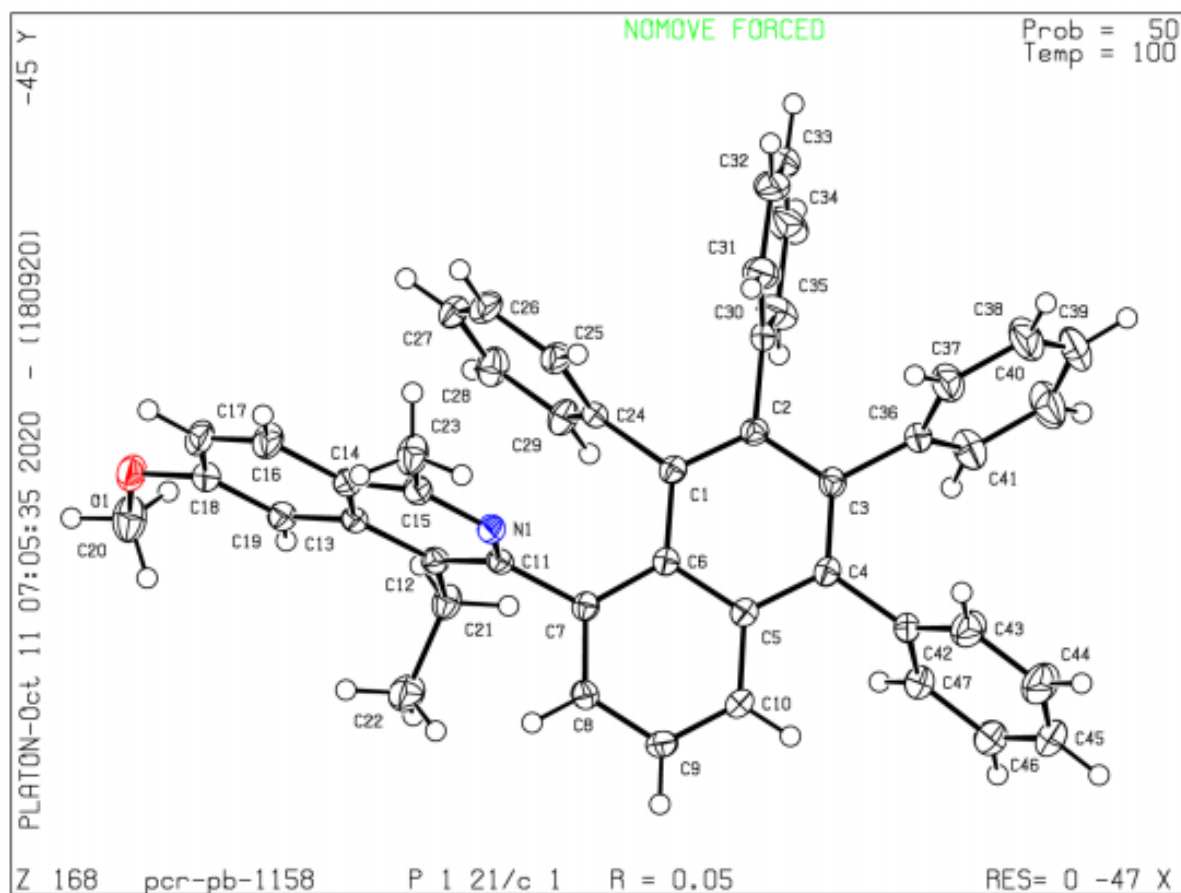
3.6 REFERENCES

1. (a) Rieger, R.; Müllen, K. Forever Young: Polycyclic Aromatic Hydrocarbons as Model Cases for Structural and Optical Studies. *J. Phys. Org. Chem.* **2010**, *23*, 315−325. (b) Narita, A.; Wang, X.-Y.; Feng, X.; Müllen, K. New Advances in Nanographene Chemistry. *Chem. Soc. Rev*. **2015**, *44, 6616−6643.* (c) Brasholz, M. "Super-Reducing" Photocatalysis: Consecutive Energy and Electron Transfers with Polycyclic Aromatic Hydrocarbons. *Angew. Chem., Int. Ed.* **2017**, *56*, 10280.

2. (a) Yang, L.; Jiang, S.; Zhao, Y.; Zhu, L.; Chen, S.; Wang, X.; Wu, Q.; Ma, J.; Ma, Y.; Hu, Z. Boron-Doped Carbon Nanotubes as Metal Free Electrocatalysts for the Oxygen Reduction Reaction. *Angew. Chem., Int. Ed.* **2011**, *50*, 7132−7135. (b) Matsuo, K.; Saito, S.; Yamaguchi, S. Photo-dissociation of B−N Lewis Adducts: A Partially Fused Trinaphthyl borane with Dual Fluorescence. *J. Am. Chem. Soc.* **2014**, *136*, 12580−12583. (c) Kahan, R. J.; Hirunpinyopas, W.; Cid, J.; Ingleson, M. J.; Dryfe, R. A. W. Well-Defined Boron/Nitrogen-Doped Polycyclic Aromatic Hydrocarbons Are Active Electrocatalysts for the Oxygen Reduction Reaction. *Chem. Mater*. **2019**, *3*1, 1891−1898. (d) Tang, R.; Wang, X. Y.; Zhang, W. Z.; Zhuang, X. D.; Bi, S.; Zhang, W. B.; Zhang, F. Aromatic Azaheterocycle-Cored Luminogens with Tunable Physical Properties via Nitrogen Atoms for Sensing Strong Acids. *J. Mater. Chem. C* **2016**, *4*, 7640−7648. (e) Li, M.; Yuan, Y.; Chen, Y. Acid-induced multicolor fluorescence of pyridazine derivative. *ACS Appl. Mater. Interfaces* **2018**, *10*, 1237− 1243. (f) Jiang, W.; Zhou, Y.; Geng, H.; Jiang, S.; Yan, S.; Hu, W.; Wang, Z.; Shuai, Z.; Pei, J. Solution-Processed, High-Performance Nanoribbon Transistors Based on Dithioperylene. *J. Am. Chem. Soc*. **2011**, *133*, 1−3.

3. (a) Miao, Q. Ten Years of N-Heteropentacenes as Semiconductors for Organic Thin-Film Transistors. *Adv. Mater*. **2014**, *26*, 5541. (b) MateoAlonso, A. Pyrene-fused pyrazaacenes: from small molecules to nanoribbons. *Chem. Soc. Rev*. **2014**, *43*, 6311. (c) Bunz, U. H. F. The Larger Linear N-Heteroacenes. *Acc. Chem. Res.* **2015**, *48*, 1676. (d) Li, J.; Zhang, Q. Linearly Fused Azaacenes: Novel Approaches and New Applications Beyond Field-Effect Transistors (FETs). *ACS Appl. Mater. Interfaces* **2015**, *7*, 28049.

4. (a) Kulkarni, A. P.; Tonzola, C. J.; Babel, A.; Jenekhe, S. A. Electron Transport Materials for Organic Light-Emitting Diodes. *Chem. Mater.* **2004**, *16*, 4556−4573. (b) Li, Y. N.; Sonar, P.; Murphy, L.; Hong, W. High mobility diketopyrrolopyrrole (DPP)-based organic semiconductor materials for organic thin film transistors and photovoltaics. *Energy Environ. Sci.* **2013**, *6*, 1684−1710. (c) Gsanger, M.; Bialas, D.; Huang, L. Z.; Stolte, M.; Wurthner, F. Organic Semiconductors based on Dyes and Color Pigments. *Adv. Mater*. **2016**, *28*, 3615−3645. (d) Wang, H.; Maiyalagan, T.; Wang, X. Review on Recent Progress in Nitrogen-Doped Graphene: Synthesis, Characterization, and Its Potential Applications. *ACS Catal.* **2012**, *2*, 781. (e) Kong, X.-K.; Chen, C.-L.; Chen, Q.-W. Doped graphene for metal-free catalysis. *Chem. Soc. Rev*. **2014**, *43*, 2841.

5. (a) Godula, K.; Sames, D. C-H Bond Functionalization in Complex Organic Synthesis. *Science* **2006**, *312*, 67–72. (b) Yamaguchi, J.; Yamaguchi, A. D.; Itami, K. C-H Bond Functionalization: Emerging Synthetic Tools for Natural Products and Pharmaceuticals. *Angew. Chem., Int. Ed*. **2012**, *51*, 8960–9009. (c) McMurray, L.; O'Hara, F.; Gaunt, M. J. Recent Developments in Natural Product Synthesis Using Metal-Catalysed C–H Bond Functionalisation. *Chem. Soc. Rev.* **2011**, *40*, 1885. (d) He, R.; Huang, Z.-T.; Zheng, Q.-Y.; Wang, C. Isoquinoline Skeleton

Synthesis via Chelation-Assisted C−H Activation. *Tetrahedron Lett.* **2014**, *55*, 5705–5713.

6. (a) Umeda, N.; Tsurugi, H.; Satoh, T.; Miura, M. Fluorescent Naphthyl- and Anthrylazoles from the Catalytic Coupling of Phenylazoles with Internal Alkynes through the Cleavage of Multiple C-H Bonds. *Angew. Chem., Int. Ed*. **2008**, *47*, 4019. (b) Shi, Z.; Tang, C.; Jiao, N. Chemoselective Synthesis of Naphthylamides and Isoquinolinones via Rhodium-Catalysed Oxidative Dehydrogenative Annulation of Benzamides with Alkynes. *Adv. Synth. Catal*. **2012**, *354*, 2695. (c) Li, S. S.; Liu, C. F.; Zhang, G. T.; Xia, Y. Q.; Li, W. H.; Dong, L. A Convenient One-Pot Route to Screw-Shaped [*5*]Azahelicenes via Rhodium(III)-Catalysed Multiple C-H Bond Activation. *Chem. - Asian J.* **2017**, *12*, 415. (d) Kong, W.-J.; Shen, Z.; Finger, L. H.; Ackermann, L. Electrochemical Access to Aza-Polycyclic Aromatic Hydrocarbons: Rhoda-Electrocatalysed Domino Alkyne Annulations. *Angew. Chem., Int. Ed*. **2020**, *59*, 5551−5556.

7. (a) Mo, J.; Wang, L.; Liu, Y.; Cui, X. Transition-Metal-Catalysed Direct C−H Functionalization under External-Oxidant-Free Conditions. *Synthesis* **2015**, *47*, 439−459. (b) Huang, H.; Ji, X.; Wu, W.; Jiang, H. Transition Metal-Catalysed C−H Functionalization of N-Oxyenamine Internal Oxidants. *Chem. Soc. Rev.* **2015**, *44*, 1155−1171.

8. (a) Guimond, N.; Gouliaras, C.; Fagnou, K. Rhodium(III)-Catalysed Isoquinolone Synthesis: The N−O Bond as a Handle for C−N Bond Formation and Catalyst Turnover. *J. Am. Chem. Soc*. **2010**, *132*, 6908–6909. (b) Guimond, N.; Gorelsky, S. I.; Fagnou, K. Rhodium(III)-Catalysed Heterocycle Synthesis Using an Internal Oxidant: Improved Reactivity and Mechanistic Studies. *J. Am. Chem. Soc*. **2011**, *133*, 6449–6457. (c) Wang, H.; Grohmann, C.; Nimphius, C.; Glorius, F. Mild

Rh(III)-Catalysed C–H Activation and Annulation with Alkyne MIDA Boronates: Short, Efficient Synthesis of Heterocyclic Boronic Acid Derivatives. *J. Am. Chem. Soc*. **2012**, *134*, 19592–19595. (d) Zhao, D.; Lied, F.; Glorius, F. Rh(III)-Catalysed C–H Functionalization/Aromatization Cascade with 1,3-Dienes: A Redox-Neutral and Regioselective Access to Isoquinolines. *Chem. Sci.* **2014**, *5*, 2869. (e) Shi, Z.; Boultadakis-Arapinis, M.; Koester, D. C.; Glorius, F. Rh(III)-Catalysed Intramolecular Redox-Neutral Cyclization of Alkenes via C–H Activation. *Chem. Commun*. **2014**, *50*, 2650. (f) Biswal, P.; Pati, B. V.; Chebolu, R.; Ghosh, A.; Ravikumar, P. C. Hydroxylamine-*O* -Sulfonic Acid (HOSA) as a Redox-Neutral Directing Group: Rhodium Catalysed, Additive Free, One-Pot Synthesis of Isoquinolines from Arylketones. *Eur. J. Org. Chem.* **2020**, *2020*, 1006−1014.

9. (a) Guimond, N.; Fagnou, K. Isoquinoline Synthesis via Rhodium-Catalysed Oxidative Cross-Coupling/Cyclization of Aryl Aldimines and Alkynes. *J. Am. Chem. Soc*. **2009**, *131*, 12050–12051. (b) Sen, M.; Kalsi, D.; Sundararaju, B. Cobalt(III)-Catalysed Dehydrative [4+2] Annulation of Oxime with Alkyne by C-H and N-OH Activation. *Chem. - Eur. J.,* **2015**, *21*, 15529–15533. (c) Pawar, A. B.; Agarwal, D.; Lade, D. M. Cp*Co(III)-Catalysed C–H/N–N Functionalization of Arylhydrazones for the Synthesis of Isoquinolines. *J. Org. Chem*. **2016**, *81*, 11409–11415. (d) Li, X.-C.; Du, C.; Zhang, H.; Niu, J.-L.; Song, M.-P. Cp*-Free Cobalt-Catalysed C–H Activation/Annulations by Traceless N,O-Bidentate Directing Group: Access to Isoquinolines. *Org. Lett.* **2019**, *21*, 2863−2866. (e) Dey, A.; Volla, C. M. R.Traceless Bidentate Directing Group Assisted Cobalt-Catalysed sp^2-C–H Activation and [4+2]-Annulation Reaction with 1,3-Diynes. *Org. Lett.* **2020**, *22*, 19, 7480–7485, and references have cited therein.

10. Liu, B.; Hu, F.; Shi, B.-F. Synthesis of Sterically Congested Polycyclic Aromatic Hydrocarbons: Rhodium(III)-Catalysed Cascade Oxidative Annulation of Aryl Ketoximes with Diphenylacetylene by Sequential Cleavage of Multiple C-H Bonds. *Adv. Synth. Catal.* **2014**, *356*, 2688.

11. Hayashi, Y. Pot Economy and One-Pot Synthesis. *Chem. Sci.* **2016**, *7*, 866−880.

12. Simmons, E. M.; Hartwig, J. F. On the Interpretation of Deuterium Kinetic Isotope Effects in C−H Bond Functionalizations by Transition-Metal Complexes. *Angew. Chem., Int. Ed.* **2012**, *51*, 3066−3072.

13. Mio, M. J.; Kopel, L. C.; Braun, J. B.; Gadzikwa, T. L.; Hull, K. L.; Brisbois, R. G.; Markworth, C. J.; Grieco, P. A. One-Pot Synthesis of Symmetrical and Unsymmetrical Bisarylethynes by a Modification of the Sonogashira Coupling Reaction. *Org. Lett.* **2002**, *4*, 3199−3202.

14. Wang, H.; Koeller, J.; Liu, W.; Ackermann, L. Cobalt(III)-Catalysed C-H/N-O Functionalizations: Isohypsic Access to Isoquinolines. *Chem. Eur. J.* **2015**, *21*, 15525–15528.

Chapter 4

N-allylbenzimidazole as a Strategic Surrogate in the Rh-catalysed Stereoselective Mono-Alkenylation of Aryl C(sp^2)-H Bonds

4.1 Abstract

4.2 Introduction

4.3 Results and Discussions

4.4 Conclusions

4.5 Experimental Section

4.6 References

Chapter 4

N-allylbenzimidazole as a Strategic Surrogate in the Rh-catalysed Stereoselective Mono-Alkenylation of Aryl C(sp²)-H Bonds
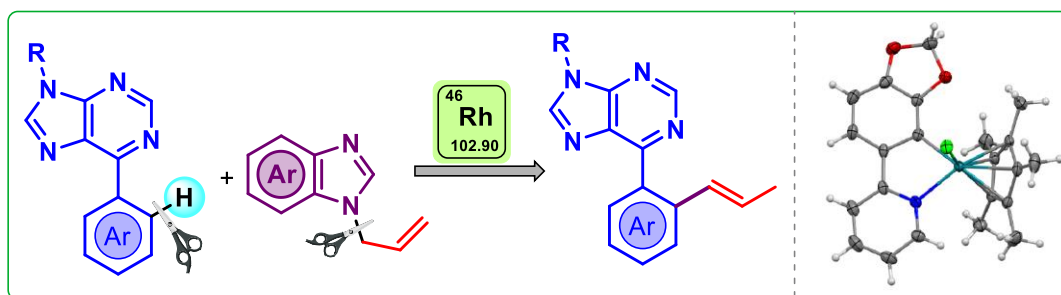
4.1 ABSTRACT

A Rh-catalysed C(sp²)-H alkenylation has been reported by taking N-allylbenzimidazole as an allylamine congener. This distinctive transformation has been observed for the first time, where a tandem process of C-H allylation followed by alkene isomerization delivers a highly stereoselective trans alkenylated product. The presence of a Lewis acid enhances the reactivity, assisting the cleavage of C(sp³)-N bond by coordinating to the N3 of N-allylbenzimidazole. Herein we report an unprecedented protocol of domino C-N bond cleavage followed by aryl C(sp²)-H alkenylation. Detailed mechanistic studies, control experiments and computational studies have been conducted to understand the mechanism. The rhodacycle-intermediates involved in the reaction have been isolated and characterized through NMR, HRMS, and single crystal X-ray analysis.

4.2 INTRODUCTION

Transition metal catalysed methodologies involving organo-halides, alcohols, alkanes, olefins have played prominent roles towards the construction of new C-C bonds.[1-3] In this context, the transition-metal catalysed Tsuji-Trost reaction[4a] has evolved

Figure 4.1 Transition metal catalysed C-H allylation *vs* alkenylation

(a) Tsuji-Trost allylation reaction:

X = OAc, Cl.. → [**PdL$_n$**]$^{\oplus}$ → Nucleophile *(enolate)* → Nu
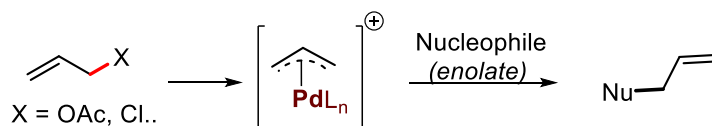
(b) Strategies used for C-N bond cleavage/activation in allylamines:

Lewis acid (LA) / H$^+$/B(OH)$_3$

weakens the C-N bond

strong C-N bond

H-bonding interaction / Protic solvent, R-OH

ML$_n$ (Pd, Ni..) → Nu-H → Nu

(η^3-allyl)ML$_n$
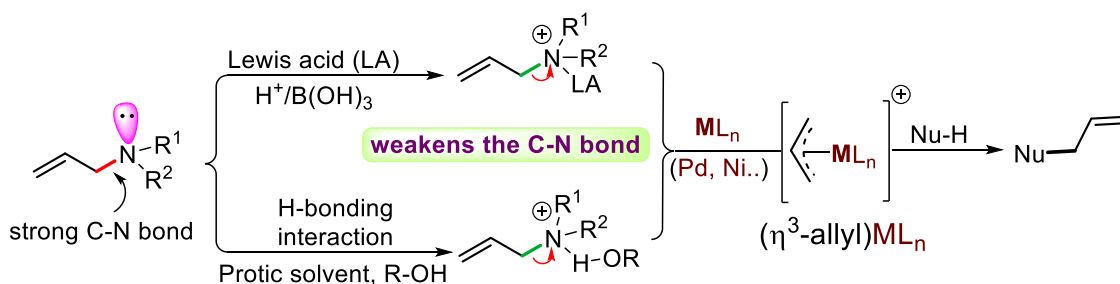
(c) Directed C-H allylation using allylamine congeners:

Wang (2018)   [Ru] TFE   [Ru] TFA, TCE   Gooben (2018)
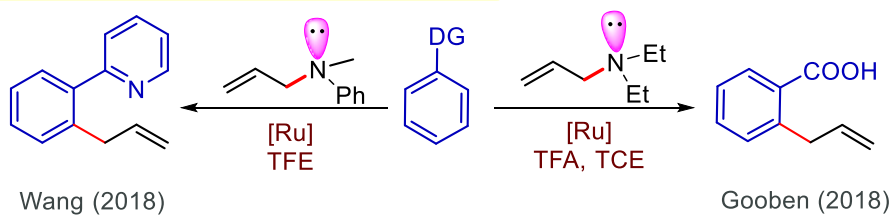
(d) A basic comparison between the reported allylamine and *N*-allylbenzimidazole:

Activator (**A**)

● 4° N-atom weakens the C-N bond (reported)

● 4° N-atom formed by relay of +ve charge (through resonance)
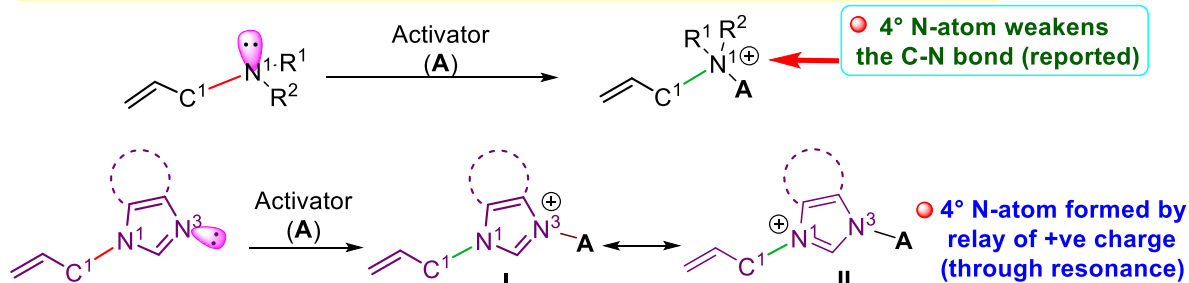
(e) This work: Rh-catalysed alkenylation by allylamine congener, *N*-allylbenzimidazole:

[Cp*RhCl$_2$]$_2$ / Zn(OAc)$_2$ / TFE

Not observed

● *Rhodium catalysed C-H alkenylation via C-N cleavage*

● *First report of N-allyl benzimidazole as alkenyl surrogate*

● *Exclusively C-H mono-alkenylation*

● *Tandem allylation and alkene isomerization*

● *Organo-Rh(III) intermediate isolation*

● *Exclusively trans-stereoselcetivity*
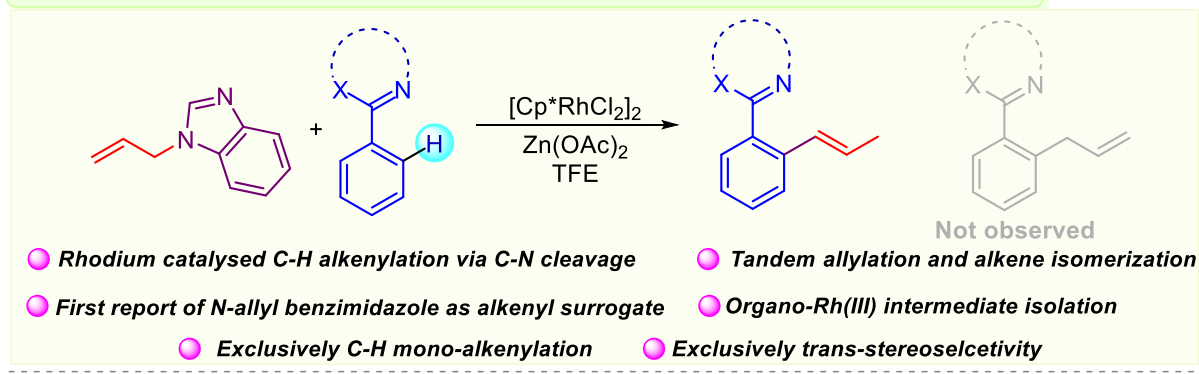
as an efficient and reliable methodology for the allylation of organo-nucleophiles using allyl halides,[5] alcohols,[6] and ester derivatives[7] as electrophilic components (Figure 4.1, a).[4-7] Here, the nucleophile attacks the metal (π-allyl) intermediate formed after C-X bond (X = halogen/OR) cleavage. However, compared to C-O/C-X bonds, C-N bonds are more thermodynamically stable due to their high bond-dissociation energy.[8] Thus, the cleavage of C-N bonds remains an under-explored area, as is the use of allylamines as electrophilic partners. Different strategies have been employed in order to activate the robust C-N bond of allylamines,[9] such as the use of strong *Lewis* acid catalysts[10] as well as exploiting hydrogen bonding interactions[11] (Figure 4.1, b). In both strategies, an amine is lost to generate a metal π-allyl cation. This, in the presence of an active nucleophile, delivers the allylated product (Figure 4.1, b). The Tian group has taken advantage of *Lewis* acid catalysts for coupling of allylic amines and boronic acids, discovering that boric acid plays a crucial role in triggering C-N bond cleavage of allylamines.[10a] This strategy has been further extended to the synthesis of structurally diverse chiral sulfones.[10b] In 2011, the Zhang group discovered an efficient Pd-catalysed α-allylation of aldehydes and ketones via C-N bond cleavage, assisted by hydrogen-bonding interactions in protic solvents.[11] This methodology was found to work well with primary, secondary and tertiary amines. Substrates bearing active methylene and methine units were also found to undergo allylation smoothly from allylamine derivatives via C-N bond cleavage.[12]

During the last few decades, transition metal-catalysed directed C-H bond functionalization has evolved as a powerful tool for step- and atom-economic transformations.[13] However, parallel C-H activation and C-N bond cleavage for C-C bond forming reactions is still in its infancy.[14] In 2018, the Wang group reported the allylation of 2-phenylpyridine via C-N bond cleavage of allyamines, in which the protic solvent trifluoroethanol (TFE) was observed to trigger the C-N cleavage via hydrogen bonding

interaction (Figure 4.1, c).[14a] Recently, the Gooben group successfully achieved *ortho-*allylation of benzoic acid using *N,N*-dialkyl allylamines as the allylating agent (Figure 4.1, c).[14b] Again, the protic solvent trichloroethanol (TCE) was found to be compatible, enhancing the reactivity.

An important aspect of catalysis is that a slight change in the electronics of the substrate and/or the reaction conditions could deliver a completely different product. Therefore, we decided to study the reactivity of *N*-allylbenzimidazole **1a** as an allylamine congener (Figure 4.1, d). The primary difference between **1a** and the previously reported allylamine is that the non-bonded electron pair on N1 is readily available for protonation/hydrogen bonding with a protic solvent as with allylamine; whereas the non-bonded electron pair on N1 of **1a** is unavailable either for hydrogen bonding or *Lewis* acid coordination as it is a part of the aromatic π-system. However, the non-bonded electrons on the N3 atom of **1a** could be used for this purpose in lieu of N1 atom. Upon chelation of N3-atom with a Lewis acid, a positivve charge can be developed over N3 which could be relayed to N1 through resonance (Figure 4.1, d). In structure **II**, C1 is attached to a quaternary nitrogen species which could activate the C-N bond. We were interested to see whether this relay effect of positive charge from N3 to N1 woulldl show the same allylation chemistry.

On this basis, we proposed to study the chemistry of *N*-allylbenzimidazole for directed $C(sp^2)$-H functionalization. We initially carried out the reaction between 2-arylpyridine derivatives **2** and *N*-allylbenzimidazole **1a** with rhodium catalysis. Surprisingly, we observed selective $C(sp^2)$-H alkenylation as opposed to allylation. Salient features of this methodology and study are (i) orthogonal transformation compared to reported reactions, (ii) selective mono-alkenylation instead of allylation, (iii) the first report of C-N cleavage of *N*-allylbenzimidazole with Rh-catalysis, (iv)

4.3 RESULTS AND DISCUSSION

Table 4.1 Optimization of reaction conditions for C(sp^2)-H alkenylation

entry	deviation from the standard conditions	yield of 3af (%)[b]
1	none	75
2	[Cp*Rh(MeCN)$_3$][SbF$_6$]$_2$	31
3	Rh(OAc)$_2$	nr
4	Rh(PPh$_3$)$_3$Cl	nr
5	MeOH	25
6	HFIP	20
7	TFT	nr
8	TFE+H$_2$O	trace
9	temperature 70 ^{o}C instead of 130 ^{o}C	nr
10	temperature 90 ^{o}C instead of 130 ^{o}C	trace
11	temperature 110 ^{o}C instead of 130 ^{o}C	40
12[c]	AgSbF$_6$ instead of LiClO$_4$	nr
13[c]	AgOAc instead of LiClO$_4$	nr
14	NaIO$_4$ instead of LiClO$_4$	20
15	**1a** (1 equiv) instead of 3 equiv	22
16	**1a** (2 equiv) instead of 3 equiv	46
17	Zn(OTf)$_2$ instead of Zn(OAc)$_2$	60
18	PivOH instead of Zn(OAc)$_2$	trace
19	Cu(OTf)$_2$ instead of Zn(OAc)$_2$	nr
20	2 h	35
21	4 h	73
22	6 h	20
23	without [Rh]	nr
24	without LiClO$_4$	trace
25[d]	without Zn(OAc)$_2$	55 (12 h)

[a]Reaction conditions: **1a** (3 equiv, 0.18 mmol), **2f** (1 equiv, 0.06 mmol), [Cp*RhCl$_2$]$_2$ (5 mol %, 0.003 mmol), LiClO$_4$ (2 equiv, 0.12 mmol), Zn(OAc)$_2$ (1.5 equiv, 0.09 mmol), TFE (0.1 M, 0.6 mL), 130 °C, N$_2$, [b]Isolated yield. [c](20 mol%, 0.2 equiv) of silver additives were used, [d]Isolated yield after 12 h.

computational studies on the mechanism of this transformation, (v) experimental support for our mechanistic proposal, (vi) characterization of Rh-intermediate, and (vii) exclusive trans alkenylation.

Our investigation began with the reaction of *N*-allylbenzimidazole **1a** and 2-(4-chlorophenyl)pyridine **2f** (Table 4.1). We were satisfied to find that 5 mol % of Cp*Rh catalyst and 2 equiv. of $LiClO_4$ in combination with 1.5 equiv of $Zn(OAc)_2$ gave mono-alkenylated product **3af** in 75% yield (Table 4.1, entry 1). The use of a cationic Rh-complex resulted in 31% yield of **3af** (Table 4.1, entry 2); whereas $Rh_2(OAc)_4$ dimer and Wilkinson's catalyst failed to deliver the product (Table 4.1, entries 3-4). When solvents other than TFE were screened, lower yields were observed (Table 4.1, entries 5-7). These results suggest that the polar protic solvent TFE plays a crucial role in the reaction. It has been reported that the use of water can enhance the hydrolysis of C-N bonds.[15] Therefore, in an attempt to enhance the rate of C-N bond cleavage of *N*-allylbenzimidazole, a 1:1 ratio of $TFE:H_2O$ was explored (Table 4.1, entry 8), but instead of an improved yield, we observed only a trace amount of product.

Our results indicated that the rate of the reaction is highly affected by the temperature; an exponential increase in the reaction yield being observed with increasing temperature (Table 4.1, entries 9-11). $LiClO_4$ works well for this protocol; whereas replacing it with silver additives such as $AgSbF_6$ and AgOAc, resulted in no reaction (Table 4.1, entries 12-13). In addition, use of $NaIO_4$ in place of $LiClO_4$ resulted in only 20% yield of the product **3af** (Table 4.1, entry 14). Varying the equivalents of *N*-allylbenzimidazole resulted in lower yields (Table 4.1, entries 15-16).

Further screening of *Lewis* and protic acid additives – $Zn(OTf)_2$, PivOH, and $Cu(OTf)_2$ – did not result in an improved yield of **3af** (Table 4.1, entries 17-19). To determine the effect of time, three parallel reactions were performed, and it was observed

that after 4 h the product begins to decompose under the reaction conditions (Table 4.1, entries 20-22). Finally, control experiments confirmed the necessity for catalyst [Cp*RhCl₂]₂, additive LiClO₄, and Zn(OAc)₂ (Table 4.1, entries 23-25). From these results, it is clear that the reaction is triggered by the addition of Lewis acid. Thus, it was confirmed that the role of LiClO₄ is crucial for this reaction and Zn(OAc)₂ acts as a promoter.

Scheme 4.1 Screening of allylamines, allyl alcohol and esters[a,b]
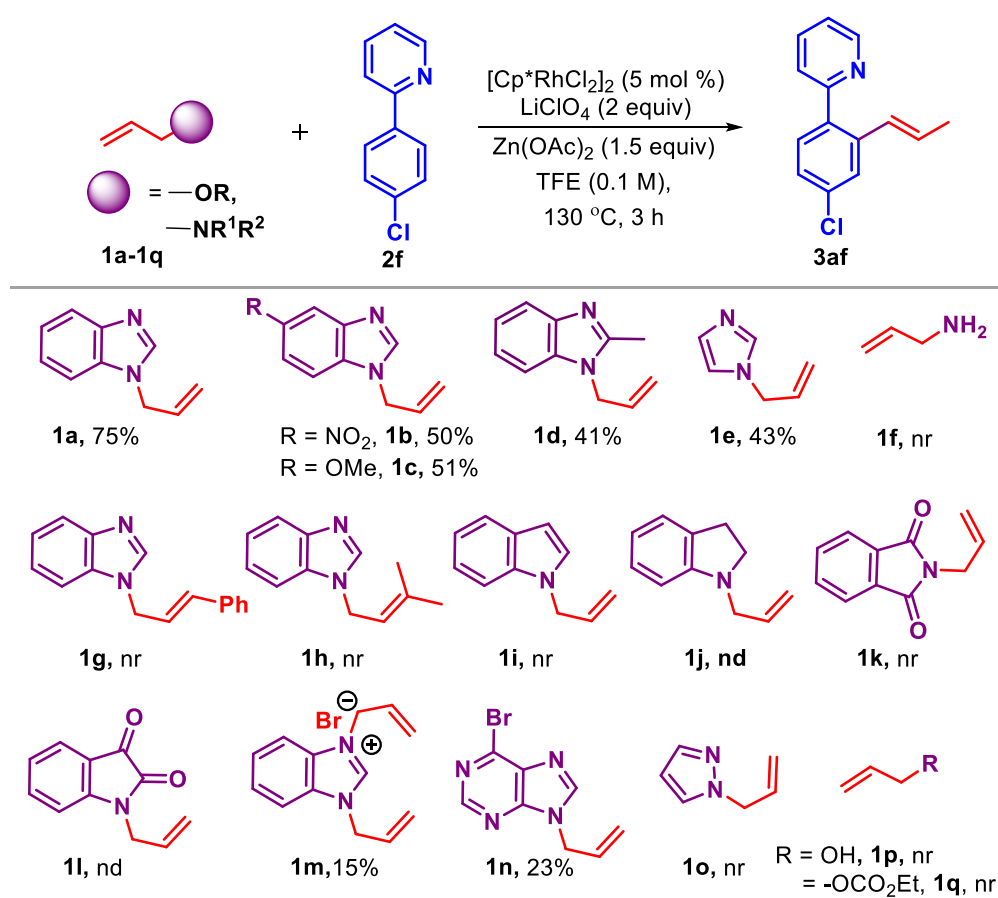
[a]Reaction conditions: **1** (3 equiv, 0.3 mmol), **2f** (1 equiv, 0.1 mmol), [Cp*RhCl₂]₂ (5 mol %, 0.05 mmol), LiClO₄ (2 equiv, 0.2 mmol), Zn(OAc)₂ (1.5 equiv, 0.15 mmol), TFE (0.1 M, 1.0 mL), 130 °C, N₂, [b]Isolated yield.
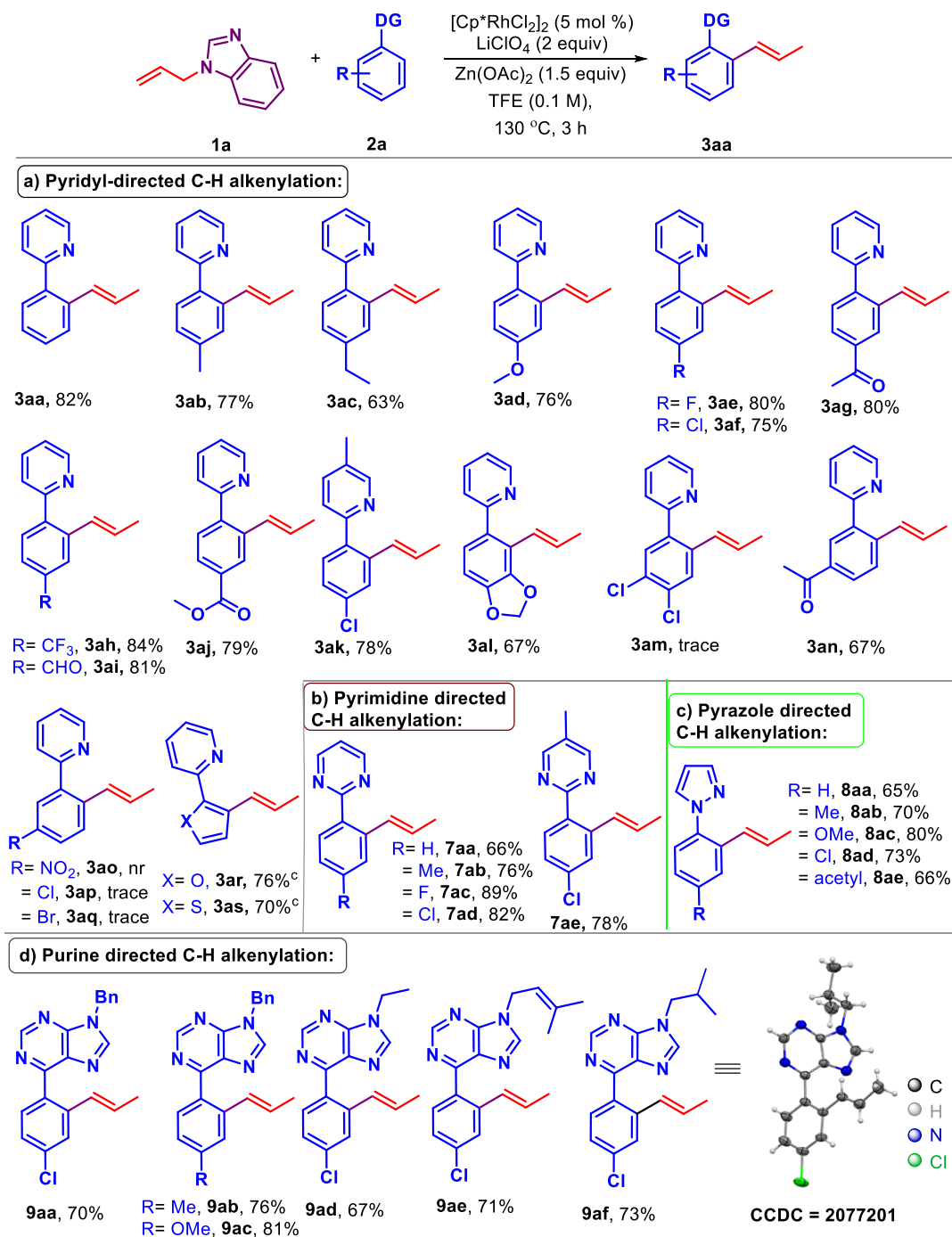
With the optimized conditions, we proceeded to study the electronic influence of the *N*-allyl coupling partner on the C-H alkenylation of 2-arylpyridines (Scheme 4.1). When **1a** contains either a π-electron-withdrawing group (EWG) such as -NO₂ (**1b**) or an electron-donating group (EDG) such as -OMe (**1c**), similar reactivity was observed; both

substrates yielding ~50% of **3af**, indicating that the nature of the substituent in the benzenoid system has no significant impact. Similarly, when 2-methyl-*N*-allylbenzimidazole **1d** was studied as an alkenylating source, **3af** was afforded in 41% yield. To check the influence of the benzene ring, *N*-allyl imidazole **1e** and allylamine **1f** were used instead of **1a**, but inferior yields were observed in both cases. These results imply that the presence of the benzene ring facilitates this transformation. Monosubstituted or disubstituted alkenes (**1g** and **1h**) did not deliver the respective alkenylated products, indicating that alkene insertion into the Rh-C bond is subject to steric constraints and occurs prior to C-N bond cleavage. To check the role of the N3 nitrogen atom of **1a**, *N*-allylindole **1i** was employed as the coupling partner. In this case, we did not observe any product **3af**, suggesting that the reaction is facilitated by interaction with the N3 atom of **1a** (likely binding by *Lewis* acid). Further, *N*-allylindoline **1j** was also tested and found to be ineffective for this transformation. When the more electron deficient *N*-allylphthalimide **1k** and *N*-allylisatin **1l** were used, the product **3af** was not obtained. Use of 1,3-diallylbenzimidazole **1m** and *N*-allyl-4-bromopurine **1n** gave mixtures of alkenylated and allylated products in poor yields. In contrast to imidazole **1e**, N-allylpyrazole **1o** did not give the product **3af**. Moreover, when aryl pyridine **2f** was subjected to the standard reaction conditions with the more frequently used allylating reagents such as allyl alcohol **1p** and allyl ethyl carbonate **1q**, none of them produced either C-H allylated or alkenylated products. The results of these studies confirm the efficiency and selectivity of N-allylbenzimidazole **1a** for this transformation.

To test the generality of this methodology by using *N*-allylbenzimidazole **1a** as a coupling partner, various substituted 2-arylpyridines were tested (Scheme 4.2, a). The aryl unit containing both EDGs (-CH$_3$, -C$_2$H$_5$, -OMe, -F, -Cl) and EWGs (-CHO, -COCH$_3$, -CF$_3$, -CO$_2$Me) were well tolerated under these conditions, delivering moderate

to very good yields of the respective C-H alkenylated products. It has been observed that

substrates with EDGs led to lesser yields (Scheme 4.2: **3ab**-**3af**, **3ak**, and **3al**) compared

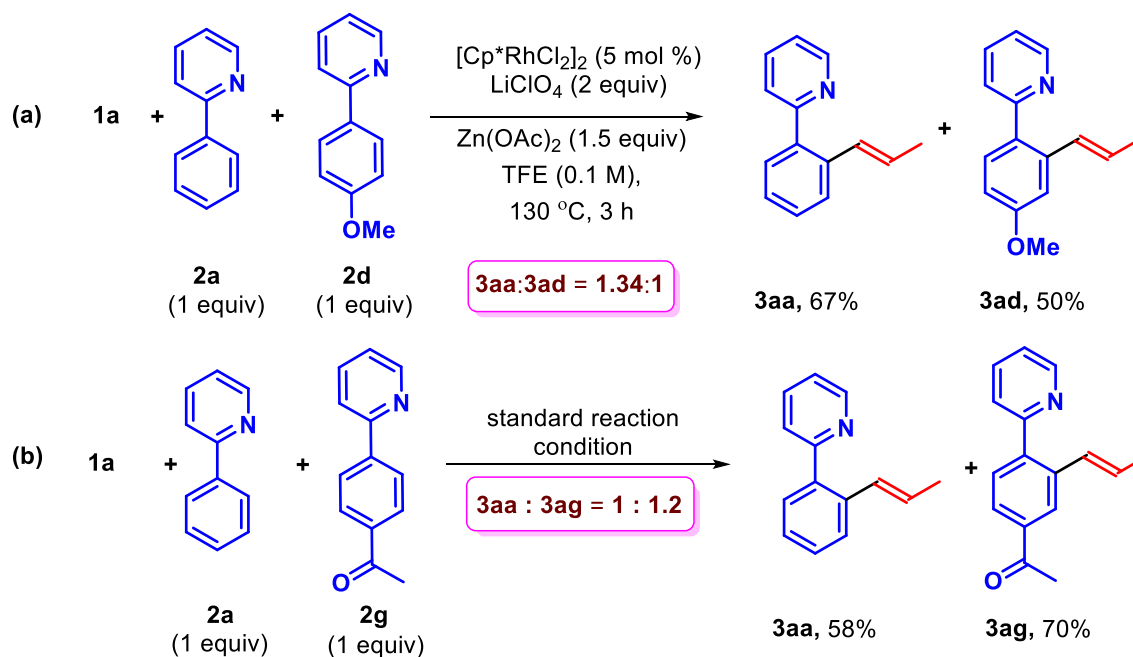**Scheme 4.2 Scopes of Rh-catalysed alkenylation reactions[a,b]**

a) **Pyridyl-directed C-H alkenylation:**

3aa, 82%   **3ab,** 77%   **3ac,** 63%   **3ad,** 76%   R= F, **3ae,** 80%   **3ag,** 80%
                                                          R= Cl, **3af,** 75%

R= CF$_3$, **3ah,** 84%   **3aj,** 79%   **3ak,** 78%   **3al,** 67%   **3am,** trace   **3an,** 67%
R= CHO, **3ai,** 81%

R= NO$_2$, **3ao,** nr   X= O, **3ar,** 76%[c]
= Cl, **3ap,** trace   X= S, **3as,** 70%[c]
= Br, **3aq,** trace

b) **Pyrimidine directed C-H alkenylation:**

R= H, **7aa,** 66%
= Me, **7ab,** 76%
= F, **7ac,** 89%
= Cl, **7ad,** 82%   **7ae,** 78%

c) **Pyrazole directed C-H alkenylation:**

R= H, **8aa,** 65%
= Me, **8ab,** 70%
= OMe, **8ac,** 80%
= Cl, **8ad,** 73%
= acetyl, **8ae,** 66%

d) **Purine directed C-H alkenylation:**

9aa, 70%   R= Me, **9ab,** 76%   **9ad,** 67%   **9ae,** 71%   **9af,** 73%   **CCDC = 2077201**
              R= OMe, **9ac,** 81%

○ C
○ H
○ N
○ Cl

[a]Reaction conditions: **1a** (3 equiv, 0.3 mmol), **2/4/5/6** (1 equiv, 0.1 mmol), [Cp*RhCl$_2$]$_2$ (5 mol %, 0.05 mmol), LiClO$_4$ (2 equiv, 0.2 mmol), Zn(OAc)$_2$ (1.5 equiv, 0.15 mmol), TFE (0.1 M, 1.0 mL), 130 °C, N$_2$. [b]Isolated yield.

to substrates with EWGs (Scheme 4.2, **3ag**-**3aj**). Interestingly, sensitive functional groups such as -formyl (**3ai**) and -ester (**3aj**) were retained in the final product. The unsymmetrical substrate bearing a dioxolane ring selectively gave **3al** in 67% yield, by activation of the *ortho*-hydrogen from the more sterically hindered site. The origin of this selectivity might be due to chelation involving the oxygen atom in the cyclometalated intermediate.[16] The scope of the reaction was extended to heterocycles such as 2-arylpyrimidines and 2-arylpyrazoles (Scheme 4.2, b and c). These heterocycles were found to deliver their corresponding mono-alkenylated products without need for variation in the standard reaction conditions. The substrates bearing EDGs or EWGs reacted smoothly, giving products in good yields (Scheme 4.2, **7aa**-**7ae**, and **8aa**-**8ae**). As a nucleobase and a core unit in nuclei acids, purine is of particular interest. Transition metal-catalysed purine-directed C-H alkenylations have been reported using phenylacetylene or vinylcarboxylic acids by the Yu[17a] and Xu groups,[17b] respectively. We envisaged that our protocol could install an alkenyl unit selectively into this system. Gratifyingly, this reaction condition was found viable for purine-directed alkenylated products **9aa**-**9af** in good yields (Scheme 4.2, d). The *trans*-stereochemistry was confirmed unambiguously from single crystal X-ray analysis of product **9af** (CCDC 2077201).
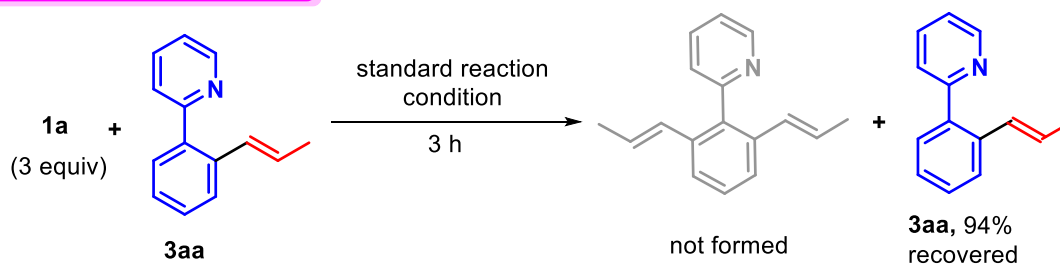
In order to gain a better understanding about the influence of electronics on the substrate, intermolecular competition experiments were conducted between different arylpyridines (Scheme 4.3). Electronically poor substrates reacted faster than electronically rich substrates with the reactivity trends **2g**>**2a**>**2d** (Scheme 3a and 3b). These results are consistent with a concerted metalation-deprotonation (CMD)[19] pathway for the C-H activation. To check the feasibility of dialkenylation under the standard reaction condition, **3aa** was employed as a substrate. However, we did not observe any

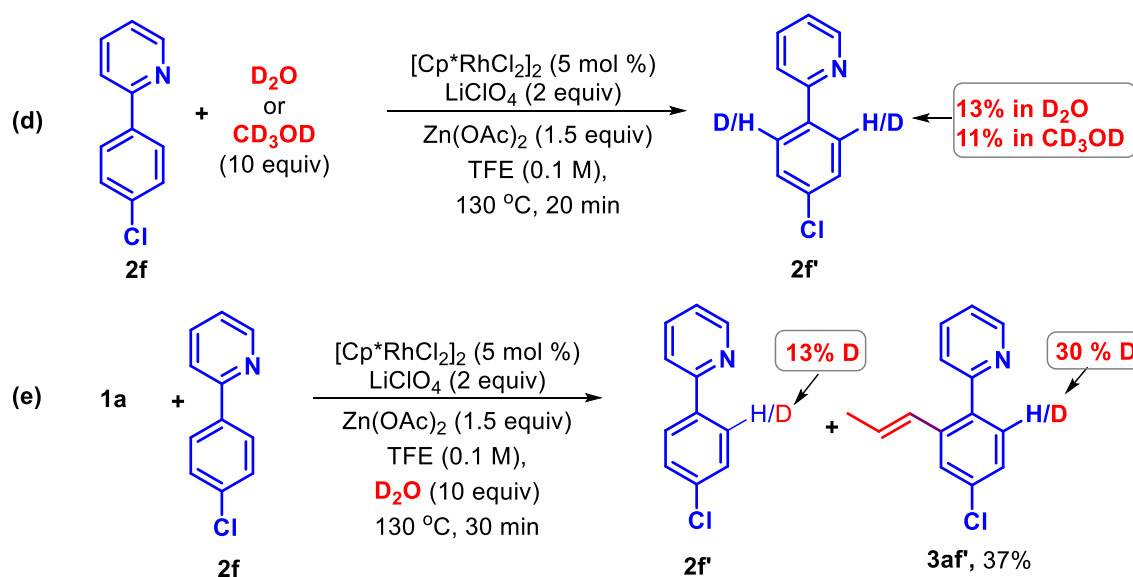**Scheme 4.3 Control experiment and mechanistic studies**

Competitive experiments:

(a) 1a + 2a (1 equiv) + 2d (1 equiv)

[Cp*RhCl₂]₂ (5 mol %)
LiClO₄ (2 equiv)

Zn(OAc)₂ (1.5 equiv)
TFE (0.1 M),
130 °C, 3 h

3aa:3ad = 1.34:1

3aa, 67%   3ad, 50%

(b) 1a + 2a (1 equiv) + 2g (1 equiv)

standard reaction condition

3aa : 3ag = 1 : 1.2

3aa, 58%   3ag, 70%

(c) Standardreaction with 3aa:

1a (3 equiv) + 3aa

standard reaction condition
3 h

not formed   +   3aa, 94% recovered

H/D Scrambling experiments:

(d) 2f + D₂O or CD₃OD (10 equiv)

[Cp*RhCl₂]₂ (5 mol %)
LiClO₄ (2 equiv)

Zn(OAc)₂ (1.5 equiv)
TFE (0.1 M),
130 °C, 20 min

2f'   D/H   H/D   13% in D₂O
11% in CD₃OD

(e) 1a + 2f

[Cp*RhCl₂]₂ (5 mol %)
LiClO₄ (2 equiv)

Zn(OAc)₂ (1.5 equiv)
TFE (0.1 M),
D₂O (10 equiv)
130 °C, 30 min

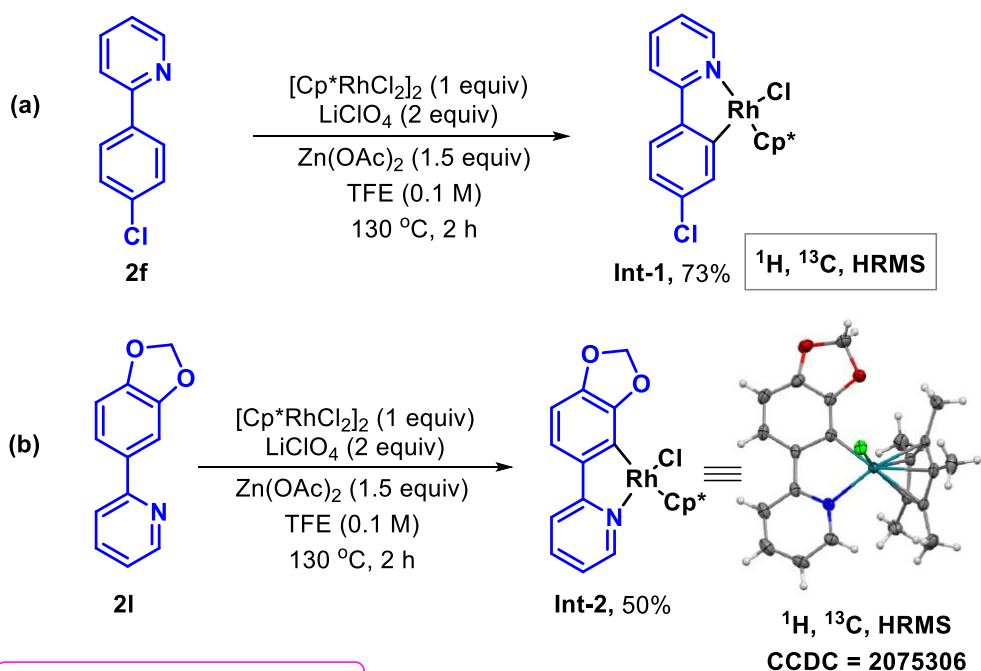2f'   13% D   H/D   +   3af', 37%   30 % D   H/D

dialkenylation; rather 94% of **3aa** was recovered (Scheme 4.3, c), which demonstrates the highly selective addition of a single alkenyl group onto the substrate.

To gain further insight into the mechanism, we conducted several mechanistic experiments (Scheme 4.3, d-e). When **2f** was allowed to react with D_2O or CD_3OD in the absence of **1a**, 13% and 11% deuterium exchange was observed, respectively (Scheme 4.3, d). Additionally, the reaction of **2f** and D_2O in the presence of **1a** resulted in 30% H/D-scrambling at the *ortho*-position of **3af** (Scheme 4.3, e). When taken together, both experiments indicate that the C-H bond metalation step is reversible.[18]
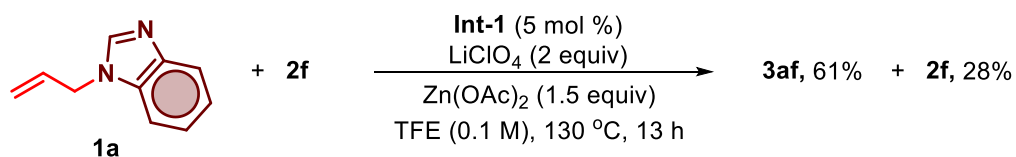
Reaction of **2f** with stoichiometric amount of [Cp*RhCl$_2$]$_2$ under the standard reaction conditions in absence of **1a** yielded a five-membered rhodacycle, **Int-1**, in 70% yield, characterized by NMR spectroscopy and HRMS (Scheme 4.4, a). Similarly, another five-membered rhodacycle, **Int-2**, was synthesized from **2l**, again confirmed by NMR spectroscopic analysis, HRMS, as well as X-ray crystallography (Scheme 4.4, b). The active involvement of **Int-1** in the catalytic cycle was confirmed when 5 mol % of **Int-1** was used as catalyst for the reaction of **2f** with **1a**, affording a 61% yield of **3af** (Scheme 4.4, c). There are several reports on transition metal-catalysed *in situ* isomerizations of terminal alkenes to internal alkenes.[19] Thus, we examined whether internal alkene **1a'** is an active coupling partner in the course of this reaction or not. A reaction employing **1a'** resulted in no product (Scheme 4.4, d), consistent with the terminal alkene **1a** participating in the reaction, not the internal alkene **1a'**. The formation of **3aa** was observed even in the presence of a stoichiometric amount of radical scavenger BHT or TEMPO in 75% and 46%, respectively, which rules out significant contribution from radical pathways (Scheme 4.4, e). To check whether the reaction is proceeding through 2'-allylphenylpyridine **3aa'** as an intermediate, **3aa'** was subjected to the standard conditions, which resulted in 67% of **2a** and 18% of **3aa.** (Scheme 4.4, f), suggesting that

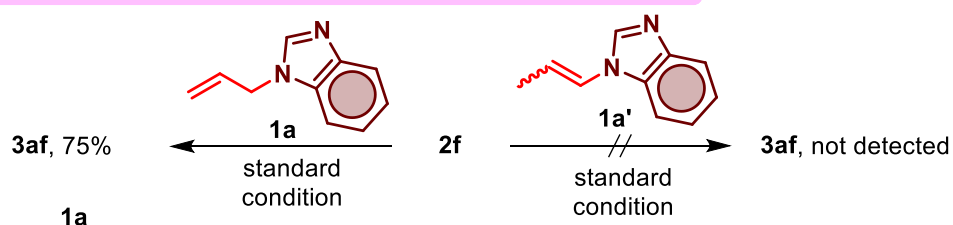## Scheme 4.4 Control experiment and mechanistic studies
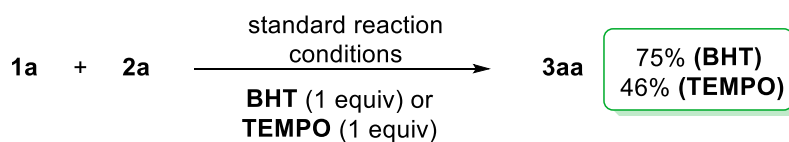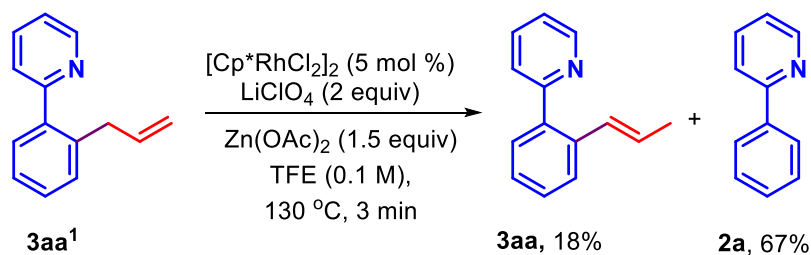
Synthesis of rhodacycle intermediates:

(a)

2f → [Cp*RhCl₂]₂ (1 equiv) / LiClO₄ (2 equiv) / Zn(OAc)₂ (1.5 equiv) / TFE (0.1 M) / 130 °C, 2 h → **Int-1**, 73% | ^{1}H, ^{13}C, HRMS

(b)

2l → [Cp*RhCl₂]₂ (1 equiv) / LiClO₄ (2 equiv) / Zn(OAc)₂ (1.5 equiv) / TFE (0.1 M) / 130 °C, 2 h → **Int-2**, 50%

^{1}H, ^{13}C, HRMS
CCDC = 2075306

(c) Standard reaction with Int-1:

1a + 2f → Int-1 (5 mol %) / LiClO₄ (2 equiv) / Zn(OAc)₂ (1.5 equiv) / TFE (0.1 M), 130 °C, 13 h → **3af,** 61% + **2f,** 28%

(d) Standard reaction with terminal alkene 1a and internal alkene 1a':

3af, 75% ← 1a + 2f / standard condition   2f + 1a' → // standard condition → **3af,** not detected

(e) Reaction with radical scavengers:

1a + 2a → standard reaction conditions / BHT (1 equiv) or TEMPO (1 equiv) → 3aa | 75% **(BHT)** / 46% **(TEMPO)**

(f) Reaction with 2'-allylphenylpyridine 3aa¹:

3aa¹ → [Cp*RhCl₂]₂ (5 mol %) / LiClO₄ (2 equiv) / Zn(OAc)₂ (1.5 equiv) / TFE (0.1 M), / 130 °C, 3 min → **3aa,** 18% + **2a,** 67%

117

this isomerization is indeed possible. The isomerization of a terminal alkene to an internal alkene,[19] as well as pyridyl directed rhodium-catalysed C-C bond cleavage of allylbenzene,[20] is well established.
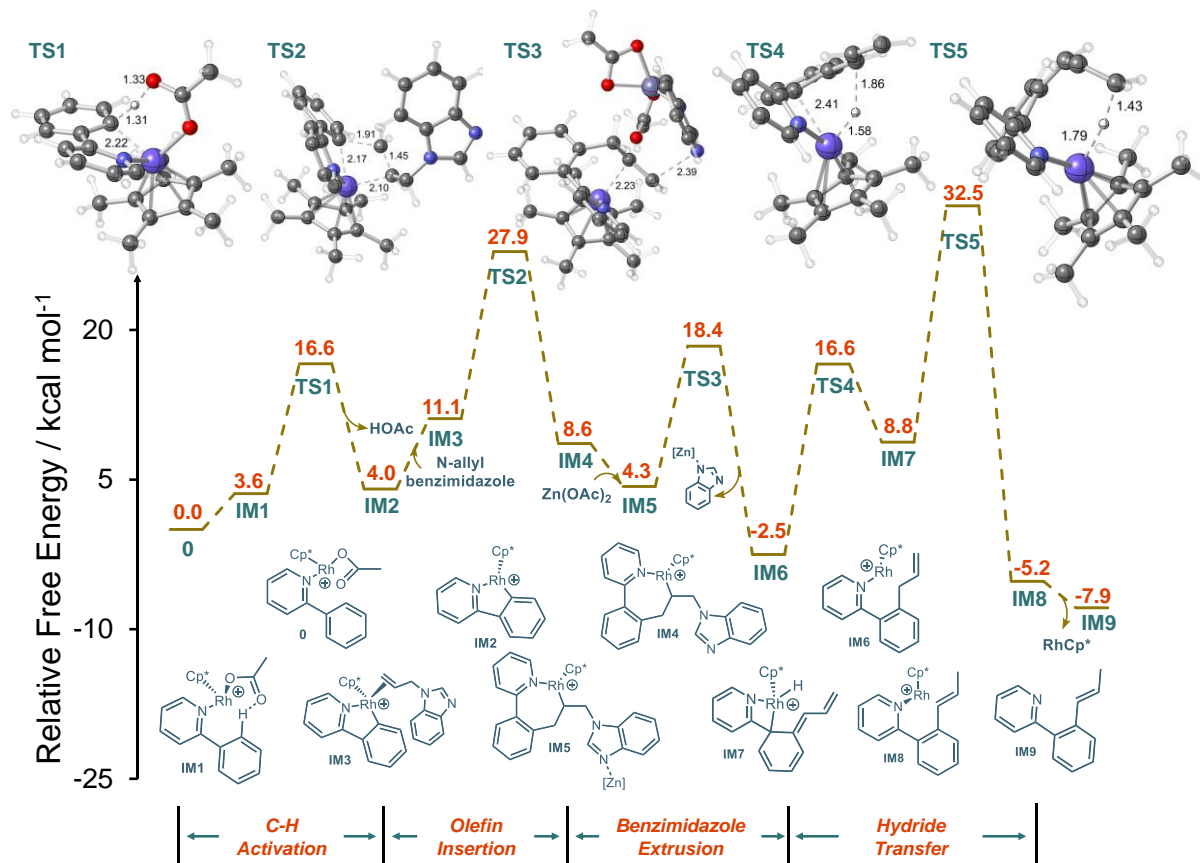

Figure 4.2. Proposed mechanism and optimized geometries of transition states structures (TSSs) with key nuclear distances for the rhodium-catalysed alkenylation of 2-phenylpyridine with *N*-allylbenzimidazole. The bond distances are in angstroms (Å). Color code: C gray, O red, H white, N blue, Zn cyan, Rh purple.

To gain additional insight into the reaction mechanism, DFT calculations at the B3LYP-D3(BJ)/Def2-TZVP/SMD (TFE)// B3LYP-D3(BJ)/Def2-SVP level of theory[21] were carried out (see Supporting Information for details on the choice of this level of theory and addition details on methods). The coupling of *N*-allylbenzimidazole **1a** with 2-phenylpyridine **2a** was used as a model reaction, as it furnished a high yield of product (82%). As the cationic catalyst [Cp*Rh(OAc)]$^+$ is proposed to be generated in the presence of Zn(OAc)$_2$ and LiClO$_4$, the complex of this catalyst with 2-phenylpyridine was selected as the starting point of the reaction. We also considered the possibility of

involvement of a triplet state, but the results of those calculations reveal that the energies of triplet species are uniformly much higher than those of the corresponding singlet state species.

Our results reveal that an *ortho-* C–H bond cleavage takes place via a CMD mechanism[22] (Figure 4.2). The intermediate **0** isomerizes to intermediate **IM1**, allowing for a CH–O interaction that presages C-H activation (the distance between acetate and *ortho-* H changes from 2.10 Å in 0 to 1.95 Å in 1). Intermediate **IM1** then undergoes energetically viable CMD through the 6-membered ring transition state structure (TSS) **TS1** (Figure 4.2) to afford the five-membered rhodacycle **IM2**. During this process, C–H bond cleavage and Rh–C bond formation occur synchronously. Alternative mechanisms were considered – σ -bond metathesis, oxidative addition, and electrophilic substitution – but our attempts to obtain the corresponding intermediates and/or TSSs failed. As shown in Figure 4.2, the overall free energy barrier for this process is predicted to be 16.6 kcal mol^{-1}. Note that CMD is predicted to be reversible, consistent with the deuteration experiments described above. Similar six-membered ring transition states for CMD mechanisms have been reported for Pd[23a-c] and Ir[23d] catalysed C–H activations. CMD is followed by dissociation of acetic acid to produce intermediate **IM2**. Upon dissociation of acetic acid, the alkene partner, *N*-allylbenzimidazole, can bind to **IM2** to form complex **IM3**, which undergoes alkene insertion via the 4-membered ring TSS **TS2** to form the 7-membered rhodacycle **IM4** (Figure 4.2).

The overall barrier to **TS2** is predicted to be 27.9 kcal mol^{-1}, viable under the experimental conditions used. Upon inclusion of Zn(OAc)$_2$, which coordinates to the sp^2-hybridized nitrogen on the benzimidazole moiety, shown in intermediate **IM5**, the benzimidazole is extruded through TSS **TS3**. This process is computed to be exergonic, forming intermediate **IM6** (Figure 4.2). Additional calculations in which the C–N

distance was scanned illuminate the necessity of the Lewis acid, as without it, C–N bond cleavage presents as an uphill battle with a saddle point possessing a barrier of 35.0 kcal mol^{-1}. We also considered that Zn(OAc)$_2$ may be necessary for the previous insertion step and ensuing steps; however the results of supplementary calculations reveal that the presence of Zn(OAc)$_2$ increases barriers for those individual steps. From **IM6**, alkene isomerization occurs, involving a hydride transfer from the benzylic carbon to the rhodium through TSS **TS4** (Figures 4.2 and 4.3). This step is predicted to involve a surmountable barrier of 19.1 kcal mol^{-1}, despite disruption of aromaticity associated with forming **IM7**. From there, another hydride transfer can occur, this time from the rhodium to the terminal carbon on the alkenyl via TSS **TS5**, forming intermediate IM8, from which the final product, **IM9**, is released upon reductive elimination of the catalyst.
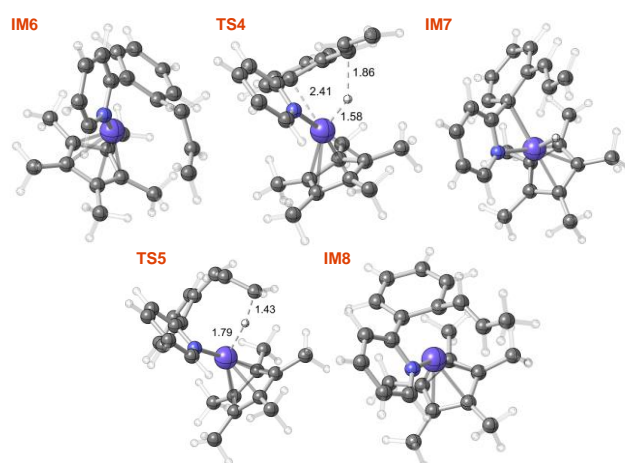
Figure 4.3. Optimized geometries of **6**, **TS4**, **7**, **TS5** and **8** (with key nuclear distances for **TS4** and **TS5**). The bond distances are in angstroms (Å). Color code: C gray, H white, N blue, Rh purple.

To assess the changes in aromatic character along the **IM6 → TS4 → IM7 → TS5 → IM8** pathway, NICSzz values 1 Å above the center of the benzene moiety[24] (more negative values are generally associated with greater aromaticity) were computed to be: -8.34, -0.19, 1.93, -1.62 and -10.70 UNITS? respectively. As expected, aromatic character is predicted for **IM6**, and although some is lost during this process, it is eventually

regained in **IM8**. The overall **IM6** → **TS5** step is predicted to be rate (turnover)-determining, possessing a barrier of 35.0 kcal mol^{-1} (36.4–45.8 kcal mol^{-1} at other levels of theory). A barrier of this magnitude is at the upper end of the range of barriers that can be overcome under the experimental reaction conditions, providing a rationale for the high temperature needed. The experimental observation of alkene isomerization (Scheme 4.3, f) under the reaction conditions is also consistent with these results.

Based on our mechanistic investigations and previous literature reports,[14,19] a catalytic cycle can be proposed (Scheme 4.5). The Rh(III) catalyst **A** initially undergoes

Scheme 4.5 Proposed mechanism
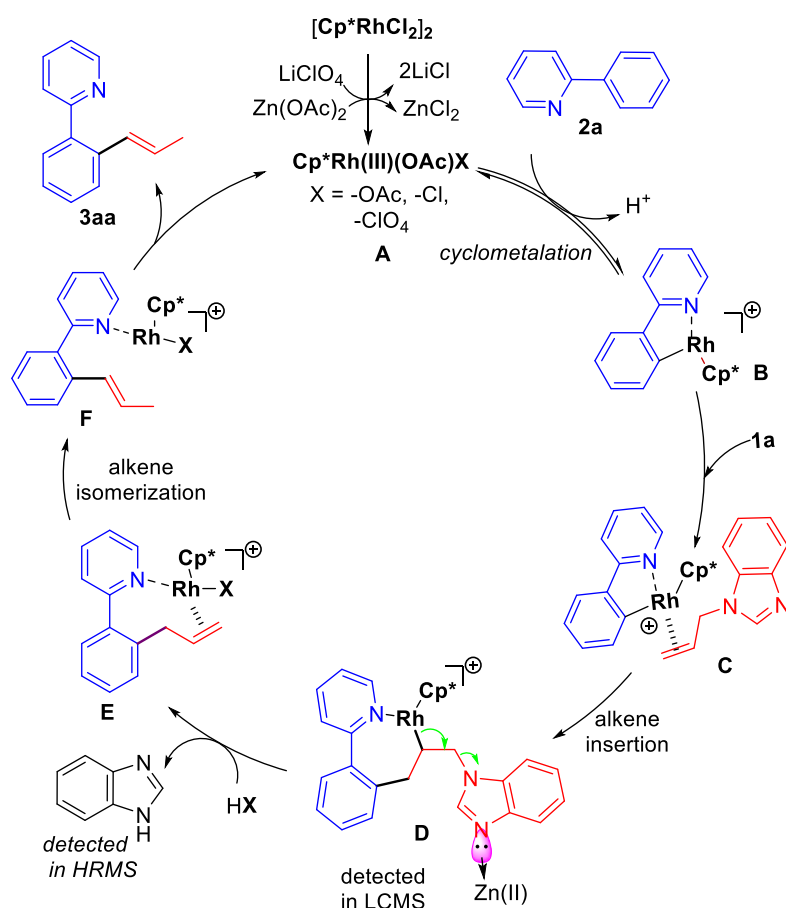
cyclometalation with **2a**, reversibly forming intermediate **B** (characterized by NMR, HRMS, and XRD analyses). π-Complexation of intermediate **B** with **1a**, followed by alkene insertion into the C- Rh bond gives intermediate **D** (detected in LCMS). The

121

elimination of benzimidazole (detected in HRMS) by the assistance of the zinc additive leads to the allylated intermediate **E**, which, upon isomerization,[19] delivers the alkenylated product **3aa**.

Scheme 4.6 Synthetic utility of this methodology
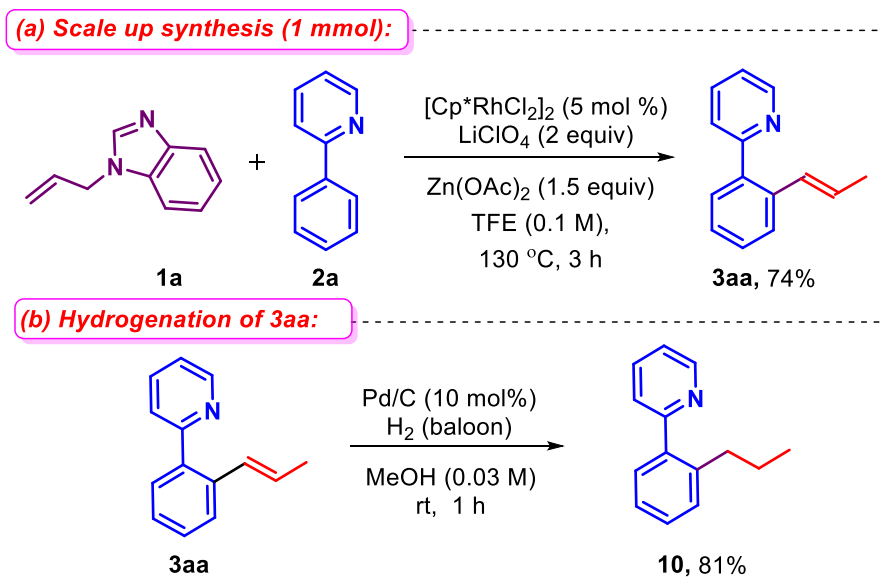
The synthetic utility of the reaction has been demonstrated by performing a 1 mmol scale reaction, which afforded 74% of **3aa** (Scheme 4.6, a). Furthermore, to show the potential utility of the alkenylated products formed by our method, hydrogenation of **3aa** was performed. The hydrogenated product 2-(2-propylphenyl)pyridine **10** was obtained in 81% of yield as a colorless oil (Scheme 4.6, b).

4.4 CONCLUSIONS

In conclusion, a rhodium(III)-catalysed trans-selective $C(sp^2)$-H alkenylation was developed by using *N*-allylbenzimidazole as allylamine surrogate. This methodology was found to be applicable to substrates with a wide range of functional groups and directing groups. More importantly, *N*-arylpurines could be stereoselectivity monoalkenylated with the developed protocol. Mechanistic studies (experimental and computational), organo-rhodium intermediate isolation and structure determination, provide a consistent picture

of the reaction pathway. The formation of *trans*-alkenes among other possibilities (e.g., allylation/cis-alkenylation) is a useful aspect of this methodology.

4.5 EXPERIMENTAL SECTION

All the starting materials were bought from Sigma Aldrich, Alfa-Aesar, Avra, TCI and Spectrochem, and used without any further purification. For column chromatography, silica gel (100-200, 230-400 mesh) from Acme Co. was used. A gradient elution using distilled hexane and ethyl acetate was performed, based on Merck aluminum TLC sheets. All isolated compounds were characterized by ^{1}H NMR (Bruker-400/700 MHz), ^{13}C NMR spectroscopy and HRMS. Copies of the ^{1}H NMR, ^{13}C NMR, ^{19}F NMR. Nuclear Magnetic Resonance spectra were recorded on a Bruker 400/700 MHz instrument. HRMS signal analysis was performed using micro TOF Q-II mass spectrometer. X-ray analysis was conducted using Rigaku Smartlab X-ray diffractometer in NISER, Bhubaneswar. Allyl carbonates,[25] and 2-(2-propylphenyl)pyridine[26] were prepared by following literature reports.

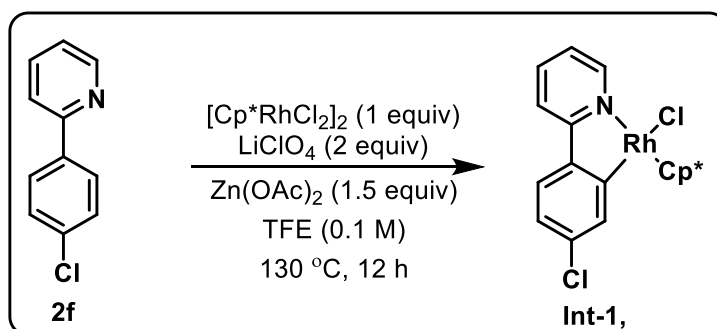**General reaction procedure for the annulation reaction:**
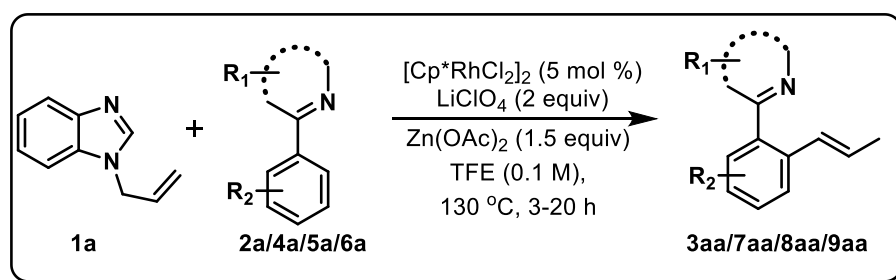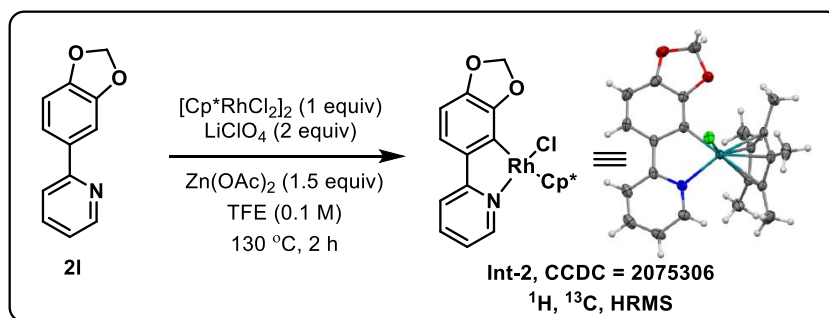

To an oven-dried 25 mL Schlenk tube charged with a magnetic stir bar, was added LiClO$_4$ (0.2 mmol, 2 equiv) and the tube was heated under reduced pressure to eliminate traces of moisture. To this dried tube, were added phenylpyridine **2**, phenylpyrimidine **4**, phenylpyrazole **5** or 9-alkyl-6-(4-chlorophenyl)-purine **6** (0.1 mmol, 1 equiv),

[Cp*RhCl$_2$]$_2$ (0.005 mmol, 5 mol %), Zn(OAc)$_2$ (0.15 mmol, 1.5 equiv), alkene **1a** (0.3 mmol, 3 equiv) and TFE (0.1 M, 1 mL) under a nitrogen atmosphere. The reaction mixture was stirred (750 rpm) in a preheated aluminum block at 130 °C. After completion of the reaction (monitored by TLC), the solvent was evaporated under reduced pressure, and the crude residue was purified by column chromatography using EtOAc/hexane as eluent to provide the corresponding alkenylated product **3aa/7aa/8aa/9aa**.

Synthesis of Intermediate-1 (Int-1):

To an oven-dried 25 mL Schlenk tube charged with a magnetic stir bar, was added LiClO$_4$ (0.1 mmol, 2 equiv) and the tube was heated under reduced pressure to eliminate traces of moisture. To this dried tube, were added 4-chlorophenylpyridine **2f** (0.05 mmol, 1 equiv), [Cp*RhCl$_2$]$_2$

 (0.05 mmol, 1 equiv), Zn(OAc)$_2$ (0.075 mmol, 1.5 equiv) and TFE (0.1 M, 0.5 mL) under a nitrogen atmosphere. The reaction mixture was stirred (750 rpm) in a preheated aluminum block at 130 ℃ for 12 h**.** The solvent was removed under reduced pressure and the residue was recrystallized from methanol/DCM. The reddish colored crystals obtained (17 mg) in 73% yield were characterized by NMR and HRMS analyses.

Synthesis of Intermediate-2 (Int-2):

3af′

To an oven-dried 25 mL Schlenk tube charged with a magnetic stir bar, was added LiClO$_4$ (0.1 mmol, 2 equiv) and the tube was heated under reduced pressure to remove traces of moisture. To this dried tube, were added 2-(benzo[*d*][*1,3*]dioxol-5-yl)pyridine 2l (0.05 mmol, 1 equiv), [Cp*RhCl$_2$]$_2$ (0.05 mmol, 1 equiv), Zn(OAc)$_2$ (0.075 mmol, 1.5 equiv) and TFE (0.1 M, 0.5 mL under a nitrogen atmosphere. The reaction mixture was stirred (750 rpm) in a preheated aluminum block at 130 °C for 2 h. Solvent was removed under reduced pressure and the residue was recrystallized from methanol/DCM. The reddish colored crystals obtained (12 mg) in 50% yield were characterized by NMR, HRMS, and single crystal X-ray analyses.

Experimental characterization data of products:

(*E*)-2-(2-(Prop-1-en-1-yl)phenyl)pyridine (3aa):
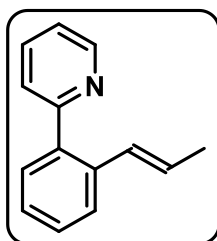
Physical State: Colorless liquid (16 mg, 82% yield). **R$_f$** = 0.5 (10% EtOAc/hexane). **^{1}H NMR (CDCl$_3$, 400 MHz):** δ 8.64 (d, *J* = 4.8 Hz, 1H), 7.65 (dt, *J* = 7.6 Hz, 1.6 Hz, 1H), 7.50 (d, *J* = 7.6 Hz, 1H), 7.38 (dd, *J* = 7.2 Hz, 1.6 Hz, 1H), 7.34 (d, *J* = 7.6 Hz, 1H), 7.30-7.16 (m, 3H), 6.40 (dd, *J* = 16.0 Hz, 1.6 Hz, 1H), 6.16-6.07 (m, 1H), 1.74 (dd, *J* = 6.4 Hz, 1.6 Hz, 3H) ppm. **^{13}C{^{1}H} NMR (CDCl$_3$, 100 MHz):** δ 159.5, 149.7, 139.0, 136.5, 136.1, 130.3, 129.8, 128.7, 127.5, 127.1, 126.4, 125.2, 121.9, 19.0 ppm. **IR** (KBr,

cm^{-1}): 3414, 2912, 1584, 1424, 964. **HRMS (ESI) m/z:** [M+H]$^+$ Calcd for C$_{14}$H$_{14}$N 196.1121; Found 196.1127.

### (E)-2-(4-Methyl-2-(prop-1-en-1-yl)phenyl)pyridine (3ab):
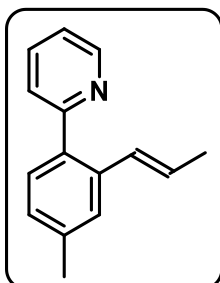
Physical State: Colorless liquid (16 mg, 77% yield). **R$_f$** = 0.3 (10% EtOAc/hexane). **^{1}H NMR (CDCl$_3$, 400 MHz):** δ 8.70 (d, J = 4.4 Hz, 1H), 7.71 (t, J = 7.6 Hz, 1H), 7.41-7.35 (m, 3H), 7.24-7.20 (m, 1H), 7.12 (d, J = 7.6 Hz, 1H), 6.47 (d, J = 16.0 Hz, 1H), 6.22-6.13 (m, 1H), 2.39 (s, 3H), 1.81 (d, J = 6.4 Hz, 3H) ppm. **^{13}C{^{1}H} NMR (CDCl$_3$, 175 MHz):** δ 159.5, 149.6, 138.4, 136.3 (2C), 136.1, 130.3, 129.9, 128.0, 127.2, 127.1, 125.2, 121.7, 21.6, 19.0 ppm. **IR** (KBr, cm^{-1}): 3458, 2913, 1608, 1585, 1464, 964. **HRMS (ESI) m/z:** [M+H]$^+$ Calcd for C$_{15}$H$_{16}$N 210.1277; Found 210.1284.

### (E)-2-(4-Ethyl-2-(prop-1-en-1-yl)phenyl)pyridine (3ac):
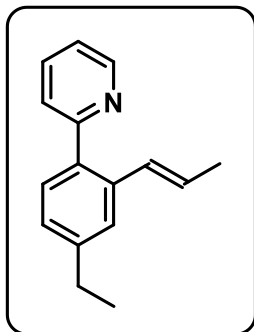
Physical State: Oily liquid (14 mg, 63% yield). **R$_f$** = 0.4 (5% EtOAc/hexane). **^{1}H NMR (CDCl$_3$, 400 MHz):** δ 8.70 (m, 1H), 7.71 (td, J = 7.6 Hz, 2.0 Hz, 1H), 7.42-7.38 (m, 3H), 7.24-7.21 (m, 1H), 7.15 (dd, J = 8.0 Hz, 1.6 Hz, 1H), 6.48 (dd, J = 15.6 Hz, 1.6 Hz, 1H), 6.23-6.14 (m, 1H), 2.69 (q, J = 7.6 Hz, 2H), 1.82 (dd, J = 6.8 Hz, 1.6 Hz, 3H), 1.27 (t, J = 7.6 Hz, 3H) ppm. **^{13}C{^{1}H} NMR (CDCl$_3$, 175 MHz):** δ 159.5, 149.6, 144.8, 136.5, 136.3, 136.1, 130.3, 130.0, 127.2, 126.9, 125.9, 125.2, 121.7, 29.1, 19.0, 15.9 ppm. **IR** (KBr, cm^{-1}): 3499, 2962, 1607, 1585, 1463, 965. **HRMS (ESI) m/z:** [M+H]$^+$ Calcd for C$_{16}$H$_{18}$N 224.1434; Found 224.1453.

***(E)*-2-(4-Methoxy-2-(prop-1-en-1-yl)phenyl)pyridine (3ad)**:
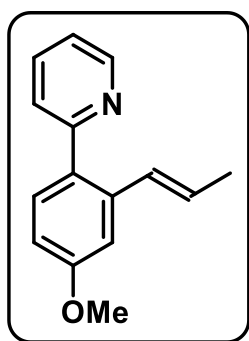
Physical State: Colorless liquid (17 mg, 76% yield), **R_f-value:** 0.3 (10% EtOAc/hexane). **^{1}H NMR (CDCl$_3$, 400 MHz):** δ 8.69 (d, J = 4.0 Hz, 1H), 7.70 (td, J = 7.6 Hz, 1.6 Hz, 1H), 7.42 (d, J = 8.4 Hz, 1H), 7.38 (d, J = 8.0 Hz, 1H), 7.22-7.19 (m, 1H), 7.08 (d, J = 2.0 Hz, 1H), 6.86 (dd, J = 8.4 Hz, 2.4 Hz, 1H), 6.49 (dd, J = 15.6 Hz, 1.6 Hz, 1H), 6.23-6.14 (m, 1H), 3.86 (s, 3H), 1.82 (dd, J = 6.4 Hz, 1.6 Hz, 3H) ppm. **^{13}C{^{1}H} NMR (CDCl$_3$, 100 MHz):** δ 160.0, 159.2, 149.6, 137.9, 136.1, 132.1, 131.7, 130.0, 127.7, 125.2, 121.5, 113.1, 111.4, 55.6, 19.0 ppm. **IR (KBr, cm^{-1}):** 3424, 2929, 1602, 1586, 1462, 963. **HRMS (ESI) m/z:** [M+H]$^+$ Calcd for C$_{15}$H$_{16}$NO 226.1226; Found 226.1230.

***(E)*-2-(4-Fluoro-2-(prop-1-en-1-yl)phenyl)pyridine (3ae):**
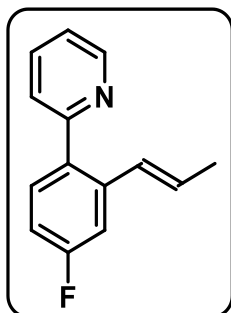
Physical State: Colorless liquid (17 mg, 80% yield). **R_f = 0.4** (10% EtOAc/hexane). **^{1}H NMR (CDCl$_3$, 700 MHz):** δ 8.70 (d, J = 4.2 Hz, 1H), 7.73 (td, J = 7.7 Hz, 2.1 Hz, 1H), 7.43 (dd, J = 6.3 Hz, 2.1 Hz, 1H), 7.38 (d, J = 8.4 Hz, 1H), 7.26-7.24 (m, 2H), 6.99 (td, J = 7.7 Hz, 2.1 Hz, 1H), 6.44 (d, J = 15.4 Hz, 1H) 6.23-6.18 (m, 1H), 1.82 (dd, J = 6.3 Hz, 1.4 Hz, 3H) ppm. **^{13}C{^{1}H} NMR (CDCl$_3$, 175 MHz):** δ 163.2 (d, J_{C-F} = 244.8 Hz), 158.6, 149.7, 138.7 (d, J_{C-F} = 8.0 Hz), 136.3, 135.1 (d, J_{C-F} = 2.8 Hz), 132.2 (d, J_{C-F} = 8.7 Hz), 129.0 (d, J_{C-F} = 2.1 Hz), 128.8, 125.2, 122.0, 114.1 (d, J_{C-F} = 21.5 Hz), 112.7 (d, J_{C-F} = 22.0), 19.0 ppm. **^{19}F NMR (CDCl$_3$, 376 MHz):** -114.1 ppm. **IR (KBr, cm^{-1}):** 3393, 2912, 1606, 1587, 1463, 1159, 963. **HRMS (ESI) m/z:** [M+H]$^+$ Calcd for C$_{14}$H$_{13}$FN 214.1027; Found 214.1030.

### (E)-2-(4-Chloro-2-(prop-1-en-1-yl)phenyl)pyridine (3af):
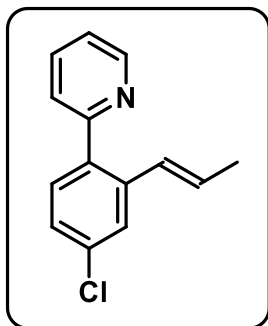
Physical State: Oily liquid (17 mg, 75% yield). R_f = 0.45 (10% EtOAc/hexane). **¹H NMR (CDCl₃, 400 MHz):** δ 8.70 (d, J = 4.4 Hz, 1H), 7.73 (td, J = 7.6 Hz, 1.6 Hz, 1H), 7.55 (d, J = 2.0 Hz, 1H), 7.41-7.38 (m, 2H), 7.28-7.24 (m, 2H), 6.42 (dd, J = 15.6 Hz, 1.6 Hz, 1H), 6.25-6.16 (m, 1H), 1.82 (dd, J = 6.8 Hz, 1.6 Hz, 3H) ppm. **¹³C{¹H} NMR (CDCl₃, 100 MHz):** δ 158.4, 149.8, 138.2, 137.3, 136.3, 134.7, 131.7, 128.9, 128.8, 127.1, 126.4, 125.1, 122.2, 19.0 ppm. **IR** (KBr, cm⁻¹): 3422, 2912, 1592, 1462, 1099, 961. **HRMS (ESI) m/z:** [M+H]⁺ Calcd for $C_{14}H_{13}ClN$ 230.0731; Found 230.0732.

### (E)-1-(3-(Prop-1-en-1-yl)-4-(pyridin-2-yl)phenyl)ethanone (3ag):
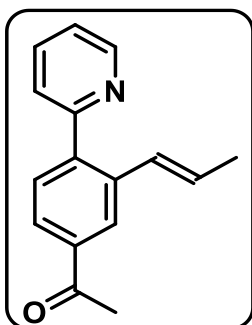
Physical State: Colorless liquid (19 mg, 80% yield). R_f = 0.4 (20% EtOAc/hexane). **¹H NMR (CDCl₃, 400 MHz):** δ 8.74 (d, J = 4.4 Hz, 1H), 8.16 (d, J = 1.6 Hz, 1H), 7.87 (dd, J = 8.0 Hz, 1.6 Hz, 1H), 7.77 (td, J = 7.6 Hz, 1.6 Hz, 1H), 7.56 (d, J = 8.0 Hz, 1H), 7.44 (d, J = 8.0 Hz, 1H), 7.31-7.28 (m, 1H), 6.49 (dd, J = 15.6 Hz, 1.6 Hz, 1H), 6.35-6.26 (m, 1H), 2.65 (s, 3H), 1.85 (dd, J = 6.8 Hz, 1.6 Hz, 3H) ppm. **¹³C{¹H} NMR (CDCl₃, 100 MHz):** δ 198.4, 158.4, 149.9, 143.1, 137.2, 137.0, 136.4, 130.7, 129.1 (2C), 126.8, 126.7, 125.2, 122.6, 27.1, 19.0 ppm. **IR** (KBr, cm⁻¹): 3429, 2915, 1683, 1584, 1356, 1240, 964. **HRMS (ESI) m/z:** [M+H]⁺ Calcd for $C_{16}H_{16}NO$ 238.1226; Found 238.1218.

(E)-2-(2-(prop-1-en-1-yl)-4-(trifluoromethyl)phenyl)pyridine (3ah):
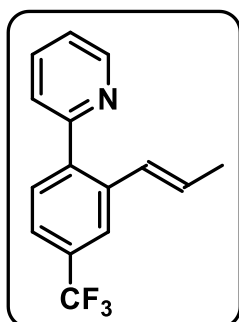
Physical State: Colorless liquid (22 mg, 84% yield). R_f = 0.5 (10% EtOAc/hexane). **^{1}H NMR (CDCl$_3$, 400 MHz):** δ 8.74 (d, J = 4.8 Hz, 1H), 7.81 (s, 1H), 7.77 (td, J = 7.6 Hz, 2.0 Hz, 1H), 7.58-7.52 (m, 2H), 7.43 (d, J = 8.0 Hz, 1H), 7.32-7.29 (m, 1H), 6.47 (dd, J = 15.6 Hz, 1.6 Hz, 1H), 6.23-6.25 (m, 1H), 1.84 (dd, J = 6.4 Hz, 1.6 Hz, 3H) ppm. **^{13}C{^{1}H} NMR (CDCl$_3$, 100 MHz):** δ 158.2, 149.9, 141.9, 137.2, 136.4, 130.8, 129.5, 129.2, 128.7, 127.2 (q, J_{C-F} = 264.0 Hz), 125.1, 123.6 (q, J_{C-F} = 3.7 Hz), 123.4 (q, J_{C-F} = 3.9 Hz), 122.6, 19.0 ppm. **^{19}F NMR (CDCl$_3$, 376 MHz):** δ -62.6 ppm. **IR** (KBr, cm^{-1}): 3460, 2915, 1651, 1586, 1336, 1124, 962. **HRMS (ESI) m/z:** [M+H]$^+$ Calcd for C$_{15}$H$_{13}$F$_3$N 264.0995; Found 264.0985.

(E)-3-(Prop-1-en-1-yl)-4-(pyridin-2-yl)benzaldehyde (**3ai**):
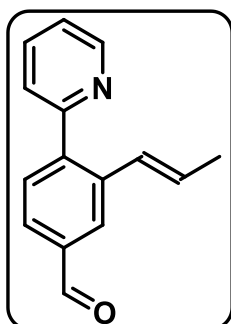
Physical State: Oily liquid (18 mg, 81% yield). R_f = 0.5 (30% EtOAc/hexane). **^{1}H NMR (CDCl$_3$, 400 MHz):** δ 10.07 (s, 1H), 8.74 (d, J = 4.0 Hz, 1H), 8.07 (d, J = 1.6 Hz, 1H), 7.81-7.75 (m, 2H), 7.63 (d, J = 7.6 Hz, 1H), 7.45 (d, J = 8.0 Hz, 1H), 7.32-7.29 (m, 1H), 6.59 (dd, J = 15.6 Hz, 1.6 Hz, 1H), 6.36-6.27 (m, 1H), 1.86 (dd, J = 6.8 Hz, 1.6 Hz, 3H) ppm. **^{13}C{^{1}H} NMR (CDCl$_3$, 100 MHz):** δ 192.5, 158.3, 150.0, 144.4, 137.6, 136.6, 136.4, 131.2, 129.5, 128.8, 128.2, 127.9, 125.1, 122.7, 19.0 ppm. **IR** (KBr, cm^{-1}): 3431, 2921, 1695, 1584, 1435, 963. **HRMS (ESI) m/z:** [M+H]$^+$ Calcd for C$_{15}$H$_{14}$NO 224.1070; Found 224.1051.

Methyl (E)-3-(prop-1-en-1-yl)-4-(pyridin-2-yl)benzoate (**3aj**):

Physical State: Oily liquid (20 mg, 79% yield). R_f = 0.4 (20% EtOAc/hexane). **^{1}H NMR (CDCl$_3$, 700 MHz):** δ 8.74 (d, J = 4.2 Hz, 1H), 8.25 (s,1H), 7.95 (dd, J = 7.7 Hz, 1.4 Hz,
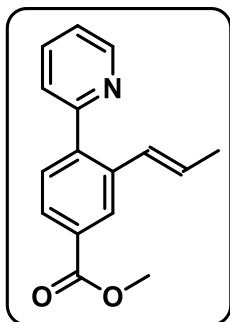
1H), 7.76 (td, J = 7.7 Hz, 1.4 Hz, 1H), 7.53 (d, J = 8.4 Hz, 1H), 7.44 (d, J = 7.7 Hz, 1H), 7.30-7.28 (m, 1H), 6.47 (d, J = 15.4 Hz, 1H), 6.34-6.29 (m, 1H), 3.94 (s, 3H), 1.84 (dd, J = 6.3 Hz, 1.4 Hz, 3H) ppm. ^{13}C{^{1}H} NMR (CDCl$_3$, 175 MHz): δ 167.3, 158.5, 149.9, 142.9, 136.8, 136.4, 130.5, 130.3, 128.9, 128.9, 128.0, 127.9, 125.2, 122.5, 52.5, 19.0 ppm. IR (KBr, cm^{-1}): 3430, 2950, 1720, 1584, 1435, 1290, 1107, 965. HRMS (ESI) m/z: [M+H]$^+$ Calcd for C$_{16}$H$_{16}$NO$_2$ 254.1176; Found 254.1151.

(E)-2-(4-Chloro-2-(prop-1-en-1-yl)phenyl)-5-methylpyridine (3ak):
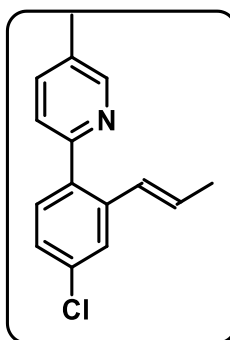
Physical State: Oily liquid (19 mg, 78% yield). R_f = 0.4 (10% EtOAc/hexane). ^{1}H NMR (CDCl$_3$, 400 MHz): δ 8.52 (d, J = 2.0 Hz, 1H), 7.53-7.50 (m, 2H), 7.37 (d, J = 8.4 Hz, 1H), 7.27-7.22 (m, 2H), 6.42 (dd, J = 15.6 Hz, 1.6 Hz, 1H), 6.23-6.14 (m, 1H), 2.40 (s, 3H), 1.83 (dd, J = 6.8 Hz, 1.6 Hz, 3H) ppm. ^{13}C{^{1}H} NMR (CDCl$_3$, 100 MHz): δ 155.5, 150.2, 138.2, 137.3, 136.9, 134.5, 131.7, 131.6, 128.9, 128.7, 127.1, 126.3, 124.6, 19.0, 18.5 ppm. IR (KBr, cm^{-1}): 3413, 2916, 1591, 1469, 1090, 962. HRMS (ESI) m/z: [M+H]$^+$ Calcd for C$_{15}$H$_{15}$ClN 244.0888; Found 244.0890.

(E)-2-(4-(Prop-1-en-1-yl)benzo[d][1,3]dioxol-5-yl)pyridine (3al):
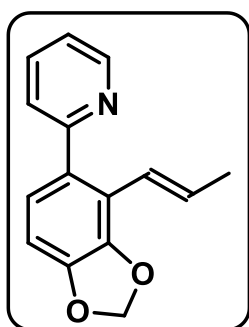
Physical State: colorless liquid (16 mg, 67% yield). R_f = 0.5 (20% EtOAc/hexane). ^{1}H NMR (CDCl$_3$, 400 MHz): δ 8.67 (d, J = 4.0 Hz, 1H), 7.70 (td, J = 7.6 Hz, 1.6 Hz, 1H), 7.37 (d, J = 8.0 Hz, 1H), 7.24-7.21 (m, 1H), 6.95 (d, J = 8.0 Hz, 1H), 6.75 (d, J = 8.0 Hz, 1H), 6.57-6.48 (m, 1H), 6.25 (dd, J = 16.0 Hz,

1.6 Hz, 1H), 6.04 (s, 2H), 1.81 (dd, J = 6.8 Hz, 1.6 Hz, 3H) ppm. **^{13}C{^{1}H} NMR (CDCl$_3$, 100 MHz):** δ 159.3, 149.6, 147.9, 145.6, 136.2, 134.0, 132.0, 125.2, 124.6, 124.2, 121.8, 119.5, 106.8, 101.3, 19.7 ppm. **IR (KBr, cm^{-1}):** 3413, 2909, 1622, 1585, 1445, 1245, 1059, 943. **HRMS (ESI) m/z:** [M+H]$^+$ Calcd for C$_{15}$H$_{14}$NO$_2$ 240.1019; Found 240.1027.

(E)-1-(4-(Prop-1-en-1-yl)-3-(pyridin-2-yl)phenyl)ethan-1-one (3an):
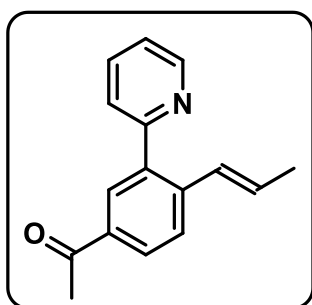
Physical State: Oily liquid (16 mg, 67% yield). **R$_f$** = 0.4 (20% EtOAc/hexane). **^{1}H NMR (CDCl$_3$, 400 MHz):** δ 8.74 (d, J = 4.4 Hz, 1H), 8.03 (d, J = 2.0 Hz, 1H), 7.95 (dd, J = 8.4 Hz, 2.0 Hz, 1H), 7.77 (td, J = 7.6 Hz, 1.6 Hz, 1H), 7.67 (d, J = 8.0 Hz, 1H), 7.44 (d, J = 8.0 Hz, 1H), 7.32-7.28

(m, 1H), 6.51 (dd, J = 15.6 Hz, 1.2 Hz, 1H), 7.39-7.30 (m, 1H), 2.60 (s, 3H), 1.85 (dd, J = 6.8 Hz, 1.6 Hz, 3H) ppm. **^{13}C{^{1}H} NMR (CDCl$_3$, 100 MHz):** δ 197.8, 158.6, 149.8, 141.1, 139.1, 136.5, 135.7, 130.9, 130.4, 129.1, 128.4, 126.6, 125.2, 122.4, 26.9, 19.2 ppm. **IR (KBr, cm^{-1}):** 3421, 2912, 1680, 1600, 1465, 1241, 964. **HRMS (ESI) m/z:** [M+H]$^+$ Calcd for C$_{16}$H$_{16}$NO 238.1226; Found 238.1239.

(E)-2-(3-(prop-1-en-1-yl)furan-2-yl)pyridine (3ar):
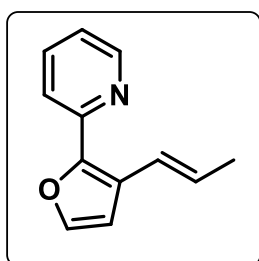
Physical State: Oily liquid (14 mg, 76% yield). **R$_f$-value:** 0.6 (5% EtOAc/hexane). **^{1}H NMR (CDCl$_3$, 700 MHz):** δ 8.62 (d, J = 4.9 Hz, 1H), 7.70-7.66 (m, 2H), 7.41-7.39 (m, 2H), 7.12-7.10 (m, 1H), 6.67 (d, J = 2.1 Hz, 1H), 6.17-6.11(m, 1H), 1.93

(dd, J = 6.3 Hz, 1.4 Hz, 3H) ppm. **^{13}C{^{1}H} NMR (CDCl$_3$, 175 MHz):** δ 151.4, 149.6, 147.0, 142.7, 136.6, 128.0, 124.1, 122.8, 121.4, 120.2, 110.3, 19.06 ppm. **IR (KBr, cm^{-1}):** 3471, 2932, 2911, 1591, 1555, 1445, 973. **HRMS (ESI) m/z:** [M+H]$^+$ Calcd for C$_{12}$H$_{12}$NO 186.0913; Found 186.0920.

(E)-2-(3-(prop-1-en-1-yl)thiophen-2-yl)pyridine (**3as**):
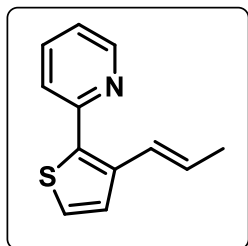
Physical State: Oily liquid (14 mg, 70% yield). R_f **-value:** 0.6 (0% EtOAc/hexane). **^{1}H NMR (CDCl$_3$, 700 MHz):** δ 8.65 (d, J = 4.2 Hz, 1H), 7.71 (td, J = 7.7 Hz, 1.4 Hz, 1H), 7.54 (d, J = 7.7 Hz, 1H), 7.28 (d, J = 4.9 Hz, 1H), 7.22 (d, J = 5.6 Hz, 1H), 7.18- 6.16 (m, 1H), 6.80 (d, J = 15.4 Hz, 1H), 6.24-6.19 (m, 1H), 1.90 (dd, J = 7.0 Hz, 1.4 Hz, 3H) ppm. **^{13}C{^{1}H} NMR (CDCl$_3$, 175 MHz):** δ 153.5, 150.0, 137.7, 137.6, 136.7, 128.6, 127.5, 126.3, 125.2, 123.1, 121.8, 19.0 ppm. **IR** (KBr, cm^{-1}): 3470, 2929, 2909, 1581, 1563, 1434, 968. **HRMS (ESI) m/z:** [M+H]$^+$ Calcd for C$_{12}$H$_{12}$NS 202.0685; Found 202.0682.

(E)-2-(2-(Prop-1-en-1-yl)phenyl)pyrimidine (**7aa**):
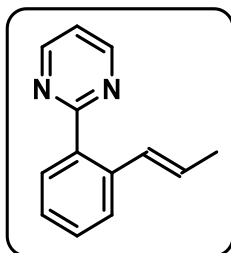
Physical State: Colorless liquid (13 mg, 66% yield. R_f = 0.2 (10% EtOAc/hexane). **^{1}H NMR (CDCl$_3$, 400 MHz):** δ 8.86 (d, J = 4.8 Hz, 2H), 7.75 (dd, J = 7.6 Hz, 1.6 Hz, 1H), 7.61 (d, J = 7.2 Hz, 1H), 7.40 (td, J = 7.6 Hz, 1.2 Hz, 1H), 7.32 (td, J = 7.6 Hz, 1.2 Hz, 1H), 7.25-7.22 (m, 1H), 6.82 (dd, J = 15.6 Hz, 1.2 Hz, 1H), 6.26-6.17 (m, 1H), 1.86 (dd, J = 6.4 Hz, 1.6 Hz, 3H) ppm. **^{13}C{^{1}H} NMR (CDCl$_3$, 100 MHz):** δ 167.7, 157.3, 137.3, 136.8, 130.9, 129.9, 129.8, 127.5, 127.1, 126.8, 118.8, 19.1 ppm. **IR** (KBr, cm^{-1}): 3433, 2912, 1567, 1553, 1414, 961. **HRMS (ESI) m/z:** [M+H]$^+$ Calcd for C$_{13}$H$_{13}$N$_2$ 197.1073; Found 197.1080.

(E)-2-(4-Methyl-2-(prop-1-en-1-yl)phenyl)pyrimidine (**7ab**):

Physical State: Colorless liquid (16 mg, 76% yield). R_f = 0.4 (10% EtOAc/hexane). **^{1}H NMR (CDCl$_3$, 400 MHz):** δ 8.8 (d, J = 4.8 Hz, 2H), 7.69 (d, J = 8.0 Hz, 1H), 7.41 (s,
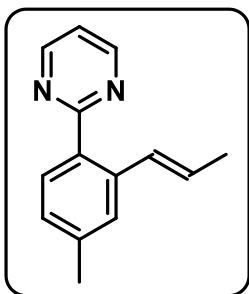
1H), 7.18 (t, J = 4.8 Hz, 1H), 7.13 (d, J = 7.2 Hz, 1H), 6.89 (dd, J = 15.6 Hz, 1.2 Hz, 1H), 6.22-6.13 (m, 1H), 2.39 (s, 3H), 1.86 (dd, J = 6.4 Hz, 1.6 Hz, 3H) ppm. $^{13}C\{^1H\}$ **NMR (CDCl$_3$, 100 MHz):** δ 167.9, 157.1, 139.8, 137.4, 134.3, 131.1, 130.3, 128.0, 127.6, 127.1, 118.6, 21.73, 19.07 ppm. **IR** (KBr, cm^{-1}): 3032, 2917, 1608, 1566, 1415, 960. **HRMS (ESI) m/z:** [M+H]$^+$ Calcd for C$_{14}$H$_{15}$N$_2$ 211.1230; Found 211.1234.

***(E)-2-(4-Fluoro-2-(prop-1-en-1-yl)phenyl)pyrimidine* (7ac)**:
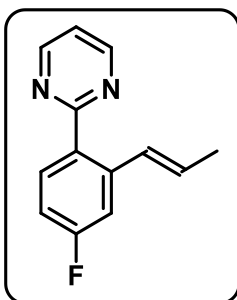
Physical State: Colorless liquid (19 mg, 89% yield). $\mathbf{R}_f$ = 0.4 (20% EtOAc/hexane). ^{1}**H NMR (CDCl$_3$, 700 MHz):** δ 8.86 (d, J = 4.9 Hz, 2H), 7.79-7.77 (m, 1H), 7.30-7.28 (m, 1H), 7.23 (t, J = 4.9 Hz, 1H), 7.03-7.00 (m, 1H), 6.86 (d, J = 16.1 Hz, 1H), 6.26-6.21 (m, 1H), 1.88-1.86 (m, 3H) ppm. $^{13}C\{^1H\}$ **NMR (CDCl$_3$, 175 MHz):** δ 166.9, 163.9 (d, $J_{C\text{-}F}$ = 248.1 Hz), 157.3, 140.0 (d, $J_{C\text{-}F}$ = 8.2 Hz), 133.3 (d, $J_{C\text{-}F}$ = 8.9 Hz), 133.0 (d, $J_{C\text{-}F}$ = 2.8 Hz), 129.2 (d, $J_{C\text{-}F}$ = 1.9 Hz), 128.8, 118.9, 114.2 (d, $J_{C\text{-}F}$ = 21.6 Hz), 113.2 (d, $J_{C\text{-}F}$ = 22.3 Hz), 19.1 ppm. ^{19}**F NMR (CDCl$_3$, 376 MHz):** δ -112.0. **IR** (KBr, cm^{-1}): 3443, 2912, 1607, 1577, 1409, 1267, 960. **HRMS (ESI) m/z:** [M+H]$^+$ Calcd for C$_{13}$H$_{12}$FN$_2$ 215.0979; Found 215.0993.

***(E)-2-(4-Chloro-2-(prop-1-en-1-yl)phenyl)pyrimidine* (7ad)**:
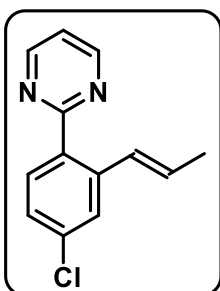
Physical State: Colorless liquid (19 mg, 82% yield). $\mathbf{R}_f$ = 0.3 (10% EtOAc/hexane). ^{1}**H NMR (CDCl$_3$, 400 MHz):** δ 8.78 (d, J = 4.8 Hz, 2H), 7.67 (d, J = 8.4 Hz, 1H), 7.51 (s, 1H), 7.23-7.16 (m, 2H), 6.77 (d, J = 15.6 Hz, 1H), 6.21-6.12 (m, 1H), 1.79 (d, J = 6.4 Hz,

3H) ppm. **¹³C{¹H} NMR (CDCl₃, 175 MHz):** δ 166.8, 157.3, 139.2, 136.0, 135.1, 132.5, 129.0, 128.9, 127.1, 126.8, 119.0, 19.1 ppm. **IR** (KBr, cm⁻¹): 3446, 2923, 1563, 1417, 1265, 1102, 961. **HRMS (ESI) m/z:** [M+H]⁺ Calcd for $C_{13}H_{12}ClN_2$ 231.0684; Found 231.0678.

(E)-2-(4-Chloro-2-(prop-1-en-1-yl)phenyl)-5-methylpyrimidine (7ae):
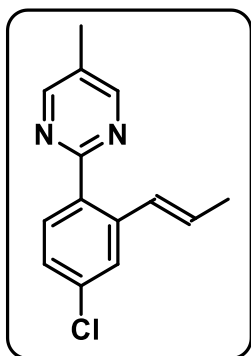
Physical State: Colorless liquid (19 mg, 78% yield). **R***f* = 0.45 (10% EtOAc/hexane). **¹H NMR (CDCl₃, 400 MHz):** δ 8.67 (s, 2H), 7.69 (d, *J* = 8.4 Hz, 1H), 7.57 (d, *J* = 2.0 Hz, 1H), 7.27 (dd, *J* = 8.4 Hz, 2.0 Hz, 1H), 6.82 (dd, *J* = 15.6 Hz, 1.6 Hz, 1H), 6.27-6.18 (m, 1H), 2.37 (s, 3H), 1.86 (dd, *J* = 6.4 Hz, 1.6 Hz, 3H) ppm. **¹³C{¹H} NMR (CDCl₃, 100 MHz):** δ 164.3, 157.5, 139.0, 135.6, 135.2, 132.3, 129.0, 128.7, 128.3, 127.1, 126.7, 19.1, 15.8 ppm. **IR** (KBr, cm⁻¹): 3452, 2924, 1588, 1429, 1101, 959. **HRMS (ESI) m/z:** [M+H]⁺ Calcd for $C_{14}H_{14}ClN_2$ 245.0840; Found 245.0843.

(E)-1-(2-(Prop-1-en-1-yl)phenyl)-1H-pyrazole (8aa):
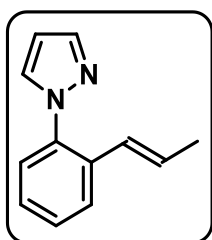
Physical State: Colorless liquid (12 mg, 65% yield). **R***f* = 0.4 (10% EtOAc/hexane). **¹H NMR (CDCl₃, 700 MHz):** δ 7.73 (s, 1H), 7.62 (s, 1H), 7.58 (d, *J* = 8.4 Hz, 1H), 7.36-7.34 (m, 2H), 7.29 (td, *J* = 7.7 Hz, 1.4 Hz, 1H), 6.44 (s, 1H), 6.21-6.20 (m, 2H), 1.82 (d, *J* = 4.2 Hz, 3H) ppm. **¹³C{¹H} NMR (CDCl₃, 175 MHz):** δ 140.8, 138.3, 133.9, 131.7, 129.0, 128.6, 127.6, 126.9, 126.6, 126.5, 106.6, 19.1 ppm. **IR** (KBr, cm⁻¹): 3424, 2912, 1691, 1517, 1393, 1044, 965. **HRMS (ESI) m/z:** [M+H]⁺ Calcd for $C_{12}H_{13}N_2$ 185. 1079; Found 185. 1085.
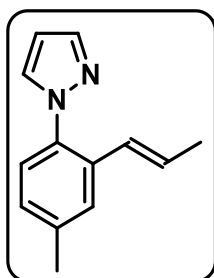
(E)-1-(4-Methyl-2-(prop-1-en-1-yl)phenyl)-1H-pyrazole (8ab):

Physical State: Colorless liquid (14 mg, 70% yield). R_f = 0.4 (5% EtOAc/hexane). **^{1}H NMR (CDCl$_3$, 700 MHz):** δ 7.71 (d, J = 1.4 Hz, 1H), 7.57 (d, J = 2.1 Hz, 1H), 7.38 (s, 1H), 7.23 (d, J = 7.7 Hz, 1H), 7.09 (d, J = 7.7 Hz, 1H), 6.42 (t, J = 2.1 Hz, 1H), 6.21-6.17 (m, 1H), 6.15 (d, J = 16.1 Hz, 1H), 2.39 (s, 3H), 1.81 (d, J = 4.9 Hz, 3H) ppm. **^{13}C{^{1}H} NMR (CDCl$_3$, 175 MHz):** δ 140.6, 138.4, 136.0, 133.6, 131.7, 128.7, 128.4, 127.2, 126.5 (2C), 106.4, 21.5, 19.1 ppm. **IR** (KBr, cm^{-1}): 3422, 2920, 1690, 1515, 1395, 965. **HRMS (ESI) m/z:** [M+H]$^+$ Calcd for C$_{13}$H$_{15}$N$_2$ 199.1230; Found 199.1238.

(E)-1-(4-Methoxy-2-(prop-1-en-1-yl)phenyl)-1H-pyrazole (8ac):
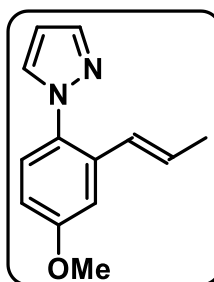
Physical State: Colorless liquid (17 mg, 80% yield). R_f = 0.2 (5% EtOAc/hexane). **^{1}H NMR (CDCl$_3$, 400 MHz):** δ 7.70 (d, J = 1.6 Hz, 1H), 7.53 (d, J = 2.4 Hz, 1H), 7.25-7.24 (m, 1H), 7.06 (d, J = 2.8 Hz, 1H), 6.82 (dd, J = 8.8 Hz, 3.2 Hz, 1H), 6.41 (t, J = 2.0 Hz, 1H), 6.21-6.14 (m, 1H), 6.09 (dd, J = 15.6 Hz, 1.2 Hz, 1H), 3.85 (s, 3H), 1.80 (dd, J = 6.4 Hz, 1.2 Hz, 3H) ppm. **^{13}C{^{1}H} NMR (CDCl$_3$, 100 MHz):** δ 159.7, 140.5, 135.5, 131.9, 131.8, 129.2, 128.0, 126.3, 113.2, 111.2, 106.3, 55.8, 19.0 ppm. **IR** (KBr, cm^{-1}): 3430, 2913, 1652, 1604, 1518, 1294, 1043, 964. **HRMS (ESI) m/z:** [M+H]$^+$ Calcd for C$_{13}$H$_{15}$N$_2$O 215.1179; Found 215.1192.

(E)-1-(4-Chloro-2-(prop-1-en-1-yl)phenyl)-1H-pyrazole (8ad):
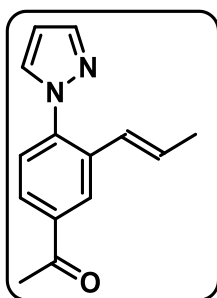
Physical State: Colorless liquid (16 mg, 73% yield). R_f = 0.4 (5% EtOAc/hexane). **^{1}H NMR (CDCl$_3$, 400 MHz):** δ 7.66 (d, J = 1.6 Hz, 1H), 7.51 (d, J = 2.0 Hz, 1H),
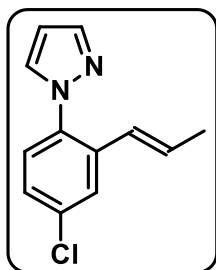
7.48 (d, J = 2.4 Hz, 1H), 7.23 (d, J = 8.4 Hz, 1H), 7.19-7.17 (m, 1H), 6.37 (t, J = 2.0 Hz, 1H), 6.21-6.12 (m, 1H), 6.08 (d, J = 16.8 Hz, 1H), 1.76 (d, J = 6.0 Hz, 3H) ppm. **^{13}C{^{1}H} NMR (CDCl$_3$, 100 MHz):** δ 141.1, 135.4, 134.4, 131.6, 130.5, 127.9, 127.6, 126.8, 125.6, 120.6, 106.9, 19.1 ppm. **IR** (KBr, cm^{-1}): 3444, 2912, 1651, 1517, 1485, 1109, 955. **HRMS (ESI) m/z:** [M+H]$^+$ Calcd for C$_{12}$H$_{12}$ClN$_2$ 219.0684; Found 219.0680.

(E)-1-(3-(Prop-1-en-1-yl)-4-(1H-pyrazol-1-yl)phenyl)ethanone (**8ae**):

Physical State: Colorless liquid (15 mg, 66% yield). **R$_f$** = 0.2 (5% EtOAc/hexane). **^{1}H NMR (CDCl$_3$, 700 MHz):** δ 7.93 (s, 2H), 7.77 (d, J = 1.4 Hz, 1H), 7.68 (d, J = 7.7 Hz, 1H), 7.65 (d, J = 2.1 Hz, 1H), 6.48 (t, J = 2.1 Hz, 1H), 6.39-6.34 (m, 1H), 6.25 (d, J = 16.1 Hz, 1H), 2.60 (s, 3H), 1.87 (dd, J = 6.3 Hz, 1.4 Hz, 3H) ppm.

^{13}C{^{1}H} NMR (CDCl$_3$, 175 MHz): δ 197.0, 141.2, 138.4, 138.2, 136.3, 132.0, 131.7, 128.1, 127.0, 125.9, 107.1, 26.9, 19.3 ppm. **IR** (KBr, cm^{-1}): 3444, 2915, 1682, 1605, 1517, 1450, 1264, 968. **HRMS (ESI) m/z:** [M+H]$^+$ Calcd for C$_{14}$H$_{15}$N$_2$O 227.1179; Found 227.1186.

*(E)-9-Benzyl-6-(4-chloro-2-(prop-1-en-1-yl)phenyl)-9H-purine* (**9aa**):
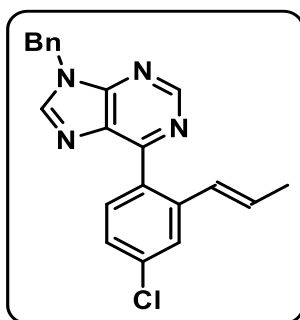
Physical State: Colorless liquid (25 mg, 70% yield). **R$_f$** = 0.3 (20% EtOAc/hexane). **^{1}H NMR (CDCl$_3$, 400 MHz):** δ 9.09 (s, 1H), 8.07 (s, 1H), 7.69 (d, J = 8.4 Hz, 1H), 7.66 (d, J = 2.0 Hz, 1H), 7.41-7.31 (m, 6H), 6.62 (dd, J = 15.6 Hz, 1.6 Hz, 1H), 6.30-6.21 (m, 1H), 5.49 (s, 2H), 1.79 (dd, J =

6.8 Hz, 1.6 Hz, 3H) ppm. **^{13}C{^{1}H} NMR (CDCl$_3$, 175 MHz):** δ 157.6, 152.7, 152.4, 144.9, 139.3, 136.3, 135.3, 132.9, 132.9, 131.7, 129.5, 129.3, 129.0, 128.4, 128.3, 127.0, 126.6, 47.7, 19.0 ppm. **IR** (KBr, cm^{-1}): 3435, 2925, 1708, 1580, 1499, 1328, 958. **HRMS (ESI) m/z:** [M+H]$^+$ Calcd for C$_{21}$H$_{18}$ClN$_4$ 361.1215; Found 361.1222.

(E)-9-Benzyl-6-(4-methyl-2-(prop-1-en-1-yl)phenyl)-9H-purine (**9ab**):
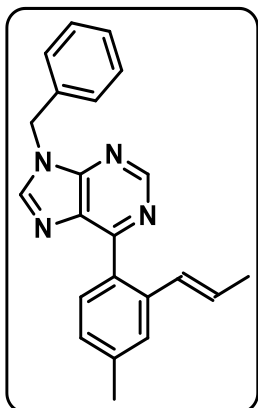
Physical State: Colorless liquid (26 mg, 76% yield). **R$_f$** = 0.3 (20% EtOAc/hexane). **^{1}H NMR (CDCl$_3$, 400 MHz):** δ 9.07 (s, 1H), 8.02 (s, 1H), 7.64 (d, J = 8.0 Hz, 1H), 7.49 (s, 1H), 7.38-7.34 (m, 5H), 7.16 (d, J = 7.6 Hz, 1H), 6.67 (d, J = 15.6 Hz, 1H), 6.24-6.16 (m, 1H), 5.48 (s, 2H), 2.41 (s, 3H), 1.77 (dd, J = 6.8 Hz, 1.2 Hz, 3H) ppm. **^{13}C{^{1}H} NMR (CDCl$_3$, 100 MHz):** δ 159.1, 152.7, 152.3, 144.5, 140.0, 137.4, 135.6, 132.7, 131.6, 130.8, 129.7, 129.5, 128.9, 128.3, 127.9, 127.4, 127.3, 47.7, 21.8, 19.0 ppm. **IR** (KBr, cm^{-1}): 3563, 2919, 2851, 1582, 1504, 1454, 963. **HRMS (ESI) m/z:** [M+H]$^+$ Calcd for C$_{22}$H$_{21}$N$_4$ 341.1761; Found 341.1773.

(E)-9-benzyl-6-(4-methoxy-2-(prop-1-en-1-yl)phenyl)-9H-purine (**9ac**):
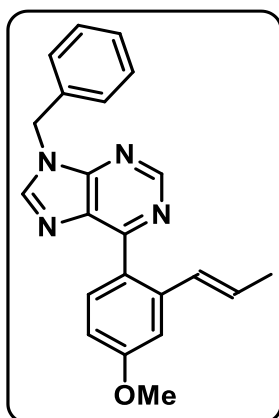
Physical State: Colorless liquid (29 mg, 81% yield). **R$_f$** = 0.4 (50% EtOAc/hexane). **^{1}H NMR (CDCl$_3$, 700 MHz):** δ 9.08 (s, 1H), 8.05 (s, 1H), 7.78 (d, J = 9.1 Hz, 1H), 7.38-7.35 (m, 5H), 7.20 (d, J = 2.1 Hz, 1H), 6.92 (dd, J = 8.4 Hz, 2.8 Hz, 1H), 6.75 (dd, J = 15.4 Hz, 1.4 Hz, 1H), 6.25-6.22 (m, 1H), 5.48 (s, 2H), 3.88 (s, 3H), 1.80 (dd, J = 7.0 Hz, 1.4 Hz, 3H) ppm. **^{13}C{^{1}H} NMR (CDCl$_3$, 175 MHz):** δ 161.1, 158.6, 152.6, 152.2, 144.4, 139.3,

135.5, 133.4, 132.4, 129.7, 129.5, 128.9, 128.2, 127.9, 126.3, 112.9, 111.9, 55.7, 47.6, 19.0 ppm. **IR** (KBr, cm^{-1}): 3487, 2934, 2910, 1579, 1504, 1454, 962. **HRMS (ESI) m/z:** [M+H]$^+$ Calcd for $C_{22}H_{21}N_4O$ 357.1710; Found 357.1710.

(E)-6-(4-chloro-2-(prop-1-en-1-yl)phenyl)-9-ethyl-9H-purine (**9ad**):
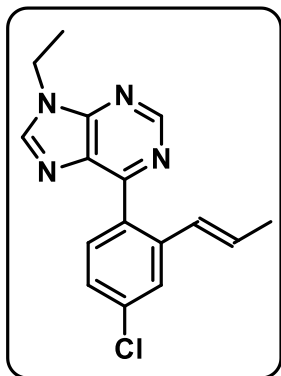
Physical State: Colorless liquid (20 mg, 67% yield). **R$_f$** = 0.2 (20% EtOAc/hexane). **^{1}H NMR (CDCl$_3$, 700 MHz):** δ 9.06 (s, 1H), 8.11 (s, 1H), 7.68-7.67 (m, 2H), 7.33 (dd, J = 8.4 Hz, 2.1 Hz, 1H), 6.61 (d, J = 15.4 Hz, 1H), 6.29-6.24 (m, 1H), 4.40 (q, J = 7.0 Hz, 2H), 1.79 (d, J = 6.3 Hz, 3H), 1.63 (d, J = 7.0 Hz, 3H) ppm. **^{13}C{^{1}H} NMR (CDCl$_3$, 175 MHz):** δ 157.5, 152.4, 152.2, 144.6, 139.2, 136.2, 132.9, 132.8, 131.8, 129.2, 128.4, 127.0, 126.6, 39.4, 19.0, 15.7 ppm. **IR** (KBr, cm^{-1}): 3503, 2935, 2915, 1582, 1501, 1445, 957. **HRMS (ESI) m/z:** [M+H]$^+$ Calcd for $C_{16}H_{16}ClN_4$ 299.1058; Found 299.1061.

(E)-6-(4-chloro-2-(prop-1-en-1-yl)phenyl)-9-(3-methylbut-2-en-1-yl)-9H-purine (**9ae**):
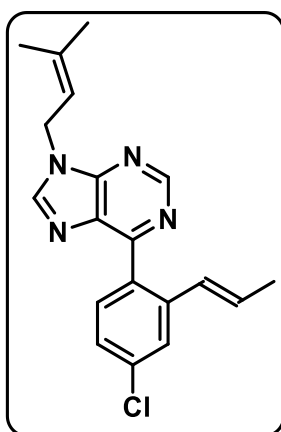
Physical State: Colorless liquid (24 mg, 71% yield). **R$_f$** = 0.2 (20% EtOAc/hexane). **^{1}H NMR (CDCl$_3$, 400 MHz):** δ 9.06 (s, 1H), 8.07 (s, 1H), 7.68-7.66 (m, 2H), 7.33-7.32 (m, 1H), 6.60 (d, J = 16.0 Hz, 1H), 6.30-6.22 (m, 1H), 5.51-5.48 (m, 1H), 4.90 (d, J = 3.2 Hz, 2H), 1.88 (s, 3H), 1.83 (s, 3H), 1.79 (d, J = 6.8 Hz, 3H) ppm. **^{13}C{^{1}H} NMR (CDCl$_3$, 175 MHz):** δ 157.4, 152.4, 152.2, 144.7, 140.2, 139.2, 136.2, 132.9, 132.7, 131.8, 129.2, 128.4, 127.0, 126.6, 117.6, 41.8, 26.0, 19.0, 18.5 ppm. **IR** (KBr, cm$^-$

^{1}): 3504, 2937, 2912, 1580, 1499, 957. **HRMS (ESI) m/z:** [M+H]$^+$ Calcd for $C_{19}H_{20}ClN_4$: 339.1371, Found: 339.1381.

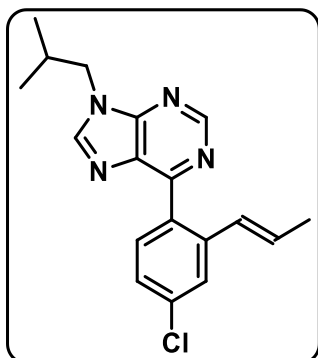**(E)-6-(4-Chloro-2-(prop-1-en-1-yl)phenyl)-9-isobutyl-9H-purine (9af)**:

Physical State: Colorless liquid (24 mg, 73% yield). $R_f =$ 0.3 (20% EtOAc/hexane). ^{1}**H NMR (CDCl$_3$, 700 MHz):** δ 9.06 (s, 1H), 8.06 (s, 1H), 7.70 (d, J = 7.7 Hz, 1H), 7.67 (s, 1H), 7.34 (d, J = 8.4 Hz, 1H), 6.62 (d, J = 15.4 Hz, 1H), 6.29-6.24 (m, 1H), 4.14 (d, J = 7.0 Hz, 2H), 2.38-2.32 (m, 1H), 1.79 (d, J = 6.3 Hz, 3H), 1.01 (d, J = 7.0 Hz, 6H) ppm. ^{13}C{^{1}H} **NMR (CDCl$_3$, 175 MHz):** δ 157.5, 152.5, 152.4, 145.4, 139.3, 136.2, 132.9, 132.5, 131.7, 129.2, 128.4, 127.0, 126.6, 51.6, 29.4, 20.3, 19.0 ppm. **IR** (KBr, cm^{-1}): 3455, 2927, 1708, 1586, 1327, 1107, 936. **HRMS (ESI) m/z:** [M+H]$^+$ Calcd for $C_{18}H_{20}ClN_4$ 327.1371; Found 327.1372.

Intermediate-1 (Int-1):
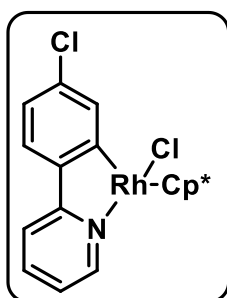
Physical State: Reddish solid (17 mg, 73% yield). R_f = 0.5 (100% EtOAc). ^{1}**H NMR (CDCl$_3$, 700 MHz):** δ 8.71 (d, J = 5.6 Hz, 1H), 7.75 (d, J = 2.1 Hz, 1H), 7.72 (d, J = 3.5 Hz, 2H), 7.52 (d, J = 7.7 Hz, 1H), 7.17-7.14 (m, 1H), 7.04 (dd, J = 7.7 Hz, 1.4 Hz, 1H), 1.63 (s, 15H) ppm. ^{13}C{^{1}H} **NMR (CDCl$_3$, 175 MHz):** δ 180.3 (d, J = 32.9 Hz), 164.7, 151.6, 142.5, 137.6, 136.4, 136.0, 124.5, 123.4, 122.5, 119.5, 96.4 (d, J = 6.1 Hz), 9.4 ppm. **HRMS (ESI) m/z:** [M-Cl]$^+$ Calcd for $C_{21}H_{22}ClNRh$ 426.0490; Found 426.0462.

Intermediate-2 (**Int-2**):
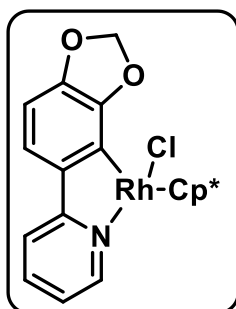
Physical State: Reddish solid CONSISTENCY THROUGHOUT (12 mg, 50% yield). $\mathbf{R}_f$ = 0.5 (100% EtOAc). **^{1}H NMR (CDCl$_3$, 400 MHz):** δ 8.66 (d, J = 5.6 Hz, 1H), 7.65 (dd, J = 4.8 Hz, 1.2 Hz, 2H), 7.28 (d, J = 8.0 Hz, 1H), 7.08-7.02 (m, 1H), 6.58 (d, J = 8.0 Hz, 1H), 6.04 (d, J = 1.6 Hz, 1H), 6.00 (d, J = 1.6 Hz, 1H), 1.67 (s, 15H) ppm. **^{13}C{^{1}H} NMR (CDCl$_3$, 100 MHz):** δ 165.7, 152.8, 152.6 (d, J = 23.2 Hz), 151.5, 147.6, 139.5, 137.2, 121.4, 119.4, 119.2, 104.3, 99.9, 96.8 (d, J = 6.3 Hz), 9.7 ppm. **HRMS (ESI) m/z:** [M-Cl]$^+$ Calcd for C$_{22}$H$_{23}$NO$_2$Rh 436.0778; Found 436.0772.

2-(2-Propylphenyl)pyridine (**10**):
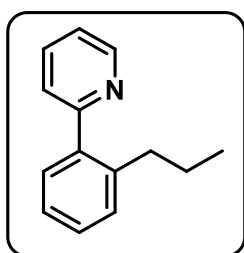
Physical State: colorless liquid (16 mg, 81% yield). $\mathbf{R}_f$ = 0.5 (10% EtOAc/hexane). **^{1}H NMR (CDCl$_3$, 700 MHz):** δ 8.68 (d, J = 4.9 Hz, 1H), 7.73 (td, J = 7.7 Hz, 1.4 Hz, 1H), 7.37 (d, J = 7.7 Hz, 1H), 7.32 (t, J = 7.7 Hz, 2H), 7.29 (d, J = 7.0 Hz, 1H), 7.25-7.23 (m, 2H), 2.67 (t, J = 7.7 Hz, 2H), 1.47 (sext, J = 7.7 Hz, 2H), 0.80 (t, J = 7.7 Hz, 3H) ppm. **^{13}C{^{1}H} NMR (CDCl$_3$, 175 MHz):** δ 160.6, 149.4, 140.8, 140.7, 136.4, 130.0, 130.0, 128.5, 126.1, 124.4, 121.9, 35.3, 24.7, 14.3 ppm. **IR (KBr, cm^{-1}):** 3404, 2929, 1585, 1468, 1022, 989. **HRMS (ESI) m/z:** [M+H]$^+$ Calcd for C$_{14}$H$_{16}$N 198.1277; Found 198.1268.

NMR spectra of (*E*)-2-(2-(Prop-1-en-1-yl)phenyl)pyridine (3aa):

3aa, ^{1}H NMR (CDCl$_3$, 400 MHz)

3aa, ^{13}C{^{1}H} NMR (CDCl$_3$, 100 MHz)
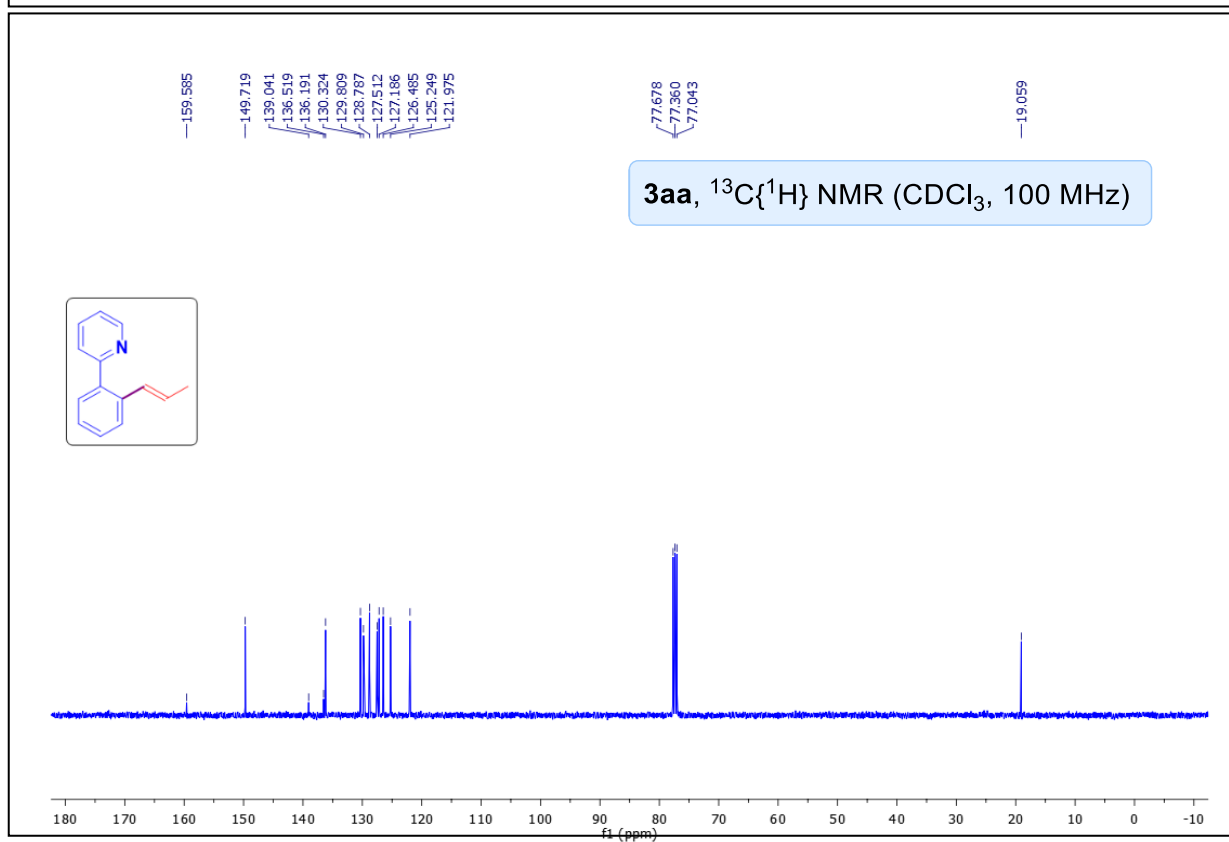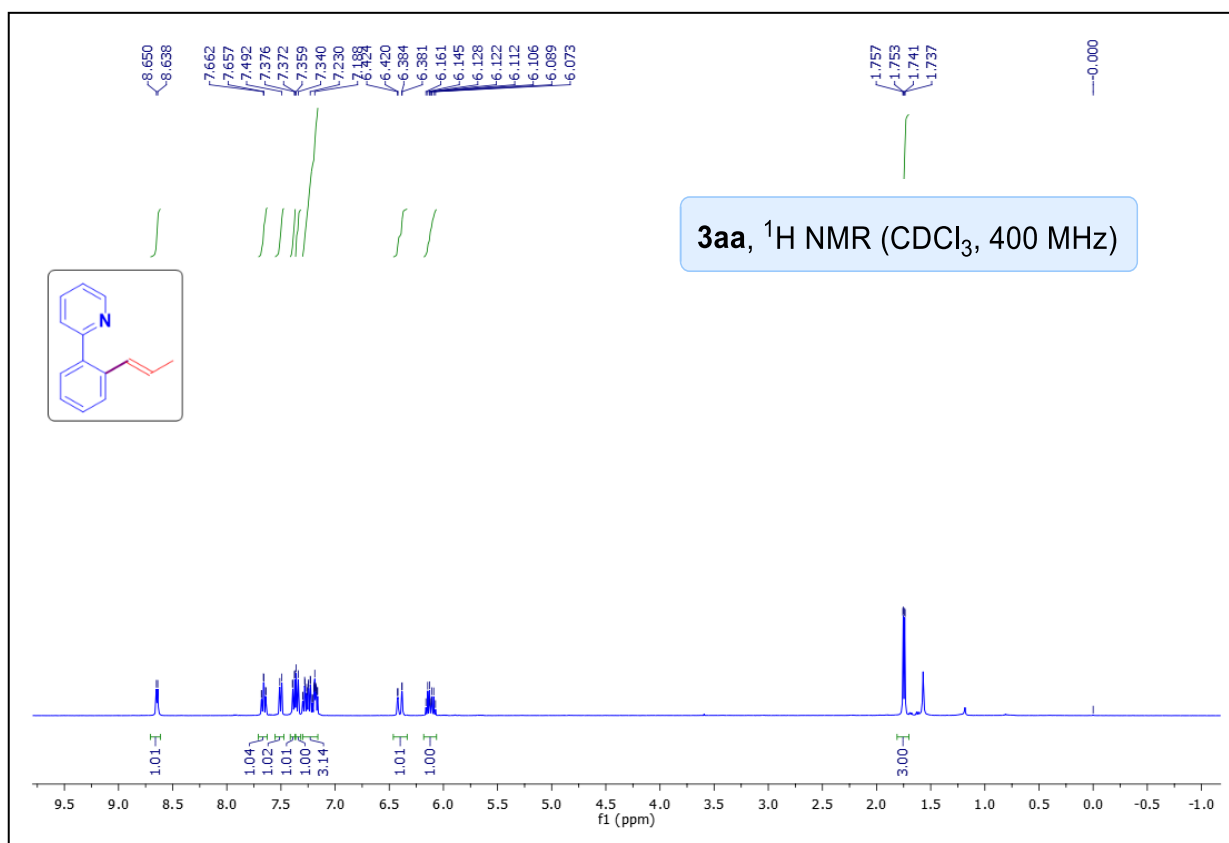
NMR spectra of Methyl (E)-3-(prop-1-en-1-yl)-4-(pyridin-2-yl)benzoate (3aj):

3aj, ^{1}H NMR (CDCl$_3$, 700 MHz)

1H NMR (CDCl$_3$, 400 MHz)

3aj, ^{13}C{^{1}H} NMR (CDCl$_3$, 175 MHz)
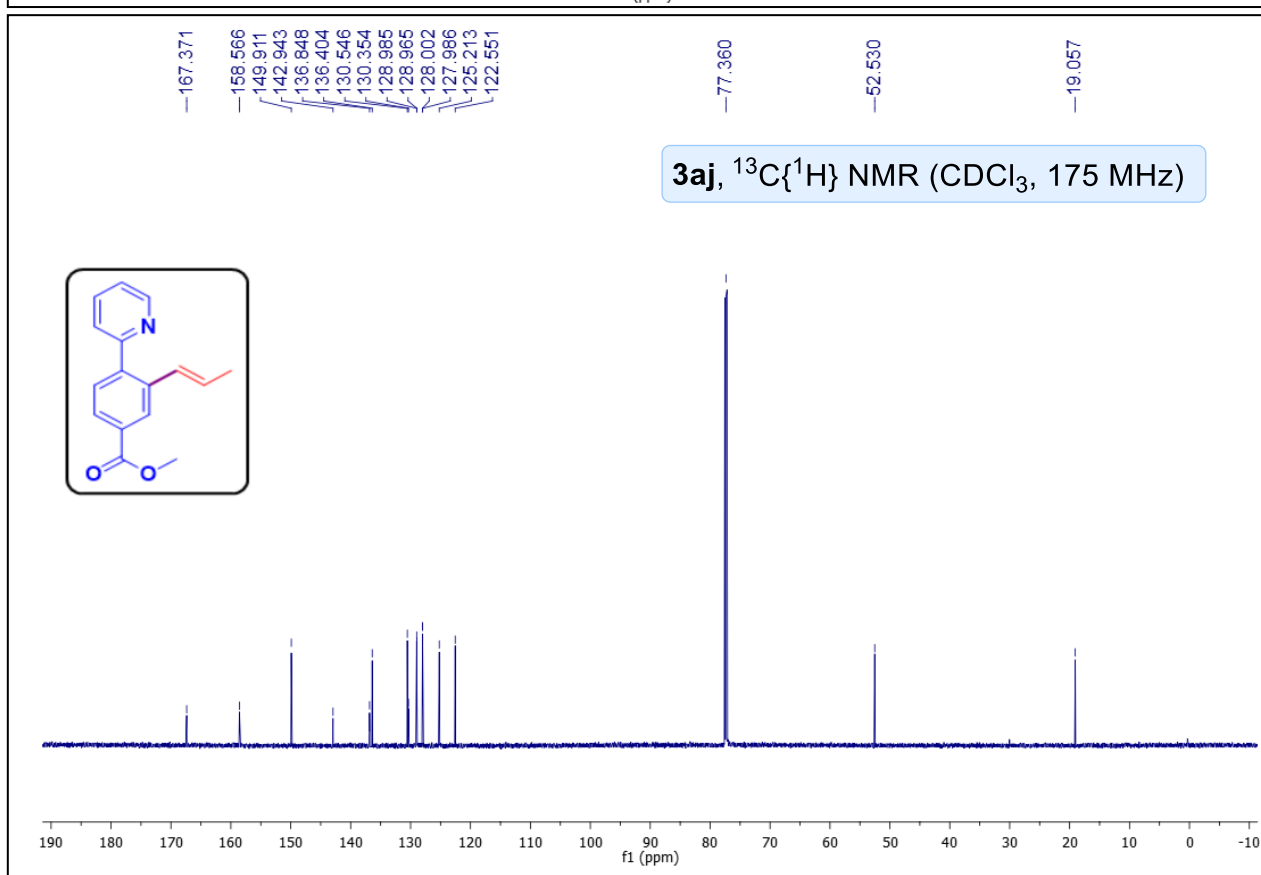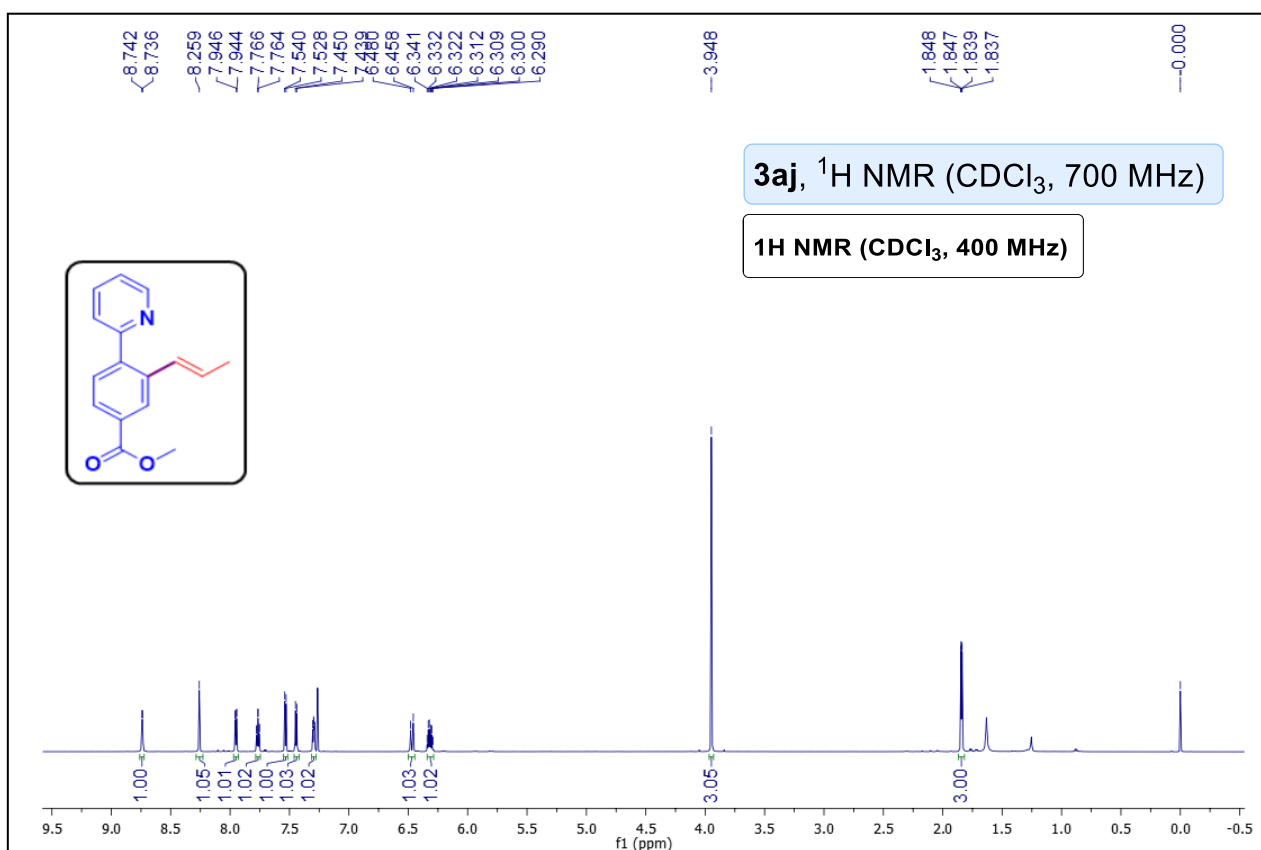
Single x-ray Crystal structure of 9af

9ab

CCDC = 2077201
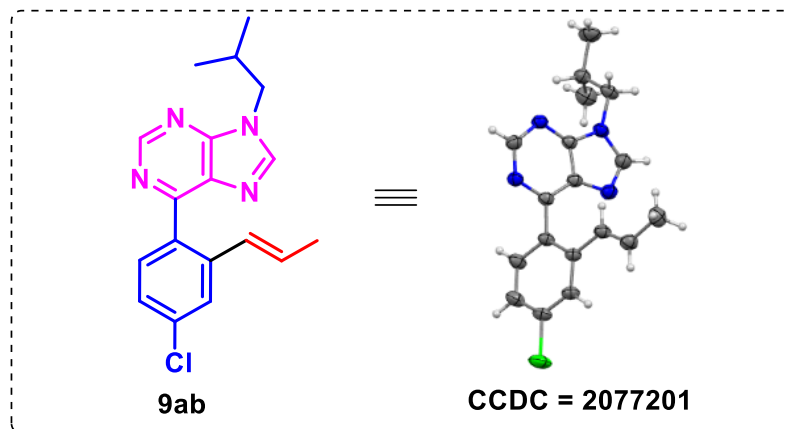
Datablock pbtn-purine - ellipsoid plot

Single x-ray Crystal structure of Int-2

Int-2, CCDC = 2075306

C
H
N
Cl
O
Rh
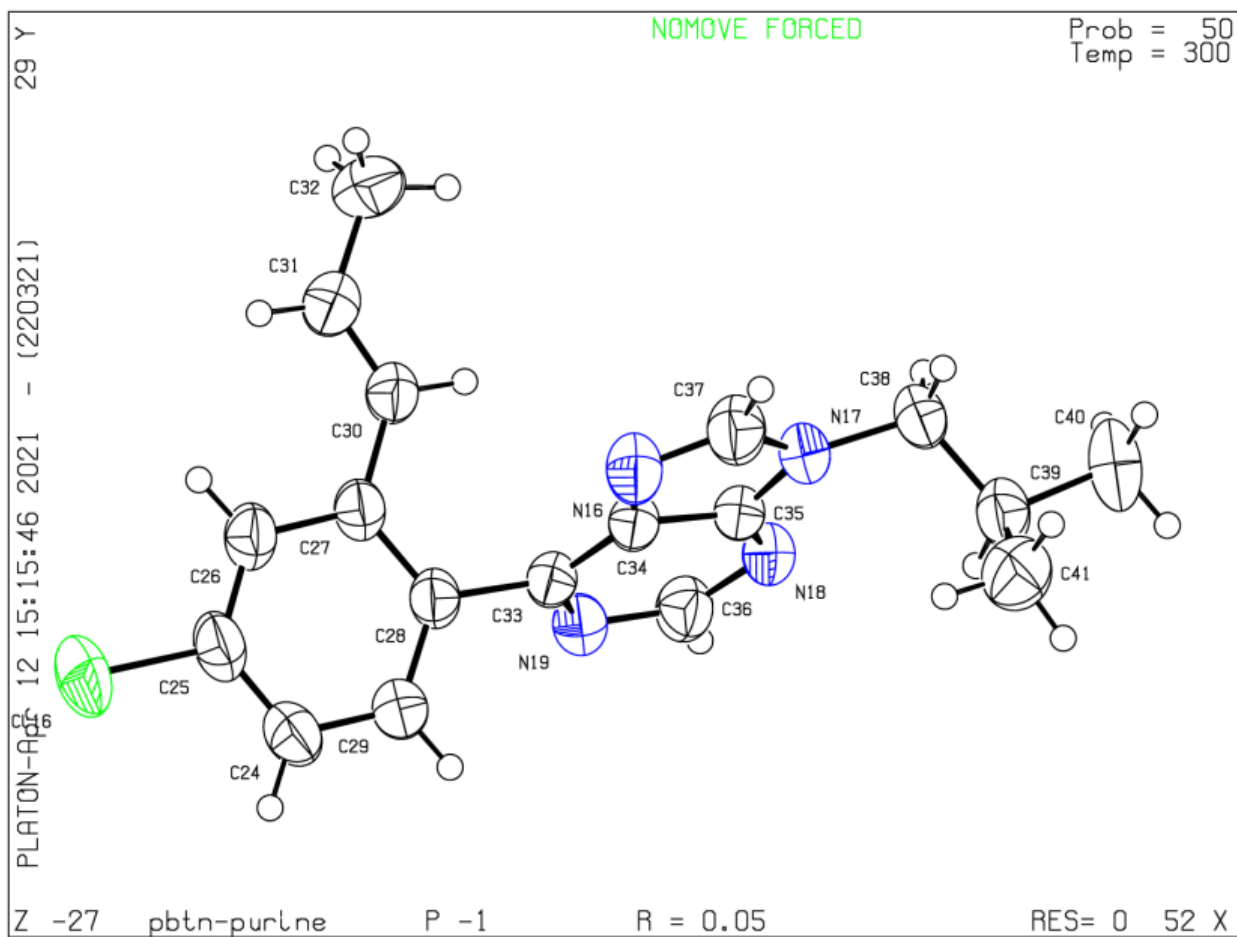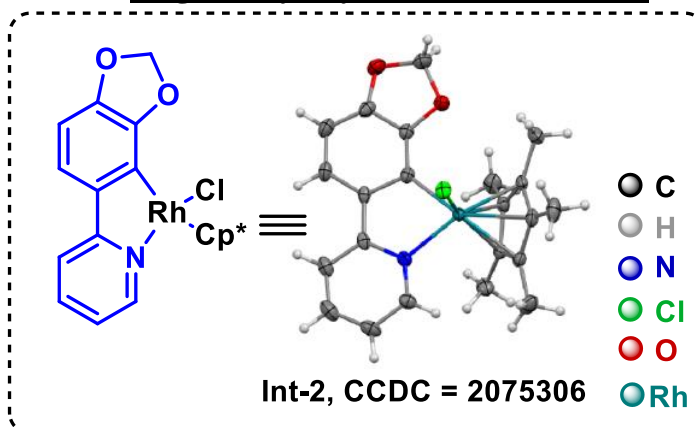
Datablock pcr-pb-tn-1nt-oxobri - ellipsoid plot
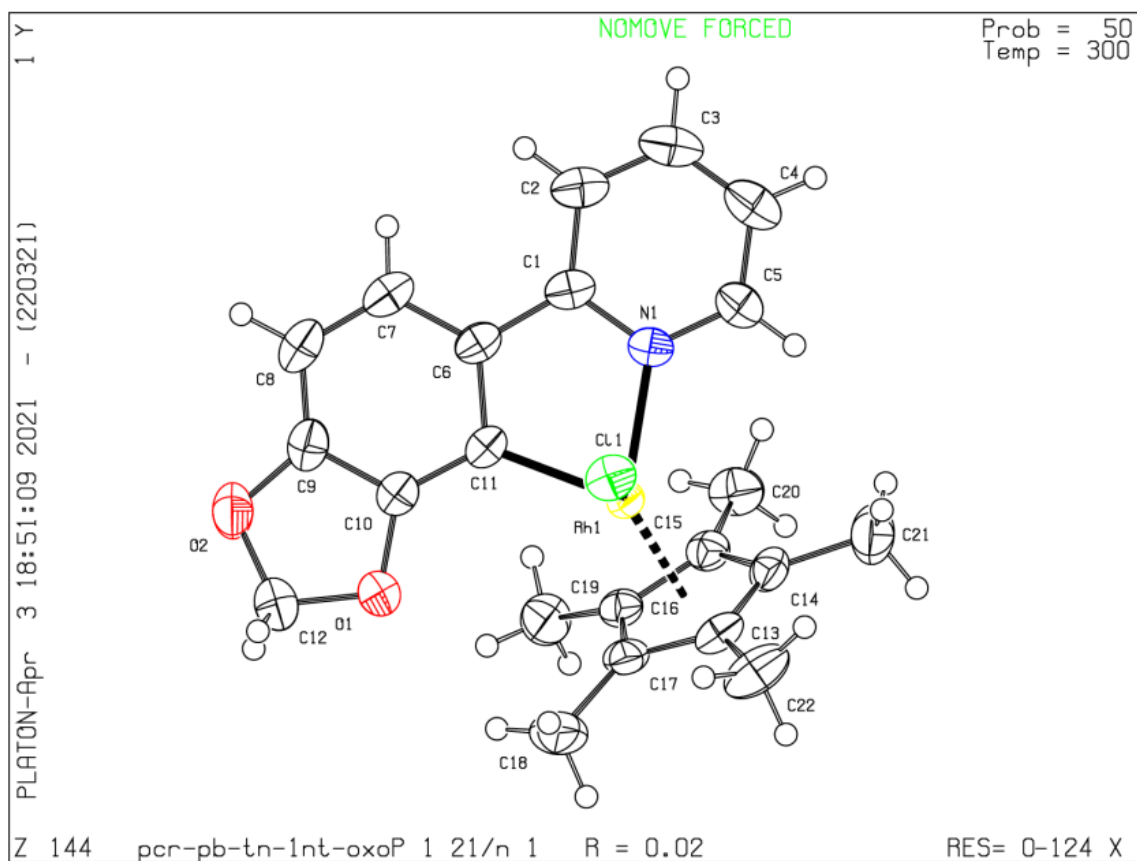
4.6 REFERENCES

1. (a) Jiang, N.; Hu, Q.; Reid, C. S.; Lu, Y.; Li, C.-J. A novel palladium-catalysed coupling of epoxides with allyl bromide mediated by indium(i)chloride: a cascade epoxide rearrangement–carbonyl allylation. *Chem. Commun.* **2003**, 2318-2319. (b) Gildner, P. G.; Gietter, A. A. S.; Cui, D.; Watson, D. A. Benzylation of Nitroalkanes Using Copper-Catalysed Thermal Redox Catalysis: Toward the Facile C-Alkylation of Nitroalkanes. *J. Am. Chem. Soc.* **2012**, *134*, 9942−9945. (c) Rezazadeh, S.; Devannah, V.; Watson, D. A. Nickel-Catalysed *C*-Alkylation of Nitroalkanes with Unactivated Alkyl Iodides. *J. Am. Chem. Soc.* **2017**, *139*, 8110−8113. (d) Devannah, V.; Sharma, R.; Watson, D. A. Nickel-Catalysed Asymmetric *C*-Alkylation of Nitroalkanes: Synthesis of Enantioenriched β-Nitroamides. *J. Am. Chem. Soc.* **2019**, *141*, 8436−8440. (e) Cristofol, A.; Escudero-Adan, E. C.; Kleij, A. W. Palladium-Catalysed (*Z*)-Selective Allylation of Nitroalkanes: Access to Highly Functionalized Homoallylic Scaffolds. *J. Org. Chem.* **2018**, *83*, 9978−9990. (f) Ankade, S. B.; Shabade, A. B.; Soni, V.; Punji, B. Unactivated Alkyl Halides in Transition-MetalCatalysed C−H Bond Alkylation. *ACS Catal.* **2021**, *11*, 3268−3292.

2. (a) Song, C. E.; Jung, D.-u.; Choung, S. Y.; Roh, E. J.; Lee, S.-g. <u>Dramatic enhancement of catalytic activity in an ionic liquid: Highly practical Friedel–Crafts alkenylation of arenes with alkynes catalysed by metal triflates</u>. *Angew. Chem., Int. Ed.* **2004**, *43*, 6183. (b) Yasuda, M.; Somyo, T.; Baba, A. Direct Carbon−Carbon Bond Formation from Alcohols and Active Methylenes, Alkoxyketones, or Indoles Catalysed by Indium Trichloride. *Angew. Chem., Int. Ed.* **2006**, *45*, 793−796. (c) X. Zhou, G. Zhang, R. Huang, H. Huang, Palladium-Catalysed Allyl–Allyl

Reductive Coupling of Allylamines or Allylic Alcohols with H_2 as Sole Reductant. *Org. Lett.* **2021**, *23*, 365−369.

3. (a) Taylor, R. D.; MacCoss, M.; Lawson, A. D. G. Rings in Drugs. *J. Med. Chem.* **2014**, *57*, 5845−5859. (b) R. B. Watson, C. S. Schindler, *Org. Lett.* **2018**, *20*, 68-71. (c) Jiang, Z.-T.; Huang, J.; Zeng, Y.; Hu, F.; Xia, Y. Rhodium Catalysed Regioselective C-H Allylation of Simple Arenes via C-C Bond Activation of Gem-difluorinated Cyclopropanes. *Angew. Chem., Int. Ed.* **2021**, *60*, 10626−10631.

4. (a) Tsuji, J.; Takahashi, H.; Morikawa, M. Organic Syntheses by Means of Noble Metal Compounds XVII. Reaction of π-Allylpalladium Chloride with Nucleophiles. *Tetrahedron Lett.* **1965**, *6*, 4387–4388. (b) Trost, B. M.; Van Vranken, D. L. Asymmetric Transition Metal-Catalysed Allylic Alkylations. *Chem. Rev.* **1996**, *96*, 395–422. (c) Trost, B. M.; Crawley, M. L. Asymmetric Transition-Metal-Catalysed Allylic Alkylations: Applications in Total Synthesis. *Chem. Rev.* **2003**, *103*, 2921–2944. (d) Mohr, J. T.; Behenna, D. C.; Harned, A. M.; Stoltz, B. M. Deracemization of quaternary stereocenters by Pd-catalysed enantioconvergent decarboxylative allylation of racemic β-ketoesters. *Angew. Chem., Int. Ed.* **2005**, *44*, 6924–6927. (e) Lu, Z.; Ma, S. Metal-Catalysed Enantioselective Allylation in Asymmetric Synthesis. *Angew. Chem., Int. Ed.* **2008**, *47*, 258–297. (f) Dutta, S.; Bhattacharya, T.; Werz, D. B.; Maiti, D. Transition-metal-catalysed C–H allylation reactions. *Chem.* **2021**, *7*, 555–605.

5. (a) Hartung, C. G.; Fecher, A.; Chapell, B.; Snieckus, V. Directed ortho Metalation Approach to C-7-Substituted Indoles. Suzuki−Miyaura Cross Coupling and the Synthesis of Pyrrolophenanthridone Alkaloids. *Org. Lett.* **2003**, *5*, 1899−1902. (b) Walker, W. K.; Anderson, D. L.; Stokes, R. W.; Smith, S. J.; Michaelis, D. J. Allylic

Aminations with Hindered Secondary Amine Nucleophiles Catalysed by Heterobimetallic Pd-Ti Complexes. *Org. Lett*. **2015**, *17*, 752–755.

6. (a) Huang, J.; Zhou, L.; Jiang, H. Palladium-Catalysed Allylation of Alkynes with Allyl Alcohols in Aqueous Media: Highly Regio- and Stereoselective Synthesis of 1,4-Dienes. *Angew. Chem., Int. Ed.* **2006**, *45*, 1945−1949. (b) Piechaczyk, O.; Thoumazet, C.; Jean, Y.; Le Floch, P. DFT study on the palladium-catalysed allylation of primary amines by allylic alcohol. *J. Am. Chem. Soc.* **2006**, *128*, 14306−14317. (c) Jiang, G.; List, B. Palladium/Brønsted Acid-Catalysed α-Allylation of Aldehydes with Allylic Alcohols. *Adv. Synth. Catal.* **2011**, *353*, 1667−1670. (d) Hu, L.; Cai, A.; Wu, Z.; Kleij, A. W.; Huang, G. A Mechanistic Analysis of the Palladium-Catalysed Formation of Branched Allylic Amines Reveals the Origin of the Regio- and Enantioselectivity through a Unique Inner-Sphere Pathway. *Angew. Chem., Int. Ed.* **2019**, 58, 14694−14702. (e) Tsai, C.-C.; Sandford, C.; Wu, T.; Chen, B.; Sigman, M. S.; Toste, F. D. Enantioselective Intramolecular Allylic Substitution via Synergistic Palladium/Chiral Phosphoric Acid Catalysis: Insight into Stereoinduction through Statistical Modeling. *Angew. Chem., Int. Ed.* **2020**, 59, 14647−14655.

7. (a) Leitner, A.; Shu, C. T.; Hartwig, J. F. Effects of catalyst activation and ligand steric properties on the enantioselective allylation of amines and phenoxides *Org. Lett*. **2005**, *7*, 1093–1096. (b) Ibrahem, I.; Cordova, A. Direct Catalytic Intermolecular α-Allylic Alkylation of Aldehydes by Combination of Transition-Metal and Organocatalysis. *Angew. Chem., Int. Ed.* **2006**, *45*, 1952−1956. (c) Zhang, P.; Brozek, L. A.; Morken, J. P. Pd-Catalysed Enantioselective Allyl–Allyl Cross-Coupling. *J. Am. Chem. Soc*. **2010**, *132*, 10686–10688. (d) Engle, K. M.; Mei, T.-S.; Wasa, M.; Yu, J.-Q. Weak coordination as powerful means for

developing broadly useful C-H functionalization reactions. *Acc. Chem. Res*. **2012**, *45*, 788–802. (e) Sha, S.-C.; Zhang, J.; Carroll, P. J.; Walsh, P. J. Raising the *pKa* Limit of "Soft" Nucleophiles in Palladium-Catalysed Allylic Substitutions: Application of Diarylmethane Pronucleophiles. *J. Am. Chem. Soc.* **2013**, *135*, 17602–17609.

8. Blanksby, S. J.; Ellison, G. B. Bond Dissociation Energies of Organic Molecules. *Acc. Chem. Res*. **2003**, *36*, 255−263.

9. (a) Garro-Helion, F.; Merzouk, A.; Guibe, F. Mild and Selectivé Palladium(0)-Catalysed Deallylation of Allylic Amines. Allylamine and Diallylamine as Very Convenient Ammonia Equivalents for the Synthesis of Primary Amines. *J. Org. Chem*. **1993**, *58*, 6109−6113. (b) Escoubet, S.; Gastaldi, S.; Timokhin, V. I.; Bertrand, M. P.; Siri, D. Thiyl Radical Mediated Cleavage of Allylic C−N Bonds: Scope, Limitations and Theoretical Support to the Mechanism. *J. Am. Chem. Soc*. **2004**, *126*, 12343−12352. (c) Trost, B. M.; Osipov, M.; Dong, G. Palladium-Catalysed Dynamic Kinetic Asymmetric Transformations of Vinyl Aziridines with Nitrogen Heterocycles: Rapid Access to Biologically Active Pyrroles and Indoles. *J. Am. Chem. Soc*. **2010**, *132*, 15800−15807. (d) Ouyang, K.; Hao, W.; Zhang, W.-X.; Xi, Z. Transition-Metal-Catalysed Cleavage of C–N Single Bonds. *Chem. Rev*. **2015**, *115*, 12045-12090. (e) Su, J. K.; Ma, X. X.; Ou, Z. L.; Song, Q. L. Deconstructive functionalizations of unstrained carbon-nitrogen cleavage enabled by difluorocarbene. *ACS Cent. Sci*. **2020**, *6*, 1819-1826. (f) García-Carceles, J.; Bahou, K. A.; Bower, J. F. Recent́ Methodologies That Exploit Oxidative Addition of C−N Bonds to Transition Metals. *ACS Catal.* **2020**, *10*, 12738−12759. (g) Dai, R.-H.; Wang, Q.; Chen, Z.-X.; Tian, S.-K. Asymmetric Aza-Claisen

Rearrangement between Enantioenriched α-Chiral Allylamines and Allenones. *J. Org. Chem*. **2021**, *86*, 3065−3073.

10. (a) Selected reports on Lewis acid catalysis: (a) Liu, C.-R.; Li, M.-B.; Cheng, D.-J.; Yang, C.-F.; Tian, S.-K. Catalyst-Free Alkylation of Sulfinic Acids with Sulfonamides via sp^3 C-N Bond Cleavage at Room Temperature. *Org. Lett*. **2009**, *11*, 2543–2545. (b) Li, M. B.; Wang, Y.; Tian, S. K. Regioselective and Stereospecific Cross-Coupling of Primary Allylic Amines with Boronic Acids and Boronates through Palladium-Catalysed C−N Bond Cleavage. *Angew. Chem., Int. Ed*. **2012**, *51*, 2968−2971. (c) Wu, X.; Chen, Y.; Li, M.; Zhou, M.; Tian, S. Direct Substitution of Primary Allylic Amines with Sulfinate Salts. *J. Am. Chem. Soc*. **2012**, *134*, 14694−14697. (d) Ma, X.-T.; Wang, Y.; Dai, R.-H.; Liu, C.-R.; Tian, S.-K. Catalytic Allylation of Stabilized Phosphonium Ylides with Primary Allylic Amines. *J. Org. Chem*. **2013**, *78*, 11071−11075. (e) Xu, J.-K.; Wang, Y.; Gu, Y.; Tian, S.-K. Palladium-Catalysed Stereospecific Allylation of Nitroacetates with Enantioenriched Primary Allylic Amines. *Adv. Synth. Catal*. **2016**, *358*, 1854. (f) Xu, Y.-N.; Zhu, M.-Z.; Tian, S.-K. Chiral α-Amino Acid/ Palladium-Catalysed Asymmetric Allylation of α-Branched β-Ketoesters with Allylic Amines: Highly Enantioselective Construction of All Carbon Quaternary Stereocenters. *J. Org. Chem*. **2019**, *84*, 14936−14942.

11. Zhao, X.; Liu, D.; Guo, H.; Liu, Y.; Zhang, W. C-N Bond Cleavage of Allylic Amines via Hydrogen Bond Activation with Alcohol Solvents in Pd-Catalysed Allylic Alkylation of Carbonyl Compounds. *J. Am. Chem. Soc*. **2011**, *133*, 19354−19357.

12. (a) Mukherjee, S.; List, B. Chiral Counteranions in Asymmetric Transition-Metal Catalysis: Highly Enantioselective Pd/Brønsted Acid-Catalysed Direct α-

Allylation of Aldehydes. *J. Am. Chem. Soc.* **2007**, *129*, 11336−11337. (b) Xu, J.-K.; Wang, Y.; Gu, Y.; Tian, S.-K. Palladium-Catalysed Stereospecific Allylation of Nitroacetates with Enantioenriched Primary Allylic Amines. *Adv. Synth. Catal.* **2016**, *358*, 1854−1858. (c) Sweeney, J. B.; Ball, A. K.; Smith, L. J. Catalytic C−C Bond Formation Using a Simple Nickel Pre-catalyst System: Base- and Activator-Free Direct C-Allylation by Alcohols and Amines. *Chem. - Eur. J.* **2018**, *24*, 7354−7357. (d) Nagae, H.; Xia, J.; Kirillov, E.; Higashida, K.; Shoji, K.; Boiteau, V.; Zhang, W.; Carpentier, J.-F.; Mashima, K. Asymmetric Allylic Alkylation of β-Ketoesters via C-N Bond Cleavage of *N*-allyl-*N*-methylaniline Derivatives Catalysed by a Nickel-Diphosphine System. *ACS Catal*. **2020**, *10*, 5828−5839. *(*e) Wu, L., Wang, T., Gao, C., Huang, W., Qu, J., Chen, Y. Skeletal Reconstruction of 3-Alkylidenepyrrolidines to Azepines Enabled by Pd-Catalysed C–N Bond Cleavage. *ACS Catal.* **2021,** *11***,** 3, 1774–1779.

13. (a) Godula, K.; Sames, D. C-H Bond Functionalization in Complex Organic Synthesis. *Science* **2006**, *312*, 67−72. (b) McMurray, L.; O'Hara, F.; Gaunt, M. J. Recent developments in natural product synthesis using metal-catalysed C-H bond functionalisation. *Chem. Soc. Rev*. **2011**, *40*, 1885−1898. (c) Yamaguchi, J.; Yamaguchi, A. D.; Itami, K. C-H Bond Functionalization: Emerging Synthetic Tools for Natural Products and Pharmaceuticals. *Angew. Chem., Int. Ed*. **2012**, *51*, 8960−9009. (d) He, R.; Huang, Z.-T.; Zheng, Q.-Y.; Wang, C. Isoquinoline skeleton synthesis via chelation-assisted C–H activation. *Tetrahedron Lett.* **2014**, *55*, 5705–5713.

14. (a) Yan, R.; Wang, Z. X. Ruthenium Catalysed C−H Allylation of Arenes with Allylic Amines. *Org. Biomol. Chem*. **2018**, *16*, 3961−3969. (b) Hu, X.-Q.; Hu, Z.;

Zhang, G.; Sivendran, N.; Gooßen, L. J. Catalytic C−N and C−H Bond Activation: *ortho*-Allylation of Benzoic Acids with Allyl Amines. *Org. Lett.* **2018**, *20*, 4337.

15. Cadierno, V.; García-Garrido, S. E.; Gimeno, J.; Nebra, N. Ru(IV)-catalysed isomerization of allylamines in water: A highly efficient procedure for the deprotection of *N*-allylic amines. *Chem. Commun.* **2005**, 4086–4088.

16. (a) Punji, B.; Song, W.; Shevchenko, G. A.; Ackermann, L. Cobalt Catalysed C−H Bond Functionalizations with Aryl and Alkyl Chlorides. *Chem. - Eur. J.* **2013**, *19*, 10605−10610. (b) Biswal, P.; Pati, B. V.; Chebolu, R.; Ghosh, A.; Ravikumar, P. C. Hydroxylamine-*O*-Sulfonic Acid (HOSA) as a Redox-Neutral Directing Group: Rhodium Catalysed, Additive Free, One-Pot Synthesis of Isoquinolines from Arylketones. *Eur. J. Org. Chem*. **2020**, *2020*, 1006−1014.

17. (a) Wang, S.; Hou, J.-T.; Feng, M.-L.; Zhang, X.-Z.; Chen, S.- Y.; Yu, X.-Q. Cobalt(III)-Catalysed Alkenylation of Arenes and 6-Arylpurines with Terminal Alkynes: Efficient Access to Functional Dyes. *Chem. Commun*. **2016**, *52*, 2709−2712. (b) Xu, C.; Zhang, L.; Xu, J.; Pan, Y.; Li, F.; Li, H.; Xu, L. Rhodium(I)-catalysed Decarbonylative Direct Olefination of 6-Arylpurines with Vinyl Carboxylic Acids Directed by the Purinyl N1 Atom. *ChemistrySelect* **2016**, *1*, 653–658.

18. Simmons, E. M.; Hartwig, J. F. On the Interpretation of Deuterium Kinetic Isotope Effects in C-H Bond Functionalizations by Transition-Metal Complexes. *Angew. Chem., Int. Ed*. **2012**, *51*, 3066−3072.

19. Selected reports on Rh-catalysed alkene isomerization: (a) Tsang, D. S.; Yang, S.; Alphonse, F.-A.; Yudin, A. K. Stereoselective isomerization of N-allyl aziridines into geometrically stable Z enamines by using rhodium hydride catalysis. *Chem. - Eur. J.* **2008**, *14*, 886−894. (b) Hassam, M.; Taher, A.; Arnott, G. E.; Green, I. R.;

van Otterlo, W. A. L. Isomerization of Allylbenzenes. *Chem. Rev.* **2015**, *115*, 5462−5569. (c) Azpíroz, R.; Di Giuseppe, A.; Urriolabeitia, A.; Passarelli, V.; Polo, V.; Pérez-Torrente, J. J.; Oro, L. A.; Castarlenas, R. Hydride-Rhodium(III)-*N*-Heterocyclic Carbene Catalyst for Tandem Alkylation/Alkenylat-ion via C-H Activation. *ACS Catal.* **2019**, *9*, 9372−9386. (d) Massad, I.; Marek, I. Alkene Isomerization through Allylmetals as a Strategic Tool in Stereoselective Synthesis. *ACS Catal.* **2020**, *10*, 5793−5804. (e) Fiorito, D.; Scaringi, S.; Mazet, C. Transition Metal-Catalysed Alkene Isomerization as an Enabling Technology in Tandem, Sequential and Domino Processes. *Chem. Soc. Rev.* **2021**, *50*, 1391−1406.

20. Onodera, S.; Ishikawa, S.; Kochi, T.; Kakiuchi, F. Direct Alkenylation of Allylbenzenes via Chelation-Assisted C–C Bond Cleavage. *J. Am. Chem. Soc.* **2018**, *140*, 9788–9792.

21. (a) Gaussian 09, Revision A.03, M. J. Frisch, G. W. Trucks, H. B. Schlegel, G. E. Scuseria, M. A. Robb, J. R. Cheeseman, G. Scalmani, V. Barone, G. A. Petersson, H. Nakatsuji, X. Li, M. Caricato, A. Marenich, J. Bloino, B. G. Janesko, R. Gomperts, B. Mennucci. (b) Grimme, S.; Antony, J.; Ehrlich, S.; Krieg, H. A Consistent and Accurate Ab Initio Parametrization of Density Functional Dispersion Correction (DFT-D) for the 94 Elements H-Pu. *J. Chem. Phys.* **2010**, *132*, 24103. (c) Weigend, F. Accurate Coulomb-Fitting Basis Sets for H to Rn. *Phys. Chem. Chem. Phys.* **2006**, *8*, 1057–1065. (d) Weigend, F.; Ahlrichs, R. Balanced Basis Sets of Split Valence, Triple Zeta Valence and Quadruple Zeta Valence Quality for H to Rn: Design and Assessment of Accuracy. *Phys. Chem. Chem. Phys.* **2005**, *7*, 3297–3305. (e) Jiao, L.; Lin, M.; Yu, Z.-X. Density Functional Theory Study of the Mechanisms and Stereochemistry of the Rh(I)-Catalysed Intramolecular [3+2] Cycloadditions of 1-Ene- and 1-Yne-

Vinylcyclopropanes. *J. Am. Chem. Soc.* **2011**, *133*, 447–461. (f) Shi, F.-Q. Density Functional Theory Study on the Mechanism of Rh-Catalysed Decarboxylative Conjugate Addition: Diffusion- and Ligand-Controlled Selectivity toward Hydrolysis or β-Hydride Elimination. *Org. Lett.* **2011**, *13*, 736–739. (g) Evans, M. E.; Burke, C. L.; Yaibuathes, S.; Clot, E.; Eisenstein, O.; Jones, W. D. Energetics of C−H Bond Activation of Fluorinated Aromatic Hydrocarbons Using a [Tp′Rh(CNneopentyl)] Complex. *J. Am. Chem. Soc.* **2009**, *131*, 13464–13473. (h) Taw, F. L.; Mueller, A. H.; Bergman, R. G.; Brookhart, M. A Mechanistic Investigation of the Carbon−Carbon Bond Cleavage of Aryl and Alkyl Cyanides Using a Cationic Rh(III) Silyl Complex. *J. Am. Chem. Soc.* **2003**, *125*, 9808–9813. (i) Xavier, E. S.; De Almeida, W. B.; da Silva, J. C. S.; Rocha, W. R. C−H Bond Activation of Methane Promoted by (H5-Phospholyl)Rh(CO)$_2$: A Theoretical Perspective. *Organometallics* **2005**, *24*, 2262–2268. (j) Grimme, S.; Ehrlich, S.; Goerigk, L. Effect of the Damping Function in Dispersion Corrected Density Functional Theory. *J. Comput. Chem.* **2011**, *32*, 1456–1465. (k) Marenich, A. V.; Cramer, C. J.; Truhlar, D. G. Universal Solvation Model Based on Solute Electron Density and on a Continuum Model of the Solvent Defined by the Bulk Dielectric Constant and Atomic Surface Tensions. *J. Phys. Chem. B* **2009**, *113*, 6378–6396.

22. (a) Lapointe, D.; Fagnou, K. Overview of the Mechanistic Work on the Concerted Metallation-Deprotonation Pathway. *Chem. Lett.* **2010**, *39*, 1118–1126. (b) Ackermann, L. Carboxylate-Assisted Transition-Metal-Catalysed C-H Bond Functionalizations: Mechanism and Scope. *Chem. Rev.* **2011**, *111*, 1315–1345. (c) Davies, D. L.; Macgregor, S. A.; McMullin, C. L. Computational Studies of Carboxylate-Assisted C-H Activation and Functionalization at Group 8-10 Transition Metal Centers. *Chem. Rev.* **2017**, *117*, 8649–8709. (d) Kapdi, A. R.

Organometallic Aspects of Transition-Metal Catalysed Regioselective C-H Bond Functionalisation of Arenes and Heteroarenes. *Dalt. Trans.* **2014**, *43*, 3021–3034. (e) Gorelsky, S. I.; Lapointe, D.; Fagnou, K. Analysis of the Concerted Metalation-Deprotonation Mechanism in Palladium-Catalysed Direct Arylation across a Broad Range of Aromatic Substrates. *J. Am. Chem. Soc.* **2008**, *130*, 10848–10849. (f) R. Stuart, D.; Alsabeh, P.; Kuhn, M.; Fagnou, K. Rhodium(III)-Catalysed Arene and Alkene C−H Bond Functionalization Leading to Indoles and Pyrroles. *J. Am. Chem. Soc.* **2010**, *132*, 18326–18339.

23. (a) Davies, D. L.; Donald, S. M. A.; Macgregor, S. A. Computational Study of the Mechanism of Cyclometalation by Palladium Acetate. *J. Am. Chem. Soc.* **2005**, *127*, 13754–13755. (b) Rousseaux, S.; Gorelsky, S. I.; Chung, B. K. W.; Fagnou, K. Investigation of the Mechanism of C(sp^3)−H Bond Cleavage in Pd(0)-Catalysed Intramolecular Alkane Arylation Adjacent to Amides and Sulfonamides. *J. Am. Chem. Soc.* **2010**, *132*, 10692–10705. (c) Xiao, B.; Fu, Y.; Xu, J.; Gong, T.-J.; Dai, J.-J.; Yi, J.; Liu, L. Pd(II)-Catalysed C−H Activation/Aryl−Aryl Coupling of Phenol Esters. *J. Am. Chem. Soc.* **2010**, *132*, 468–469. (d) Davies, D. L.; Donald, S. M. A.; Al-Duaij, O.; Macgregor, S. A.; Pölleth, M. Electrophilic C−H Activation at {Cp*Ir}: Ancillary-Ligand Control of the Mechanism of C−H Activation. *J. Am. Chem. Soc.* **2006**, *128*, 4210–4211.

24. (a) Schleyer, P. V. R.; Maerker, C.; Dransfeld, A.; Jiao, H.; Van Eikema Hommes, N. J. R. Nucleus-Independent Chemical Shifts: A Simple and Efficient Aromaticity Probe. *J. Am. Chem. Soc.* **1996**, *118*, 6317–6318. (b) Chen, Z.; Wannere, C. S.; Corminboeuf, C.; Puchta, R.; von Ragué Schleyer, P. Nucleus-Independent Chemical Shifts (NICS) as an Aromaticity Criterion. *Chem. Rev.* **2005**, *105*, 3842–3888. (c) Merino, G.; Heine, T.; Seifert, G. The Induced Magnetic Field in Cyclic

Molecules. *Chem. - A Eur. J.* **2004**, *10*, 4367–4371. (d) Wolinski, K.; Hinton, J. F.; Pulay, P. Efficient Implementation of the Gauge-Independent Atomic Orbital Method for NMR Chemical Shift Calculations. *J. Am. Chem. Soc.* **1990**, *112*, 8251–8260. (e) Ebrahimi, H. P.; Shaghaghi, H.; Tafazzoli, M. Gauge Invariant Atomic Orbital-Density Functional Theory Prediction of Accurate Gas Phase ^{1}H and ^{13}C NMR Chemical Shifts. *Concepts Magn. Reson. Part A Bridg. Educ. Res.* **2011**, *38 A*, 269–279.

25. L. Hoang, Z Yang, M. Smith, R Pal, L. Miska, E. Pérez, W. Pelter, X. Cheng Z, M. Takacs. Enantioselective Desymmetrization via Carbonyl-Directed Catalytic Asymmetric Hydroboration and Suzuki–Miyaura Cross-Coupling. *Org. Lett.* **2015**, *17*, 940-943.

26. Ramachandran, K.; Anbarasan, P. Cobalt(III)-Catalysed Allylation of Arene C–H Bonds. *Eur. J. Org. Chem.* **2017**, *2017*, 3965–3968.

Chapter 5

Rhodium-Catalysed Synthesis of 2-Methylindole via

C-N bond Cleavage of *N*-allylbenzimidazole

Chapter 5

Rhodium-Catalysed Synthesis of 2-Methylindole via C-N bond Cleavage of *N*-allylbenzimidazole

- **easy access to diverse indole scaffold** ● **product diversification to drug molecule**
- **[3+2] annulation via C-H/C-N bond cleavage**
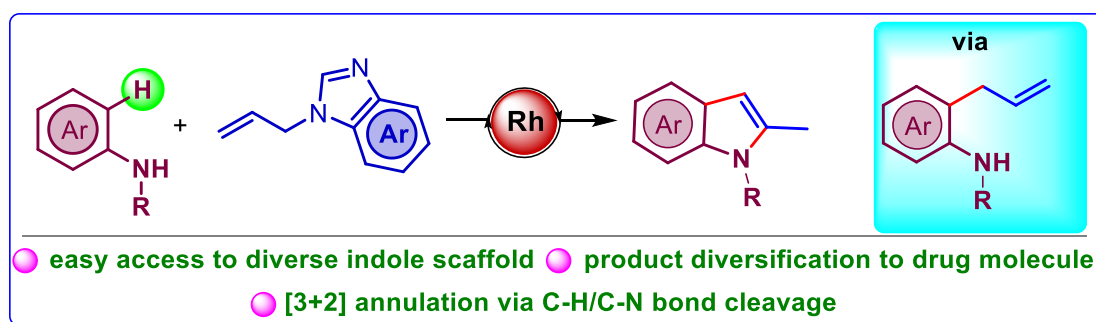
5.1 ABSTRACT

A rhodium catalysed oxidative C-H/N-H dehydrogenative [3+2] annulation strategy is reported between anilines and N-allylbenzimidazole for the synthesis of 2-methylindole scaffolds. An unactivated alkene N-allylbenzimidazole has been used and, more importantly, this transformation involves the cleavage of thermodynamically stable C-N bond of allylamine. Detailed mechanistic studies have been performed and a key intermediate was detected in HRMS.

5.2 INTRODUCTION

In transition metal-catalysed directed C-H bond functionalization processes, several reacting partners (coupling partners) have been used for synthetic transformations. Coupling partners such as alkynes[1], alkenes[2], organo halides[3], diazo compounds[4], boronic acid[5], alcohols[6], amines[7] have been well documented for forming C-C/C-hetero bonds. Among these, the unique reactivity of alkenes has occupied a significant place in synthesis, particularly for olefination, alkylation and annulation reactions (Figure 5.1, a). In this context, electronically activated or biased alkenes such as acrylates, styrenes, vinylsulfones, and acrylamides have been extensively explored as compared to
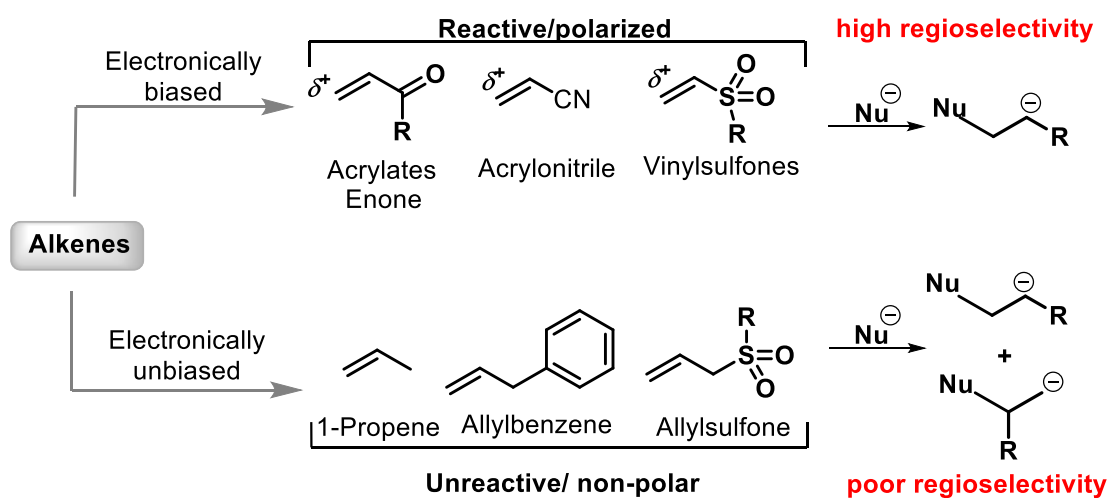
unactivated or unbiased alkenes.[8] The presence of an electron-withdrawing substituent defines the biased reactivity of the alkene and hence they show high site-selectivity (Figure 5.1, b).

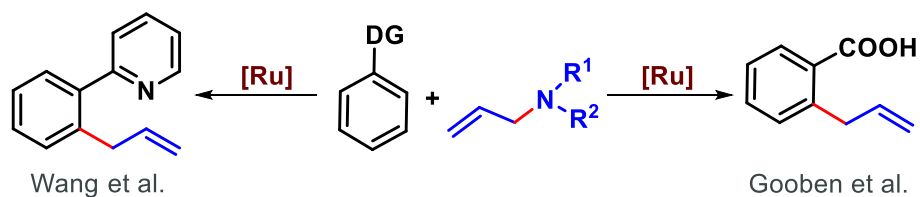**Figure 5.1 Reactivities of different types of alkenes**

(a) Common reactivity of alkene as a reacting partner in directed C-H functionalization:
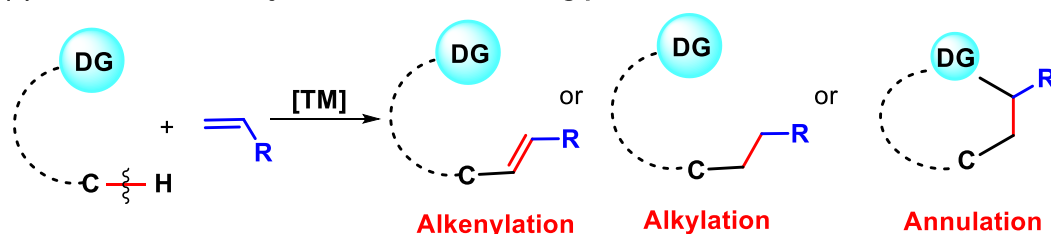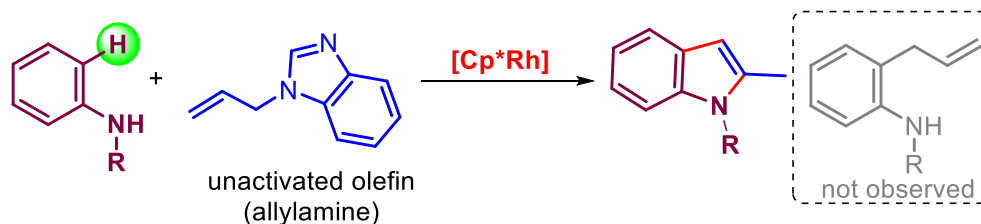

(b) Reactivity comparison between electronically biased/unbiased alkene:

(c) Previous work with allylamine: Ruthenium catalysed allylation:

(d) This work: Rhodium catalysed oxidative [3+2] annulation with allylamine:
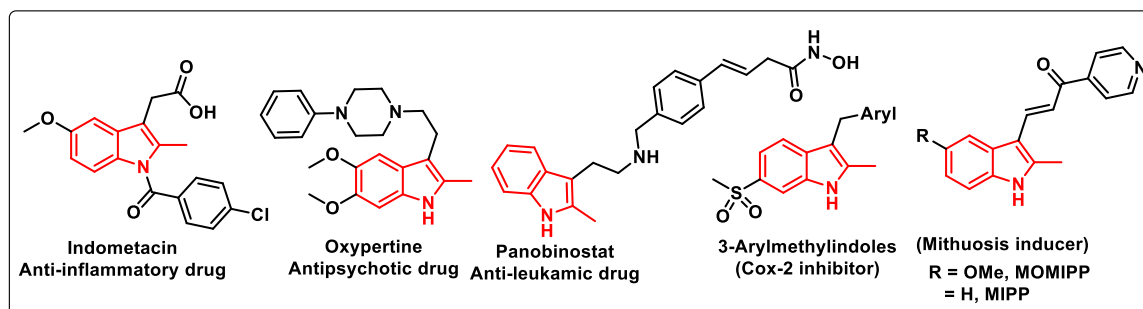

160

In contrast, the absence of such functional groups make the alkene unactivated or unbiased, which are associated with challenges such as (i) poor reactivities, and (ii) poor site-selectivity (linear vs branched product) (Figure 5.1, b).[9] However, notable progress has been made for electronically unbiased alkenes such as, methylenecyclopropanes, allyl alcohols, allyl carboxylates, and allyl sulfones.[10] Recently, Jeganmohan and co-workers reported the $C(sp^2)$-H olefination/alkylation on aryl carboxylic acids and unsaturated amides using unactivated alkenes.[11] The Chatani group reported a picolinamide-directed alkylation reaction with terminal alkenes where the acid additive plays an important role for achieving site-selectivity.[12a] They also disclosed the branch-selective alkenylation of anilines with the unactivated terminal alkene trimethylvinylsilane.[12b] In addition to the aforementioned alkenes, allylamine also possesses a terminal unbiased olefinic group and, in classical organic synthesis, allylamines have been utilized for allylation reactions for valuable transformations.[13] However, there are only two reports on ruthenium-catalysed directed $C(sp^2)$-allylation reactions by Gooben and Wang (Figure 5.1, c).[14] The allylation chemistry proceeds via the cleavage of a thermodynamically stable C-N bond.[15] Unlike C-O bond cleavage (allylcarboxylates), C-N bond cleavage is relatively more difficult and challenging.[15] We proposed exploring the reactivity of an allylamine congener with anilines. Surprisingly, the reaction of *N*-pyridylanilne with *N*-allylbenzimidazole under rhodium catalysis delivered 2-methylindole instead of the *ortho*-allylation observed with anilines; which could be possible through a pyridyl directed dehydrogenative [3+2] annulation pathway (Figure 5.1, d).

2-methylindole is a valuable scaffold present in so many drug molecules and natural products (Figure 5.2).[16] Synthesis of such biologically useful scaffold including

exploration of the synthetic applications of allylamine prompted us to investigate this transformation.

**Figure 5.2 Selected examples of biologically active molecules with 2-methylindole moiety**

Indometacin
Anti-inflammatory drug

Oxypertine
Antipsychotic drug

Panobinostat
Anti-leukamic drug

3-Arylmethylindoles
(Cox-2 inhibitor)

(Mithuosis inducer)
R = OMe, MOMIPP
= H, MIPP

5.3 RESULTS AND DISCUSSION

N-pyridylaniline **1a**, *N*-allylbenzimidazole **2a** were chosen as model substrates and [Cp*RhCl$_2$]$_2$ as catalyst; which were subjected to a series of reaction conditions (Table 5.1). Initially we explored various protic solvents (TFE, MEOH, ^{t}Amyl-OH) and aprotic solvents (toluene, 1,4-dioxane, acetonitrile, chlorobenzene) (Table 5.1, entries 2 and 3). Among them, toluene was found to be the most effective affording the indole **3aa** in 76% yield. The role of the additive is crucial as only a trace amount of **3aa** was observed in absence of LiClO$_4$ (Table 5.1, entry 4). Therefore, commonly used silver additives such as AgOAc, AgSbF$_6$ and alkali metal salts such as K$_2$CO$_3$, KOAc were also screened (Table 5.1, entries 5-7). Notably, the alkali metal salts were found tob e more productive than silver based additives. Moreover, tetrabutylammonium salts TBAB or TBAI were able to produce 70% of **3aa**. Lowering the additive equivalence to 1.5 equiv decreased the product yield to 63%, while increasing the additive equivalence gave almost same yield (Table 5.1, entries 8,9). A control experiment without Zn(OTf)$_2$ additive afforded only 33% of yield of 3aa after 12 h (Table 5.1, entry 10). Having observed this catalytic behaviour, we screened other *Lewis* acids. Attempts using In(OTf)$_3$, boric acid or Zn(OAc)$_2$ (Table 5.1, entries 11,13) were not productive. To understand the effect of

Table 5.1 Optimization for the Rh-catalysed oxidative annulation of *N*-pyridyl aniline with *N*-allylamine[a,b]
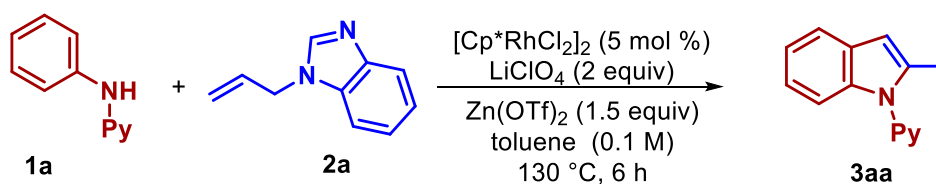
entry	deviation from the standard conditions	yield of 3aa(%)[b]
1	none	76
2	protic solvents such as MeOH or TFE instead of toluene	46, 51
3	protic solvents such as DCE or PhCl instead of toluene	46, 49
4	without LiClO$_4$	trace
5[c]	AgOAc or AgSbF$_6$ instead of LiClO$_4$	24, trace
6[d]	K$_2$CO$_3$ or KOAc instead of LiClO$_4$	45, 37
7[e]	TBAB or TBAI instead of LiClO$_4$	70, 69
8	1.5 equiv. of LiClO$_4$ instead of 2 equiv.	63
9	2.5 equiv. of LiClO$_4$ instead of 2 equiv.	77
10	without Zn(OTf)$_2$	33[f]
11	In(OTf)$_3$, B(OH)$_3$ as additive instead of Zn(OTf)$_2$	23, nr
12	Zn(OAc)$_2$ as instead of Zn(OTf)$_2$	15
13	1 equiv. of Zn(OTf)$_2$	39
14	reaction temperature 140 °C, 120 °C	73, 61[g]
15	without [Cp*RhCl$_2$]$_2$	nr
16	[Cp*Rh(CH$_3$CN)$_3$][SbF$_6$]$_2$ instead of [Cp*RhCl$_2$]$_2$	17

I, 76%   II, 51%   III, nd   IV, nd   V, nd
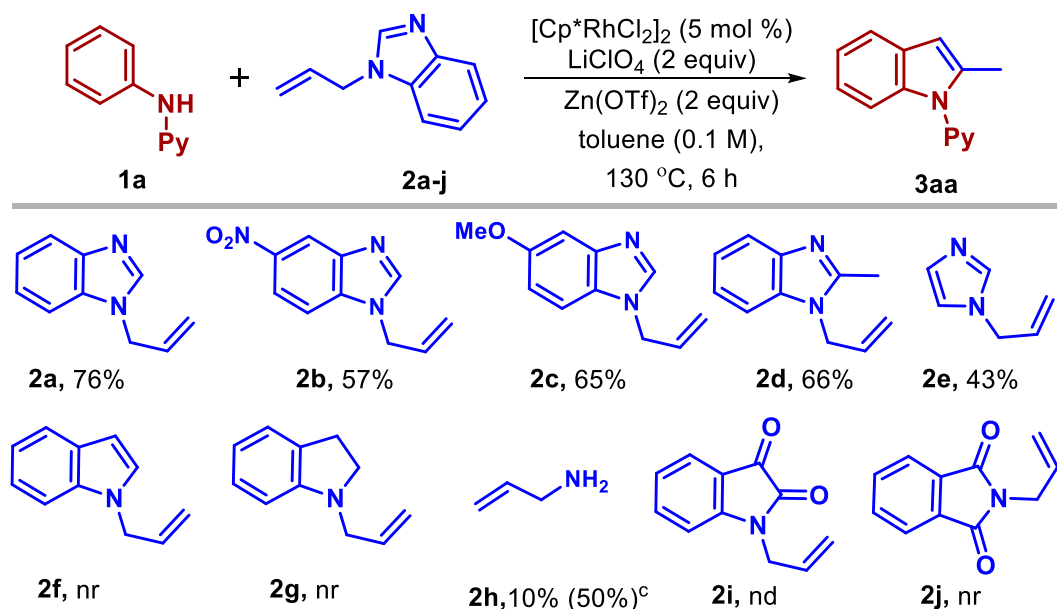
VI, nr   VII, nr   VIII, nr
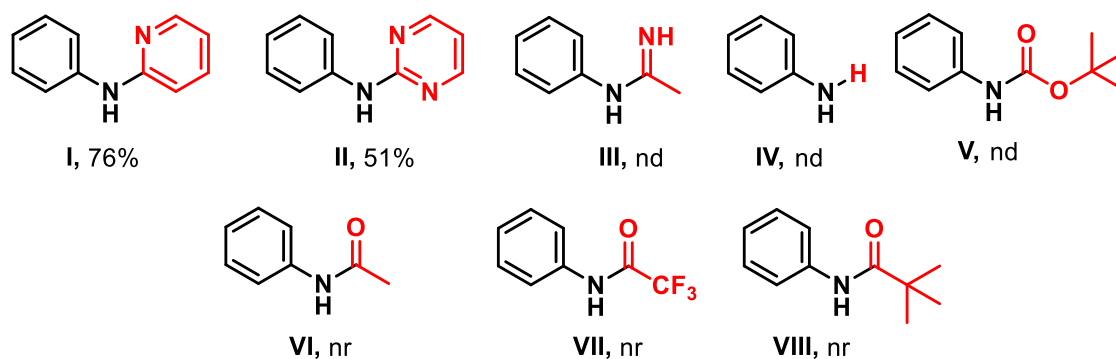
[a]Reaction conditions: **1a** (0.032 mmol, 1 equiv), **2a** (0.096 mmol, 3 equiv), [Cp*RhCl$_2$]$_2$ (5 mol %), LiClO$_4$ (0.064 mmol, 2 equiv), Zn(OTf)$_2$ (0.048 mmol, 1.5 equiv), toluene (0.1 M), 130 °C, 6 h. [b]Isolated yield. nr-no reaction.[c]0.2 equiv of additive. [d]1 equiv of additive.[e]2 equiv of additive. [f]brsm yield after 12 h. [g]yield after 12 h.

temperature, reactions were performed at different temperatures (Table 5.1, entry 14) and 130 °C was found as the optimal temperature. No product was formed in the absence of Rh-catalyst and only 17% of the product **3aa** was produced with the cationic catalyst [Cp*Rh(CH$_3$CN)$_3$][SbF$_6$]$_2$ (Table 5.1, entry 16).

After an exhaustive study of the reaction parameters, use of [Cp*RhCl$_2$]$_2$ (5 mol %), LiClO$_4$ (2 equiv), Zn(OTf)$_2$ (1.5 equiv), toluene as solvent, and 130 °C reaction temperature was concluded to be the optimized reaction condition. We further have screened this optimized condition to understand the effect of substituents over the *N*-atom of the aniline (Table 5.1). Among all substragtes, pyridyl and pyrimidyl protected anilines were found to be viable substrates under the standard reaction conditions delivering 76% and 51% of their respective annulated products. In contrast, *N*-aryl amidine **III**, *N*-arylcarbamate **V**, or other carbonyl protected anilines (**VI**-**VIII**) were found unsuccessful.
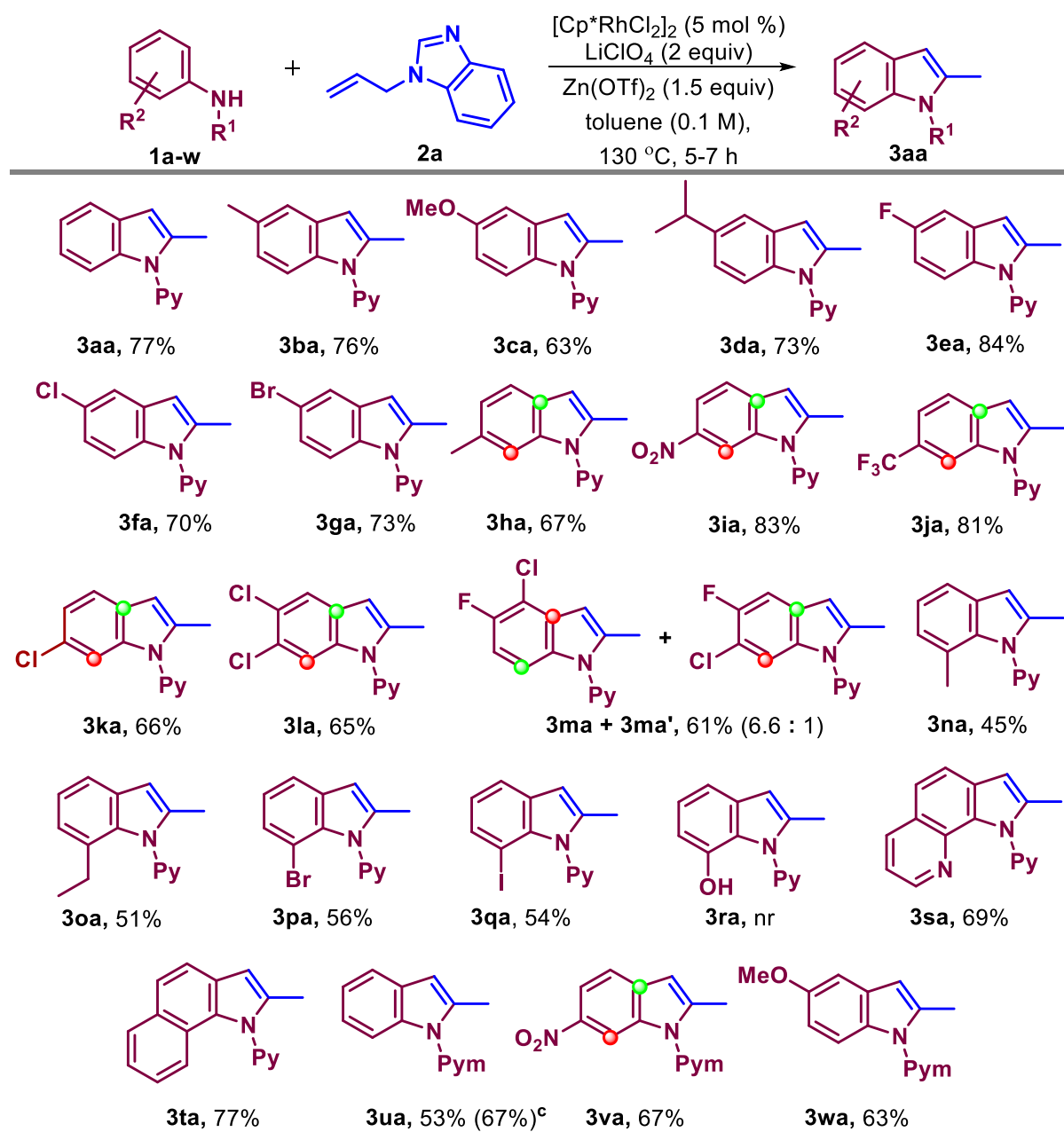
Scheme 5.1 Evaluation of various *N*-allylamines[a,b]

2a, 76%   **2b,** 57%   **2c,** 65%   **2d,** 66%   **2e,** 43%

2f, nr   **2g,** nr   **2h,** 10% (50%)[c]   **2i,** nd   **2j,** nr

[a]Reaction conditions: **1a** (0.1 mmol, 1 equiv), **2** (0.3 mmol, 3 equiv), [Cp*RhCl$_2$]$_2$ (5 mol %), LiClO$_4$ (0.2 mmol, 2 equiv), Zn(OTf)$_2$ (0.15 mmol, 1.5 equiv), toluene (0.1 M), 130 °C, 6 h. [b]Isolated yield. [c]brsm yield after 12 h. nr- no reaction.

With the pyridyl directing group, we screened a series of *N*-allylamine derivatives

2 (Scheme 5.1). Compared to *N*-allylbenzimidazole **2a**, the presence of an electron

withdrawing group (-NO$_2$) **2b** or donating group (-OMe, -Me) **2c**, **2d** on the

benzimidazole unit failed to produce better yields. When *N*-allylimidazole **2e** was used

Scheme 5.2 Scope Of Anilines for Cp*Rh(III)-catalysed 2-methylindole Synthesis[a,b]

3aa, 77%	3ba, 76%	3ca, 63%	3da, 73%	3ea, 84%
3fa, 70%	3ga, 73%	3ha, 67%	3ia, 83%	3ja, 81%
3ka, 66%	3la, 65%	3ma + 3ma', 61% (6.6 : 1)		3na, 45%
3oa, 51%	3pa, 56%	3qa, 54%	3ra, nr	3sa, 69%
3ta, 77%	3ua, 53% (67%)[c]	3va, 67%	3wa, 63%	

[a]Reaction conditions: **1a** (0.032 mmol, 1 equiv), **2** (0.096 mmol, 3 equiv), [Cp*RhCl$_2$]$_2$ (5 mol %), LiClO$_4$ (0.064 mmol, 2 equiv), Zn(OTf)$_2$ (0.048 mmol, 1.5 equiv), toluene (0.1 M), 130 °C, 6 h. [b]Isolated yield. [c]brsm yield after 12 h. nr-no reaction.

instead of **2a**, a reduced yield was observed. Notably, *N*-allylindole was found to be completely unreactive for this annulation reaction. Hence, these results show the very crucial role of the nitrogen atom at C-3 of indole. Similarly, attempts with indoline **2g**, isatin **2i** and isoindolonone **2j** failed to produce **3aa**. The simple allylamine gave only 10% yield of **3aa**. From all these screenings, *N*-allylbenzim-idazole **2a** was found to give the best yield.
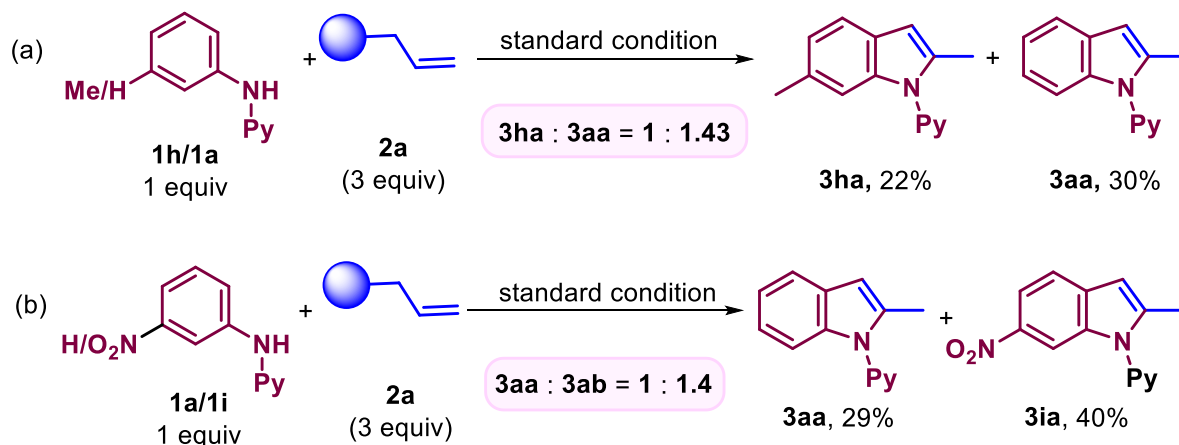
After determining the optimized reaction conditions, we moved on to explore the generality of this methodology with different anilines (Scheme 5.2). Substrates bearing electron donating groups (-Me, -Et, -OMe, -^{i}Pr), halo groups (-F, -Cl, -Br, -I) or electron withdrawing groups (-NO$_2$, -CF$_3$) were found to be viable substrates. Anilines with methyl, methoxy and *iso*propyl substituents produced **3ba**, **3ca**, and **3da** in 76%, 63%, and 73% yields respectively. Halogen substituted anilines were observed to produce good to very good yields of indoles **3ea**, **3fa**, **3ga**, **3ka**, **3la**, **3ma**, **3pa** and **3qa**. As usual, the functionalization was observed at the sterically less hindered site of *meta*-substituted anilines giving their respective annulated products **3ha**, **3ia**, **3ja**. As compared to the *para-* and *meta-* substituted anilines, *ortho*-substituted anilines were found to be less effective substrates (**3na-3qa**). This might well be due to steric resistance from the *ortho*-substituent. Importantly, 2-methyl-pyrrolo[3,2-*h*]quinoline **3sa**, and 2-methyl-benzo[*g*]indole **3ta** could be synthesized from 1-aminonaphthalene and 8-aminoquinoline substrate in 69% and 77% respectively. Along with the pyridyl directed annulation, the scope of this methodology was found viable for the pyrimidine directing groups for the synthesis of **3ua**, **3va**, and **3wa**.

To gain insight into this Rh-catalysed annulation reaction, control experiments and mechanistic studies were performed (Scheme 5.3). Intermolecular competition
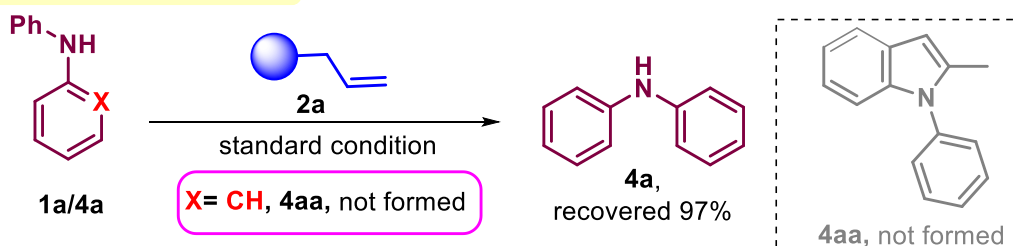
reactions were performed between electron rich substrate **1h** and neutral substrate **1a** with

2a. A product ratio 1/1.43 was obtained for the annulated products **3ha/3aa** respectively
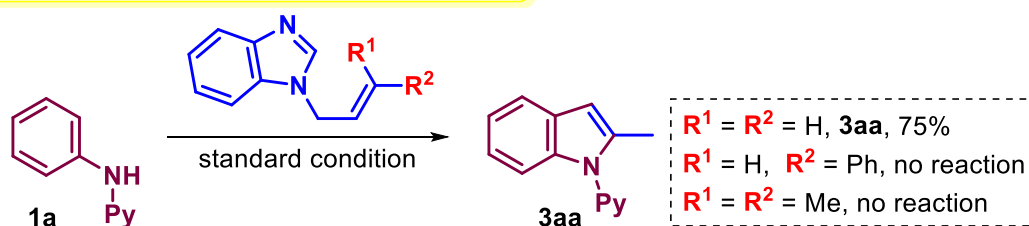
Scheme 5.3 Competitive studies and control experiments:

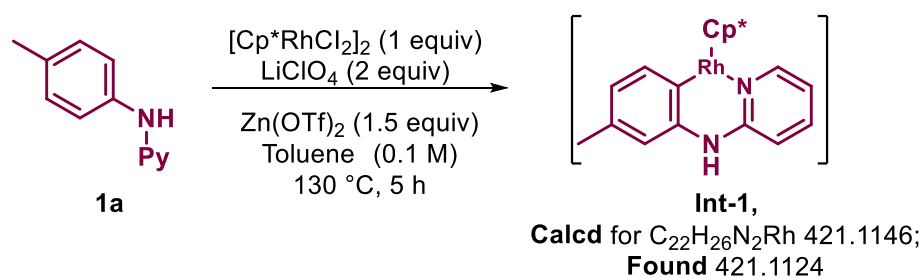Comeptition studies between substrates:

(a)

1h/1a
1 equiv

2a
(3 equiv)

standard condition

3ha : 3aa = 1 : 1.43

3ha, 22%   **3aa,** 30%

(b)

1a/1i
1 equiv

2a
(3 equiv)

standard condition

3aa : 3ab = 1 : 1.4

3aa, 29%   **3ia,** 40%

(c) Role of chelating N-atom:

1a/4a

2a

standard condition

X= CH, 4aa, not formed

4a,
recovered 97%

4aa, not formed

(d) Substituent effect of alkene on the reactivity:

1a

standard condition

3aa

R¹ = R² = H, 3aa, 75%
R¹ = H, R² = Ph, no reaction
R¹ = R² = Me, no reaction

(e) Detection of rhodacycle intermediate in HRMS:

1a

[Cp*RhCl₂]₂ (1 equiv)
LiClO₄ (2 equiv)

Zn(OTf)₂ (1.5 equiv)
Toluene (0.1 M)
130 °C, 5 h

Int-1,
Calcd for $C_{22}H_{26}N_2Rh$ 421.1146;
Found 421.1124
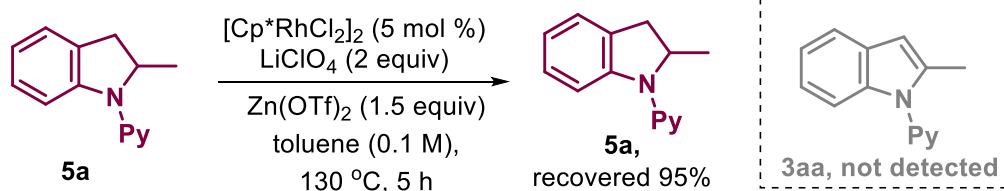
(Scheme 5.3, a). In support of this reactivity, a similar product distribution ratio was also obtained for **3aa**/**3ia** (Scheme 5.3, b). Both of these experiments indicate that this annulation reaction is significantly favoured by electron-withdrawing groups. Next, in order to investigate the role of the *N*-atom in the pyridyl directing group, diphenylamine **4a** was subjected to the standard reaction conditions (Scheme 5.3, c). In contrary to **1a**, no product was detected for **4a**; rather 97% of **4a** was recovered from the reaction mixture. This implies the crucial role of the pyridyl *N*-atom as a co-ordinating atom in this transformation.

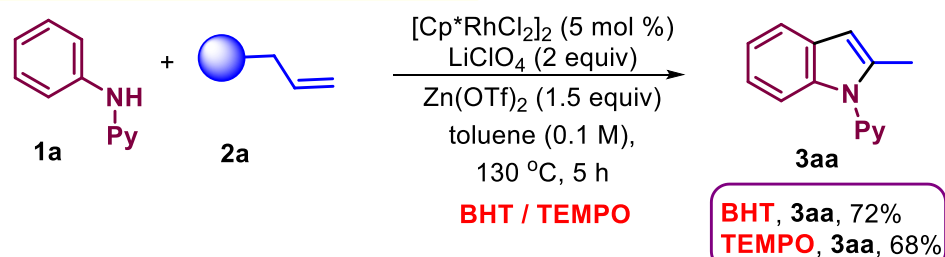**Scheme 5.4 Competitive studies and control experiments:**

(a) Standard reaction with *N*-(2-allylphenyl)pyridin-2-amine (1a"):

[Cp*RhCl₂]₂ (5 mol%)
LiClO₄ (2 equiv)
Zn(OTf)₂ (1.5 equiv)
toluene (0.1 M)
130 °C, 5 h

no reaction in absence of [Rh]

1a"   **3aa,** 48%   **1a",** 43% (recovered)
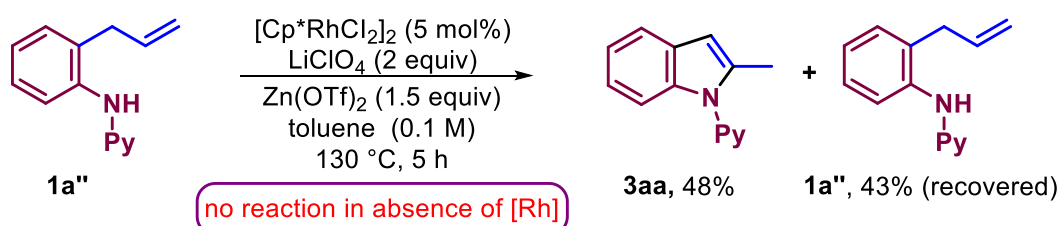
(b) Reaction of 2-methyl-1-(pyridin-2-yl)indoline:

[Cp*RhCl₂]₂ (5 mol %)
LiClO₄ (2 equiv)
Zn(OTf)₂ (1.5 equiv)
toluene (0.1 M),
130 °C, 5 h

5a   **5a,** recovered 95%   **3aa, not detected**

(c) Reaction of with radical scavengers:

[Cp*RhCl₂]₂ (5 mol %)
LiClO₄ (2 equiv)
Zn(OTf)₂ (1.5 equiv)
toluene (0.1 M),
130 °C, 5 h

BHT / TEMPO

1a   **2a**   **3aa**

BHT, **3aa,** 72%
TEMPO, **3aa,** 68%

The substituent effects of the alkene on the reactivity were examined by taking mono- or disubstituted derivative of terminal alkene **2a** (Scheme 5.3, d). No product was detected

from the terminal substituted alkenes, which suggests that insertion of the alkene into the C-Rh bond is inhibited by substituents on the terminal alkene. The intermediate **Int-1** was detected by HRMS from a control experiment performed in absence of alkene **2a** (Scheme 5.3, e).

The pre-synthesized substrate **1a″**, upon being subjected to the standard conditions yielded a 92% yield of **3aa**; supporting that the pathway involves allylation followed by intramolecular cyclization (Scheme 5.4, a). We did not observe the formation of **3aa** in absence of the rhodium catalyst, which also confirms the need of Rh-catalyst for this intramolecular cyclization. However, **5a** failed to produce **3aa**, which suggests that **5a** is not an active intermediate for this transformation (Scheme 5.4, b). Additionally, reactions were performed in presence of radical scavengers BHT/TEMPO (Scheme 5.4, c), furnishing **3aa** in 72% and 68% yields respectively. These experiments rule out a radical pathway for this reaction.

Based on the above mechanistic studies and literature reports,[14,17] a catalytic cycle can be proposed (Scheme 5.5). The active rhodium catalyst A undergoes cyclometalation ir-reversibly with *N*-pyridylaniline 1a giving the cyclometallated intermediate B. Migratory insertion of alkene 2a into the C-Rh bond, followed by elimination of benzimidazole unit delivers the intermediate E. The addition of the *N*-Rh bond to the alkene carbon leads to the intermediate **F**. The intermediate **G** can be derived by *β*-hydride elimination of **F**. Finally, aromatization of **G** delivers the final product **3aa**.

A 1 mmol scale reaction was performed to observe the synthetic viability of this protocol at larger scale, delivering **3aa** in 74% yield (Scheme 5.6, a). The annulated product **3aa** may be used as a synthetic precursor for the synthesis of useful derivatives

(Scheme 5.6, b). The formyl group was installed at C-3 of **3aa** giving 80% of **4** via the Vilsmeier– Haack formylation reaction. Similarly, removal of the pyridyl group,
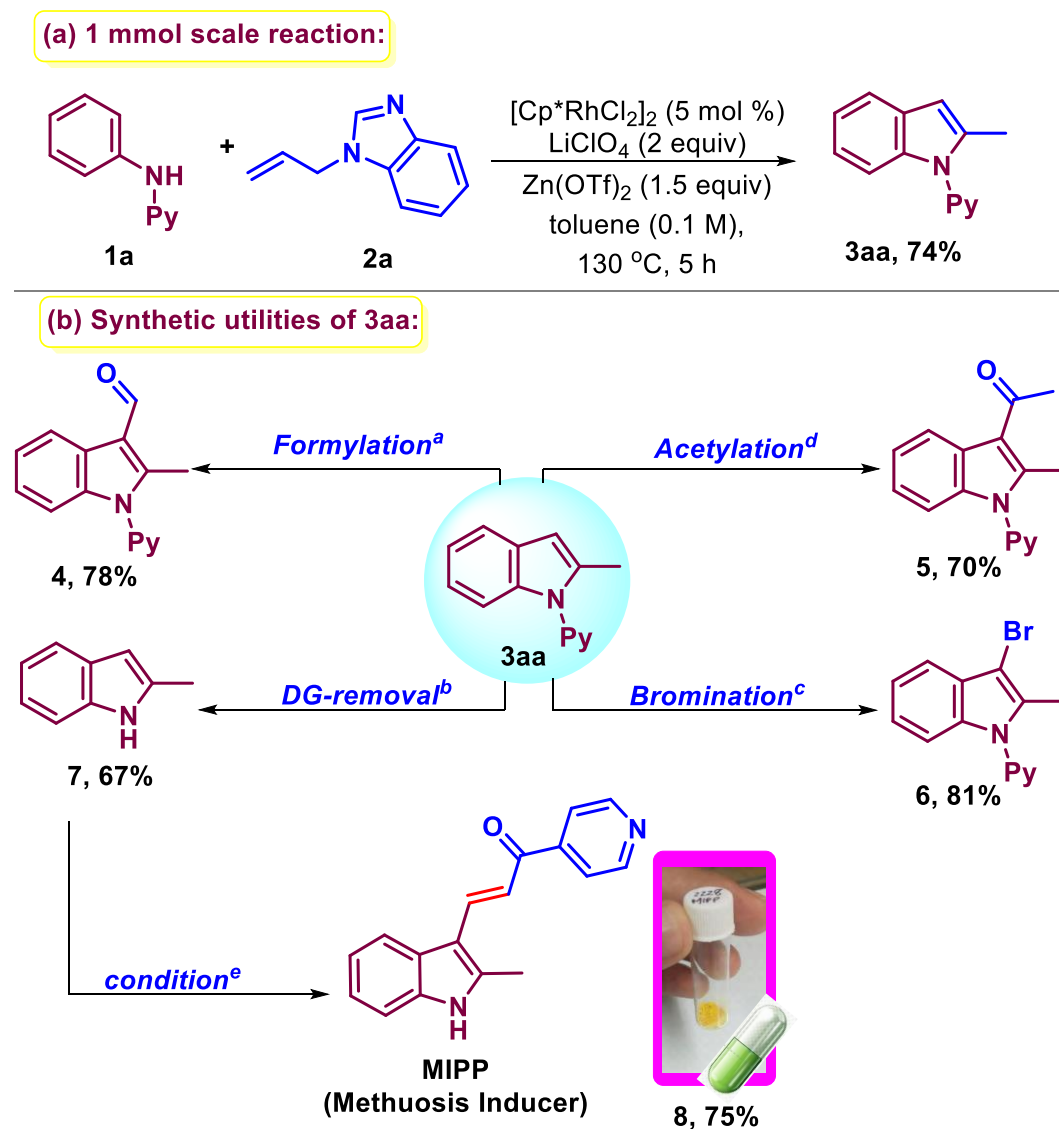
Scheme 5.5 Proposed catalytic cycle
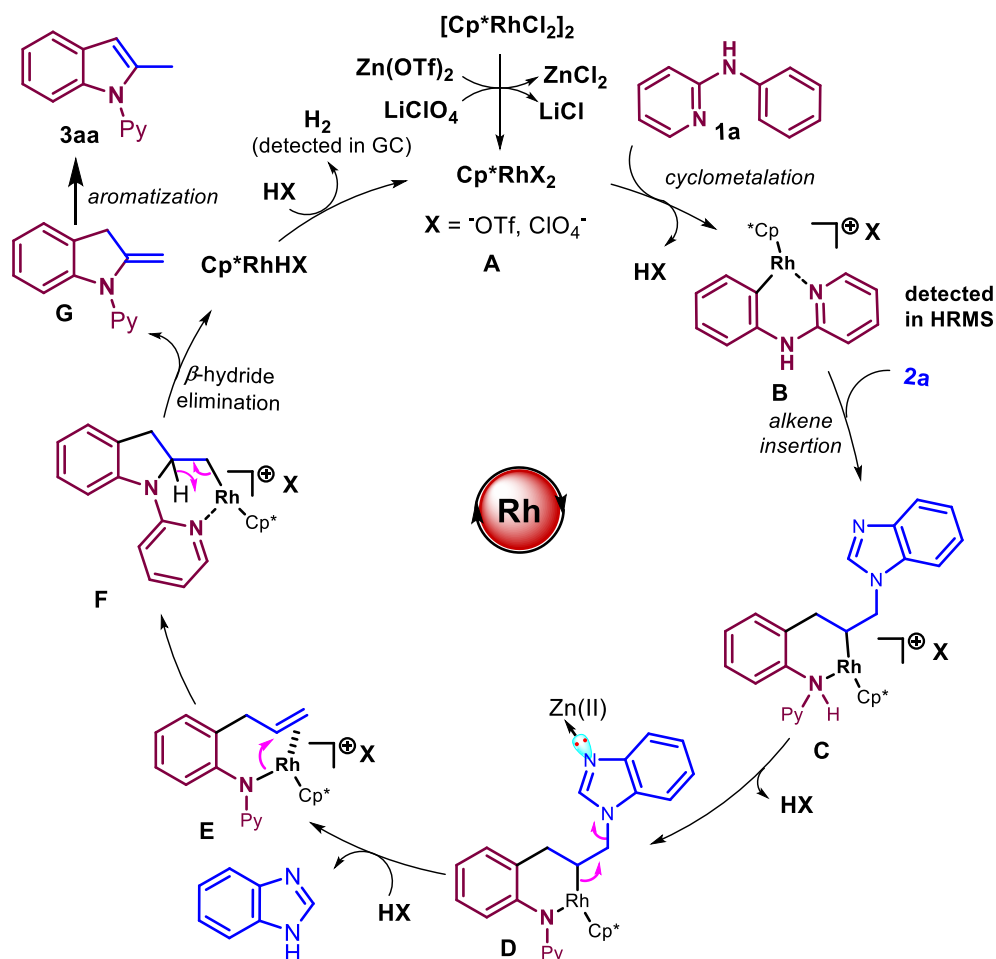
bromination, and acetylation have been achieved, to deliver the respective products **5, 6,** and **7** in good yields. The synthetic application of this methodology has been further extended for the synthesis of drug molecule (Scheme 5.6, b). 2-methylindole derived product 3-(2-methyl-1H-indol-3-yl)-1-(4-pyridinyl)-2-propen-1-one (MIPP) **8** is known as a methuosis inducer in glioblastoma and other types of cancer cells.[16b] The drug molecule MIPP was synthesized from **5** in 75% yield. This methodology could also be

useful for the preparation of a series of MIPP derivatives, which could be helpful for further biological studies.

Scheme 5.6 Synthetic applications:

Reaction conditions: (a) DMF, (COCl)$_2$, DCM, -10 °C-rt, 1 h; (b) (i) MeOTf, DCM, 0°C-rt, 12 h; (ii) 2M NaOH, MeOH, 60 °C, 10 h; (c) NBS, CHCl$_3$, rt, 5 h; (d) AcCl, SnCl$_4$, toluene, 0 °C, 2 h; (e) (i) DMF, (COCl)$_2$, DCM, rt, 1 h. (ii) 4-acetylpyridine, piperidine, MeOH, reflux, 18 h.

5.4 CONCLUSION

In summary, a regioselective synthesis of 2-methylindole and its derivatives has been reported by the oxidative [3+2] annulation of anilines and *N*-allylbenzimidazole

through rhodium catalysis. The unactivated alkene *N*-allyl benzimidazole, has been used as the reacting substrate and this transformation proceeds through cleavage of a thermodynamically stable C-N bond. The catalytic cycle was determined from a series of control experiments, which confirm a cascade of C-H allylation followed by intramolecular cyclization. Moreover, a late-stage synthetic application has been extended for the synthesis of the drug molecule MIPP.

5.5 EXPERIMENTAL SECTION

All the starting materials were bought from Sigma Aldrich, Alfa-Aesar, Avra, TCI and Spectrochem, and used without any further purification. For column chromatography, silica gel (100-200, 230-400 mesh) from Acme Co. was used. A gradient elution using distilled hexane and ethyl acetate was performed, based on Merck aluminum TLC sheets. All isolated compounds were characterized by ^{1}H NMR (Bruker-400/700 MHz), ^{13}C NMR spectroscopy and HRMS. Copies of the ^{1}H NMR, ^{13}C NMR, and ^{19}F NMR can be found in the Supporting Information. Nuclear Magnetic Resonance spectra were recorded on a Bruker 400/700 MHz instrument. HRMS signal analysis was performed using micro TOF Q-II mass spectrometer. All ^{1}H NMR experiments were reported in parts per million (ppm), and were measured relative to the signals for residual chloroform (7.26 ppm) in the deuterated solvent. All ^{13}C NMR spectra were reported in ppm relative to CDCl$_3$ (77.36 ppm). *N*-arylpyridine[18], and *N*-arylpyrimidine[18], acetimidamide[19], *N*-acetyl aniline[20], *N*-trifluoroacetyl aniline[20], *N*-pivaloyl aniline[20], tert-butylphenylcarbamate[21] were prepared by following the literature reports.

General reaction procedure for Rh-catalysed annulation reaction:

To an oven-dried 25 mL Schlenk tube charged with a magnetic stir bar, was added LiClO$_4$ (0.2 mmol, 2 equiv) and the tube was heated under reduced pressure to remove traces of

water. To this dried Schlenk tube, were added *N*-pyridylaniline or *N*-pyrimidylaniline **1** (0.1 mmol, 1 equiv), [Cp*RhCl$_2$]$_2$ (0.005 mmol, 5 mol %), Zn(OTf)$_2$ (0.15 mmol, 1.5 equiv), alkene **2a** (0.3 mmol, 3 equiv) and toluene (0.1 M, 1 mL) under a nitrogen atmosphere. The reaction mixture was stirred (700 rpm) in a preheated aluminum block at 130 °C. After completion of the reaction (monitored by TLC), the solvent was evaporated under reduced pressure, and the crude residue was purified by column chromatography using EtOAc/hexane as eluent to furnish the corresponding annulated product.

Experimental characterization data of products:

2-Methyl-1-(pyridin-2-yl)-1H-indole (**3aa**)[17]:
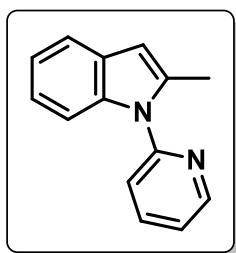
Physical State: Colorless liquid (16 mg, 77% yield). **R$_f$** = 0.8 (10% EtOAc/hexane). **^{1}H NMR (CDCl$_3$, 400 MHz):** δ 8.65 (d, *J* = 4.8 Hz, 1H), 7.87 (t, *J* = 8.0 Hz, 1H), 7.56-7.54 (m, 1H), 7.20 (d, *J* = 8.0 Hz, 1H), 7.38-7.36 (m, 1H), 7.32-7.29 (m, 1H), 7.13-7.10 (m, 2H), 6.42 (s, 1H), 2.46 (s, 3H) ppm. **^{13}C{^{1}H} NMR (CDCl$_3$, 101 MHz):** δ 151.8, 149.9, 138.5, 137.4, 137.1, 129.0, 122.1, 121.8, 121.1, 120.9, 120.0, 110.5, 103.6, 14.3 ppm. **IR** (KBr, cm^{-1}): 3052, 2957, 2853, 1466.

2,5-Dimethyl-1-(pyridin-2-yl)-1H-indole (**3ba**)[17]:
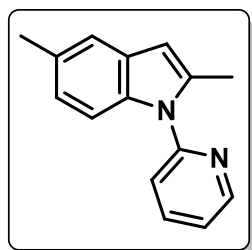
Physical State: Colorless liquid (17 mg, 76% yield). **R$_f$** = 0.7 (10% EtOAc/hexane). **^{1}H NMR (CDCl$_3$, 400 MHz):** δ 8.64 (d, *J* = 4.8 Hz, 1H), 7.86 (t, *J* = 8.0 Hz, 1H), 7.40 (d, *J* = 8.0 Hz, 1H), 7.33 (s, 1H), 7.29-7.25 (m, 2H), 6.93 (d, *J* = 8.4 Hz, 1H), 6.33 (s, 1H), 2.45 (s, 3H), 2.43 (s, 3H) ppm. **^{13}C{^{1}H} NMR (CDCl$_3$, 101 MHz):** δ 152.0,

149.8, 138.4, 137.2, 135.8, 130.2, 129.3, 123.3, 121.9, 120.9, 119.9, 110.2, 103.3, 21.7, 14.3 ppm. **IR** (KBr, cm^{-1}): 3016, 2917, 2857, 1442.

5-Methoxy-2-methyl-1-(pyridin-2-yl)-1H-indole (**3ca**)[23]:
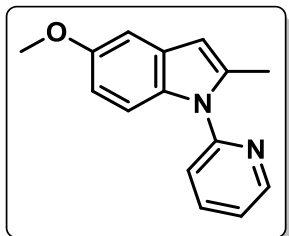
Physical State: Oily liquid (15 mg, 63% yield). **R**$_f$ = 0.5 (10% EtOAc/hexane). **^{1}H NMR (CDCl$_3$, 400 MHz):** δ 8.64 (d, J = 4.8 Hz, 1H), 7.86 (t, J = 8.0 Hz, 1H), 7.39 (d, J = 8.0 Hz, 1H), 7.30-7.25 (m, 2H), 7.02 (s, 1H), 6.76 (d, J = 8.8 Hz, 1H), 6.34 (s, 1H), 3.85 (s, 3H), 2.43 (s, 3H) ppm. **^{13}C{^{1}H} NMR (CDCl$_3$, 101 MHz):** δ 155.1, 151.9, 149.8, 138.4, 137.7, 132.5, 129.6, 121.9, 120.8, 111.4, 111.3, 103.6, 102.4, 56.1, 14.4 ppm. **IR** (KBr, cm^{-1}): 2999, 2923, 2830, 1447, 1337, 1034.

5-Isopropyl-2-methyl-1-(pyridin-2-yl)-1H-indole (**3da**):
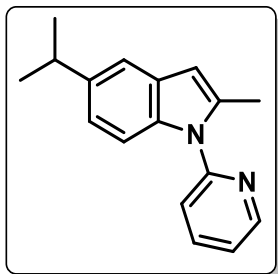
Physical State: Pale yellow solid (18 mg, 73% yield). **mp** 57-59 °C. **R**$_f$ = 0.8 (10% EtOAc/hexane). **^{1}H NMR (CDCl$_3$, 400 MHz):** δ 8.64 (d, J = 4.4 Hz, 1H), 7.86 (t, J = 7.6 Hz, 1H), 7.42-7.39 (m, 2H), 7.32-7.28 (m, 2H), 7.01 (d, J = 8.4 Hz, 1H), 6.36 (s, 1H), 3.02-2.95 (m, 1H), 2.45 (s, 3H), 1.29 (d, J = 6.8 Hz, 6H) ppm. **^{13}C{^{1}H} NMR (CDCl$_3$, 101 MHz):** δ 152.0, 149.8, 141.7, 138.4, 137.2, 136.0, 129.2, 121.9, 120.9, 120.8, 117.1, 110.3, 103.5, 34.4, 24.9, 14.3 ppm. **IR** (KBr, cm^{-1}): 3085, 3056, 2922, 2866, 1440. **HRMS (ESI) m/z:** [M+Na]$^+$ Calcd for C$_{17}$H$_{18}$N$_2$Na 273.1362; Found 273.1376.

5-Fluoro-2-methyl-1-(pyridin-2-yl)-1H-indole (**3ea**)[17]:

Physical State: Colorless liquid (19 mg, 84% yield). **R**$_f$ = 0.4 (10% EtOAc/hexane). **^{1}H NMR (CDCl$_3$, 400 MHz):** δ 8.66-8.65 (m, 1H), 7.88 (td, J = 7.6 Hz, 2.0 Hz, 1H), 7.39 (d, J = 8.0 Hz, 1H), 7.33-7.25 (m, 2H), 7.18 (dd, J = 9.6 Hz, 2.8 Hz, 1H), 6.84 (td, J = 9.2 Hz,
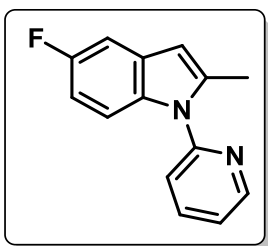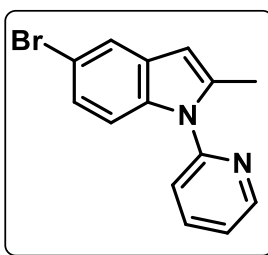
2.4 Hz, 1H), 6.37 (s, 1H), 2.44 (s, 3H) ppm. **^{13}C{^{1}H} NMR (CDCl$_3$, 101 MHz):** δ 158.8 (d, J_{C-F} = 233 Hz), 151.6, 149.9, 138.7, 138.6, 134.0, 129.5 (d, J_{C-F} = 10.2 Hz), 122.3, 121.0, 111.3 (d, J_{C-F} = 9.4 Hz), 109.7 (d, J_{C-F} = 25.6 Hz), 105.0 (d, J_{C-F} = 23.4 Hz), 103.6 (d, J_{C-F} = 4.2 Hz), 14.3 ppm. **^{19}F NMR (CDCl$_3$, 376 MHz):** -124.0 ppm. **IR** (KBr, cm^{-1}): 3061, 2059, 2922, 2853, 1452, 1020.

5-Chloro-2-methyl-1-(pyridin-2-yl)-1H-indole (3fa)[17]:
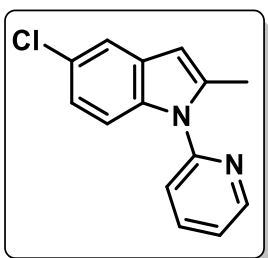
Physical State: Pale yellow solid (17 mg, 70% yield). **mp** 60-62 °C. **R$_f$** = 0.45 (10% EtOAc/hexane). **^{1}H NMR (CDCl$_3$, 400 MHz):** δ 8.65 (d, J = 4.4 Hz, 1H), 7.89 (t, J = 7.6 Hz, 1H), 7.50 (s, 1H), 7.38 (d, J = 8.0 Hz, 1H), 7.33 (t, J = 6.0 Hz, 1H), 7.28-7.26 (m, 1H), 7.06 (d, J = 8.8 Hz, 1H), 6.35 (s, 1H), 2.44 (s, 3H) ppm. **^{13}C{^{1}H} NMR (CDCl$_3$, 100 MHz):** δ 151.4, 150.0, 138.7, 138.5, 135.8, 130.1, 126.4, 122.5, 122.0, 121.0, 119.4, 111.6, 103.1, 14.3 ppm. **IR** (KBr, cm^{-1}): 3088, 3019, 2921, 2851, 1466, 782.

### 5-Bromo-2-methyl-1-(pyridin-2-yl)-1H-indole (3ga)[23]:

Physical State: Pale brown solid (21 mg, 73% yield). **mp** 59-61 °C. **R$_f$** = 0.4 (20% EtOAc/hexane). **^{1}H NMR (CDCl$_3$, 400 MHz):** δ 8.65 (d, J = 4.8 Hz, 1H), 7.89 (t, J = 7.6 Hz, 1H), 7.66 (s, 1H), 7.38 (d, J = 8.0 Hz, 1H), 7.35-7.32 (m, 1H), 7.25-7.17 (m, 2H), 6.35 (s, 1H), 2.44 (s, 3H) ppm. **^{13}C{^{1}H} NMR (CDCl$_3$, 100 MHz):** δ 151.3, 150.0, 138.7, 138.4, 136.1, 130.7, 124.6, 122.5 (2C), 121.0, 114.1, 112.1, 103.0, 14.2 ppm. **IR** (KBr, cm^{-1}): 3066, 2920, 2851, 1445, 661.

### 2,6-Dimethyl-1-(pyridin-2-yl)-1H-indole (3ha)[17]:
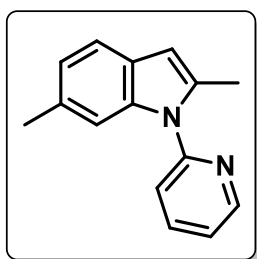
Physical State: Colorless liquid (15 mg, 67% yield). R_f = 0.5 (10% EtOAc/hexane). **^{1}H NMR (CDCl$_3$, 400 MHz):** δ 8.65 (d, J = 4.4 Hz, 1H), 7.88 (t, J = 7.6 Hz, 1H), 7.41 (t, J = 7.2 Hz, 2H), 7.30 (t, J = 6.0 Hz, 1H), 7.17 (s, 1H), 6.95 (d, J = 7.6 Hz, 1H), 6.36 (s, 1H), 2.43 (s, 3H), 2.40 (s, 3H) ppm. **^{13}C{^{1}H} NMR (CDCl$_3$, 101 MHz):** δ 151.9, 149.8, 138.4, 137.8, 136.4, 131.6, 126.8, 122.5, 122.0, 121.1, 119.7, 110.6, 103.4, 22.1, 14.3 ppm. **IR** (KBr, cm^{-1}): 3460, 2915, 1651, 1586, 1336, 1124, 962.

2-Methyl-6-nitro-1-(pyridin-2-yl)-1H-indole (3ia):
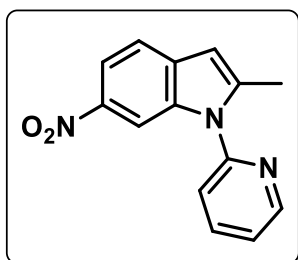
Physical State: Yellow solid (21 mg, 83% yield). **mp** 121-123 °C. R_f = 0.6 (20% EtOAc/hexane). **^{1}H NMR (CDCl$_3$, 400 MHz):** δ 8.72-8.71 (m, 1H), 8.26 (d, J = 2.0 Hz, 1H), 8.05-8.03 (m, 1H), 7.98 (td, J = 8.0 Hz, 2.0 Hz, 1H), 7.57 (d, J = 8.8 Hz, 1H), 7.45-7.43 (m, 2H), 6.53 (s, 1H), 2.50 (s, 3H) ppm. **^{13}C{^{1}H} NMR (CDCl$_3$, 176 MHz):** δ 150.4, 150.4, 143.6, 143.2, 139.2, 136.2, 134.0, 123.4, 121.3, 119.7, 116.7, 107.6, 104.2, 14.54 ppm. **IR** (KBr, cm^{-1}): 3108, 2919, 2849, 1443. **HRMS (ESI) m/z:** [M+Na]$^+$ Calcd for $C_{14}H_{11}N_3O_2Na$ 276.0743; Found 276.0715.

2-Methyl-1-(pyridin-2-yl)-6-(trifluoromethyl)-1H-indole (3ja)[17]:
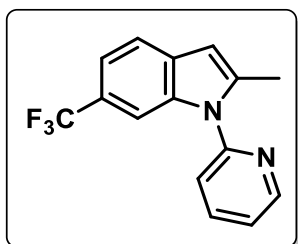
Physical State: Oily liquid (22 mg, 81% yield). R_f = 0.4 (20% EtOAc/hexane). **^{1}H NMR (CDCl$_3$, 400 MHz):** δ 8.70-8.68 (m, 1H), 7.96-7.91 (m, 1H), 7.62-7.60 (m, 2H), 7.42-7.34 (m, 3H), 6.47 (s, 1H), 2.47 (s, 3H) ppm. **^{13}C{^{1}H} NMR (CDCl$_3$, 176 MHz):** δ 151.0, 150.2, 140.1, 138.9, 136.5, 131.4, 125.6 (q, J_{C-F} = 271.2 Hz), 123.9 (q, J_{C-F} = 31.6 Hz), 122.9, 121.2, 120.2, 117.7 (q, J_{C-F} = 3.6 Hz), 108.1 (q, J_{C-F} = 4.4

Hz), 103.6, 14.3 ppm. **^{19}F NMR (CDCl$_3$, 376 MHz):** -60.4 ppm. **IR** (KBr, cm^{-1}): 2959, 2925, 2858, 1446, 1018.

6-Chloro-2-methyl-1-(pyridin-2-yl)-1H-indole (3ka):
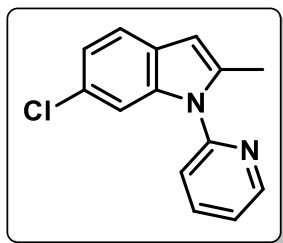
Physical State: Oily liquid (16 mg, 66% yield). **R$_f$** = 0.6 (10% EtOAc/hexane). **^{1}H NMR (CDCl$_3$, 400 MHz):** δ 8.66 (d, J = 4.4 Hz, 1H), 7.90 (t, J = 7.6 Hz, 1H), 7.44 (d, J = 8.4 Hz, 1H), 7.39 (d, J = 8.0 Hz, 1H), 7.36-7.32 (m, 2H), 7.08 (d, J = 8.4 Hz, 1H), 6.38 (s, 1H), 2.43 (s, 3H) ppm. **^{13}C{^{1}H} NMR (CDCl$_3$, 176 MHz):** δ 151.3, 150.0, 138.7, 137.9, 137.8, 127.8, 127.5, 122.6, 121.5, 121.1, 120.8, 110.7, 103.5, 14.2 ppm. **IR** (KBr, cm^{-1}): 3019, 2920, 2854, 2781, 1441, 782. **HRMS (ESI) m/z:** [M+Na]$^+$ Calcd for C$_{14}$H$_{11}$ClN$_2$Na 265.0503; Found 265.0528.

5,6-Dichloro-2-methyl-1-(pyridin-2-yl)-1H-indole (3la):
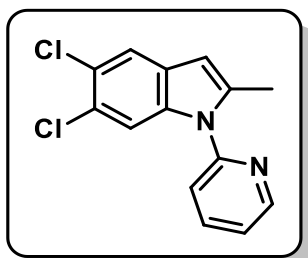
Physical State: Pale yellow solid (18 mg, 65% yield). **mp** 68-70 °C. **R$_f$** = 0.5 (10% EtOAc/hexane). **^{1}H NMR (CDCl$_3$, 400 MHz):** δ 8.66 (d, J = 4.4 Hz, 1H), 7.92 (t, J = 7.6 Hz, 1H), 7.59 (s, 1H), 7.46 (s, 1H), 7.37-7.36 (m, 2H), 6.33 (s, 1H), 2.42 (s, 3H) ppm. **^{13}C{^{1}H} NMR (CDCl$_3$, 101 MHz):** δ 150.9, 150.1, 139.2, 138.9, 136.3, 128.6, 125.5, 124.7, 122.8, 120.9 (2C), 112.3, 102.9, 14.3 ppm. **IR** (KBr, cm^{-1}): 3060, 2922, 2852, 1447, 782. **HRMS (ESI) m/z:** [M+H]$^+$ Calcd for C$_{14}$H$_{11}$Cl$_2$N$_2$ 277.0294; Found 277.0294.

4-Chloro-5-fluoro-2-methyl-1-(pyridin-2-yl)-1H-indole (3ma + 3ma'):

**Physical State:** Oily liquid (16 mg, 61% yield). **R$_f$** = 0.4 (20% EtOAc/hexane). **^{1}H NMR (CDCl$_3$, 400 MHz):** δ 8.67 (d, J = 4.4 Hz, 1H), 7.91 (d, J = 7.6 Hz, 1H), 7.40-7.34 (m, 3H), 7.27-7.25 (m, 1H), 6.36 (s, 1H), 2.42 (s, 3H) ppm. **^{13}C{^{1}H} NMR**
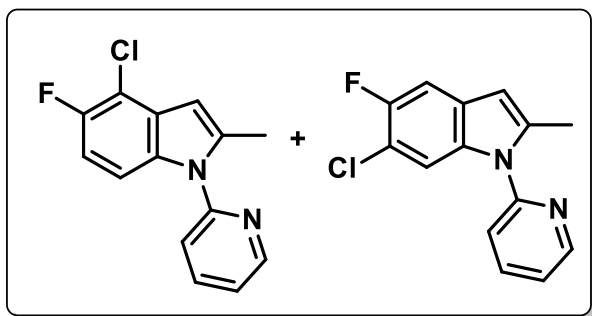
(CDCl$_3$, 176 MHz): δ 153.9 (d, $J_{C\text{-}F}$ = 238.3 Hz), 151.1, 150.1 (2C), 139.2, 138.8 (2C), 133.8, 127.9 (d, $J_{C\text{-}F}$ = 9.1 Hz), 122.8, 122.7, 121.1, 120.9, 115.2 (d, $J_{C\text{-}F}$ = 20.7 Hz), 120.0, 110.4 (d, $J_{C\text{-}F}$ = 24.9 Hz), 109.6 (d, $J_{C\text{-}F}$ = 8.6 Hz), 106.1 (d, $J_{C\text{-}F}$ = 5.8 Hz), 103.5 (d, $J_{C\text{-}F}$ = 4.0 Hz), 102.1 (d, $J_{C\text{-}F}$ = 4.7 Hz), 14.3 (2C) ppm. **^{19}F NMR (CDCl$_3$, 376 MHz):** -126.1, 128.2 ppm. **IR** (KBr, cm^{-1}): 3021, 2921, 2851, 1465, 1026. **HRMS (ESI) m/z:** [M+H]$^+$ Calcd for C$_{14}$H$_{11}$ClFN$_2$ 261.0589; Found 261.0596.
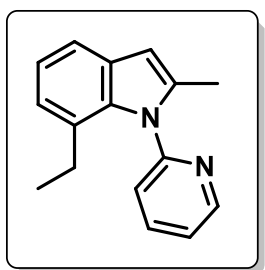
2,7-Dimethyl-1-(pyridin-2-yl)-1H-indole (3na)[17]:
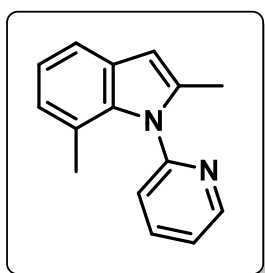
Physical State: Colorless liquid (10 mg, 45% yield). **R$_f$** = 0.6 (10% EtOAc/hexane). **^{1}H NMR (CDCl$_3$, 700 MHz):** δ 8.65 (d, J = 3.5 Hz, 1H), 7.85 (td, J = 7.7 Hz, 2.1 Hz, 1H), 7.42-7.39 (m, 2H), 7.30 (d, J = 7.7 Hz, 1H), 7.01 (t, J = 7.7 Hz, 1H), 6.85 (d, J = 7.0 Hz, 1H), 6.37 (s, 1H), 2.20 (s, 3H), 1.85 (s, 3H) ppm.

^{13}C{^{1}H} NMR (CDCl$_3$, 176 MHz): δ 153.5, 149.4, 138.0, 137.8, 136.9, 129.5, 124.4, 124.3, 123.5, 121.2, 120.7, 118.0, 102.6, 19.5, 13.6 ppm. **IR** (KBr, cm^{-1}): 2959, 2920, 2855, 2816, 1437.

7-Ethyl-2-methyl-1-(pyridin-2-yl)-1H-indole (3oa)[23]:

Physical State: Colorless liquid (12 mg, 51% yield). **R$_f$** = 0.7 (10% EtOAc/hexane). **^{1}H NMR (CDCl$_3$, 700 MHz):** δ 8.68 (brd, 1H), 7.88 (t, J = 7.0, 1H), 7.42 (d, J = 7.7 Hz, 2H), 7.34 (d, d = 7.7 Hz, 1H), 7.08 (t, J = 7.0 Hz, 1H), 6.95 (d, J = 7.7 Hz,

1H), 6.41 (s, 1H), 2.21-2.18 (m, 5H), 0.96 (t, *J* = 7.7 Hz, 3H) ppm. **¹³C{¹H} NMR (CDCl₃, 176 MHz):** δ 153.9, 149.5, 138.1, 138.0, 136.3, 129.9, 127.7, 124.1, 123.5, 122.2, 120.8, 118.0, 102.8, 25.1, 14.8, 13.7 ppm. **IR** (KBr, cm⁻¹): 2965, 2924, 2872, 1436.

7-Bromo-2-methyl-1-(pyridin-2-yl)-1H-indole (**3pa**):
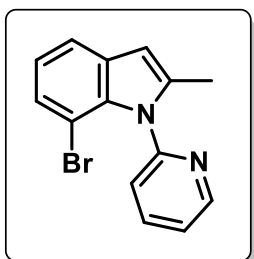
Physical State: colorless liquid (16 mg, 56% yield). R_f = 0.6 (20% EtOAc/hexane). **¹H NMR (CDCl₃, 400 MHz):** δ 8.66 (d, *J* = 4.4 Hz, 1H), 7.90 (t, *J* = 7.6 Hz, 1H), 7.66 (s, 1H), 7.38 (d, *J* = 8.0 Hz, 1H), 7.34 (t, *J* = 6.8 Hz, 1H), 7.24-7.17 (m, 2H), 6.36 (s, 1H), 2.44 (s, 3H) ppm. **¹³C{¹H} NMR (CDCl₃, 176 MHz):** δ 151.4, 150.0, 138.7, 138.4, 136.2, 130.7, 124.6, 122.5, 122.5, 121.1, 114.1, 112.1, 103.0, 14.3 ppm. **IR** (KBr, cm⁻¹): 3063, 3009, 2918, 2890, 566. **HRMS (ESI) m/z:** [M+H]⁺ Calcd for $C_{14}H_{12}BrN_2$ 287.0178; Found 287.0183. **m/z**: [M+H]⁺ Calcd for $C_{14}H_{12}Br^{81}N_2$ 289.0158; found, 289.0165

7-Iodo-2-methyl-1-(pyridin-2-yl)-1H-indole (**3qa**):
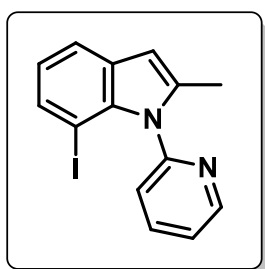
Physical State: Colorless liquid (18 mg, 54% yield). R_f = 0.7 (10% EtOAc/hexane). **¹H NMR (CDCl₃, 400 MHz):** δ 8.65 (dd, *J* = 4.8 Hz, 1.2 Hz, 1H), 7.87 (td, *J* = 8.0 Hz, 2.0 Hz, 1H), 7.56-7.52 (m, 1H), 7.42 (d, *J* = 8.0 Hz, 1H), 7.37-7.33 (m, 1H), 7.31-7.28 (m, 1H), 7.12-7.09 (m, 1H), 6.41 (s, 1H), 2.45 (s, 3H) ppm. **¹³C{¹H} NMR (CDCl₃, 176 MHz):** δ 151.8, 149.9, 138.5, 137.4, 137.1, 129.1, 122.1, 121.8, 121.1, 121.0, 120.0, 110.5, 103.6, 14.3 ppm. **IR** (KBr, cm⁻¹): 3053, 3028, 2919, 2858, 1466, 660. **HRMS (ESI) m/z:** [M+H]⁺ Calcd for $C_{43}H_{12}IN_2$ 333.9961; Found 333.9971.

2-Methyl-1-(pyridin-2-yl)-1H-pyrrolo[3,2-h]quinoline (3sa):

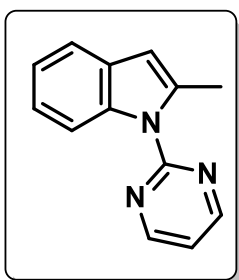**Physical State:** Colorless liquid (18 mg, 69% yield). R_f = 0.7 (10% EtOAc/hexane).
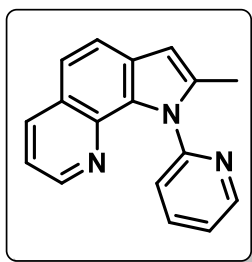
^{1}H NMR (CDCl$_3$, 400 MHz): δ 8.68-8.67 (m, 1H), 8.38 (dd, J = 4.0 Hz, 1.6 Hz, 1H), 8.10 (dd, J = 8.0 Hz, 1.6 Hz, 1H), 7.88 (dt, J = 7.6 Hz, 2.0 Hz, 1H), 7.72 (d, J = 8.4 Hz, 1H), 7.46-7.41 (m, 3H), 7.17-7.14 (m, 1H), 6.56 (d, J = 0.8 Hz, 1H), 2.33 (d, J = 0.8 Hz, 3H) ppm. **^{13}C{^{1}H} NMR (CDCl$_3$, 175 MHz):** δ 154.0, 149.1, 147.9, 138.8, 138.1, 137.8, 136.2, 131.1, 128.3, 125.4, 124.5, 123.3, 121.2, 120.6, 118.7, 103.7, 13.7 ppm. **IR** (KBr, cm^{-1}): 3070, 2922, 2852, 1469. **HRMS (ESI) m/z:** [M+H]$^+$ Calcd for C$_{17}$H$_{14}$N$_3$ 260.1182; Found 260.1163.

### 2-Methyl-1-(pyridin-2-yl)-1H-benzo[g]indole (3ta):
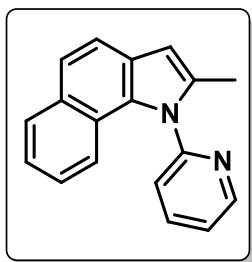
Physical State: Colorless liquid (20 mg, 77% yield). R_f = 0.4 (10% EtOAc/hexane). **^{1}H NMR (CDCl$_3$, 700 MHz):** δ 8.78 (d, J = 4.9 Hz, 1H), 7.95 (t, J = 7.0 Hz, 1H), 7.86 (d, J = 7.7 Hz, 1H), 7.67 (d, J = 8.4 Hz, 1H), 7.54-7.51 (m, 2H), 7.41 (d, J = 7.7 Hz, 1H), 7.27-7.25 (m, 1H), 7.10 (t, J = 7.7 Hz, 1H), 6.83 (d, J = 8.4 Hz, 1H), 6.53 (s, 1H), 2.28 (s, 3H) ppm. **^{13}C{^{1}H} NMR (CDCl$_3$, 175 MHz):** δ 154.1, 150.4, 139.1, 136.7, 131.4, 131.3, 129.4, 125.9, 125.1, 124.1, 123.2, 122.4, 122.0, 120.6 (2C), 120.5, 103.7, 13.6 ppm. **IR** (KBr, cm^{-1}): 3054, 2920, 2852, 1437. **HRMS (ESI) m/z:** [M+H]$^+$ Calcd for C$_{18}$H$_{15}$N$_2$ 259.1230; Found 259.1219.

2-Methyl-1-(pyrimidin-2-yl)-1H-indole (**3ua**)[22]:

Physical State: Colorless liquid (11 mg) in 53% yield and 67% of brsm yield. R_f = 0.7 (10% EtOAc/hexane). **¹H NMR (CDCl₃, 400 MHz):** δ 8.79 (d, J = 4.4 Hz, 2H), 8.28 (d, J = 8.0 Hz, 1H), 7.50 (d, J = 7.6 Hz, 1H), 7.21-7.12 (m, 3H), 6.43 (s, 1H), 2.71 (s, 3H) ppm. **¹³C{¹H} NMR (CDCl₃, 175 MHz):** δ 158.7, 158.4, 138.1, 137.1, 129.7, 122.6, 122.1, 119.8, 117.2, 114.2, 107.0, 16.9 ppm. **IR** (KBr, cm⁻¹): 3051, 2920, 2850, 2784, 1427.

2-Methyl-6-nitro-1-(pyrimidin-2-yl)-1H-indole (**3va**):
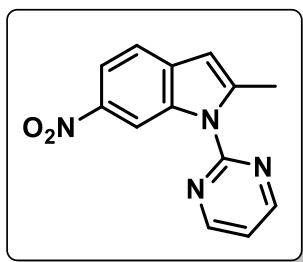
Physical State: Yellow solid (17 mg, 67% yield). **mp** 147-149 °C. R_f = 0.2 (5% EtOAc/hexane). **¹H NMR (CDCl₃, 700 MHz):** δ 9.24 (d, J = 1.4 Hz, 1H), 8.86 (d, J = 4.2 Hz, 2H), 8.10 (dd, J = 9.1 Hz, 2.1 Hz, 1H), 7.54 (d, J = 9.1 Hz, 1H), 7.27-7.26 (m, 1H), 6.53 (s, 1H), 2.78 (s, 3H) ppm. **¹³C{¹H} NMR (CDCl₃, 175 MHz):** δ 158.8, 158.0, 144.4, 143.8, 135.7, 134.7, 119.4, 118.3, 117.8, 111.48, 107.2, 17.3 ppm. **IR** (KBr, cm⁻¹): 3044, 2918, 2851, 1510. **HRMS (ESI) m/z:** [M+Na]⁺ Calcd for $C_{13}H_{10}N_4O_2Na$ 277.0697; Found 277.0705.

5-Methoxy-2-methyl-1-(pyrimidin-2-yl)-1H-indole (**3wa**)[22]:
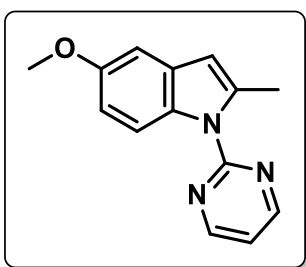
Physical State: Colorless liquid (15 mg, 63% yield). R_f = 0.4 (10% EtOAc/hexane). **¹H NMR (CDCl₃, 700 MHz):** δ 8.75 (d, J = 4.9 Hz, 2H), 8.24 (d, J = 9.1 Hz, 1H), 7.09 (t, J = 4.9 Hz, 1H), 6.98 (d, J = 2.1 Hz, 1H), 6.83 (dd, J = 9.1 Hz, 2.1 Hz, 1H), 6.35 (s, 1H), 3.85 (s, 3H), 2.71 (s, 3H) ppm. **¹³C{¹H} NMR (CDCl₃, 176**

MHz): δ 158.7, 158.3, 155.7, 138.8, 132.0, 130.5, 116.9, 115.4, 111.4, 107.0, 102.4, 56.0, 17.3 ppm. **IR** (KBr, cm^{-1}): 3043, 2922, 2831, 2774, 1426, 1292.
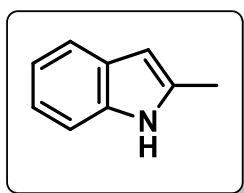
2-Methyl-1-(pyridin-2-yl)-1H-indole-3-carbaldehyde (**4**)[23]:
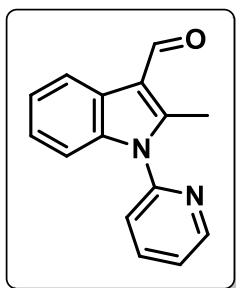
Physical State: Colorless liquid (19 mg, 80% yield). **R$_f$** = 0.2 (20% EtOAc/hexane). **^{1}H NMR (CDCl$_3$, 400 MHz):** δ 10.3 (s, 1H), 8.73-8.71 (m, 1H), 8.32 (d, *J* = 8.0 Hz, 1H), 7.98 (td, *J* = 3.6 Hz, 2.0 Hz, 1H), 7.47-7.44 (m, 2H), 7.32-7.28 (m, 1H), 7.23 (d, *J* = 3.6 Hz, 2H), 2.69 (s, 3H) ppm. **^{13}C{^{1}H} NMR (CDCl$_3$, 176 MHz):** $\delta$ 185.4, 150.4, 150.0, 148.0, 139.1, 137.2, 126.1, 124.0, 123.9, 123.7, 122.1, 121.3, 116.1, 110.7, 11.8 ppm. **IR** (KBr, cm^{-1}): 3061, 2927, 2843, 1437, 650.

2-Methyl-1H-indole (**5**)[24]:

Physical State: Brown solid (44 mg, 67% yield). **R$_f$** = 0.5 (10% EtOAc/hexane). **^{1}H NMR (CDCl$_3$, 700 MHz):** δ 7.82 (brd, 1H), 7.50 (s, 1H), 7.26 (s, 1H), 7.09-7.05 (m, 2H), 6.21 (s, 1H), 2.43 (s, 3H) ppm. **^{13}C{^{1}H} NMR (CDCl$_3$, 176 MHz):** δ 136.3, 135.3, 129.4, 121.2, 119.9, 110.5, 100.7, 14.0 ppm. (One peak is merging). **IR** (KBr, cm^{-1}): 3394, 3052, 2939, 2850, 1402.

### *3-Bromo-2-methyl-1-(pyridin-2-yl)-1H-indole* (**6**):
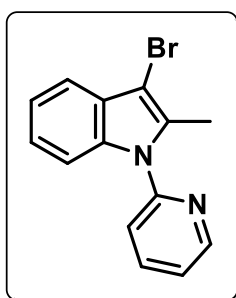
Physical State: Colorless liquid (23 mg, 81% yield). **R$_f$** = 0.3 (5% EtOAc/hexane). **^{1}H NMR (CDCl$_3$, 400 MHz):** δ 8.65 (dd, *J* = 4.8 Hz, 1.2 Hz, 1H), 7.88 (td, *J* = 8.0 Hz, 2.0 Hz, 1H), 7.55-7.53 (m, 1H), 7.40-7.31 (m, 3H), 7.24-7.15 (m, 2H), 2.46 (s, 3H) ppm. **^{13}C{^{1}H} NMR (CDCl$_3$, 176 MHz):** δ 151.2, 150.0, 138.7,

136.2, 134.3, 127.9, 123.2, 122.6, 121.7, 121.1, 118.9, 110.7, 94.2, 12.8 ppm. **IR** (KBr, cm^{-1}): 3058, 3019, 2920, 1466. **HRMS (ESI) m/z:** [M+H]$^+$ Calcd for $C_{14}H_{12}BrN_2$ 287.0178; Found 287.0180. **m/z**: [M+H]$^+$ Calcd for $C_{14}H_{12}Br^{81}N_2$ 289.0158; found, 289.0169.

1-(2-Methyl-1-(pyridin-2-yl)-1H-indol-3-yl)ethan-1-one (7)[23]:
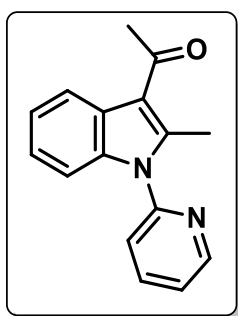
**Physical State:** White solid (18 mg, 72% yield). **R$_f$** = 0.3 (40% EtOAc). **^{1}H NMR (CDCl$_3$, 700 MHz):** δ 8.74 (d, J = 4.2 Hz, 1H), 8.07 (d, J = 7.7 Hz, 1H), 7.97 (d, J = 7.7 Hz, 1H), 7.47-7.45 (m, 1H), 7.41(d, J = 7.7 Hz, 1H), 7.30-7.28 (m, 1H), 7.19 (d, J = 3.5 Hz, 2H), 2.72 (s, 3H), 2.68 (s, 3H) ppm. **^{13}C{^{1}H} NMR (CDCl$_3$, 176 MHz):** δ 195.4, 150.5, 150.3, 144.7, 139.0, 137.1, 126.8, 123.9, 123.1, 123.0, 122.7, 121.2, 116.3, 111.0, 32.1, 14.4 ppm. **IR** (KBr, cm^{-1}): 3462, 2984, 1750, 1718, 1373, 1267.

2-Methyl-1H-indole-3-carbaldehyde (7a)[26]:
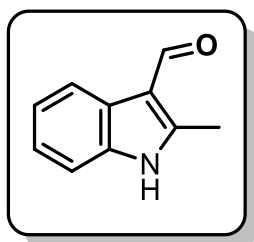
Physical State: Pale yellow solid (60 mg, 94% yield). **R$_f$** = 0.2 (40% EtOAc/hexane). **^{1}H NMR (CDCl$_3$, 700 MHz):** δ 10.19 (s, 1H), 8.70 (brd, 1H), 8.24 (d, J = 7.0 Hz, 1H), 7.33 (d, J = 7.7 Hz, 1H), 7.27-7.26 (m, 1H), 7.25-7.23 (m, 1H), 2.74 (s, 3H) ppm. **^{13}C{^{1}H} NMR (CDCl$_3$, 176 MHz):** δ 184.9, 146.9, 135.2, 126.4, 123.8, 123.1, 121.2, 115.1, 111.0, 12.6 ppm. **IR** (KBr, cm^{-1}): 3188, 3056, 2927, 2806, 1775, 1468.

(E)-3-(2-Methyl-1H-indol-3-yl)-1-(pyridin-4-yl)prop-2-en-1-one (**8**)[16b]:
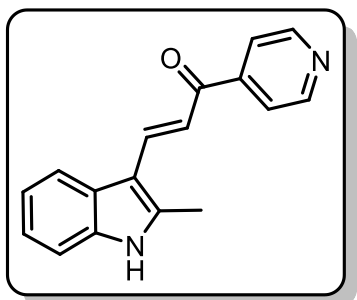
Physical State: Yellow solid (49 mg, 75% yield). R_f = 0.2 (40% EtOAc/hexane). **^{1}H NMR (DMSO-d$_6$, 400 MHz):** δ 11.93 (brd, 1H), 8.81-8.80 (m, 2H), 8.10 (d, J = 15.2 Hz, 1H), 8.05-8.03 (m, 1H), 7.94 (dd, J = 4.4 Hz, 1.6 Hz, 2H), 7.45 (d, J = 15.2 Hz, 1H), 7.43-7.39 (m, 1H), 7.23-7.18 (m, 2H), 2.59 (s, 3H) ppm. **^{13}C{^{1}H} NMR (DMSO-d$_6$, 176 MHz):** 188.9, 151.5, 146.5, 145.8, 140.4, 137.1, 126.7, 123.3, 122.4, 122.3, 121.2, 114.0, 112.6, 110.3, 12.8 ppm. **IR** (KBr, cm^{-1}): 2959, 2847, 2741, 1641, 1413.

NMR spectra of 2-Methyl-1-(pyridin-2-yl)-1H-indole (3aa):

3aa, ^{1}H NMR (CDCl$_3$, 400 MHz)

3aa, ^{13}C{^{1}H} NMR (CDCl$_3$, 100 MHz)

1H NMR (CDCl$_3$, 400 MHz)
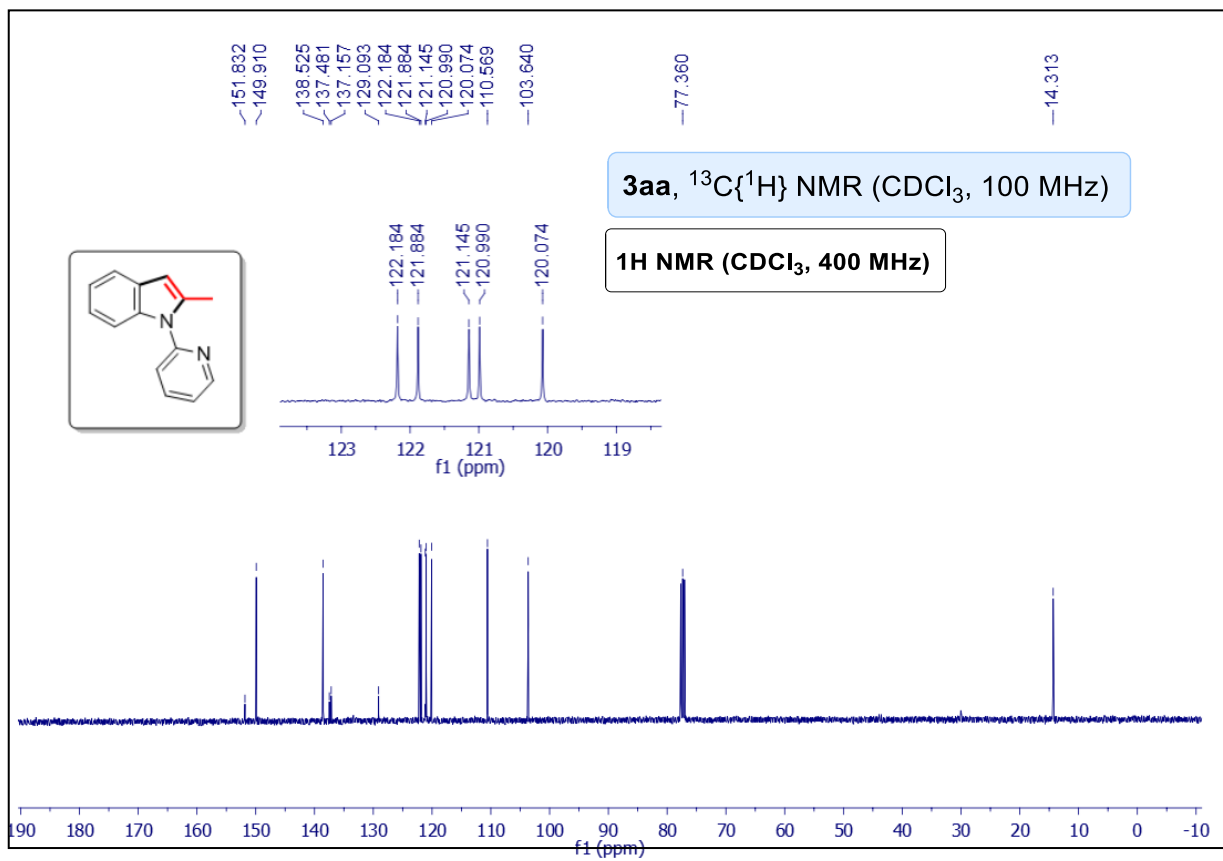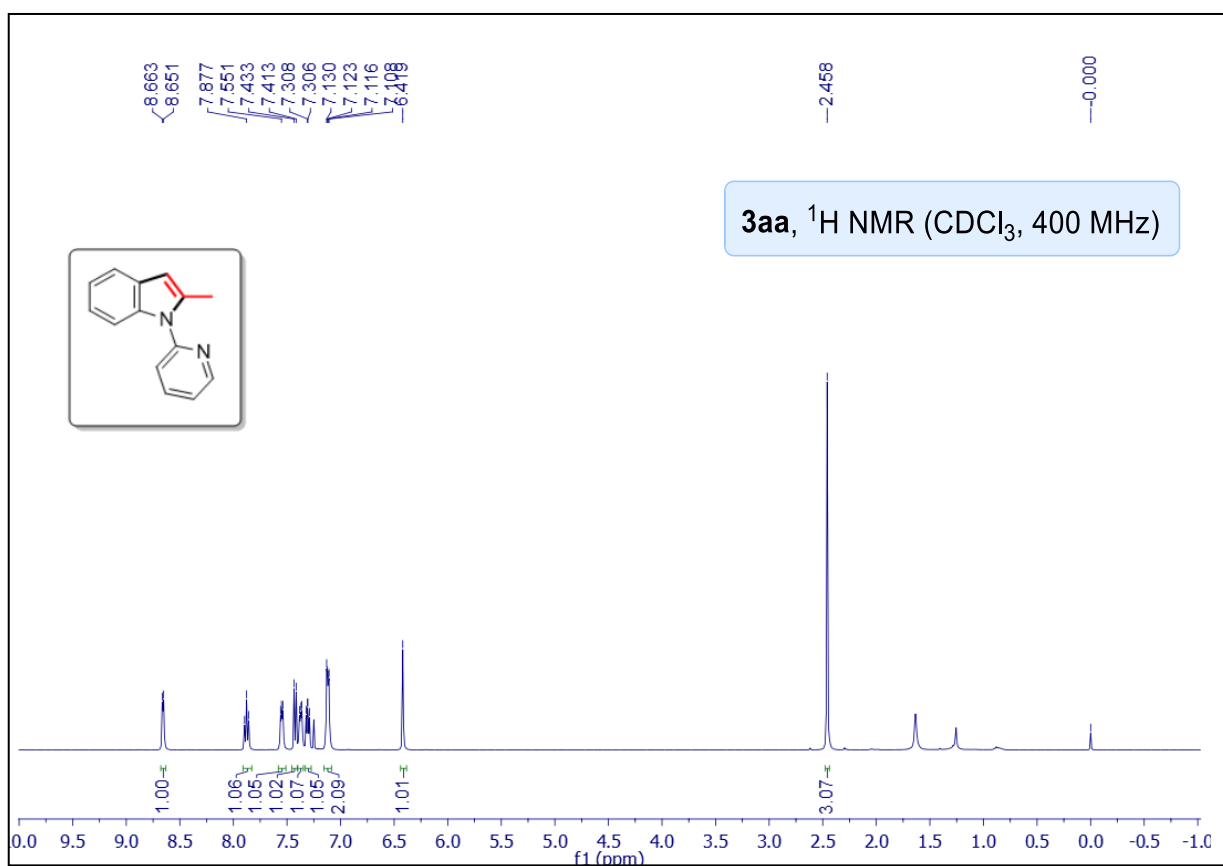
NMR spectra of 5-Isopropyl-2-methyl-1-(pyridin-2-yl)-1H-indole (3da):

3da, ^{1}H NMR (CDCl$_3$, 400 MHz)

3da, ^{13}C{^{1}H} NMR (CDCl$_3$, 100 MHz)

8, ^{1}H NMR (DMSO-D6, 400 MHz)

8, ^{13}C{^{1}H} NMR (DMSO-D6, 176 MHz)

1H NMR (CDCl$_3$, 400 MHz)

5.6 REFERENCES

1. (a) Manan, R. S.; Zhao, P. *Nat. Commun*. **2016**, *7*, 11506–11517. (b) Zheng, L.; Hua, R. C–H Activation and Alkyne Annulation via Automatic or Intrinsic Directing Groups: Towards High Step Economy. *Chem. Rec.* **2018**, *18*, 556–569. (c) Ye, X.; Wang, C.; Zhang, S.; Wei, J.; Shan, C.; Wojtas, L.; Xie, Y.; Shi, X. Facilitating Ir-Catalysed C-H Alkynylation with Electrochemistry: Anodic Oxidation-Induced Reductive Elimination. *ACS Catal.* **2020**, *10* (20), 11693–11699.

2. (a) Dong, Z.; Ren, Z.; Thompson, S. J.; Xu, Y.; Dong, G. Transition-Metal-Catalysed C-H Alkylation Using Alkenes. *Chem. Rev.* **2017**, *117*, 9333–9403. (b) Li, J.-J.; Wang, C.-G.; Yu, J.-F.; Wang, P.; Yu, J.-Q. Cu-Catalysed C-H Alkenylation of Benzoic Acid and Acrylic Acid Derivatives with Vinyl Boronates. *Org. Lett.* **2020**, *22*, 4692–4696.

3. (a) Luo, Y.-C.; Yang, C.; Qiu, S.-Q.; Liang, Q.-J.; Xu, Y.-H.; Loh, T.-P. Palladium(II)-Catalysed Stereospecific Alkenyl C-H Bond Alkylation of Allylamines with Alkyl Iodides. *ACS Catal.* **2019**, *9*, 4271–4276. (b) Ankade, S. B.; Shabade, A. B.; Soni, V.; Punji, B. Unactivated Alkyl Halides in Transition-Metal-Catalysed C-H Bond Alkylation. *ACS Catal.* **2021**, *11*, 3268–3292.

4. (a) Vorobyeva, D. V.; Osipov, S. N. Selective Synthesis of 2-and 7-Substituted Indole Derivatives via Chelation-Assisted Metallocarbenoid C–H Bond Functionalization. *Synthesis* **2018**, *50*, 227–240. (b) Xiang, Y.; Wang, C.; Ding, Q.; Peng, Y. Diazo Compounds: Versatile Synthons for the Synthesis of Nitrogen Heterocycles *via* Transition Metal-Catalysed Cascade C–H Activation/Carbene Insertion/Annulation Reactions. *Adv. Synth. Catal.* **2019**, *361*, 919-944.

5. (a) Moon, S.; Nishii, Y.; Miura, M. Thioether-Directed Peri-Selective C-H Arylation under Rhodium Catalysis: Synthesis of Arene-Fused Thioxanthenes. *Org. Lett.* **2019**, *21*, 233–236 (b) Zhang, J.; Liu, Y.; Jia, Q.; Wang, Y.; Ma, Y.; Szostak, M. Ruthenium(II)-Catalysed C–H Arylation of *N,N*-Dialkyl Thiobenzamides with Boronic Acids by Sulfur Coordination in 2-Me THF. *Org. Lett.* **2020**, *22*, 6884–6890.

6. (a) Chen, Y.-Q.; Wu, Y.; Wang, Z.; Qiao, J. X.; Yu, J.-Q. Transient Directing Group Enabled Pd-Catalysed γ-C(sp^3)–H Oxygenation of Alkyl Amines. *ACS Catal.* **2020**, *10*, 5657–5662. (b) Jin, L.; Zhang, X.-L.; Guo, R.-L.; Wang, M.-Y.; Gao, Y.-R.; Wang, Y.-Q. Palladium-catalysed dehydrogenative fluoroalkoxylation of benzaldehydes. *Org. Lett.* **2021**, *23*, 1921–1927. (c) Shinde, Vikki N.; Rangan, K.; Kumar, D.; Kumar, A. Palladium-Catalysed Weakly Coordinating Lactone-Directed C−H Bond Functionalization of 3-Arylcoumarins: Synthesis of Bioactive Coumestan Derivatives. *J. Org. Chem.* **2021**, *86*, 14, 9755–9770.

7. Park, Y.; Kim, Y.; Chang, S. Transition metal-catalysed C–H amination: scope, mechanism, and applications. *Chem. Rev.* **2017**, *117*, 9247–9301.

8. (a) Yang, L.; Correia, C. A.; Li, C.-J. Rhodium-catalysed C–H activation and conjugate addition under mild conditions. *Org. Biomol. Chem.* **2011**, *9*, 7176-7179. (b) Potter, T. J.; Ellman, J. A. Rh(III)-Catalysed C–H Bond Addition/Amine-Mediated Cyclization of Bis-Michael Acceptors. *Org. Lett.* **2016**, *18*, 3838–3841 (c) Boerth, J. A.; Ellman, J. A. Rh(III)-catalysed diastereoselective C–H bond addition/cyclization cascade of enone tethered aldehydes *Chem. Sci.* **2016**, *7*, 1474. (d) Manna, M. K.; Bhunia, S. K.; Jana, R. Ruthenium(II)-catalysed intermolecular synthesis of 2-arylindolines through C–H activation/ oxidative cyclization cascade *Chem. Commun.* **2017**, *53*, 6906. (e) Banjare, S.-K.; Biswal, P.; Ravikumar, P.-C.

Cobalt-Catalysed One-Step Access to Pyroquilon and C-7 Alkenylation of Indoline with Activated Alkenes Using Weakly Coordinating Functional Groups. *J. Org. Chem.* **2020**, *85*, 5330–5341. (f) Kumar, M.; Verma, S.; Verma, A. K. Ru(II)-Catalysed Oxidative Olefination of Benzamides: Switchable Aza-Michael and Aza-Wacker Reaction for Synthesis of Isoindolinones. *Org. Lett.* **2020**, *22*, 4620–4626. (g) Onodera, S.; Togashi, R.; Ishikawa, S.; Kochi, T.; Kakiuchi, F. Catalytic, Directed C–C Bond Functionalization of Styrenes. *J. Am. Chem. Soc.* **2020**, *142*, 7345–7349.

9. (a) Crisenza, G. E. M.; Sokolova, O. O.; Bower, J. F. Branch-Selective Alkene Hydroarylation by Cooperative Destabilization: Iridium-Catalysed ortho-Alkylation of Acetanilides. *Angew. Chem., Int. Ed.* **2015**, *54*, 14866–14870 (b) Deb, A.; Maiti, D. Emergence of Unactivated Olefins for the Synthesis of Olefinated Arenes. *Eur. J. Org. Chem.* **2017**, *2017*, 1239–1252. (c) Zell, D.; Bursch, M.; Mueller, V.; Grimme, S.; Ackermann, L. Full Selectivity Control in Cobalt(III)-Catalysed C–H Alkylations by Switching of the C–H Activation Mechanism *Angew. Chem., Int. Ed.* **2017**, *56*, 10378–10382. (d) Liu, Y.; Yang, Y.; Wang, C.; Wang, Z.; You, J. Rhodium(III)- Catalysed Regioselective Oxidative Annulation of Anilines and Allylbenzenes via C(sp^3)−H/C(sp^2)−H Bond Cleavage. *Chem. Commun.* **2019**, *55*, 1068−1071 (e) Lee, S.; Semakul, N.; Rovis, T. Direct Regio- and Diastereoselective Synthesis of δ-Lactams from Acrylamides and Unactivated Alkenes Initiated by Rh(III)-Catalysed C–H Activation. *Angew. Chem., Int. Ed.* **2020**, *59*, 4965–4969.

10. (a) Kozhushkov, S. I.; Yufit, D. S.; Ackermann, L. Ruthenium-Catalysed Hydroarylations of Methylene- cyclopropanes: Mild C-H Bond Functionalizations with Conservation of Cyclopropane Rings. *Org. Lett.* **2008**, *10*, 3409-3412. (b)

Schinkel, M.; Marek, I.; Ackermann, L. Carboxylate-Assisted Ruthenium(II)-Catalysed Hydro- arylations of Unactivated Alkenes through C-H Cleavage. *Angew. Chem., Int. Ed.* **2013**, *52*, 3977-3980 (c) Kumar, G. S.; Kapur, M. Ruthenium-Catalysed, Site-Selective C-H Allylation of Indoles with Allyl Alcohols as Coupling Partners. *Org. Lett.* **2016**, *18*, 1112-1115 (d) Jambu, S.; Tamizmani, M.; Jeganmohan, M. *Org. Lett.* **2018**, *20*, 1982−1986. (e) Manikandan, R.; Madasamy, P.; Jeganmohan, M. Ruthenium-Catalysed Oxidant Free Allylation of Aromatic Ketoximes with Allylic Acetates at Room Temperature. *Chem. - Eur. J.* **2015**, *21*, 13934-13938 (f) Trita, A. S.; Biafora, A.; Pichette Drapeau, M.; Weber, P.; Gooßen, L. J. Regiospecific ortho-C−H Allylation of Benzoic Acids. *Angew. Chem., Int. Ed*. **2018**, *57*, 14580−14584. (h) Dana, S.; Giri, C. K.; Baidya, M. Ruthenium(II)-Catalysed Regioselective C–H Olefination of Aromatic Ketones and Amides with Allyl Sulfones. *Org. Lett.* **2021**, *23*, 17, 6855–6860.

11. (a) Jambu, S.; Jeganmohan, M. Rhodium(III)-Catalysed C–H Olefination of Aromatic/Vinyl Acids with Unactivated Olefins at Room Temperature. *Org. Lett.* **2020**, *22*, 5057–5062 (b) Shambhavi, C. N.; Jeganmohan, M. Ruthenium(II)-Catalysed Redox-Neutral C-H Alkylation of Arylamides with Unactivated Olefins. *Org. Lett.* **2021**, *23*, 4849-4854. (c) ambu, S.; Shambhavi, C. N.; Jeganmohan, M. Aerobic Oxidative C–H Olefination of Arylamides with Unactivated Olefins via a Rh(III)-Catalysed C–H Activation. *Org. Lett.* **2021**, *23*, 2964-2970.

12. (a) Das, A.; Chatani, N. Cp*Rh(II)-Catalysed C–H Alkylation of Benzylamines with Unactivated Alkenes: The Influence of Acid on Linear and Branch Selectivity. *Org. Lett.* **2021**, *23*, 4273−4278. (b) Khake, S. M.; Yamazaki, K.; Ano, Y.; Chatani, N. Iridium(III)-Catalysed Branch-Selective C-H Alkenylation of Aniline Derivatives with Alkenes. *ACS Catal.* **2021**, *11*, 5463–5471. (c) Khake, S. M.;

Chatani, N. Rh(III)-Catalysed [3+2] Annulation of Aniline Derivatives with Vinylsilanes via C−H Activation/Alkene Cyclization: Access to Highly Regioselective Indoline Derivatives *ACS Catalysis* **2021**, *11*, 12375-12383.

13. (a) Mukherjee, S.; List, B. Chiral Counteranions in Asymmetric Transition-Metal Catalysis: Highly Enantioselective Pd/Brønsted Acid-Catalysed Direct α-Allylation of Aldehydes. *J. Am. Chem. Soc.* **2007**, *129*, 11336−11337. (b) Li, M. B.; Wang, Y.; Tian, S. K. Regioselective and Stereospecific Cross-Coupling of Primary Allylic Amines with Boronic Acids and Boronates through Palladium-Catalysed C−N Bond Cleavage. *Angew. Chem., Int. Ed*. **2012**, *51*, 2968−2971. (c) Nagae, H.; Xia, J.; Kirillov, E.; Higashida, K.; Shoji, K.; Boiteau, V.; Zhang, W.; Carpentier, J.-F.; Mashima, K. Asymmetric Allylic Alkylation of *β*-Ketoesters via C-N Bond Cleavage of *N*-allyl-*N*-methylaniline Derivatives Catalysed by a Nickel-Diphosphine System. *ACS Catal.* **2020**, *10*, 5828−5839. (d) Wu, L., Wang, T., Gao, C., Huang, W., Qu, J., Chen, Y. Skeletal Reconstruction of 3-Alkylidenepyrrolidines to Azepines Enabled by Pd-Catalysed C–N Bond Cleavage. *ACS Catal*. **2021**, *11*, 3, 1774–1779.

14. (a) Yan, R.; Wang, Z. X. Ruthenium Catalysed C−H Allylation of Arenes with Allylic Amines. *Org. Biomol. Chem*. **2018**, *16*, 3961−3969. (b) Hu, X.-Q.; Hu, Z.; Zhang, G.; Sivendran, N.; Gooßen, L. J. Catalytic C−N and C−H Bond Activation: ortho-Allylation of Benzoic Acids with Allyl Amines. *Org. Lett.* **2018***, 20*, 4337.

15. Blanksby, S. J.; Ellison, G. B. Bond Dissociation Energies of Organic Molecules. *Acc. Chem. Res*. **2003**, *36*, 255−263.

16. (a) Sravanthi, T. V.; Manju, S. L. Indoles-A promising scaffold for drug development. *Eur. J. Pharm. Sci.* **2016**, *91*, 1–10. (b) Robinson, M. W.; Overmeyer, J. H.; Young, A. M.; Erhardt, P. W.; Maltese, W. A. Synthesis and evaluation of

indole-based chalcones as inducers of methuosis, a novel type of nonapoptotic cell death. *J. Med. Chem*. **2012**, *55*, 1940–1956.

17. Manna, M. K.; Bairy, G.; Jana, R. Sterically Controlled Ru(II)-Catalysed Divergent Synthesis of 2-Methylindoles and Indolines through a C–H Allylation/Cyclization Cascade. *J. Org. Chem.* **2018***, 83*, 8390–8400.

18. Mishra, N. K.; Choi, M.; Jo, H.; Oh, Y.; Sharma, S.; Han, S. H.; Jeong, T.; Han, S.; Lee, S.-Y.; Kim, I. S. Direct C–H alkylation and indole formation of anilines with diazo compounds under rhodium catalysis. *Chem. Commun*. **2015**, *51*, 17229-17232.

19. G. Brasche, S. L. Buchwald. C-H Functionalization/C-N Bond Formation: Copper-Catalysed Synthesis of Benzimidazoles from Amidines *Angew. Chem. Int. Ed*. 2008, *47*, 1932.

20. Ueda, S.; Nagasawa, H. Copper-Catalysed Synthesis of Benzoxazoles via a Regioselective C−H Functionalization/C−O Bond Formation under an Air Atmosphere. *J. Org. Chem.* **2009**, *74*, 4272–4277.

21. Chankeshwara, S. V.; Chakraborti, A. K. Catalyst-Free Chemoselective *N-tert-*Butyloxycarbonylation of Amines in Water. *Org. Lett.* **2006**, *8*, 3259–3262.

22. Manna, M. K.; Bairy, G.; Jana, R. Sterically Controlled Ru(II)-Catalysed Divergent Synthesis of 2-Methylindoles and Indolines through a C–H Allylation/Cyclization Cascade. *J. Org. Chem.* **2018**, *83*, 8390–8400.

23. Ni, S.; Hribersek, M.; Baddigam, S. K.; Ingner, F. J. L.; Orthaber, A.; Gates, P. J.; Pilarski, L. T. Mechanochemical Solvent-Free Catalytic C-H Methylation. *Angew. Chem., Int. Ed.* **2021**, *60*, 6660–6666.

24. Tonin, M. D. L.; Zell, D.; Müller, V.; Ackermann, L. Ruthenium(II)-Catalysed C−H Methylation with Trifluoroborates. *Synthesis* **2017**, *49*, 127.

25. Zhang, X.-W.; Jiang, G.-Q.; Lei, S.-H.; Shan, X.-H.; Qu, J.-P.; Kang, Y.-B. Iron-Catalysed *α,β*-Dehydrogenation of Carbonyl Compounds *Org. Lett.* **2021**, *23*, 1611–1615.

26. Mandrekar, Ketan S.; Tilve, Santosh G. Molecular iodine mediated oxidative cleavage of the C–N bond of aryl and heteroaryl (dimethylamino)methyl groups into aldehydes. *New J. Chem.* **2021**, *459*, 4152-4155.

SUMMARY OF THE THESIS

Isoquinolines
Chapter-2

N-PAHs
Chapter-3

Alkenylation
Chapter-4

2-Methyl
indoles
Chapter-5